

NO-R164 149

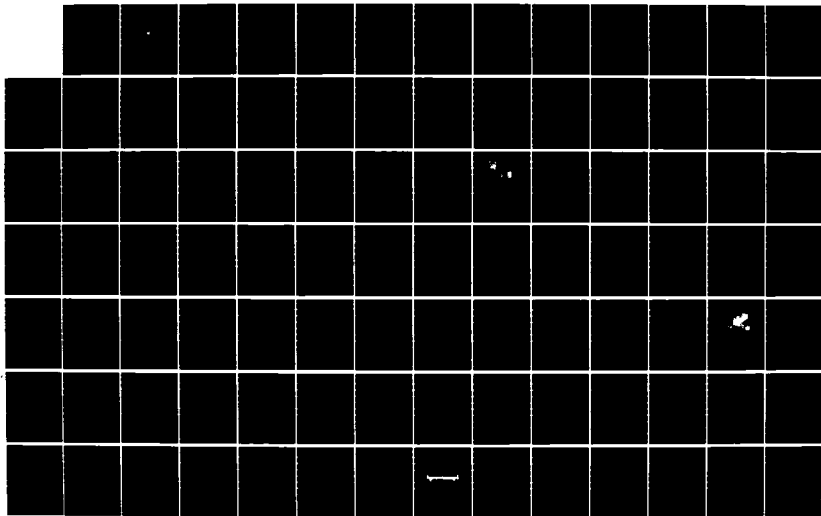
RECIPROCITY CALIBRATION IN A PLANE WAVE RESONATOR(U)
NAVAL POSTGRADUATE SCHOOL MONTEREY CA C L BURNASTER
DEC 85 NPS61-86-006

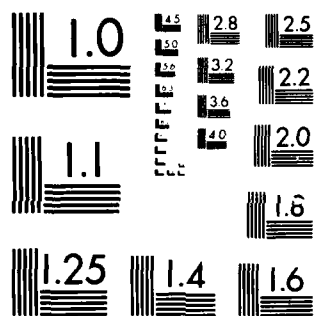
1/5

UNCLASSIFIED

F/G 14/2

NL





MICROCOPY RESOLUTION TEST CHART
NATIONAL BUREAU OF STANDARDS-1963-A

2

NPS61-86-006

NAVAL POSTGRADUATE SCHOOL

Monterey, California

AD-A164 149



DTIC
COPY
E

THESIS

RECIPROCITY CALIBRATION
IN
A PLANE WAVE RESONATOR

by

Charles Lyman Burmaster

December 1985

Dissertation Supervisor:

S. L. Garrett

DTIC FILE COPY

Approved for public release; distribution unlimited

Prepared for: The Office of Naval Research
Arlington, Virginia

86 2 13 053

NAVAL POSTGRADUATE SCHOOL
Monterey, Ca 93943

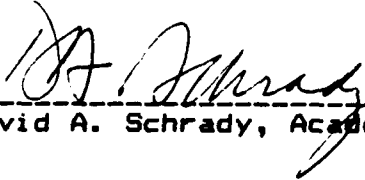
Rear Admiral R. H. Shumaker
Superintendent

D. A. Schrady
Provost

This thesis prepared in conjunction with research sponsored in part by The Office of Naval Research under NPS61-86-004.

Reproduction of all or part of this report is authorized.

Released by:



David A. Schrady, Academic Dean

UNCLASSIFIED

SECURITY CLASSIFICATION OF THIS PAGE

AD-A164 149

REPORT DOCUMENTATION PAGE

1a REPORT SECURITY CLASSIFICATION		1b. RESTRICTIVE MARKINGS	
SECURITY CLASSIFICATION AUTHORITY		3 DISTRIBUTION/AVAILABILITY OF REPORT	
DECLASSIFICATION/DOWNGRADING SCHEDULE		Approved for public release; distribution unlimited	
4 PERFORMING ORGANIZATION REPORT NUMBER(S)		5 MONITORING ORGANIZATION REPORT NUMBER(S)	
NPS61-86-006			
6a. NAME OF PERFORMING ORGANIZATION	6b OFFICE SYMBOL (If applicable)	7a. NAME OF MONITORING ORGANIZATION	
Naval Postgraduate School	61	Naval Postgraduate School	
6c ADDRESS (City, State, and ZIP Code)		7b. ADDRESS (City, State, and ZIP Code)	
Monterey, California 93943 - 5100		Monterey, California 93943 - 5100	
8a NAME OF FUNDING/SPONSORING ORGANIZATION	8b. OFFICE SYMBOL (If applicable)	9. PROCUREMENT INSTRUMENT IDENTIFICATION NUMBER	
The Office of Naval Research	code 1112	N0001485AF00001	
8c ADDRESS (City, State, and ZIP Code)		10 SOURCE OF FUNDING NUMBERS	
Sciences Directorate, Physics Div. 800 N. Quincy St. (code 1112) Arlington, Va., zip. 22217		PROGRAM ELEMENT NO 61153N	
		PROJECT NO RR011-08-01	
		TASK NO 384-938	
		WORK UNIT ACCESSION NO N0001485WR 24031	
11 TITLE (Include Security Classification)			
RECIPROCITY CALIBRATION IN A PLANE WAVE RESONATOR			
12 PERSONAL AUTHOR(S)			
Charles Lyman Burmaster			
13a TYPE OF REPORT	13b TIME COVERED	14 DATE OF REPORT (Year, Month, Day)	15 PAGE COUNT
Doctoral Dissertation	FROM _____ TO _____	1985 December	434
16 SUPPLEMENTARY NOTATION			
This work supported by The Office of Naval Research			
17 COSATI CODES			18 SUBJECT TERMS (Continue on reverse if necessary and identify by block number)
FIELD	GROUP	SUB-GROUP	Acoustic Calibration, Reciprocity
			Microphone Calibration Reciprocity Calibration
			Condenser Microphone Resonant Reciprocity
19 ABSTRACT (Continue on reverse if necessary and identify by block number)			
<p>A non-standard method for the electroacoustic reciprocity calibration of a condenser microphone is theoretically developed and experimentally employed to calibrate a WE640AA laboratory standard microphone. The average experimental calibration so obtained was found to be in absolute agreement with a pressure coupler comparison calibration of the same microphone made at the National Bureau of Standards to within an experimental uncertainty (sigma) of 0.03 dB over the frequency range of 245 to 1470 Hz. using a 70 cm. plane wave resonant cavity, and to within an experimental uncertainty (sigma) of 0.06 dB over the frequency range of 735 to 1470 Hz. using a 23 cm. plane wave resonant cavity. Above 1470 Hz., the difference between the resonant plane wave reciprocity calibrations and the pressure coupler comparison calibration increased linearly with frequency to a maximum of 0.61 dB at 5145 Hz.</p> <p>Beginning with theory previously published by Isadore Rudnick, reciprocity equations for the open circuit voltage receiving sensitivity are optimized for experimental</p>			
20 DISTRIBUTION AVAILABILITY OF ABSTRACT		21 ABSTRACT SECURITY CLASSIFICATION	
<input checked="" type="checkbox"/> UNCLASSIFIED UNLIMITED <input type="checkbox"/> SAME AS RPT <input type="checkbox"/> DTIC USERS		Unclassified	
22a NAME OF RESPONSIBLE INDIVIDUAL		22b TELEPHONE (Include Area Code)	22c OFFICE SYMBOL
L. Garrett		408-646-2540	61Gx

DD FORM 1473, 84 MAR

83 APR edition may be used until exhausted

All other editions are obsolete

SECURITY CLASSIFICATION OF THIS PAGE

UNCLASSIFIED

Block 18 continued.

Plane wave resonator Transfer Impedance Computer aided test

Block 20 continued.

measurements in a plane wave resonant cavity to include the effects of finite microphone compliance and the non-adiabatic boundary conditions. Two right cylindrical plane wave resonant cavities of different dimensions were constructed to provide a self consistency check on the method.

A preliminary comparison of the theory for a free field reciprocity calibration, a pressure coupler reciprocity calibration, and a plane wave resonant reciprocity calibration is made to illustrate the common physics pertinent to the reciprocity principle that underlies the three methods.

Experimental calibrations based upon free field reciprocity were made alternately with plane wave resonant reciprocity calibrations to provide an ongoing experimental comparison when combined with published diffraction effects for a standard mounting of a WE640AA laboratory standard microphone. The National Bureau of Standards comparison calibration was based upon an absolute pressure coupler reciprocity calibration and was obtained shortly after the resonant reciprocity calibration measurements were complete.

Accession For	
NTIS GRA&I	<input checked="" type="checkbox"/>
DTIC TAB	<input type="checkbox"/>
Unannounced	<input type="checkbox"/>
Justification	
By _____	
Distribution/	
Availability Codes	
Dist	Special

Approved for public release; distribution unlimited.

Reciprocity Calibration in a Plane Wave Resonator

by

Charles Lyman Burmaster
Lieutenant Commander, United States Navy
B.S. Arizona State University, 1966
M.S. Naval Postgraduate School, 1978

Submitted in partial fulfillment of the
requirements for the degree of

DOCTOR OF PHILOSOPHY

From the

NAVAL POSTGRADUATE SCHOOL
December, 1985

Author:
Approved by:

Charles Lyman Burmaster
Charles Lyman Burmaster

S. L. Garrett
S. L. Garrett
Physics
Dissertation Supervisor

O. B. Wilson
O. B. Wilson, Jr.
Professor of Physics

W. E. Zajac
W. E. Zajac
Associate Professor of Physics

P. H. Moos
P. H. Moos
Associate Professor of
Electrical Engineering

G. W. Morris
G. W. Morris
Professor of Mathematics

L. J. Zimek
L. J. Zimek
Assistant Professor of
Electrical Engineering

Approved by:

James T. Sanders
James T. Sanders, Chairman, Engineering Association
Academic Committee

Approved by:

David A. Conrady
David A. Conrady, Academic Dean

ABSTRACT

A non-standard method for the electroacoustic reciprocity calibration of a condenser microphone is theoretically developed and experimentally employed to calibrate a W.E.640AA laboratory standard microphone. The average experimental calibration so obtained was found to be in absolute agreement with a pressure coupler comparison calibration of the same microphone made at the National Bureau of Standards to within an experimental uncertainty (σ) of $\sim .03$ dB over the frequency range of 245 to 1470 Hz using a 70 cm. plane wave resonant cavity, and to within an experimental uncertainty (σ) of $\sim .06$ dB over the frequency range of 735 to 1470 Hz using a 23 cm. plane wave resonant cavity. Above 1470 Hz, the difference between the resonant plane wave reciprocity calibrations and the pressure coupler comparison calibration increased linearly with frequency to a maximum of $\sim .61$ dB at 5145 Hz.

Beginning with theory previously published by Isadore Rudnick, reciprocity equations for the open circuit voltage receiving sensitivity are optimized for experimental measurements in a plane wave resonant cavity to include the effects of finite microphone compliance and the non-adiabatic boundary conditions. Two right cylindrical

plane wave resonant cavities of different dimensions were constructed to provide a self consistency check on the method.

A preliminary comparison of the theory for a free field reciprocity calibration, a pressure coupler reciprocity calibration, and a plane wave resonant reciprocity calibration is made to illustrate the common physics pertinent to the reciprocity principle that underlies the three methods.

Experimental calibrations based upon free field reciprocity were made alternately with plane wave resonant reciprocity calibrations to provide an ongoing experimental comparison when combined with published diffraction effects for a standard mounting of a W.E.640AA laboratory standard microphone. The National Bureau of Standards comparison calibration was based upon an absolute pressure coupler reciprocity calibration and was obtained shortly after the resonant reciprocity calibration measurements were complete.

THESIS DISCLAIMER

The reader is cautioned that computer programs developed in this research may not have been exercised for all cases of interest. While every effort has been made, within the time available, to ensure that the programs are free of computational and logic errors, they cannot be considered validated. Any application of these programs without additional verification is at the risk of the user.

TABLE OF CONTENTS

I.	THE PRINCIPLE OF ACOUSTICAL RECIPROCITY IN MICROPHONE CALIBRATION -----	27
A.	INTRODUCTION -----	27
B.	HISTORY -----	30
C.	A GENERAL THEORY OF ACOUSTICAL RECIPROCITY ----	34
D.	ACOUSTIC RECIPROCITY CALIBRATION OF MICROPHONE SENSITIVITY -----	43
	1. General Acoustic Reciprocity Calibration of Electroacoustic Transducers -----	43
	2. General Determination of The Reciprocity Factor "J" -----	53
	a. The Calculation of "J" for a Pressure Coupler Reciprocity Calibration -----	57
	b. The Calculation of "J" for a Free Field Reciprocity Calibration -----	59
	c. The Calculation of "J" for The Plane Wave Reciprocity Calibration -----	62
	3. A Summary of The Three Reciprocity Methods Compared in this Experiment -----	78
	a. Plane Wave Resonant Reciprocity Calibration -----	78
	b. Free Field Reciprocity Calibration -----	79
	c. Pressure Coupler Reciprocity Calibration -----	80

II.	EXPERIMENTAL CONSIDERATIONS FOR A PLANE WAVE RESONANT RECIPROCITY CALIBRATION -----	81
A.	INTRODUCTION -----	81
B.	DEVELOPMENT OF THE EXPERIMENTAL PLANE WAVE RECIPROCITY EQUATIONS USING CYLINDRICAL GEOMETRY -----	83
1.	Experimental Considerations -----	83
2.	Two Comparison Calibrations for Microphone "C"-----	100
3.	The Comparison Calibration of Microphones "A" and "B" With Respect to Each Other -----	109
C.	THE IMPRESSED PRESSURE CORRECTION -----	111
III.	EXPERIMENTAL PROCEDURES -----	127
A.	INTRODUCTION -----	127
B.	EXPERIMENTAL APPARATUS -----	129
1.	Plane Wave Resonant Cavities -----	129
2.	The Microphone Translator for Free Field Calibrations -----	137
C.	SIGNAL FLOW AND COMPUTER CONTROL WITH PLANE WAVE RESONANT RECIPROCITY -----	145
D.	THE CALCULATION OF EXPERIMENTAL ERROR -----	150
1.	Introduction -----	150
2.	Measuring the Ratio e_1/i_1 -----	153
a.	The Electrical Circuit -----	153
b.	Measuring The Input Capacitance of Preamplifiers -----	159
c.	The Calculation of e_1 -----	164
d.	The Calculation of i_1 -----	169
e.	Measuring The Signal Preamplifier Gain -	175

f.	Measuring Non-Linearity in The Lock-in Detector -----	180
g.	Computation of The Probable Error in e_1/i_1 -----	183
3.	The Measurement of V_{ca}/V_{cb} -----	187
4.	Calculating The Reciprocity Factor, "J" ----	189
a.	Measuring Atmospheric Pressure -----	190
b.	Uncertainty in Resonant Frequency and Quality Factor -----	193
c.	Calculating The Effect of The Non- Adiabatic Boundary Conditions Upon The Stiffness of The Gas Within The Resonant Cavity -----	199
d.	Volume Measurements in the Plane Wave Resonant Cavities -----	207
e.	Measuring Temperature and Relative Humidity -----	212
5.	A Summary of Experimental Uncertainty For The Plane Wave Resonant Reciprocity Experiment -----	214
E.	SIGNAL FLOW AND COMPUTER CONTROL FOR THE FREE FIELD COMPARISON CALIBRATION -----	218
1.	Introduction -----	218
2.	Experimental Considerations for a Free Field Comparison Calibration -----	219
3.	Measurement of the Sensitivity Ratio, $M(640R)/M(688R)$ -----	222
4.	Free Field Reciprocity Measurements -----	227
F.	EXPERIMENTAL ERROR FOR THE FREE FIELD COMPARISON CALIBRATION -----	235
1.	Introduction -----	235
2.	Measuring The Open Circuit Receiving Voltage, e_4 -----	238

a.	Analysis of The Electrical Circuit Used to Measure ϵ_4 -----	238
b.	Determination of Gain Uncertainty for The Ithaco 1201 Preamplifier -----	240
c.	Computation of The Uncertainty in The Measure of ϵ_4 -----	242
3.	Analytical Considerations for The Measure of "Vdrop" -----	243
4.	Analytical Considerations Made in The Measurement of R4 -----	245
5.	Measuring The "Acoustic" Separation Distance	246
a.	Introduction -----	246
b.	Determination of Spherical Spreading ---	248
6.	Calculating The Uncertainty in The Ratio Vb/Va -----	251
7.	A Summary of Experimental Error for The Free Field Comparison Calibration -----	253
IV.	SELF CONSISTENCY OF THE PLANE WAVE RESONANT RECIPROCITY CALIBRATION -----	256
A.	INTRODUCTION -----	256
B.	THE OBSERVATION OF EXPERIMENTAL PRECISION -----	260
C.	THE PRECISION FOR THE ROUND-ROBIN COMPARISON ---	264
D.	THE PRECISION ASSOCIATED WITH THE SWAP OF SIDE "A" AND SIDE "B" ELECTRONICS -----	266
E.	THE PRECISION OBTAINED BY REPLACING THE SIDE "B" RECIPROCAL MICROPHONE WITH ONE HAVING A SIGNIFICANTLY DIFFERENT SENSITIVITY (4 dB) -----	267
F.	THE PRECISION ASSOCIATED WITH REPLACING THE LONG TUBE WITH THE SHORT TUBE AS THE PLANE WAVE RESONANT CAVITY -----	268
G.	A SUMMARY OF THE EXPERIMENTAL PRECISION FOUND FOR THE PLANE WAVE RESONANT RECIPROCITY CALIBRATION METHOD -----	269

V.	ABSOLUTE ACCURACY OF EXPERIMENTAL RESULTS -----	271
	A. INTRODUCTION -----	271
	B. CALCULATION OF THE IMPRESSED PRESSURE CORRECTION	275
	C. THE CORRECTION TO THE BULK MODULUS OF ELASTICITY WITHIN THE PLANE WAVE RESONANT CAVITY DUE TO THE NON-ADIABATIC BOUNDARY CONDITIONS -----	284
	D. THE ELECTRICAL DRIVING POINT IMPEDANCE CORRECTION -----	286
	E. THE CORRECTION DUE TO REVISED VALUES OF MICROPHONE AND TOTAL BIAS SUPPLY CAPACITANCE -----	293
	F. THE COUPLING CAPACITANCE CORRECTION, -----	296
	G. THE ABSOLUTE PLANE WAVE RESONANT RECIPROCITY CALIBRATION -----	297
	1. Introduction -----	297
	2. Experimental Results for The Plane Wave Resonant Reciprocity Calibration Compared With a NBS Pressure Coupler Comparison Calibration Obtained For The Same Microphone	298
	H. THE CORRECTED FREE FIELD COMPARISON CALIBRATION-	304
	I. A SUMMARY OF PLANE WAVE RESONANT RECIPROCITY CALIBRATIONS -----	309
VI.	CONCLUSION -----	314
	A. SUMMARY -----	314
	B. FURTHER EXPERIMENTS AND THEORETICAL INVESTIGATIONS -----	318
	APPENDIX A - HARMONICITY IN PLANE WAVE RESONANT RECIPROCITY CALIBRATION -----	320
	APPENDIX B - ONE EXAMPLE OF THE COMPUTER PROGRAM USED FOR PLANE WAVE RESONANT RECIPROCITY CALIBRATIONS--	326
	A. INTRODUCTION -----	326
	B. FUNCTIONAL DESCRIPTION OF THE PROGRAM -----	328
	C. PROGRAM LISTING -----	330

	D. VARIABLE DEFINITIONS USED IN THE PROGRAM --	346
APPENDIX C -	DESCRIPTION OF THE PROGRAM USED TO OBTAIN THE COMPARISON RATIO, v_b/v_a IN THE FREE FIELD COMPARISON CALIBRATION -----	352
	A. INTRODUCTION -----	352
	B. FUNCTIONAL DESCRIPTION OF THE PROGRAM -----	353
	C. PROGRAM LISTING -----	355
	D. VARIABLE DEFINITIONS USED IN THE PROGRAM --	356
APPENDIX D -	DESCRIPTION OF THE PROGRAM USED TO OBTAIN THE FREE FIELD COMPARISON CALIBRATION.-----	357
	A. INTRODUCTION -----	357
	B. FUNCTIONAL DESCRIPTION OF THE PROGRAM -----	359
	C. PROGRAM LISTING -----	363
	D. VARIABLE DEFINITIONS USED IN THE PROGRAM --	373
APPENDIX E -	THE D. C. BLOCKING CAPACITOR CORRECTION -----	377
APPENDIX F -	THE OPEN CIRCUIT VOLTAGE SENSITIVITY CALIBRATION OBTAINED FROM OBSERVING A CHANGE IN MICROPHONE CAPACITANCE WITH A CHANGE IN BIAS VOLTAGE -----	383
APPENDIX G -	A PRINTOUT OF RAW DATA FOR THE PLANE WAVE RESONANT RECIPROCITY CALIBRATION IN BOTH A LONG AND A SHORT TUBE -----	389
	2 MAY DATA TAPE, LONG TUBE, A SIDE - 815 W/ET, B SIDE - 1248 -----	391
	2 MAY DATA TAPE, LONG TUBE, A SIDE - 1248, B SIDE - 815 W/ET -----	397
	2 MAY DATA TAPE, LONG TUBE, A SIDE - 1248, B SIDE - 1082 W/ET -----	403
	2 MAY DATA TAPE, LONG TUBE, A SIDE - 1082 W/ET, B SIDE - 815 -----	409
	22 NOV DATA TAPE, LONG TUBE, A SIDE - 1082, B SIDE - 815 W/ET -----	415

22 NOV DATA TAPE, SHORT TUBE, A SIDE - 1248, B SIDE - 815 (ET ALONGSIDE) -----	421
22 NOV DATA TAPE, SHORT TUBE, A SIDE - 1248, B SIDE - 1082 (ET ALONGSIDE) -----	424
LIST OF REFERENCES -----	427
INITIAL DISTRIBUTION LIST -----	431

LIST OF TABLES

3.1	Percent relative change from run to run under manual control as compared to computer control for a selected sample -----	149
3.2	Measured capacitances of bias boxes and microphones -----	158
3.3	Measured values of capacitances boxes used as "Cv" in the determination of preamplifier input capacitance -----	161
3.4	Measured ratios for [a/b] -----	162
3.5	Calculated input capacitances for signal preamplifiers used in experiment -----	163
3.6	Measured change in capacitance due to the application of a bias voltage to a condenser microphone -----	172
3.7	Linearity data obtained using ratio transformer serial #304 -----	181
3.8	Linearity data obtained using ratio transformer serial #572 -----	182
3.9	Temperature normalized resonance frequencies and the associated quality factors for three different modes -----	196
3.10	Volume measurements obtained for the plane wave cavity resonators -----	208
3.11	Summary of probable error in experimental parameters -----	216
3.12	A summary of probable error for the free field comparison calibration -----	253

4.1	W.E.640AA calibration data -----	263
4.2	Round robin comparison between Ma and Mab to obtain the "modal" experimental precision -----	265
4.3	A summary of precision in plane wave resonant reciprocity calibrations -----	269
5.1	Equivalent volumes for extreme W.E.640AA laboratory standard condenser microphones -----	278
5.2	Tabulated values of acoustic impedance for four W.E.640AA microphones -----	279
5.3	Tabulated values of the impressed pressure correction obtained using equivalent volumes of extreme samples of the WE640AA population and the difference between these corrections----	281
5.4	D. C. blocking capacitor corrections -----	296
5.5	Absolute plane wave resonant reciprocity calibrations obtained using the 70 cm tube compared with the NBS comparison calibrations---	298
5.6	Absolute plane wave resonant reciprocity calibrations obtained using the 23 cm tube compared with the NBS comparison calibrations---	299
5.7	W.E.640AA Serial #1248 calibrations -----	302
5.8	NBS vs Free field data -----	307
B.1	Functional program listing for plane wave resonant reciprocity calibration -----	329
C.1	The functional program listing for Vratio which calculates the ratio of microphone sensitivities for free field reciprocity -----	354
D.1	Functional program listing for free field comparison calibration -----	362
E.1	Program listing for Cc correction -----	380

E.2	Comparison calculation between the HP-15c and the IBM-XT with C_b and $C_c = .01 \text{ uf}$ -----	381
F.1	HP-15c program for Open circuit voltage receiving sensitivity, M_o , obtained using the change in microphone capacitance with an increase in bias voltage -----	387

LIST OF FIGURES

1.1	Cavity with rigid walls into which sound is projected -----	37
1.2	Electro-acoustic two port network -----	43
1.3	Four port electro-acoustic network -----	46
1.4	Reciprocal electroacoustic system -----	48
1.5	A cylindrical plane wave resonator -----	62
1.6	Modal resonances in a 23.3 cm, air filled brass pipe of 2.5 cm diameter at room temperature [22 deg C] -----	66
1.7	Differential volume under consideration -----	71
2.1	Modified four port network -----	85
2.2	Geometry of the offset microphone used in the calculation of $G_1(n)$ -----	87
2.3	Scheme used to obtain comparison voltages ---	90
2.4	Reciprocal microphones mounted in the ends of a plane wave resonator -----	111
2.5	Different terminations for the plane wave tubes -----	118
2.6	A copy of the original engineering drawings showing the backplate design for the WE640AA condenser microphone -----	125
3.1	Computer control of the microphone translator	139
3.2	The comparison calibration between the Altec type 688 and the W.E.640AA microphones -----	144

3.3	Schematic diagram of the signal flow for the plane wave resonant reciprocity calibration -	145
3.4	Receiving signal flowgraph -----	153
3.5	Receiving signal input circuit -----	154
3.6	Simplified input circuit for acoustic signal	157
3.7	Circuit used to measure the input capacitance of signal preamplifiers -----	159
3.8	Simplified circuit for measuring the acoustic signal -----	165
3.9	Analog to digital signal flow chart -----	167
3.10	Circuit used to measure voltage across microphone when the magnitude of the source voltage is under computer control -----	170
3.11	Circuit used to measure amplifier gain -----	176
3.12	Measured gain for HP-465A serial #95 -----	177
3.13	Measured gain for HP-465A serial #93 -----	178
3.14	Circuit used to determine non-linearity in the lock-in detector -----	180
3.15	The pressure sensor signal path -----	191
3.16	Pressure sensor vs. pressure reference -----	192
3.17	Data sample of a modal resonance from which a ravine F_n , Q_n , and amplitude are obtained -	194
3.18	Fractional error in quality factor plotted on probability paper. The linear correlation coefficient is equal to .98 -----	197

3.19	Fractional error in resonant frequency plotted on probability paper. The linear correlation coefficient is equal to .97 -----	198
3.20	Correction to the ratio of specific heats due to the non-adiabatic boundary conditions within a right circular brass cavity 70.1 cm long and 1.73 cm radius, filled with air ----	203
3.21	Correction to M_0 due to the change in stiffness of the gas within the cavity caused by the non-adiabatic boundary conditions ----	205
3.22	Signal flow used in measuring V_b/V_a inside the anechoic chamber -----	222
3.23	The sensitivity ratio obtained for 640R/688R-	224
3.24	M_0 for the W.E.640AA serial #'s 1248 & 609 (top) and the Altec type 688A (bottom) -----	225
3.25	Signal flow in the free field comparison calibration based upon free field reciprocity	227
3.26	Raw data output from "N28" -----	231
3.27	Quality control output from "N28" -----	232
3.28	A sample of the final distance versus M_0 calculated by program "N28" -----	233
3.29	Measured gain for the Ithaco preamplifier ---	241
3.30	Measuring the voltage drop [Vdrop] across the current resistor -----	243
3.31	A plot showing the correction for the "acoustic" separation distance at 490 Hz ----	249
3.32	The sensitivity ratio obtained for 640R/688R-	251

3.33	The variation of the 490 Hz microphone sensitivity with separation distance -----	255
4.1	An illustration of the "electronics swap" ---	257
4.2	The relative sizes of plane wave resonant cavities used in comparing calibrations -----	258
4.3	Electromechanical configurations used in the plane wave resonant reciprocity calibrations-	260
5.1	Raw data from both the long and short resonant tubes for plane wave resonant reciprocity calibrations -----	272
5.2	Calculated values of the impressed pressure correction applicable to the "long" tube plane wave resonant reciprocity calibration -	282
5.3	Calculated values of the impressed pressure correction applicable to the "short" tube plane wave resonant reciprocity calibration -	283
5.4	The microphone plus bias box capacitance correction plotted for all six experimental combinations -----	295
5.5	Plane wave resonant reciprocity calibration vs NBS comparison pressure coupler calibration of W.E.640AA serial #1248 type L laboratory standard microphone -----	300
5.6	The corrected free field comparison calibration for W.E.640AA serial #1248 condenser microphone -----	305
5.7	Low frequency detail in the corrected free field comparison calibration -----	306
5.8	Plane wave reciprocity calibrations for W.E.640AA serials #815, and #1082 listed top to bottom -----	309

5.9	The effect of radial and azimuthal modes on the plane wave resonant reciprocity calibration -----	311
5.10	Comparison calibration for the type BT-1751 Knowles subminiature transducer -----	312
5.11	Manufacturer's calibration curves for the Type BT-1751 and Type BT-1757 Knowles subminiature transducers -----	313
A.1	Resonant frequency re. 20 degrees centigrade plotted vs. mode number -----	322
A.2	Harmonicity as measured with data obtained from condenser microphone W.E.640AA serial# 1248 -----	323
E.1	The input electronics circuit for the acoustic signal -----	378
E.2	The bias voltage blocking capacitor correction to the open circuit voltage receiving sensitivity (plotted in dB) -----	382

LIST OF PHOTOGRAPHS

1.1	Some of the microphones used in this experiment -----	33
1.2	Right cylindrical circular resonant cavity used to obtain the modal resonances shown in figure 1.6 -----	65
2.1	In this photograph, the "ports" for the comparison microphone are mounted on the side wall of the cylinder -----	88
2.2	The relative sizes of the Knowles subminiature transducer mounted alongside the one inch condenser microphone -----	106
2.3	The relative size of the Knowles subminiature transducer alongside both a one inch W.E.640AA and a one half inch General Radio microphone--	107
3.1	The 70.12 cm brass tube used as a plane wave resonant cavity -----	130
3.2	Mounting ports, end view -----	132
3.3	The "short" tube -----	133
3.4	A closeup of the comparison microphone mounted in the wall of the short tube -----	134
3.5	The microphone port in the wall of the short tube -----	135
3.6	A comparison photograph showing the physical differences in the end microphone mounts between the short and the long tube -----	136
3.7	The microphone translator -----	138
3.8	The mounting of the drive motor and the optical shaft encoder -----	140
3.9	The equipment setup at the entrance to the anechoic chamber -----	142

ACKNOWLEDGEMENTS

I am indebted and forever thankful for the patience, love, and faithful support provided by my wife Jan who has been all any husband could ever ask for throughout the five years of days, evenings, and weekends involved in completing this dissertation. To my dissertation supervisor and friend, Dr. Steven L. Garrett, I give my thanks not only for his immeasurable contribution to this work, but also for his continuous encouragement, unbounded enthusiasm, and his willingness to share his abilities and gifts as an experimentalist at all hours of the day or night regardless of circumstance.

I am also indebted to each member of my doctoral committee for providing me with knowledge, criticism, direction, and encouragement. To Dr. Bryan Wilson, my thanks for steadfast encouragement, an introduction to the fascinating subject of transducers, and for inviting me to join the faculty at the Naval Postgraduate School. Without your interest and encouragement from the beginning, this work could not have begun. To Dr. Bill Zeleny, my thanks for the many indispensable hours you spent early on in my acoustics education answering questions as you introduced me to non-linear acoustics. You remain the only professor that

I have had who has (so far as I am aware) never made a mistake on the blackboard during a lecture. I thank you not only for your example of excellence in teaching, which I have tried to follow, but also for your warm humor and encouragement when times were difficult. To Dr. Paul Moose, my thanks for many interesting and stimulating discussions on decision and estimation theory as applied to acoustical signal processing and communications theory. At the time I studied these subjects, I had no idea that they would intrude so often into the professional applications that I have encountered at the United States Naval Academy. To Dr. George Morris, I am especially thankful for the perspective and philosophical discussions on both the subject of graduate education and the application of mathematics via numerical methods. Your example as a christian gentleman and scholar has been and continues to be a witness to me. To Dr. Larry Ziomek, my thanks for, "You will never go wrong if you start with basic principles, formulate the most general solution, and then simplify when possible with reasonable assumptions". Your friendly encouragement and considered advice has been greatly appreciated throughout this work.

To my colleagues and friends both at the Naval Postgraduate School in Monterey and here at the United States Naval Academy I owe a debt of thanks and gratitude

for the innumerable comments, discussions, suggestions, and efforts made on my behalf.

A special thanks is extended to Mr. Kerry Yarber who patiently sought out data at long range and passed it on to me across the continent. His willingness to help and respond even to the most unusual and untimely requests leaves me deeply in his debt and forever thankful for such a fine colleague and friend.

I would like to thank machinists Tom Maris and Bob Moeller for their absolutely excellent work in machining and modifying the plane wave resonant cavities. To Bob Moeller, I extend an additional thanks and my appreciation for your example of professional excellence in the construction and subsequent maintenance of the microphone translator. In a quote from Professor Steve Garrett, "Not only is Bob Moeller the most important man in the physics department here at Monterey, he also is the second most important man..." I totally agree and will always fondly remember your christian kindness to students and faculty alike.

To Bob Smith, my thanks for technical assistance in building the bias box switching circuits and your scholarly assistance in the arena of practical electronics.

To the physics department secretaries on both coasts; Lena C. Langton, Carolyn Cruz, Patricia A. Vardaro, Sue C. Chung, Lucille G. Marlar, Donna Stroshine, Joan S. Evenson,

Jan Siwicki, Marge Bem, and Judy Katzwinkle, I extend my thanks for the many times you provided administrative assistance and a listening ear.

I would like to acknowledge Dr. John Fontenalla and Dr. Mary Wintersgill for their help with computer graphics at the Naval Academy and for the wonderful spirit of helpfulness that they extended at all hours of the day and night while the dissertation was in its final stages. To Cdr. Buzz Shaw, my grateful thanks for your unending financial support, warm friendship, and spiritual support. To Dr. Murray S. Korman, my thanks for your steadfast friendship when times were difficult, your encouragement, a ready smile, and good advice.

To Dr. John Ertel and Lcdr. Mike Trent at the United States Naval Academy, my thanks for your immediate response in copying and mailing replacement floppy discs for the originals that were "eaten by a california computer" as I prepared the final draft of the dissertation.

Finally, I would like to thank Alice M. Burmaster, Charles D. Burmaster, Bob and Janell Selman, Charles, Matthew, and Melissa Burmaster, and Florence Lyman for their continuing interest and encouragement to help me see everything in its proper perspective.

May God bless and keep you all in the years to come.

I. THE PRINCIPLE OF ACOUSTICAL RECIPROCITY
IN MICROPHONE CALIBRATION

A. INTRODUCTION

In any experiment requiring absolute acoustic measurements there exists a need for an accurate calibrated standard microphone, or its equivalent, to be used to directly measure acoustic data or to be used as a sensitivity reference. *The primary subject of this paper is an unconventional method for obtaining such a calibration on a standard microphone.* First described by Isadore Rudnick [Ref. 1], this unconventional method results in an acoustical reciprocity pressure calibration of a standard microphone. It is unconventional in that it uses a plane wave resonant cavity instead of a free field or a small pressure chamber for the calibration. The method of plane wave resonant reciprocity calibration [Ref. 1] has been satisfactorily employed by G.W. Swift, A. Migliori, S.L. Garrett, and J.C. Wheatley, to calibrate a dynamic pressure transducer from 0 to 400 hertz in a 1-MPa helium gas. The dynamic pressure calibration so obtained was experimentally verified by another calibration method based upon a mercury

manometer to within an instrumental uncertainty of one percent [Ref. 2].

Conventional methods for obtaining acoustic pressure calibrations of microphones are published by The American National Standards, Inc. (ANSI)[Ref. 3], and include pressure coupler reciprocity calibration and free field reciprocity calibration. These two acoustic reciprocity microphone calibration techniques are well reported in the literature [Refs.4,5,6,7,8,9,10,11,12].

In this dissertation, the application of acoustical reciprocity to microphone sensitivity calibrations will include *theory* for all three types of acoustical reciprocity calibrations and *experimental measurements* of microphone sensitivity based upon plane wave resonant reciprocity, free field reciprocity, and pressure-reciprocity calibration performed in a closed coupler. The coupler calibrations provided here were performed by the National Bureau of Standards. Essential to the derivation of the general theory for a plane wave resonant reciprocity calibration is a "microphone that feels no impressed pressure" [Ref. 1]. This describes a perfectly rigid microphone for which the mechanical impedance is infinite. Here, the finite impedance of the microphone is included and a correction to the plane wave resonant reciprocity calibration is predicted and experimentally verified at low frequencies.

When calibrating microphones in a gas it is interesting to note, and will be shown, that all three methods of acoustic reciprocity calibration require (to within a multiplicative constant) the measurement of experimental variables that can be expressed in a similar way. These variables are; a volume, the frequency of sound, the barometric pressure, the ratio of specific heats, and basic electrical measurements. As a consequence of this common descriptive set, acoustical reciprocity calibrations are classified as *primary* methods of acoustic microphone calibration after Bobber [Ref. 10], where a primary method is defined as requiring only basic measurements of voltage, current, electrical and acoustical impedance, length, mass (or density), and time (or frequency). Secondary methods are those in which a microphone, or some other reference, has been calibrated by a primary method and is used as a reference standard.

To appreciate the impact that acoustical reciprocity calibrations have had upon acoustical science, it is useful to review the history of acoustical reciprocity in the context of historical attempts to measure acoustic pressure, particle displacement, and particle velocity.

B. HISTORY

The acoustical reciprocity principle was introduced first in Lord Rayleigh's (John William Strutt) paper on "Some General Theorems relating to Vibration"[Ref. 13] in 1873. In that paper he gave the following example of reciprocity and credited Helmholtz with a proof in the case of a uniform fluid without friction:

"In a space occupied by air, let A and B be two sources of disturbance. The vibration excited at A will produce at B the same relative amplitude and phase as if the places were exchanged." [Ref. 13: p. 181]

In 1877, in his treatise on The Theory of Sound [Ref. 14], Lord Rayleigh gave as an example of the reciprocity theorem in acoustics the following:

"let A and B be two points of a space occupied by air, between which are situated obstacles of any kind. Then a sound originating at A is perceived at B with the same intensity as that with which an equal sound originating at B would be perceived at A." [Ref. 14: Vol I, p. 134]

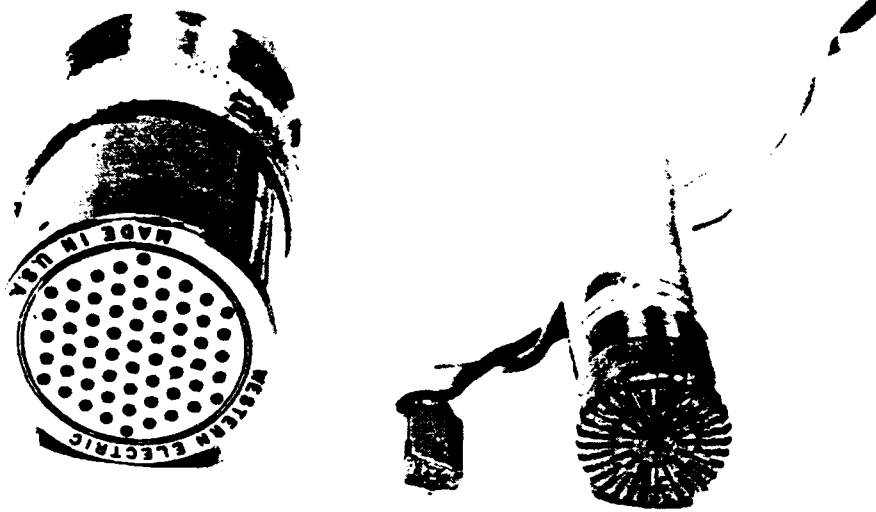
In various examples, Lord Rayleigh applied the reciprocity principle to a harmonic transverse force and a resulting displacement in a bar [Ref. 14: Vol I, p. 153], and to periodic electromotive forces and the resultant currents in electrical circuits [Ref. 14: Vol I, p. 155].

Lord Rayleigh proposed to measure the acoustic particle velocity in a sound field with the "Rayleigh disk" in 1882 [Ref. 9: p. 148]. When the theory for the performance of the Rayleigh disk was set down by Koenig [Ref. 9: p. 148], it became widely used as a tool in acoustical measurements. Other investigators measured the acoustic particle amplitude but in general these techniques yielded measurements which were accurate to within a few percent at best [Ref. 9: pp. 159-160].

A primary source of sound was invented by Gwozdz [Ref. 9: p. 169], a Russian engineer, in 1907 when he used a wire heated by electricity as a source of sound. This thermophone was improved on by Lange [Ref. 15] when he invented a thermophone with substantial acoustical output in 1914. H. D. Arnold and I. B. Crandall [Ref. 16], developed a quantitative theory to explain the workings of the thermophone, and both S. Ballantine [Ref. 17] and E.C. Wente [Ref. 18] improved upon the theory. The thermophone remains today as a primary sound source with accuracies on the order of 1 dB re 1V/ubar [Ref. 9: p. 171]. In 1917, developments in the field of vacuum tube amplifiers with their high input impedance made the design of a condenser microphone by Wente [Ref. 19] practical. The first calibration of Wente's condenser microphone was accomplished using a thermophone of his own construction [Ref. 19]. It remained for MacLean

[Ref. 4] and independently, Cook [Ref. 5] to first apply Rayleigh's reciprocity theorem to the electroacoustic system in a manner such that absolute acoustic reciprocity calibrations of the receiving (and transmitting) sensitivity of a microphone were obtained.

G.S.K. Wong and T.F.W. Embleton [Ref. 12], have predicted the best accuracies for a condenser microphone calibration to date using the pressure coupler reciprocity calibration method, with the uncertainty of the absolute open circuit sensitivity level expected to be less than .005 dB re 1V/ubar. This dissertation will theoretically and experimentally explain the calibration of the open circuit receiving sensitivity obtained with the method of plane wave resonant reciprocity for a standard Western Electric 640AA condenser microphone.



Photograph 1.1 Some of the microphones used in this experiment.

In the photograph above, a W.E.640AA one inch laboratory standard condenser microphone is shown on the left, in the center is a Knowles type BT 1751 subminiature transducer, and on the right is a General radio type 1434 condenser microphone. Both the W.E.640AA and the GR 1434 condenser microphones have locally made electrical connectors for BNC connectors partially visible in this photo.

C. A GENERAL THEORY OF ACOUSTICAL RECIPROACITY

Prior to discussing acoustical reciprocity, the following symbols are defined:

- ϕ_A - velocity potential due source "A"
- ϕ_B - velocity potential due source "B"
- p_A - acoustic pressure field due source "A"
- p_B - acoustic pressure field due source "B"
- \vec{u}_A - acoustic particle velocity due source "A"
- \vec{u}_B - acoustic particle velocity due source "B"
- \dot{V}_A - volume velocity of source "A"
- \dot{V}_B - volume velocity of source "B"
- ρ_0 - equilibrium density of acoustic medium
- ω - angular frequency of either monofrequency source
- e - open circuit receiving voltage
- i - short circuit transmitting current
- Z - general term for impedance [acoustic or electrical]
- m_0 - open circuit receiving sensitivity
- S_i - transmitting sensitivity (current)
- J - reciprocity factor (acoustic transfer admittance)
- γ - ratio of specific heats for the acoustic medium
- γ_E - ratio of specific heats for medium corrected for non-adiabatic boundary conditions and for the effects of relative humidity.
- p_0 - equilibrium (ambient) pressure
- V_0 - cavity volume used in reciprocity scheme
- λ - acoustic wavelength

- c - acoustic phase speed in unbounded medium
- $\langle \mathcal{E} \rangle_t$ - time averaged energy density
- Q_N - quality factor of the Nth resonance
- $\Delta \mathcal{E}$ - energy dissipated per cycle
- L - length of cylindrical plane wave resonator
- A_0 - end cross sectional area of cylindrical plane wave resonator
- N - the mode number of the longitudinal resonance
- f_1 - fundamental frequency of longitudinal resonances
- f - frequency (Hz)
- k - wavenumber, equal to $(2\pi)/(\text{wavelength})$
- k_N - modal wavenumber (for rigid boundary conditions in the ends of the cylindrical resonant cavity, equal to $(\text{mode number} \cdot \pi)/(\text{length of tube})$)

A theory of passive linear electroacoustic transducers was developed by L.L. Foldy and H. Primakoff in a two part paper published in 1945 [Ref. 20] and in 1947 [Ref. 21]. In their theory, the pressure and normal velocity at each point on a transducer's surface and the voltage and current at a transducer's electrical terminals were shown to be related by a set of linear integral equations. Solving the wave equation using Green's functions for the medium in which the transducer was immersed and using the equations defining the electrical termination of the transducer, they showed that the behavior of a transducer could be completely characterized in terms of four parameters. These four

parameters were shown to be: the voltage across the electrical terminals of a transducer, the current flowing into these terminals, the acoustic pressure at any point on the surface of the transducer, and the normal velocity of the surface at every point on the face of the transducer [Ref. 20]. In part II of the paper, L.L. Foldy and H. Primakoff developed the conditions necessary for the validity of the electroacoustic reciprocity theorem in a wide variety of physical systems. They found that,

"transducers possessing: electrostatic coupling only, or electromagnetic coupling only, obey the 'reciprocity relations' providing that the polarizability, the susceptibility, the Hooke's law, and the conductivity tensors are symmetric; on the other hand, transducers possessing piezoelectric coupling only, or magnetostrictive coupling only, demand in addition (for the satisfaction of the 'reciprocity relations'), the equality of the direct and inverse piezoelectric and magnetostrictive coupling tensors. The symmetry and equality of the tensors under discussion is always satisfied at sufficiently low frequencies; whether or not it holds in general depends on the detailed physical mechanism of the medium and of its electroacoustic coupling, in particular, on whether or not dissipative phenomena of the 'relaxation' type are present..."[Ref. 21]

The four parameter transducer description of L.L. Foldy and H. Primakoff is used for a condenser microphone in this paper.

To demonstrate resonant reciprocity in a cavity, consider the volume shown in figure 1.1. The walls are rigid

and there are two reciprocal transducers flush mounted in the walls. In the ensuing discussion each transducer will be used alternately as a sound source and as a sound receiver.

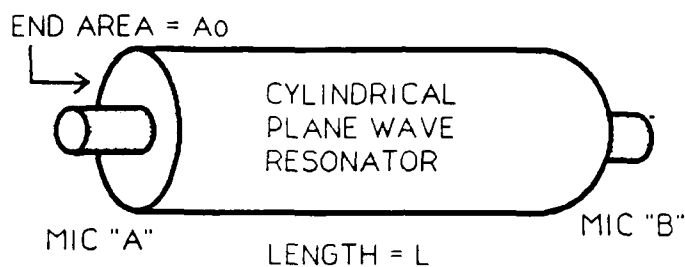


Figure 1.1 Cavity with rigid walls into which sound is projected.

When the sound fields within the cavity are irrotational, the acoustic particle velocity is given by the gradient of the velocity potential. Following Kinsler, Frey, Coppens, and Sanders [Ref. 11: p.165], we apply a vector identity to the two velocity potentials associated with the two sources to obtain,

$$\nabla \cdot (\phi_A \nabla \phi_B) = \nabla \phi_A \cdot \nabla \phi_B + \phi_A \nabla^2 \phi_B \quad \text{Equation 1.1}$$

When the vector identity is again applied, after reversing the order of the velocity potentials, we obtain,

$$\nabla \cdot (\phi_B \nabla \phi_A) = \nabla \phi_B \cdot \nabla \phi_A + \phi_B \nabla^2 \phi_A \quad \text{Equation 1.2}$$

These two equations are now subtracted and the result is integrated over the volume shown in figure 1.1. This yields the integral equation,

$$\int_{\text{Vol.}} \nabla \cdot (\phi_A \nabla \phi_B - \phi_B \nabla \phi_A) dV = \int_{\text{Vol.}} (\phi_A \nabla^2 \phi_B - \phi_B \nabla^2 \phi_A) dV \quad \text{Equation 1.3}$$

If the divergence theorem is applied to the left side we obtain Green's Theorem,

$$\oint_{\text{Surface}} (\phi_A \nabla \phi_B - \phi_B \nabla \phi_A) \cdot \hat{n} dS = \int_{\text{Vol.}} (\phi_A \nabla^2 \phi_B - \phi_B \nabla^2 \phi_A) dV \quad \text{Equation 1.4}$$

where \hat{N} is the unit vector normal to the surface. Now, if we operate both sources at the same frequency,

$$\nabla^2 \phi_A = -k^2 \phi_A$$

Equation 1.5

and,

$$\nabla^2 \phi_B = -k^2 \phi_B$$

Equation 1.6

upon substituting equations 1.5 and 1.6 into equation 1.4, we obtain,

$$\oint_{\text{SURFACE}} (\phi_A \nabla \phi_B - \phi_B \nabla \phi_A) \cdot \hat{N} dS = \int_{\text{VOL.}} (\phi_A [-k^2 \phi_B] - \phi_B [-k^2 \phi_A]) dV$$

Equation 1.7

and on the left side of equation 1.4, all that remains is the integral.

$$\oint_{\text{SURFACE}} (\phi_A \nabla \phi_B - \phi_B \nabla \phi_A) \cdot \hat{N} dS = 0$$

Equation 1.8

The acoustic particle velocity and the acoustic velocity potential are related by,

$$\vec{u} = \nabla \phi \quad \text{Equation 1.9}$$

and from the linearized Euler equation in a medium with constant density, we have,

$$p = -\rho_0 \frac{\partial \phi}{\partial t} = -j\omega \rho_0 \phi \quad \text{Equation 1.10}$$

Now, prior to substituting equations 1.9 and 1.10 into Equation 1.8, if we consider the integral in equation 1.8 to consist of one portion over the rigid walls and the other portion over the surfaces of each simple source exposed to the inside cavity volume, equation 1.8 can be simplified,

$$\int_{\text{RIGID WALLS}} (\phi_A \nabla \phi_B - \phi_B \nabla \phi_A) \cdot \hat{n} ds + \int_{\text{SIMPLE SOURCES}} (\phi_A \nabla \phi_B - \phi_B \nabla \phi_A) \cdot \hat{n} ds = 0 \quad \text{Equation 1.11}$$

Since the normal component of the particle velocity is zero at the rigid walls, the integral over the surface of the walls is zero and we are left with the integral over the exposed faces of the transducers. For harmonic velocity potentials, equations 1.9 and 1.10 are substituted into equation 1.8 where we obtain,

$$\int_{\text{SOURCE FACES}} (p_A \vec{u}_B - p_B \vec{u}_A) \cdot \hat{n} ds = 0$$

Equation 1.12

With the definition of the following parameters,

$p_{ab}(\vec{r})$ = pressure at "A" when "B" is transmitting as a function of position, \vec{r} , on A's surface.

$p_{ba}(\vec{r}')$ = pressure at "B" when "A" is transmitting as a function of position, \vec{r}' , on B's surface.

$\vec{u}_a(\vec{r})$ = velocity of the "face" of source "A" as a function of position, \vec{r} .

$\vec{u}_b(\vec{r}')$ = velocity of the "face" of source "B" as a function of position, \vec{r}' .

And provided the acoustic pressure over the face of the transducer acting as a receiver is uniform, we are able to write the following form of the statement of acoustic reciprocity:

$$\frac{1}{\rho_{AB}(\vec{r})} \int_{\text{source "B"}} \vec{u}_B(\vec{r}') \cdot \hat{n} dS_B = \frac{1}{\rho_{BA}(\vec{r})} \int_{\text{source "A"}} \vec{u}_A(\vec{r}) \cdot \hat{n} dS_A \quad \text{Equation 1.13}$$

When only simple sources are involved and each integral of the normal component of the velocity over the face of the source is replaced by the respective volume velocity this becomes,

$$\frac{\dot{U}_B}{\rho_{AB}} = \frac{\dot{U}_A}{\rho_{BA}} \quad \text{Equation 1.14}$$

This is analogous to Rayleigh's statement:

"....the vibration excited at A will produce at B the same relative amplitude and phase as if the places were exchanged." [Ref. 13]

The principle of acoustic reciprocity will now be applied to electroacoustic transducers so that we can obtain what is termed a *reciprocity calibration* of the microphone open circuit receiving sensitivity.

D. ACOUSTIC RECIPROCALITY CALIBRATIONS OF MICROPHONE SENSITIVITY

1. General Acoustic Reciprocity Calibration of Electroacoustic Transducers

When we describe the general properties of a simple source it is often correct to consider the simple source as a linear two port electroacoustic network [Ref. 20],

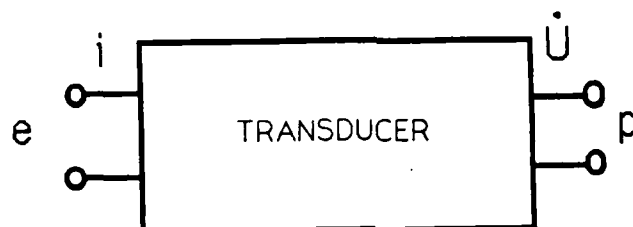


Figure 1.2 Electro-Acoustic Two Port Network.

From Foldy and Primakoff [Refs. 20, 21], the equations describing the relationship between the open circuit receiving voltage, e , the pressure at the receiver surface, $p(\vec{r})$, the transmit current, i , and the transmitter normal velocity, $\vec{u}_n(\vec{r})$, at the face of the transducer are,

$$\begin{aligned}
 e &= [Z_B]i + \int_{\text{SURFACE}} h'(\vec{r}') \vec{u}_n(\vec{r}') d\vec{r}' \\
 p &= [h(\vec{r})]i + \int_{\text{SURFACE}} Z(\vec{r}, \vec{r}') \vec{u}_n(\vec{r}') d\vec{r}'
 \end{aligned}$$

Equations 1.15

The reciprocity relations that are required of any transducer used in a reciprocity calibration are [Ref. 21]:

$$\frac{h(\vec{r})}{h(\vec{r}')} = e^{i\alpha} ; \quad \alpha \text{ A real function, NOT dependent upon } \vec{r}.$$

$$Z(\vec{r}, \vec{r}') = Z(\vec{r}', \vec{r})$$

Equations 1.16

The variables used above are defined by L.L. Foldy and H. Primakoff to be [Ref. 21]:

- Z_B = the blocked electrical impedance of the transducer
- $h(\vec{r})$ = the speaker transfer impedance
- $h'(\vec{r}')$ = the microphone transfer impedance
- $Z(\vec{r}, \vec{r}')$ = the generalized open circuit normal acoustic impedance of the transducer surface.

The first equation simply states that the speaker transfer impedance and the microphone transfer impedance are equal in magnitude and the phase angle between them is the same at all points of the transducer surface.

When equations 1.15 are recast in matrix form, $h(\vec{r})$ and $h'(\vec{r}')$ are equal to Z_{21} and Z_{12} respectively, the generalized acoustic impedance is constant over the transducer's surface and is replaced with Z_{22} , the integrals of the normal velocity over the transducer surface are replaced by the volume velocity \dot{U} , and Z_b is replaced with Z_{11} .

$$\begin{bmatrix} e \\ p \end{bmatrix} = \begin{bmatrix} Z_{11} & Z_{12} \\ Z_{21} & Z_{22} \end{bmatrix} \begin{bmatrix} i \\ \dot{U} \end{bmatrix}$$

Equations 1.17

In particular, with the voltage-pressure and current-volume velocity formulation shown above, if Z_{12} equals $(+,-)Z_{21}$ then the transducer is said to be a reciprocal(+) or an antireciprocal(-) transducer [Ref. 22]. The impedances are now described by:

Z_{11} = open circuit voltage / short circuit current

Z_{12} = open circuit voltage / volume velocity

Z_{21} = received acoustic pressure / short circuit current

Z_{22} = received acoustic pressure / volume velocity

When two such transducers are connected by an acoustic medium, a four port network will represent the system,

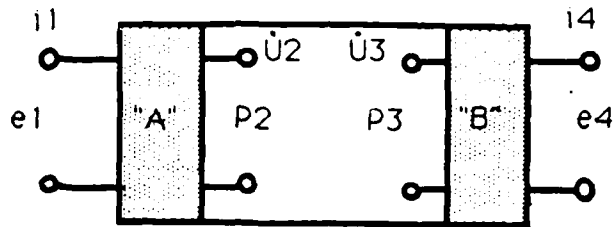


Figure 1.3 Four Port Electro-Acoustic Network

If we choose all the receiving sensitivities to be the open circuit voltage receiving sensitivities and all the transmitting sensitivities to be the current transmitting sensitivities, we have the following definitions:

$$M_A = e_1 / p_2$$

Equation 1.18

$$S_A = p_3 / i_1$$

Equation 1.19

$$M_B = e_4 / p_3$$

Equation 1.20

$$S_B = P_2 / i_4$$

Equation 1.21

Dividing equation 1.18 by 1.19 we obtain,

$$\frac{M_A}{S_A} = \frac{e_1 i_1}{P_2 P_3}$$

Equation 1.22

and dividing equation 1.20 by equation 1.21, we obtain,

$$\frac{M_B}{S_B} = \frac{e_4 i_4}{P_3 P_2}$$

Equation 1.23

Where we define:

e_1 = open circuit voltage at port (1) when transducer "B" is transmitting.

i_1 = input current at port (1) when transducer "A" is transmitting.

P_2 = acoustic pressure at port (2) when transducer "B" is transmitting.

P_3 = acoustic pressure at port (3) when transducer "A" is transmitting.

e_4 = open circuit voltage at port (4) when transducer "A" is transmitting.

i_4 = input current at port(4) when transducer "B" is transmitting.

Now, if both of the transducers and the medium are "reciprocal", meaning that $Z_{12}=Z_{21}$, $Z_{23}=Z_{32}$, and $Z_{34}=Z_{43}$, the equations representing the reciprocal system are,

$$\begin{bmatrix} e_1 \\ e_4 \end{bmatrix} = \begin{bmatrix} Z_{11} & Z_{14} \\ Z_{41} & Z_{44} \end{bmatrix} \begin{bmatrix} i_1 \\ i_4 \end{bmatrix}$$

Equations 1.24

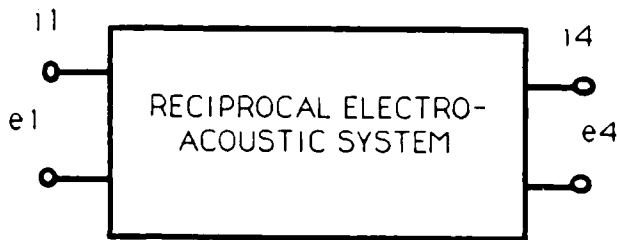


Figure 1.4 Reciprocal Electro-Acoustic System

By definition, e_1 and i_1 do not coexist in time. Similarly, e_4 and i_4 do not coexist in time. Thus if 1 receives when 4 transmits,

$$e_1 = \cancel{[Z_{11}]}(0) + [Z_{14}][i_4]$$

Equation 1.25

and when 1 transmits and 4 receives,

$$e_4 = [Z_{41}][i_1] + \cancel{[Z_{44}]}(0)$$

Equation 1.26

If the network described by equation 1.22 is reciprocal or antireciprocal, then $Z_{14} = (+) Z_{41}$ so that,

$$\frac{e_1}{i_4} = (+) \frac{e_4}{i_1}$$

Equation 1.27

This is the electrical analog of Rayleigh's statement of acoustical reciprocity [Ref. 14]. Substituting this into equations 1.22 and 1.23 we obtain,

$$\frac{M_A}{S_A} = \frac{e_1 i_1}{P_2 P_3} = \frac{e_4 i_4}{P_3 P_2} = \frac{M_B}{S_B}$$

Equation 1.28

Following L.L. Beranek [Ref. 9] and R.J. Bobber [Ref. 10] we define this ratio as the reciprocity factor, "J" and we have,

$$\frac{M_A}{S_A} = \frac{M_B}{S_B} \equiv J \quad \text{Equation 1.29}$$

Provided that the medium and both transducers are reciprocal, and if both transducers are *ideal*, we have shown that the reciprocity factor "J" depends only upon the medium (including its boundaries) and is independent of the transducers used.

To obtain a comparison between the two transducer's receiving sensitivities, a separate sound source is used to generate the same acoustic pressure that in turn is sampled at the same position by each of the receiving microphones. The ratio of the received voltages yields the desired comparison.

$$P(\text{same}) = \frac{V_A}{M_A} = \frac{V_B}{M_B} \quad \text{Equation 1.30}$$

V_a and V_b are the open circuit receiving voltages of transducers "A" and "B" respectively when the third separate sound source is transmitting. Equations 1.29 and 1.30 yield two expressions for M_a which we multiply together to obtain the square of the open circuit receiving sensitivity for transducer A.

$$(M_A)^2 = \left(M_B \frac{V_A}{V_B} \right) (S_A J) \quad \text{Equation 1.31}$$

Applying the definitions of S_a and M_b found in equations 1.19 and 1.20, we obtain the solution for the open circuit receiving sensitivity for microphone "A".

$$M_A = \left(\frac{e_4}{i_1} \frac{V_A}{V_B} J \right)^{1/2} \quad \text{Equation 1.32}$$

Using a similar procedure for transducer "B" we obtain,

$$M_B = \left(\frac{e_1}{i_4} \frac{V_B}{V_A} J \right)^{1/2} \quad \text{Equation 1.33}$$

If the voltages and currents in equations 1.32 and 1.33 can be measured, the only parameter remaining to be calculated in order to obtain a complete solution for the receiving sensitivities M_a and M_b is the reciprocity factor, "J". The physical meaning of the reciprocity factor "J" will be explained in the next section.

2. General Determination of The Reciprocity Factor, "J"

When the dimensions of the reciprocity factor, "J" are considered, we find that it can be interpreted as having dimensions of volume velocity over pressure. This is an acoustic admittance. After Rudnick [Ref. 1], we proceed to determine the solution for the reciprocity factor by considering as our reversible transducer one that is small compared to a wavelength, and is so noncompliant that its introduction at a point in the sound field never alters the sound pressure at that point. By the same token, when used as a speaker its volume velocity is independent of the acoustic load. Let both transducers be identical and of this type. The restriction that they be identical can be lifted trivially by the introduction of a third receiver as was done previously in the development of equation 1.30. For "A" transmitting and "B" receiving we obtain, using equations 1.17 for transducer "A",

$$\begin{aligned} e_1 &= Z_{11} \dot{U}_1 + Z_{12} \dot{U}_2 \\ 0 &= Z_{21} \dot{U}_1 + Z_{22} \dot{U}_2 \end{aligned} \qquad \text{Equations 1.34}$$

The second equation has a zero on the left because there is no impressed pressure and the *ideal* transducer does not feel the pressure that is self generated. For transducer "B" we

have,

$$e_4 = \cancel{z_{44}}(0) + z_{43} \dot{u}_3$$

$$p_3 = \cancel{z_{34}}(0) + z_{33} \dot{u}_3$$

Equation 1.35

since we have identical transducers in this example,

$$\frac{e_4}{p_3} = M_B = M_A = \frac{z_{12}}{z_{22}} = \frac{z_{43}}{z_{33}}$$

Equation 1.36

and,

$$S_A = \frac{p_3}{i_1}$$

Equation 1.37

We solve the second equation in 1.34 for the current, i_1 ,

$$i_1 = - \frac{z_{22}}{z_{21}} \dot{u}_2 = - \frac{\dot{u}_2}{M_A}$$

Equation 1.38

Substituting the result for i_1 into equation 1.37 and

manipulating the terms, we obtain equation 1.39 and thereby have shown that the reciprocity factor "J" is the acoustic transfer admittance.

$$\frac{M_{A,B}}{S_{A,B}} = - \frac{\dot{U}_2}{P_3} = - \frac{\dot{U}_3}{P_2} \quad \text{Equation 1.39}$$

Since the acoustic transfer admittance depends upon the medium through which the acoustic signal moves, and on the boundaries of this medium, the solutions obtained for the microphone voltage receiving sensitivities will only be valid if the medium and its boundaries are unchanged over the duration of the experimental measurements.

When setting out to calculate an analytical form for the reciprocity factor, different geometries of the medium between the two transducers will result in apparent differences in the forms found for "J". However, as mentioned earlier, it is important to note that (to within a multiplicative constant) all of these solutions for "J" will have the same form; The product of a volume and a frequency divided by the adiabatic bulk modulus of elasticity for the medium. To show this, three different "volumes" as shown in figure 1.1 will be utilized. For a gas medium, the adiabatic bulk modulus is expressed as the product of the

barometric pressure and the ratio of specific heats. Short descriptions of the dimensions involved in these different physical environments follow:

Volume 1: All dimensions are much smaller than the acoustic wavelength [Refs. 3, 9, 12].

Volume 2: Free field [Refs. 4, 5, 7, 8, 9, 10, 11].

Volume 3: One dimension is greater than or equal to half an acoustic wavelength with the other two dimensions smaller than an acoustic wavelength (cylindrical cavity) [Refs. 1, 2].

The solutions to be obtained for "J" in the next section will allow the equations for M_a and M_b to be defined in terms of basic electrical and physical measurements.

a. The Calculation of "J" for a Pressure Coupler
Reciprocity Calibration

For all dimensions much smaller than an acoustical wavelength, "volume 1" in the previous section, the magnitude and phase of the pressure will be essentially the same everywhere within the cavity. Using the adiabatic form of the ideal gas law,

$$pV^\gamma = \text{CONSTANT}$$

Equation 1.40

we take the natural log of both sides and differentiate,

$$\frac{dp}{p} + \gamma \frac{dV}{V} = 0$$

Equation 1.41

If the acoustic pressure is harmonic then it can be written as,

$$dp = p = p_0 e^{j\omega t}$$

Equation 1.42

then considering the change in acoustic pressure with respect to time,

$$\frac{dp}{dt} = j\omega p \quad \text{Equation 1.43}$$

Recognizing that the volume velocity may be expressed as the time rate of change of the volume we can write the time derivative of equation 1.41 as,

$$\frac{j\omega p}{\rho_0} + \gamma \frac{\dot{V}}{V_0} \cong 0 \quad \text{Equation 1.44}$$

consequently,

$$\frac{\dot{V}}{V_0} = \frac{-j\omega V_0}{\gamma \rho_0} \quad \text{Equation 1.45}$$

This is the reciprocity factor for a "small" cavity. Without any manipulation it is seen to follow the general form given earlier for "J".

b. The Calculation of "J" for a Free Field Reciprocity Calibration

For the free field we make use of equation 1.14 which shows that the ratio of the acoustic pressure at the face of a transducer acting as a receiver to the volume velocity of that transducer acting as a source is the same for any simple source. We are therefore able to choose a simple sphere to represent the source. It can be shown [Ref. 11: p. 164], that for an oscillating sphere of radius "a", where "a" is much less than a wavelength, we have,

$$p(r,t) = j\rho_0 c u_0 \left(\frac{a}{r}\right) (ka) e^{j(\omega t - kr)} \quad \text{Equation 1.46}$$

The volume velocity for the simple spherical source will be,

$$\dot{Q} = (4\pi a^2) u_0 e^{j\omega t} \quad \text{Equation 1.47}$$

Combining equations 1.46 and 1.47 to obtain a form of the acoustic transfer admittance, we have,

$$\frac{\dot{U}}{P} = \frac{4\pi r e^{j(kr - \pi/2)}}{\rho_0 c k}$$

Equation 1.48

substituting,

$$k = \frac{2\pi}{\lambda}$$

Equation 1.49

we obtain for the magnitude of the free field reciprocity factor "J",

$$\frac{\dot{U}_3}{P_2} = \frac{2\lambda r}{\rho_0 c}$$

Equation 1.50

When the numerator is multiplied by the wavelength, and the denominator is multiplied by the phase speed divided by the frequency, we see that,

$$\frac{\dot{U}_3}{P_2} = \frac{2f[\lambda^2 r]}{\rho_0 c}$$

Equation 1.51

This also is the general form given earlier for "J", where the effective volume is a rectangular solid with length and width equal to a wavelength and a height of $2r$.

c. The Calculation of "J" for The Plane Wave Resonant Reciprocity Calibration

To illustrate the final case where the acoustic wavelength is much larger than two dimensions and equal to or smaller than twice the third dimension of the cavity, a plane wave cylindrical resonator is used. For this case, the reciprocal transducers are mounted in the ends.

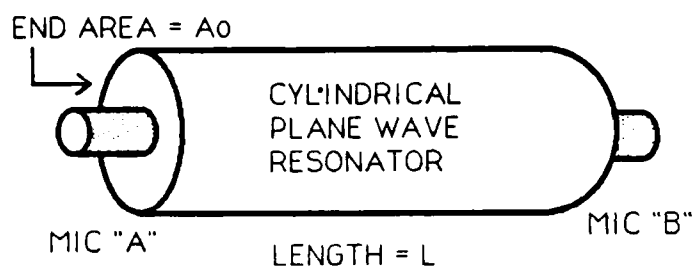


Figure 1.5 A Cylindrical Plane Wave Resonator

Solutions of the wave equation within such a cavity predict three kinds of resonance modes; radial, azimuthal, and longitudinal. When the dimensions of the cylinder are chosen so that the lowest azimuthal and radial resonance modes occur at frequencies *higher* than the highest longitudinal resonance in the frequency range of interest,

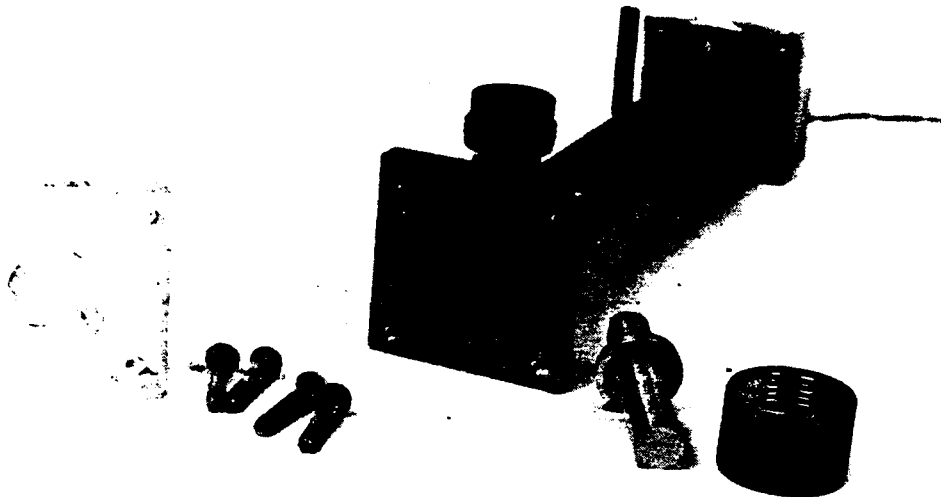
then below this frequency, only longitudinal (or plane wave) resonances can occur. For a cavity with rigid walls and ends, the pressure field within the resonant cavity is given by,

$$p(r, \theta, z) \propto \frac{\cos(m\theta)}{\sin} \cos\left(\frac{\omega_z z}{c}\right) J_m\left(\frac{\omega_r r}{c}\right) e^{j\omega t} \quad \text{Equation 1.52}$$

Here, $J_m()$ refers to a cylindrical Bessel function and not to the reciprocity factor.

From Morse [Ref. 22: p.398], the ratio of the fundamental azimuthal mode to the fundamental longitudinal mode is found to be .586 times the length to radius ratio of the cylindrical cavity. The ratio of the fundamental radial mode to the fundamental longitudinal mode is found to be 1.22 times the length to radius ratio of the cylindrical cavity. A photograph of the cylindrical plane wave resonant cavity used to experimentally observe the different resonant modes is shown next. All three different modes are then seen in figure 1.6, as a relative plot of the microphone voltage output vs frequency. A Knowles Type BT-1751 subminiature transducer acted as the microphone and was mounted on the curved wall of the 23.3 cm long cylindrical

cavity shown in the photograph. The source was a W.E.640AA
condenser microphone, Serial #1248, mounted on one end.



Photograph 1.2 Right cylindrical resonant cavity
used to obtain the modal resonances shown in figure 1.6

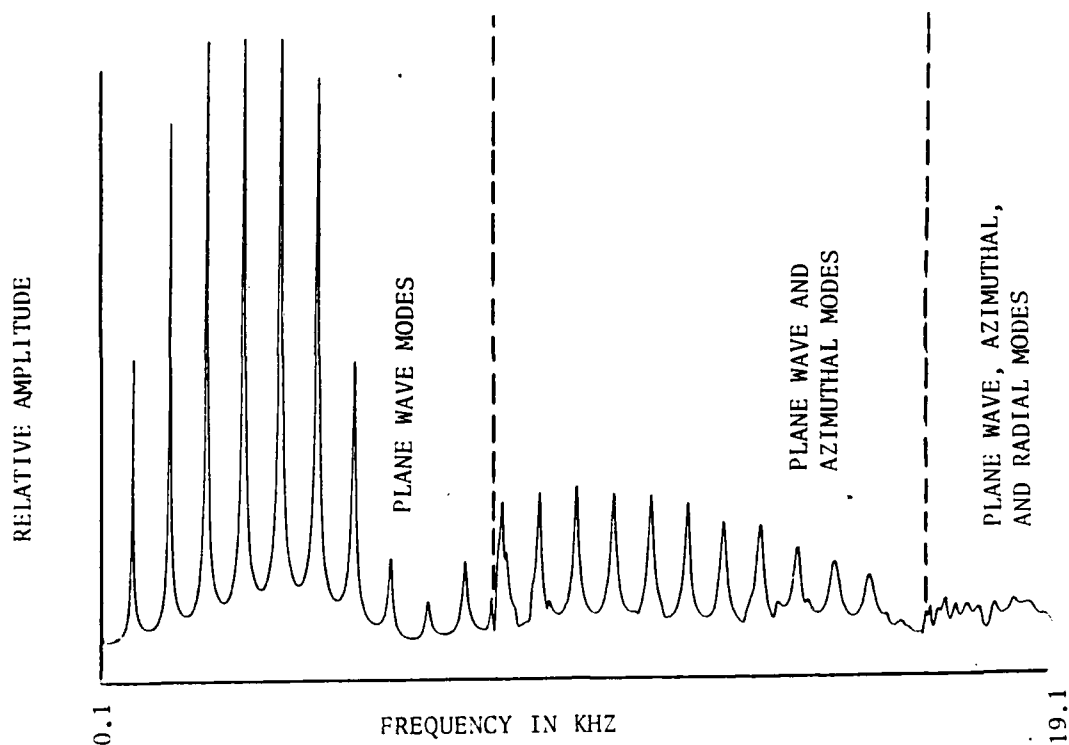


Figure 1.6 Modal resonances in a 23.3 cm, air filled brass pipe of 2.5 cm diameter at room temperature[22 deg C]

Following G.W. Swift, A. Migliori, S.L. Garrett, and J.C. Wheatley [Ref. 2], the calculation of acoustical transfer admittance is as follows:

The dot product of the acoustic particle velocity with both sides of the linearized Euler equation of motion yields,

$$\vec{u} \cdot \rho_0 \frac{\partial \vec{u}}{\partial t} = \vec{u} \cdot (-\nabla P)$$

Equation 1.53

Next, the equation of continuity of mass, written to first order in the acoustic density, is multiplied on both sides by the acoustic pressure,

$$\rho \left(\frac{1}{\rho_0 c^2} \right) \frac{\partial p}{\partial t} = \rho (-\nabla \cdot \vec{u}) \quad \text{Equation 1.54}$$

adding equations 1.53 and 1.54 we have,

$$\vec{u} \cdot \rho_0 \frac{\partial \bar{u}}{\partial t} + \frac{\rho}{\rho_0 c^2} \frac{\partial p}{\partial t} = \vec{u} \cdot (-\nabla p) + \rho (-\nabla \cdot \vec{u}) \quad \text{Equation 1.55}$$

this equation can be rewritten as,

$$\frac{\partial}{\partial t} \left(\frac{1}{2} \rho_0 \bar{u}^2 + \frac{p^2}{2 \rho_0 c^2} \right) = -\nabla \cdot (\rho \vec{u}) \quad \text{Equation 1.56}$$

This is an equation of continuity for energy density. The terms in the leftmost bracket are the kinetic energy density and the potential energy density respectively. The product

of acoustic pressure and acoustic particle velocity is the acoustic intensity. This equation is integrated over the volume within the resonant cavity to obtain,

$$\int_{VOL} \frac{\partial}{\partial t} \left(\frac{1}{2} \rho_0 u^2 + \frac{p^2}{2\rho_0 c^2} \right) dV = - \int_{VOL} \nabla \cdot (p\vec{u}) dV \quad \text{Equation 1.57}$$

Applying the divergence theorem to the right hand side of this equation and reversing the order of integration and differentiation on the left hand side, the equation becomes,

$$\frac{d}{dt} (E_{TOTAL}) = - \oint_{Surface} p \vec{u} \cdot \hat{n} ds \quad \text{Equation 1.58}$$

For plane waves at a longitudinal resonance, the acoustic pressure amplitude is uniform over each end of the cylindrical cavity. Additionally, with the *ideal* receiving microphone (the mechanical impedance is infinite), the integral of the normal component of the particle velocity over the rigid wall of the cavity volume is zero everywhere except on the surface of the source microphone,

$$\frac{d}{dt} [E_{\text{TOTAL}}] = - P_{\text{END}} \int_{\text{SOURCE FACE}} \vec{u} \cdot \hat{n} ds$$

Equation 1.59

Taking the average over one cycle yields,

$$-\frac{1}{T} \int_0^T \frac{dE_T}{dt} dt = \frac{1}{T} \int_0^T (P_{\text{END}} \dot{U}_{\text{END}}) dt$$

Equation 1.60

Here we have obtained the incremental change per cycle of the plane wave energy within the cavity due to the work per cycle done by the source microphone.

$$\Delta E = \frac{1}{f} \left[\frac{1}{T} \int_0^T (P_{\text{END}} \dot{U}_{\text{END}}) dt \right]$$

Equation 1.61

Within the cavity, the energy dissipated per cycle equals the work done per cycle to drive the source when a steady state longitudinal resonance is maintained. Thus, the change in the total plane wave energy available above as a result of the average work done by the source over one cycle must be the energy input per cycle required to sustain the

plane wave resonance. Here the energy dissipated per cycle is expressed in terms of the source pressure, the source volume velocity and the sound frequency.

If the velocity of the driving face is considered to be harmonic and if the acoustical system being driven is at a longitudinal resonance, then the acoustic impedance at the source is purely resistive and the particle velocity and acoustic pressure are in phase at the face of the driving transducer. In this case we have,

$$P_{END} = P_0 \cos(\omega t)$$

$$\dot{U}_{END} = \dot{U}_0 \cos(\omega t)$$

Equation 1.62

Now the energy per cycle required to sustain the resonance can be written as,

$$\frac{\Delta E}{\text{cycle}} = \frac{P_0 \dot{U}_0}{2f} = \frac{P_{rms} \dot{U}_{rms}}{f}$$

Equation 1.63

The terms for energy density found in equation 1.56 can now be used to calculate the total acoustical energy found within the cavity. Consider a differential volume of length

dx and cross sectional area equal to that of the cylinder located at position " x " within the tube.

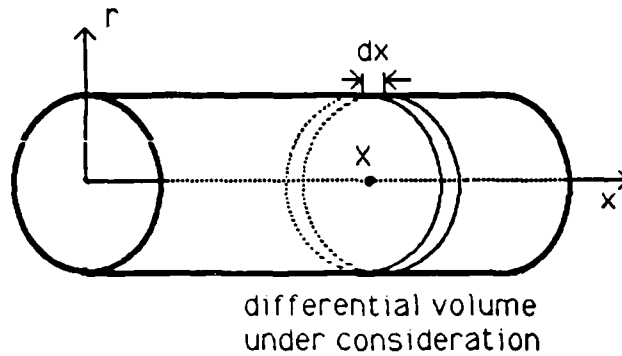


Figure 1.7 Differential volume under consideration

For rigid ends, the pressure standing waves due to longitudinal resonances within the cavity are given by,

$$P(x,t) = P_0 \cos(kx) e^{j\omega t}$$

Equation 1.64

From the linearized Euler equation in a medium with constant density we have,

$$\rho_0 \frac{\partial \vec{u}}{\partial t} = -\nabla P$$

Equation 1.65

Taking minus the gradient of equation 1.64 we obtain,

$$-\nabla p = p_0 k_n \sin(k_n x) e^{j\omega_n t} \quad \text{Equation 1.66}$$

Substituting into equation 1.65 and solving for the derivative of the particle speed with respect to time,

$$\frac{\partial u}{\partial t} = \frac{p_0 k_n}{\rho_0} \sin(k_n x) e^{j\omega_n t} \quad \text{Equation 1.67}$$

Integrating, we obtain the acoustic particle speed,

$$u(x,t) = \frac{p_0 k_n}{j\omega_n \rho_0} \sin(k_n x) e^{j\omega_n t} \quad \text{Equation 1.68}$$

Keeping the real part of the complex acoustic particle speed we have,

$$u(x,t) = \frac{p_0}{\rho_0 c_0} \sin(k_n x) \sin(\omega_n t)$$

Equation 1.69

From equation 1.64 the real part of the complex acoustic pressure is,

$$p(x,t) = p_0 \cos(k_n x) \cos(\omega_n t)$$

Equation 1.70

The total mechanical energy within the differential volume shown is the sum of the differential kinetic energy and the differential potential energy contained within.

$$dE_T = dE_{KE} + dE_{PE}$$

Equation 1.71

The differential kinetic energy from equation 1.56 is given by,

$$dE_{KE} = \frac{1}{2} \rho_0 u^2 A_0 dx$$

Equation 1.72

and the differential potential energy from equation 1.56 is given by,

$$dE_{P.E.} = \frac{\rho^2}{2\rho_0 c^2} A_0 dx \quad \text{Equation 1.73}$$

Combining equations 1.69, 1.70, 1.72 and 1.73, the differential of the total mechanical energy of the standing waves within the small slice of volume is obtained,

$$dE_T = \frac{1}{2} \rho_0 \left[\frac{\rho_0}{\rho_0 c_0} \sin(k_0 x) \sin(\omega_0 t) \right]^2 A_0 dx + \frac{1}{2} \frac{1}{\rho_0 c_0^2} \left[\rho_0 \cos(k_0 x) \cos(\omega_0 t) \right]^2 A_0 dx \quad \text{Equation 1.74}$$

Integrating over the cavity volume we obtain the integral form of the total mechanical energy within the plane wave resonant cavity,

$$E_T = \frac{\rho_0^2 A_0}{2\rho_0 c_0^2} \int_{x=0}^{x=h} \left[\sin^2(k_0 x) \sin^2(\omega_0 t) + \cos^2(k_0 x) \cos^2(\omega_0 t) \right] dx \quad \text{Equation 1.75}$$

For rigid ends within the plane wave cavity, the modal wave number is,

$$k_N = \frac{N\pi}{L} \quad \text{Equation 1.76}$$

Upon substitution into equation 1.75 and integration we obtain,

$$E_T = \frac{P_o^2 A_o L}{4 \rho_o c_o^2} \quad \text{Equation 1.77}$$

Using the root mean square value for the acoustic pressure,

$$E_T = \frac{P_{rms}^2 A_o L}{2 \rho_o c_o^2} \quad \text{Equation 1.78}$$

Where "Q" is the quality factor of the plane wave longitudinal resonance we have [Ref. 11],

$$\frac{E_T}{\Delta E/\text{cycle}} = \frac{Q}{2\pi} \quad \text{Equation 1.79}$$

we can substitute the values previously determined to obtain,

$$\frac{Q_N}{2\pi} = \frac{\left(\frac{P_{RMS}^2 A_0 L}{2 \rho_0 c_0^2} \right)}{\left(\frac{P_{RMS} \dot{L}_{RMS}}{f_N} \right)} \quad \text{Equation 1.80}$$

From the ideal gas equation of state, we have,

$$\rho_0 \gamma = \rho_0 c_0^2 \quad \text{Equation 1.81}$$

Since at a longitudinal resonance in a plane wave resonant cavity with rigid ends, the pressures at each end are equal in magnitude, we can write for the magnitude of the acoustical transfer admittance of the plane wave resonator,

$$\frac{\dot{L}_3}{P_2} = \frac{\pi V_0 f_N}{\rho_0 \gamma Q_N} \quad \text{Equation 1.82}$$

Inasmuch as the quality factor for the Nth resonance is dimensionless and is computed from a set of basic electrical measurements at frequencies in the vicinity of resonance, we have once again the general form given earlier for "J".

The complete representation of the reciprocity equations which may be considered for experimental implementation in all three different geometries will next be summarized.

3. A Summary of The Three Reciprocity Methods Compared in This Experiment

a. Plane Wave Resonant Reciprocity Calibration

For the case of the plane wave resonant cavity reciprocity calibration, we can combine equations 1.32 and 1.82 to obtain,

$$M_A = \left(\frac{e^4 V_A \pi V_o f_N}{i l V_B \rho_o \gamma Q_N} \right)^{1/2} \quad \text{Equation 1.83}$$

This is the *initial* form of the solution for the open circuit voltage receiving sensitivity found using the plane wave resonant reciprocity method of microphone calibration. In chapter II, the difficulties associated with experimentally obtaining the required measurements of the basic electrical and physical parameters used in the above equation will be addressed.

b. Free Field Reciprocity Calibration

For the case of the free field reciprocity calibration, equations 1.32 and 1.50 yield,

$$M_A = \left(\frac{e_4 V_A 2\lambda r}{i_1 V_B \rho_0 c_0} \right)^{1/2} \quad \text{Equation 1.84}$$

This is the solution for reciprocity calibration that was initially obtained by W.R. MacLean [Ref. 4] and independently by R.K. Cook [Ref. 5] in 1940.

c. Pressure Coupler Reciprocity Calibration

Finally, for the case of the pressure coupler reciprocity calibration, combining equations 1.32 and 1.45 we obtain,

$$M_A = \left(\frac{e_4 V_A}{i_1 V_B} \frac{2\pi f V_0}{\rho_0 \gamma} \right)^{1/2} \quad \text{Equation 1.85}$$

With these pedagogical solutions for the open circuit receiving sensitivity complete, we are now able to consider the form of the solution shown in equation 1.83 with regard to the experimental methods used to obtain the basic electrical and physical measurements which, when substituted into equation 1.83, ultimately yield M_A .

II. EXPERIMENTAL CONSIDERATIONS FOR A RESONANT RECIPROCITY CALIBRATION

A. INTRODUCTION

The form of the equations derived in Chapter I for the microphone open circuit voltage receiving sensitivity found using the method of plane wave resonant reciprocity was not optimized for experimental implementation. Consider the following equations:

$$M_A = \left(\frac{e_1 V_A \pi V_0 f_w}{i_1 V_B \rho_0 \gamma Q_N} \right)^{1/2}$$

Equations 2.1

$$M_B = \left(\frac{e_1 V_B \pi V_0 f_w}{i_1 V_A \rho_0 \gamma Q_N} \right)^{1/2}$$

To reduce the amount of experimental error introduced by the method of the experiment, it is useful to consider the impact of practical considerations upon the analytical form of equations 2.1. Therefore, the following questions will be addressed in this chapter:

1. How can the ratio V_A/V_B best be measured to reduce experimental error?

2. How can a self consistency check on the experimental results be incorporated into the experiment?
3. Is it possible to reduce the number of basic electrical measurements experimentally made?
4. What is the correction required in the experimentally obtained value for the open circuit voltage receiving sensitivity as a result of the non-ideal character of the compliant microphones used in the experiment?

Additionally, the experimental measurement of the quality factor of the n th resonance can be very difficult to obtain with any accuracy. Only with the experiment under computer control using a technique such as that developed by D.V. Conte and S.L. Garrett [Ref. 23] or by J.B. Mehl [Ref. 24] is this source of error reduced.

With these considerations in mind, we will proceed in the development of the equations required to experimentally measure the open circuit voltage receiving sensitivity of a microphone using the method of absolute plane wave reciprocity calibration.

B. DEVELOPMENT OF THE EXPERIMENTAL PLANE WAVE RECIPROcity EQUATIONS USING CYLINDRICAL GEOMETRY

1. Experimental Considerations

When the method to be used in measuring the ratio V_a/V_b is considered, two basic approaches are possible. In the first, the voltage ratio is measured as an experimental event unique unto itself. The final result is the ratio V_a/V_b . The difficulties associated with this experimental approach are primarily related to the difficulty to be found in the *precise repositioning* of the microphones on one end of the resonant cavity to obtain the same reference pressure generated by a source at the other end. It is preferable to design a "hands-off" experiment that will eliminate the introduction of any such re-positioning error and will allow computer control of all the experimental measurements including those used to determine the quality factor, Q . When the reference source is mounted at a third port in the wall of the resonant cavity, the "hands-off" experiment is possible. However, there already exist two such sources of sound within the resonant cavity in the form of the reciprocal transducers mounted at each end. An experimentally productive alternative is to mount instead, a receiving microphone as a reference in the third port. It will be shown that by mounting a reference microphone in the wall of the resonant cavity, not only will we be able to

measure the ratio V_a/V_b , but we can also obtain a comparison calibration of the reference microphone and a six way round-robin self consistency check of the experimental precision of the calibration for each mode. The calibrations of microphone receiving sensitivities so obtained will be as follows:

- Ma - based upon absolute plane wave reciprocity.
- Mb - based upon absolute plane wave reciprocity.
- Mca - A comparison calibration of the reference microphone based upon the absolute reciprocity calibration of microphone A.
- Mcb - A comparison calibration of the reference microphone based upon the absolute reciprocity calibration of microphone B.
- Mab - A comparison calibration of microphone A based upon the absolute reciprocity calibration of microphone B.
- Mba - A comparison calibration of microphone B based upon the absolute reciprocity calibration of microphone A..

The modifications required for equations 2.1 which yield an analytical solution for resonant plane wave reciprocity sensitivity calibrations and which use a reference receiver mounted in the wall of the resonant cavity will now be derived.

When the development of the four port acoustical reciprocity network is expanded to include the comparison microphone mounted in the side of the cylinder, some

modifications to the analytical development for the solution of M_a are necessary. Consider figure 2.1 below.

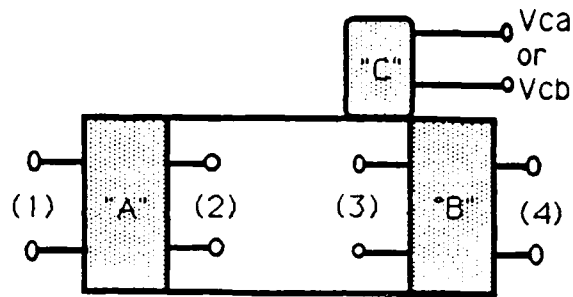


Figure 2.1 Modified four port network.

The relationships between the receiving and transmitting sensitivities for the two reciprocal microphones mounted on the ends can still be represented as before,

$$M_A = S_A J$$

$$M_B = S_B J$$

Equations 2.2

To obtain a comparison between transducer "A" and transducer "B" with the geometry shown above, it is necessary to relate the pressure at the face of microphone "C" to the pressure

at each end. Thus, when "A" is transmitting,

$$M_c = \frac{V_{CA}}{P_{CA}}$$

Equation 2.3

and when "B" is transmitting,

$$M_c = \frac{V_{CB}}{P_{CB}}$$

Equation 2.4

At a longitudinal plane wave resonance, the rms acoustic pressure at the right end of the cavity can be related to the rms pressure "felt" by the comparison microphone, with a pressure standing wave correction factor, $G_1(n)$, which depends upon the frequency of the plane wave resonance, and the position of the comparison microphone in the tube.

$$P_{CA} = [P_3] [G_1(n)]$$

Equation 2.5

The pressure standing wave correction factor, $G_1(n)$ is obtained by spatially averaging the longitudinal variations

in acoustic pressure at a plane wave resonance over the face of the reference microphone assuming the microphone sensitivity is independent of position over the face.

It is worth noting that even though the comparison calibration of the microphone "C" sensitivity obtained with the previous assumption may be in error, this assumption has no effect upon the measurement of the absolute sensitivity of microphones "A" and "B". Refer to figure 2.2.

$$[P_3] G_1(\omega) = \left[\frac{2 P_0}{\text{MIC AREA}} \right] \int_{x=a}^{x=b} \left[\cos\left(\frac{\omega T x}{L}\right) \right] \left[\left(\frac{b-a}{2}\right)^2 - \left(x - \frac{b+a}{2}\right)^2 \right]^{1/2} dx \quad \text{Equation 2.6}$$

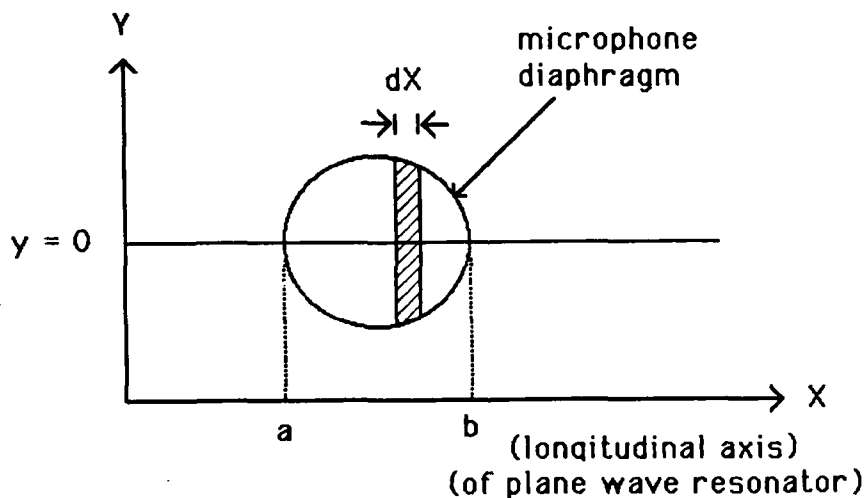


Figure 2.2 Geometry of the offset microphone used in the calculation of $G_1(\omega)$.

In the figure above, the curvature of the sides is not involved since the spatial variation of the acoustic pressure occurs only in the longitudinal direction at a plane wave resonance.



Photograph 2.1 In this photograph, the "ports" for the comparison microphone are mounted on the side wall of the cylinder

The side wall mounts in the "long" tube were unused in the final experimental measurements since there was room to mount the Knowles subminiature transducers in the ends alongside the one inch condenser microphones. The side wall

mounts in the above photograph are entirely functional and were used in preliminary experiments using electret and dynamic microphones. In the "short" tube, the side wall mounts were necessary when a 1/2 inch microphone was used as the comparison microphone.

To evaluate the relationship between the pressures at the two ends of the resonant cavity consider the general solution for standing plane waves in a cylinder driven at the left end at $X=0$ by transducer "A", with mechanical impedance Z_{ma} , and terminated at the right end at $X=L$ by transducer "B", with mechanical impedance Z_{mb} . The acoustic pressure in the cylindrical cavity can be represented as the superposition of a left going wave and a right going wave and will then be of the form,

$$P(x,t) = A e^{j(\omega t + k[L-x])} + B e^{j(\omega t - k[L-x])}$$

Equation 2.7

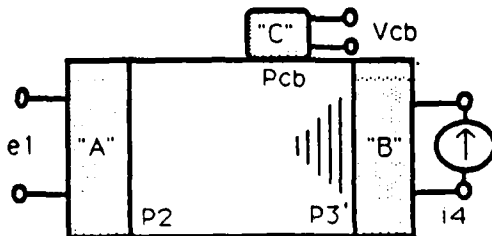
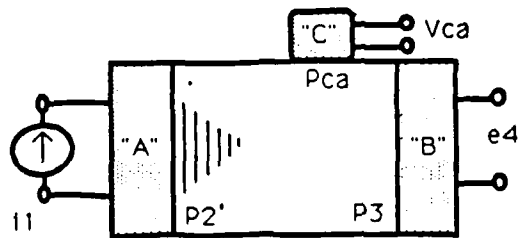


Figure 2.3 Scheme used to obtain comparison voltages.

Referring to figure 2.3 above, when microphone "A" is used as the source, the ratio of the pressure at $X=0$, (P_2') to the pressure at $X=L$, (P_3), will be,

$$\frac{P_2'}{P_3} = \frac{Ae^{jkl} + Be^{-jkl}}{A + B} \quad \text{Equation 2.8}$$

Since the force on the termination is pressure times the cross sectional area and the particle speed for a plane acoustic wave is given by,

$$u = - \frac{1}{\rho_0} \int \frac{\partial P}{\partial x} dt$$

Equation 2.9

We can use the definition for mechanical impedance to solve for the ratio of A/B in equation 2.8. For the microphone mounted in a rigid end, the mechanical impedance will be in general,

$$Z = \frac{\text{force APPLIED}}{\text{resulting speed.}}$$

Equation 2.10

which upon substitution of equations 2.7 and 2.9 into equation 2.10 at $x = L$, becomes,

$$Z_{mB} = \rho_0 c A_B \left(\frac{A + B}{A - B} \right)$$

Equation 2.11

Where A_B is the cross sectional area of microphone B. Solving for the ratio A/B we obtain,

$$\frac{A}{B} = \frac{Z_{mB} + \rho_0 c A_B}{Z_{mB} - \rho_0 c A_B}$$

Equation 2.12

Substituting into the equation for P_2'/P_3 we obtain,

$$\frac{P_2'}{P_3} = \cos(kL) + j \left[\frac{\rho_0 c A_B}{Z_{mB}} \right] \sin(kL) \quad \text{Equation 2.13}$$

Where P_2' is the pressure at $x=0$, and P_3 is the pressure at $x=L$ when transducer "A" is transmitting. With a similar but symmetrical development with transducer "B" transmitting we obtain,

$$\frac{P_3'}{P_2} = \cos(kL) + j \left[\frac{\rho_0 c A_A}{Z_{mA}} \right] \sin(kL) \quad \text{Equation 2.14}$$

Where P_3' is the pressure at the right end and P_2 is the pressure at the left end when transducer "B" is transmitting. Considering the previous sketch of the two different situations, the open circuit receiving sensitivity for microphone C can be found in each case,

$$M_C = \frac{V_{CA}}{P_{CA}} = \frac{V_{CB}}{P_{CB}} \quad \text{Equation 2.15}$$

When the standing wave scale factor is used to express the pressure at the offset comparison microphone as a function of the pressure at the end for both values of M_c , we have,

$$\frac{V_{CA}}{P_3 G_1(N)} = \frac{V_{CB}}{P_3' G_1(N)} \quad \text{Equation 2.16}$$

Solving for the pressure ratio as a function of wavenumber,

$$\frac{P_3}{P_2} = \frac{V_{CA}}{V_{CB}} \left[\cos(kL) + j \frac{\rho_0 c A_A}{Z_{MA}} \sin(kL) \right] \quad \text{Equation 2.17}$$

This pressure ratio will allow the ratio M_a/M_b to be expressed in terms of voltage ratios alone, provided the term in the brackets in equation 2.17 is equal to unity. If kL is equal to some multiple of π , as it is with perfectly rigid ends, then this assertion is correct. Experimentally, the deviation of the value of kL from an exact multiple of π is determined at a plane wave resonance by examining the harmonicity of the modal resonances in the plane wave resonant cavity. [See Appendix A.] If they are multiples of

the fundamental then KL will be a multiple of pi with $\sin(KL)=0$ and $\cos(KL)=(+-)1$. From the theory shown in Appendix A., the values of KL at resonance are exact multiples of pi only in the case of a perfectly rigid boundary or in the limit when the frequency goes to infinity. When the fundamental of the highest plane wave resonant frequency measured was calculated and compared to the lowest plane wave resonant frequency, the ratio so found was an estimate of how close the worst case KL came to being an exact multiple of pi. As shown in Appendix A., the worst case occurred as expected at the lowest plane wave resonance. In this worst case, the value of KL was measured as $.9927*\pi$, to four significant figures. Since the voltage ratio used in equation 2.18 comes in under the square root in the calculation for microphone sensitivity, the value of unity for $\cos(KL)$ will introduce an approximate .001 db re 1 V/ubar worst case error. Since other experimental uncertainties will be shown to be larger than this value by at least one order of magnitude, equation 2.17 will be used in the form shown below.

$$\frac{P_3}{P_2} = \frac{V_{CA}}{V_{CB}}$$

Equation 2.18

AD-A164 149

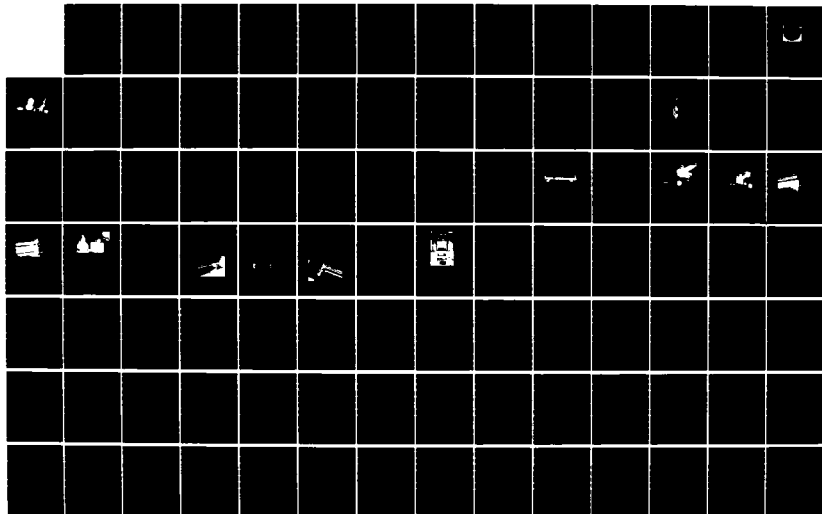
RECIPROCITY CALIBRATION IN A PLANE WAVE RESONATOR(U)
NAVAL POSTGRADUATE SCHOOL MONTEREY CA C L BURMASTER
DEC 85 NPS61-86-006

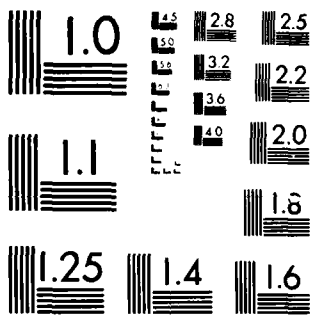
2/5

UNCLASSIFIED

F/G 14/2

NL





MICROCOPY RESOLUTION TEST CHART
NATIONAL BUREAU OF STANDARDS 1963-A

Now the ratio of M_A/M_B becomes,

$$\frac{M_A}{M_B} = \left(\frac{e_1}{P_2} \right) \left(\frac{P_3}{e_4} \right) = \left(\frac{e_1}{e_4} \right) \left(\frac{V_{CA}}{V_{CB}} \right) \quad \text{Equation 2.19}$$

Combining Equations 2.2 and 2.19 we obtain for the square of M_A ,

$$M_A^2 = \left[M_B \left(\frac{e_1}{e_4} \right) \left(\frac{V_{CA}}{V_{CB}} \right) \right] \left[S_A J \right] \quad \text{Equation 2.20}$$

When the definitions for S_A and M_B are substituted into equation 2.20 and we solve for M_A , we obtain,

$$M_A = \left(\frac{e_1}{i_1} \frac{V_{CA}}{V_{CB}} J \right)^{1/2} \quad \text{Equation 2.21}$$

Similarly,

$$M_B = \left(\frac{e_4}{i_4} \frac{V_{CB}}{V_{CA}} J \right)^{1/2} \quad \text{Equation 2.22}$$

By using the reciprocity relationship; $e_{41} = e_{14}$, we can eliminate the requirement to experimentally measure i_4 ,

$$M_B = \left(\left(\frac{e_4}{e_1} \right) \left(\frac{e_4}{i_1} \right) \left(\frac{V_{CB}}{V_{CA}} \right) J \right)^{1/2} \quad \text{Equation 2.23}$$

Having considered the practical consequences and experimental advantages of the method chosen to measure V_a/V_b , the consequences of a compliant microphone with regard to the calculation of the voltage ratio representing M_a/M_b , and having just reduced the number of basic electrical measurements required by one, consideration must now be given to the experimental determination of the reciprocity factor, "J". Consider the form of the acoustic transfer admittance derived in Chapter 1.

$$J = \left[\frac{\pi V_0 f_N}{\rho_0 \gamma Q_N} \right] \quad \text{Equation 2.24}$$

The temperature, pressure and density of the medium within the resonant cavity were found to vary over the duration of

the experiment. Since the reciprocity factor "J" represents the acoustical transfer admittance of the medium within the resonant cavity during the measurement of parameters used to calculate a plane wave resonance reciprocity calibration, some modification in the value used for "J" must be made to properly account for medium changes. When "A" is transmitting this becomes,

$$\frac{U_2}{P_3} = \frac{\pi V_0 f_N}{\rho_0 \gamma Q_{ATBR}} \quad \text{Equation 2.25}$$

Where the subscripts "ATBR" stand for "A transmitting and B receiving". When "B" is transmitting we obtain,

$$\frac{U_3}{P_2} = \frac{\pi V_0 f_N}{\rho_0 \gamma Q_{BTAR}} \quad \text{Equation 2.26}$$

Where the subscripts "BTAR" stand for "B transmitting and A receiving". Now Equations 2.21 and 2.25 are used to obtain the open circuit receiving sensitivity for transducer "A".

$$M_A = \left(\frac{e_1 V_{CA} \pi V_0 f_N}{i_1 V_{CB} \rho_0 \gamma Q_{ATBR}} \right)^{1/2} \quad \text{Equation 2.27}$$

Similarly, equations 2.23 and 2.26 are used to obtain the open circuit receiving sensitivity for transducer "B".

$$M_B = \left(\frac{e_4 e_4 V_{CB} \pi V_0 f_N}{e_1 i_1 V_{CA} \rho_0 \gamma Q_{STAR}} \right)^{1/2} \quad \text{Equation 2.28}$$

Equations 2.27 and 2.28 are the solutions we set out to obtain for a plane wave reciprocity calibration which uses a reference microphone mounted in a third port in the resonant cavity.

It is experimentally significant that the solutions for M_a and M_b using the method of plane wave reciprocity appear to be independent of the position used for the mounting of the reference microphone within the resonant cavity when in fact they are not. This is because it is possible to select a location for the reference microphone in the wall of the plane wave resonant cavity that will cause large experimental errors to occur in the solutions for M_a and M_b . Additionally, the error in the absolute calibration will cause any comparison calibration made *in situ* and based upon the absolute reciprocity calibration to be in error as well. These sources of potential error and the solutions

devised to avoid them will be discussed in the next section.

2. Two Comparison Calibrations for Microphone "C"

The need for a six way round-robin *in situ* experimental check on the precision of each modal calibration requires careful consideration of the experimental methods and calculations used to obtain any calibrations of the reference microphone. From an analytical point of view, two comparison calibrations of the reference microphone can be obtained that are based upon the absolute reciprocity solutions for M_a and M_b . Combining the reciprocity calibration obtained for M_a , the definition of M_c , and the pressure standing wave correction factor, we obtain M_c as a function of M_a and refer to this calibration as M_{cA} .

$$M_{cA} = \left(\frac{M_a}{e_1} \right) \left(\frac{V_{cB}}{G_1(N)} \right) \quad \text{Equation 2.29}$$

Similarly, using the reciprocity calibration for M_b we obtain,

$$M_{cB} = \left(\frac{M_b}{e_4} \right) \left(\frac{V_{cA}}{G_1(N)} \right) \quad \text{Equation 2.30}$$

The difference in these two values for M_c is a measure of the experimental precision obtained.

With regard to the reference microphone, two different sizes and positions were used at different times. The first reference microphone was a B&K type 4134 condenser microphone which had a 1/2 inch diameter while the second was a Knowles subminiature transducer type BT-1751 with an outside diameter of .055 inches. In separate configurations, both were used initially in the side of the cylindrical resonant cavity. The final configuration used the type BT-1751 mounted adjacent to the one inch WE640AA. This position was used in the larger cavity where the cavity inner diameter was sufficiently large to accommodate both microphones in the end cap. Experimental considerations yield two pragmatic reasons for selecting the end mounting in preference to the side mounting. When the cylindrical plane wave resonant cavity is driven at a longitudinal resonance, the standing waves within such a cavity, (when the ends are ~ rigid) will vary as $\cos(Kx)$, where x gives the longitudinal position, K equals $n\pi/L$, n is the mode number, and L is the length of the cylindrical cavity. At the fundamental mode, there will exist an acoustic standing wave pressure node at $x = L/2$. When higher modal resonances occur, there will be "n" nodes found along the longitudinal axis of the tube. *If the location of the reference*

microphone is at one of these pressure nodes, then no comparison voltages representing M_a/M_b can be obtained for that frequency. Additionally, if the microphone is mounted in the end, $G_1(n)$ becomes identically one, otherwise, there is a finite error associated with the calculation of $G_1(n)$ for any reference microphone position. While the end mounting removes the problem of finding a node at the reference microphone's position and the inaccuracies associated with computing $G_1(n)$, an additional but removable problem arises. The placement of the reference microphone in the end of the cavity next to one of the reciprocal microphones will cause a decrease in the acoustical impedance at that end. For a given source strength, this will result in a decrease in the signal amplitude for the larger microphone. This situation will appear to yield a lower sensitivity calibration for the reciprocal microphone than that obtained in the absence of the immediate presence of the reference microphone. If the reciprocity calibration on which the comparison calibration is based is taken from the microphone mounted separately, this potential error is avoided.

An estimate of the magnitude of this effect can be made by comparing the volume velocity in this problem to the analogous current in an electrical circuit. Because the transverse dimensions in the end are much less than a

wavelength, the lumped parameter analogy to the electrical circuit is possible. When the reciprocal microphone is alone in one end, mounted in the rigid supporting wall, then the volume velocity through the plane of this end occurs only as a result of the motion of the diaphragm of this microphone. This is analogous to a current source providing all its output to a single impedance placed across its output terminals. When the additional reference microphone "C" is introduced adjacent to the reciprocal microphone "B", the situation is analogous to the electrical current source having a second impedance placed in parallel across the first. When this is done, by current division, the magnitude of the current through the first impedance is reduced. Referring to equation 1.35, it is seen that the open circuit signal voltage is directly proportional to the volume velocity of the microphone. Since the magnitude of the signal voltage is one of the measured electrical parameters used in the calculation of M_b , the value so obtained for M_b is lower than that obtained when only microphone "B" is mounted in the end. Since the change in the calculated microphone sensitivity is found to be proportional to the change in the acoustical impedance in the end of the cavity, the relative change in acoustic impedance is used to approximate the relative change in the calculated microphone sensitivity.

$$\frac{\Delta Z}{Z} = \left(\frac{Z_B - \frac{Z_B Z_C}{Z_B + Z_C}}{Z_B} \right) = \frac{\Delta M}{M} \quad \text{Equation 2.31}$$

If the assumption of rigid walls is correct and if there are no leaks in the mountings used for the microphones, and if the transverse dimensions of the microphones are much less than a wavelength, then the solution above is valid. To obtain an estimate of the magnitude of the relative change in sensitivity, consider the following: Since both transducers are operating well below their respective mechanical resonances, they are both operating in the stiffness control region. The stiffness of the volume of the Knowles subminiature transducer is modeled as that of a small Helmholtz resonator [Ref. 11: p.226], and the stiffness of a W.E.640AA condenser microphone is well known in published literature [Ref. 3: p. 32]. When the mechanical impedance found using the stiffness is divided by the square of the cross sectional areas, the resulting acoustical impedances can be substituted into equation 2.31 to yield,

$$\frac{\Delta M}{M} \approx 1 - \frac{\left(\frac{\rho_0 c^2}{V_0 (\text{KNOWLES})} \right)}{k (640AA) + \left(\frac{\rho_0 c^2}{V_0 (\text{KNOWLES})} \right)} \quad \text{Equation 2.32}$$

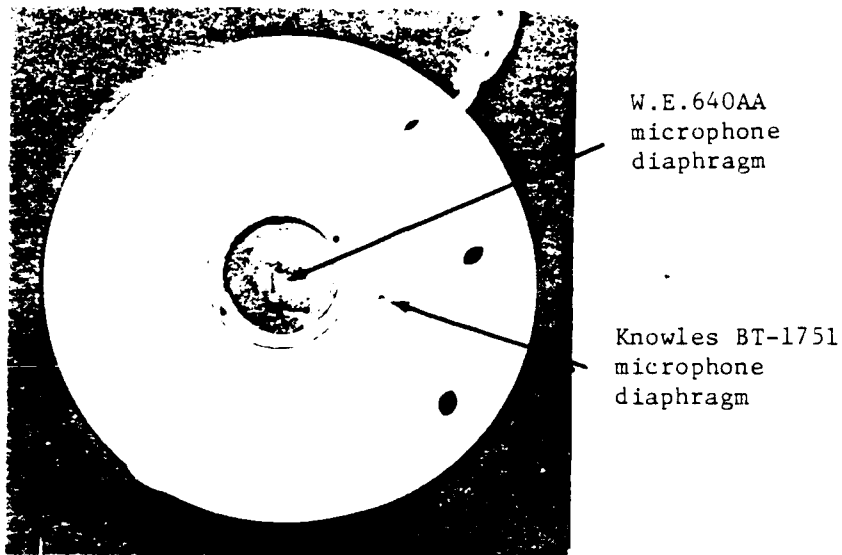
Since the volume within the Knowles subminiature microphone has roughly the same dimensions as the neck of the Knowles subminiature type BT-1751 transducer which is cylindrical in shape with a neck diameter of 1.4mm and a neck length of 1.57mm, and the acoustic impedance of a W.E.640AA condenser microphone is $\sim 1.64E+12 \text{ NM}^{-5}$ (the stiffness of the 640AA) divided by the angular frequency, [Ref: 3: p.32] substitution into equation 2.32 using a density of 1.21 kg/M^3 and a sound speed of 343 m/s yields,

$$\frac{\Delta M}{M} \cong 0.027$$

Equation 2.33

This corresponds to an expected decrease of 0.24 db re 1v/ubar in the calculated microphone "B" sensitivity when microphone "C" is mounted alongside. Experimentally, a decrease of 0.22 (+-)0.10 db re 1v/ubar was obtained by comparing the first ten plane wave reciprocity modal calibrations for W.E. 640AA serial#815 with and without the Knowles type BT-1751 subminiature reference transducer mounted alongside. With this observed change, care must be made in the comparison calculations for M_c , to use only the

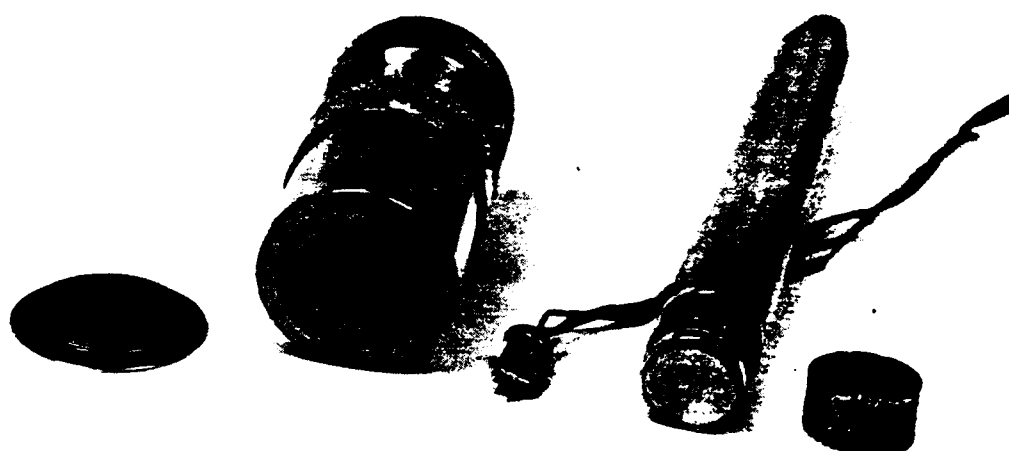
reciprocity calibrations obtained where the reciprocal microphone is mounted alone. The next two photographs show the relative sizes of the microphones involved in the calibration experiment.



Photograph 2.2 The relative sizes of the Knowles subminiature transducer mounted alongside the one inch condenser microphone.

In the photograph above, the relative position of the small Knowles subminiature transducer is approximately at the "three o'clock" position relative to the one inch WE640AA condenser microphone. The end mount shown here was intended for use only in the larger (~70 cm) plane wave resonant cavity. The inner diameter of the smaller (~23 cm) plane wave cavity did not allow sufficient room for both to be mounted in the same end. As previously described, the

acoustic impedance in the end of the resonant cavity is slightly changed when the subminiature transducer is included alongside the larger one inch condenser microphone.



Photograph 2.3 The relative size of the Knowles subminiature transducer alongside both a one inch WE640AA and a one half inch General Radio microphone.

In this photograph, the previous end mounting is removed and the microphone casings and diaphragms are visible. The subminiature transducer's FET preamplifier (inherent to the "type BT-1751" as obtained from the manufacturer) is in the extended case behind the neck and opening leading to the diaphragm. It is this portion that was previously modeled

as a small Helmholtz resonator to estimate the change in acoustic impedance at the end.

To complete the data required for a six way round robin check on the experimental precision for each modal calibration, we will next consider the comparison calibration of each reciprocal microphone based upon the absolute reciprocity calibrations already obtained for Ma and Mb.

3. The Comparison Calibration of Microphones "A" and "B" With Respect to Each Other

In order to complete the six way round robin comparison check on the experimental precision, comparison calibrations of the reciprocal microphones based upon each other are needed for each modal calibration. Refer to Equation 2.18, which gives the ratio M_A/M_B . Solving in turn for each open circuit receiving sensitivity we obtain,

$$M_{AB} = M_B \left(\frac{e_1}{e_4} \right) \left(\frac{V_{CA}}{V_{CB}} \right) \quad \text{Equation 2.34}$$

and,

$$M_{BA} = M_A \left(\frac{e_4}{e_1} \right) \left(\frac{V_{CB}}{V_{CA}} \right) \quad \text{Equation 2.35}$$

The apparent change in sensitivity for microphone "B" resulting from the change in acoustical impedance at the end containing both microphones as described in the previous section, will not adversely effect the round robin precision of an individual modal calibration. The values of M_{BA} and M_{AB} shown above are still based upon e_4 , the measured signal

voltage of microphone "B". As such, the value for M_{ba} will still be the "same" as that found for M_b . Similarly, M_{ab} will be the "same" as M_a since while the apparent value of M_b goes down as a result of the change in the acoustical impedance, the ratio of e_1/e_4 will go up a proportionate amount. The relative precision of the experiment is determined by computing either $(M_a - M_{ab}) / (M_a + M_{ab})$, $(M_b - M_{ba}) / (M_b + M_{ba})$, or $(M_{ca} - M_{cb}) / (M_{ca} + M_{cb})$. All three computations result in the same value of the experimental precision.

While the equations developed for M_a , M_b , M_{ca} , M_{cb} , M_{ab} and M_{ba} will allow a six way round robin consistency check of the experimental precision for each modal plane wave resonance, there remains one simplifying assumption upon which these equations are based, that remains to be discussed. This is the assumption, necessary for the solution for "J" given in Chapter I, that the microphones used "feel no impressed pressure". When the solution for "J" is modified to account for a microphone with a finite mechanical impedance, a correction to the solutions for M_a and M_b is required. This is the subject of the next section.

C. THE IMPRESSED PRESSURE CORRECTION

When the acoustic transfer admittance that is used in the reciprocity calibration was derived in chapter 1, the derivation was unique to a microphone that felt *no impressed pressure*. The assumption of "zero pressure sensitivity" was then incorporated in equations 1.34. This was the same as saying that the mechanical impedance of the microphone was infinite. However, real microphones have a finite mechanical impedance and the effect of this finite impedance upon the reciprocity calibration must be considered. Refer to figure 2.4 for an illustration of two different but reciprocal condenser microphones mounted in the ends of a plane wave resonant cavity.

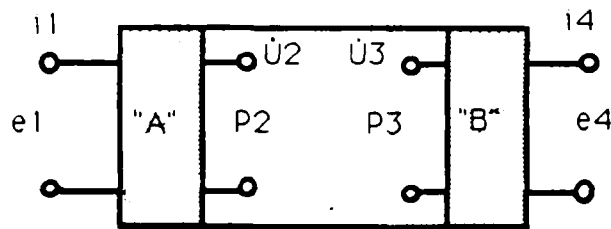


Figure 2.4 Reciprocal microphones mounted in the ends of a plane wave resonator

Referring to Equations 1.17, with interpretation of the coefficients as shown by Beranek [Ref.9:p.117] for the general case of both acoustical and electrical excitation, we can write for each reciprocal microphone,

$$\begin{array}{l}
 V_1 = (Z_{11})(i_1) + (b)(\dot{U}_2) \\
 P_2' = (b)(i_1) + (Z_{22})(\dot{U}_2)
 \end{array}
 \left. \vphantom{\begin{array}{l} V_1 \\ P_2' \end{array}} \right\} \begin{array}{l} \text{ACTING AS} \\ \text{A SOURCE} \end{array}$$

$$\begin{array}{l}
 e_1 = (Z_{11})(\dot{U}_1) + (b)(\dot{U}_2) \\
 P_2 = (b)(\dot{U}_1) + (Z_{22})(\dot{U}_2)
 \end{array}
 \left. \vphantom{\begin{array}{l} e_1 \\ P_2 \end{array}} \right\} \begin{array}{l} \text{ACTING AS} \\ \text{A RECEIVER} \end{array}$$

Equations 2.36

- Where:
- $Z_{12} = Z_{21} = b$, the transduction coefficient.
 - V_1 = voltage across the transducer's electrical terminals when the transducer is used as a speaker.
 - i_1 = current flowing in the transducer when it is used as a speaker.
 - P_2' = pressure at the speaker end of the resonant cavity when the driving frequency is at a longitudinal resonance.
 - e_1 = open circuit receiving voltage.
 - P_2 = acoustic pressure at face of receiving microphone.
 - \dot{U}_2 = volume velocity of speaker.
 - \dot{U}_2' = volume velocity of microphone.
 - Z_{11} = blocked electrical impedance plus the electrical load (or generator) impedance.
 - Z_{22} = the open circuit acoustical impedance plus acoustic radiation impedance as seen at acoustic port #2.

Dividing the third and fourth equations, we obtain for M_A ,

$$M_A = \frac{b}{Z_{22}}$$

Equation 2.37

Solving the second equation in equations 2.36 for i_1 ,

$$i_1 = \frac{p_2' - (z_{22}) \dot{u}_2}{b} \quad \text{Equation 2.38}$$

Substituting this value for i_1 into the definition for S_a we obtain,

$$S_A = \frac{P_3}{i_1} = \frac{P_3}{(p_2' - (z_{22}) \dot{u}_2) / b} \quad \text{Equation 2.39}$$

We now define the previously derived transfer admittance for the longitudinally resonant plane wave cavity to be,

$$J_0 = \left| \frac{\dot{u}_2}{P_3} \right| = \frac{\pi V_0 f_n}{\rho_0 \gamma_E Q_n} \quad \text{Equation 2.40}$$

Where "n" is the mode number of the longitudinal resonance. Since, J equals M_a/S_a and at resonance within the plane wave resonant cavity, P_2' and P_3 are equal in magnitude, equation

2.39 can be substituted into equation 1.29 and reduced to,

$$J = \left(\frac{-\dot{U}_2}{P_3} \right) \left\{ 1 - \frac{\left(\frac{1}{Z_{22}} \right) \left(\frac{P_2'}{P_3} \right)}{\left(\frac{\dot{U}_2}{P_3} \right)} \right\} \quad \text{Equation 2.41}$$

The first part of the above equation for the reciprocity factor "J", is the transfer impedance as derived in chapter one. Note however, that the assumption of a "rigid" ideal microphone is the same as stating that Z_{22} is infinite. In this ideal case, the correction term goes to zero without the assumption that P_2' is necessarily zero. In fact, in a plane wave resonant cavity, as previously shown in equation 2.13, this is not the case. With a finite impedance, it remains to be shown that the correction term multiplying $(-\dot{U}_2/P_3)$ is small. To do so requires the determination of the value of Z_{22} as shown in the canonical equations when the reciprocal microphone is terminated with an acoustic plane wave resonator.

The normal acoustic impedance (Z_{22}) is shown by Beranek [Ref.9:p.117] for the general case of simultaneous electric and acoustic excitation, as being equal to the sum of the open circuit normal acoustic impedance and the acoustic radiation impedance. In the case of plane wave resonant reciprocity, the resonant acoustic cavity can be shown to be

"loading" the faces of the microphones mounted at each end. This impedance load for the transducer attached to a plane wave tube is given by [Ref. 11: p.201]:

$$\frac{Z_{m0}}{\rho_0 c A_T} = \frac{\frac{Z_{mL}}{\rho_0 c A_T} + j \tan(k'L)}{1 + j \frac{Z_{mL}}{\rho_0 c A_T} \tan(k'L)} \quad \text{Equation 2.42}$$

where,

- Z_{m0} = mechanical impedance of the tube seen at $X=0$ in the plane wave resonant cavity.
- Z_{mL} = mechanical impedance at the $X=L$ termination.
- ρ_0 = gas density
- c = sound speed
- k = wavenumber $[w/c]$
- k' = complex wavenumber $[k - ja]$
- a = absorption coefficient
- L = length along the longitudinal axis of the resonator.
- A_T = cross sectional area of tube & diaphragm.

If the cavity is a multiple of a half wavelength and is made to resonate longitudinally, the value of kL has been shown (appendix A.) to be an integral multiple of π . Additionally, if there is a low loss (high Q) acoustic system so that hyperbolic sine and cosine are well represented by the first term in a series expansion, then the mechanical impedance looking into the resonant tube is approximately equal to the mechanical impedance found at the opposite end.

$$\frac{Z_{mo}}{\rho_0 c A_T} \cong \frac{\frac{Z_{mL}}{\rho_0 c A_T} + j \left(-j \frac{a c}{2 f_1} \right)}{1 + j \frac{Z_{mL}}{\rho_0 c A_T} \left(-j \frac{a c}{2 f_1} \right)} \cong \frac{Z_{mL}}{\rho_0 c A_T} \quad \text{Equation 2.43}$$

When this load impedance is added to the open circuit mechanical impedance of the microphone and then expressed in terms of acoustical impedances, we have for Z_{22} :

$$Z_{22} \cong \left[Z_A(x=0) + Z_A(x=L) \right] \quad \text{Equation 2.44}$$

When this interpretation of Z_{22} is combined with the results shown in equation 2.13, equation 2.41 is reduced to:

$$J \cong J_0 \left[1 - \frac{1}{Z_{22} J_0} \right] \quad \text{Equation 2.45}$$

The quantity J/J_0 is the ratio of the normal acoustic admittance of the microphone at acoustic port #2 to the acoustic admittance of the medium. When equation 2.45 is combined with equation 2.44, we see that the finite acoustic impedance of the transfer results in a

change in microphone sensitivity as compared to that expected for a perfectly rigid termination. If "Mao" is used to identify the magnitude of the open circuit receiving sensitivity calculated using equation 2.27, we have:

$$\frac{M_A}{M_{\neq 0}} = \left[1 - \frac{1}{Z_{22} \bar{J}_0} \right]^{\frac{1}{2}} \quad \text{Equation 2.46}$$

It is important to consider the acoustic system as a whole when the value of Z22 is determined. The following considerations are in addition to those previously presented where the diaphragm area is equal to the tube area.

When equations 2.36 were employed to determine the impressed pressure correction, the four port network used as the system model, required Z22 (or J22) to be associated with acoustic port #2. This means that the influence on Z22 of the difference in the cross section area of the tube and the area of the microphone diaphragm must also be considered. This difference in areas will act as an acoustic transformer and will serve to increase the acoustic impedance of that port over that which would occur if the tube and diaphragm areas were the same [Ref.9:p.125]. The multiplicative correction to Zmic that accounts for this increase in acoustic impedance at the end is the ratio of

the tube area to the diaphragm area. Consider the sequence of acoustic terminations shown in the next figure:

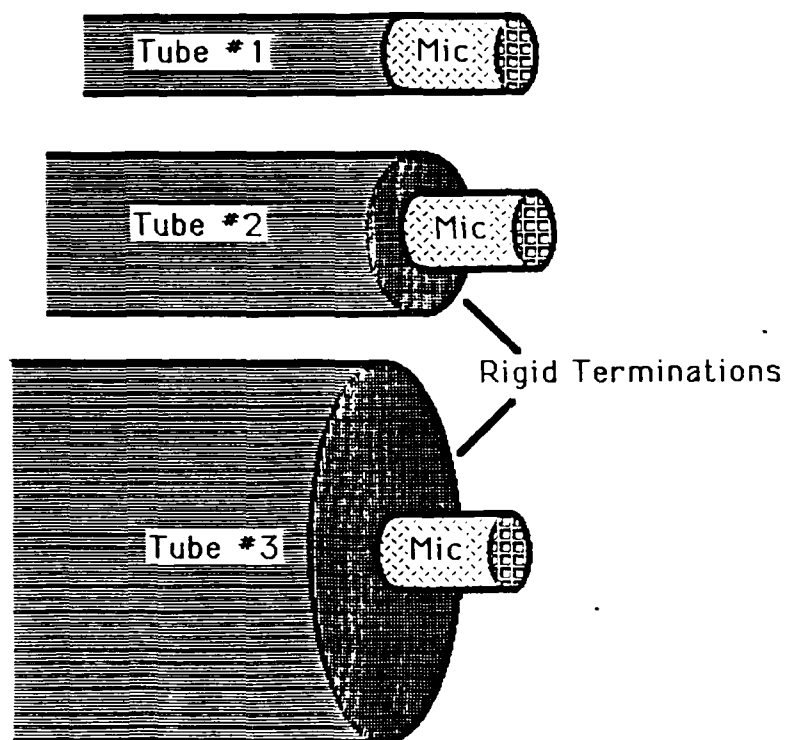


Figure 2.5 Different terminations for the plane wave tubes.

In the first tube, the area of the tube matches the area of the diaphragm. The acoustic impedance at the end of this tube is simply the acoustic impedance of the microphone. In the bottom tube, the majority of the end is a rigid wall. In this case, the limit of the acoustic impedance tends to infinity as the area of the large tube becomes much greater than the area of the diaphragm. While an experiment with

either the first or last situation is possible, it is the termination shown in tube #2 that is of practical interest in the plane wave resonant cavities used in this experiment. To illustrate the influence of the different terminations, the definition of mechanical impedance is applied to the acoustic port at the end of the tube,

$$Z_m(\text{end}) = \frac{\int_{\text{END}} p dA}{u} = \frac{P_{\text{END}} A_T}{u} \quad \text{Equation 2.47}$$

where: Z_m = mechanical impedance of the acoustic port at the end of the tube.
 P_{end} = acoustic pressure at the end of the tube.
 u = the resulting speed.
 A_T = cross section area at the end of the tube.

Since the only resulting speed at port #2 is that of the microphone diaphragm, and rewriting equation 2.47 in terms of the acoustic impedance of the microphone, we have:

$$Z_A(\text{END}) = \frac{\left[\frac{P_{\text{END}} A_d}{u} \right] \left[\frac{A_T}{A_d} \right]}{A_d^2} = Z_A(\text{mic}) \left[\frac{A_T}{A_d} \right] \quad \text{Equation 2.48}$$

where, A_d = cross section area of the diaphragm.
 Z_A = acoustic impedance.

When the effects of the acoustic transformer action due to the different areas (Beranek [Ref.9:p.125] and equation 2.48) and the loading due to longitudinal resonance (equation 2.43) are included in the value of Z_{22} ; and provided that the "non-diaphragm" areas in the ends are approximately rigid, then:

$$Z_{22} \cong \left[Z_A \left(\frac{A_T}{A_{dA}} \right) + Z_A \left(\frac{A_T}{A_{dB}} \right) \right] \quad \text{Equation 2.49}$$

It is this form of the value of Z_{22} that must be used in the computed correction to M_{ao} . To illustrate the magnitude of this correction, assume for simplicity that both microphones are identical and that the cross section area of the tube is equal to the diaphragm area. With these simplifying assumptions,

$$Z_{22} \cong 2 \left[R_A + j \left(\omega M_A - \frac{R_A}{\omega} \right) \right] \quad \text{Equation 2.50}$$

Where the subscript "a" refers to the lumped acoustical parameters associated with the microphone being considered. If the acoustical impedance of a microphone is known for the

frequency range of interest, $J_{22} = 1/Z_{22}$ can be calculated and the value of J_{22}/J_0 can be determined.

When the various reciprocity factors representing the different experimental geometries are examined, it is apparent that the magnitude of the impressed pressure correction will be different. Refer to equations 2.51 below.

$$J_0 \left(\begin{array}{l} \text{Pressure} \\ \text{coupler} \end{array} \right) = (2\pi V_0) \left(\frac{f_n}{\rho_0 \gamma_E} \right)$$

$$J_0 \left(\begin{array}{l} \text{PLANE} \\ \text{WAVE} \\ \text{RESONATOR} \end{array} \right) = \left(\frac{\pi V_0}{Q_n} \right) \left(\frac{f_n}{\rho_0 \gamma_E} \right)$$

Equations 2.51

$$J_0 \left(\begin{array}{l} \text{FREE} \\ \text{FIELD} \end{array} \right) = (2r\lambda^2) \left(\frac{f_n}{\rho_0 \gamma_E} \right)$$

The parameter values to be used for a rough numerical comparison are given below:

$R_a = 3.27E+7$ NSecM ⁻⁵	(acoustic resistance, [Ref. 3: p. 32] W.E.640AA)
$M_a = 4.77E+2$ KgM ⁻⁴	(acoustic mass [Ref. 3: p. 32])
$K_a = 1.64E+12$ NM ⁻⁵	(average acoustic stiffness [same ref])
$P_0 = 101330$ pa	(~atmospheric pressure)
$\gamma_E = 1.39$	(ratio of specific heats [Ref 25])
$f_n = 2450$ Hz	(10th modal resonance in long tube)
$c = 343$ M/sec	(phase speed in unbounded medium)
$r = .20 - .40$ M	(separation distances for free field)
$Q_n \sim 165$	(quality factor for 70 cm plane wave resonant cavity)
$V_0 \sim 6.498E-4$ M ³	(volume of plane wave resonant cavity)
$V_0 \sim 4.6E-7$ M ³	(volume of pressure coupler [Ref. 3: p.12])

The case of the pressure coupler is similar to that of the plane wave resonant cavity. In the first case, due to the small dimensions of the cavity, $KL \sim 0$, whereas in the plane wave resonant cavity $KL \sim N\pi$. In the case of the free field calibration, the correction must use a different value for $1/Z_{22}$. Substituting the appropriate values into equation 2.46 yields:

$$\frac{M_A}{M_{A0}} = \begin{cases} \sim .95, & \text{Pressure Coupler} \\ & (KL \ll 1) \\ \sim .99, & \text{Plane wave resonator} \\ & (KL = N\pi) \\ \sim 1.00, & \text{FREE field} \\ & (\text{variable } KL) \end{cases} \quad \text{Equations 2.52}$$

As expected, these quantitatively different results simply reflect the fact that the effect of the compliance of the acoustic system is the greatest in the small pressure coupler cavity, least in the free field geometry, and somewhere in between in the larger plane wave resonant cavity geometry. These fractional compliance corrections, if ignored, correspond to microphone sensitivity changes of $\sim -.45$, $\sim -.10$, and $\sim -.001$ db re 1V/ubar respectively.

Since the parameter values used to obtain this comparison are only approximate, a different method of computing "J22/Jo" will now be used in the case of a plane wave resonant cavity to obtain a further comparison.

Consider the analytical form of the transduction coefficient found in the literature for an condenser microphone when the open circuit mechanical impedance of the microphone is so much greater than the radiation impedance that the radiation impedance is negligible [Ref. 11: p350]:

$$b = \frac{C_0 E_0}{2 \pi f_n \epsilon_0 A_e A_d} \quad \text{Equation 2.53}$$

Where: C_0 = microphone capacitance.
 E_0 = condenser microphone bias voltage.
 f_n = modal frequency of resonance.
 ϵ_0 = permittivity of free space.
 A_e = the effective backplate area of the condenser microphone.
 and A_d = the diaphragm area of the microphone.

If we can include the influence of the acoustic load due to the plane wave resonant cavity in the above solution for the electroacoustic transduction coefficient, we can use the previous equation determined for "Jo" to obtain an analytical form for the ratio "1/Z22*Jo".

With constant environmental conditions (atmospheric pressure, temperature, humidity, and density) the absolute pressure sensitivity under open circuit electrical conditions is a property of the microphone [Refs. 3 and 29]. Under the free field conditions that result in the value for "b" shown above, the value of Z_{22} used in equation 2.37 is the open circuit acoustic impedance of the microphone. For identical microphones at each end of the plane wave resonant cavity, the invariance of M_a requires a $[2A_t/A_d]$ multiplicative correction to equation 2.53 to cancel a similar increase to the open circuit acoustic impedance as shown in equation 2.49. When this is done, the value of M_a calculated in equation 2.37 remains the same. The magnitude of the ratio " $1/Z_{22} \cdot J_0$ " becomes:

$$\frac{1}{Z_{22} J_0} = \frac{M_a \rho_0 \gamma_E \epsilon_0 A_e A_d^2 Q_N}{A_t C_0 E_0 V_0} \quad \text{Equation 2.54}$$

Since the quantities involved in equation 2.54 are known or can be experimentally measured, an estimate of the magnitude of this ratio and its effect upon the value computed for M_a can be made.

When the ratio "J22/Jo" is now calculated for the long tube and substituted into Equation 2.46, we obtain essentially the same result as calculated previously (~ 1 % relative change).

$$\frac{M_A}{M_{A0}} \cong 0.98, \text{ PLANE WAVE RESONATOR (RL=10\pi)} \quad \text{Equation 2.55}$$

These different impressed pressure corrections may be significant if calibration accuracies to within (+-) ~ 0.5 db re 1V/ubar or better are desired. A more careful comparison between experimental results obtained using different cylindrical dimensions for the plane wave resonator will be discussed in the chapter on experimental corrections. In these discussions the ratio of areas given by At/Ad will be included in the calculation of Z22.

III. EXPERIMENTAL PROCEDURES

A. INTRODUCTION

The experimental procedures and equipment required for two different methods of absolute reciprocity calibration of microphones are presented in this chapter. The method of primary interest was the plane wave resonant reciprocity calibration. The secondary free field comparison calibration, when corrected for diffraction [Ref. 3: p.31], was used as a low frequency consistency check for the results of the primary method.

The separate apparatus built for these two methods are described first. The resonant reciprocity part of the experiment used two different right circular cylindrical cavities to obtain a self consistency check on the associated plane wave resonant reciprocity calibrations. The free field calibration used a microphone translator that operated under computer control. Both methods used commercial electronics equipment which will be described in the appropriate section.

Following the description of the apparatus, the procedures and signalflow are presented for both calibration methods. Both a *plane wave resonant reciprocity calibration*

of a laboratory standard type W.E.640AA condenser microphone and a standard *free field reciprocity calibration* for an electrodynamic microphone are described. The free field reciprocity calibration of the electrodynamic microphone in turn yielded a *comparison calibration* of the previously calibrated W.E.640AA condenser microphone.

The basic experimental parameters obtained from measurements which occur in the experiment are; voltage, current, resistance, frequency, capacitance, temperature, length, barometric pressure, and relative humidity. The uncertainties in experimentally measured electrical and physical parameters are presented in an error analysis of these fundamental measurements. The propagation of error in the computed microphone open circuit voltage receiving sensitivity is then made resulting in an estimate of probable error. In addition, the experimental methods used to determine the system linearity, voltage transfer function(s), and the stability of different voltage amplifiers will be explained. Experimental procedures which result in a reduction of systematic error will be discussed whenever applicable. The final results for probable error will be summarized in the last section of this chapter.

B. EXPERIMENTAL APPARATUS

1. Plane Wave Resonant Cavities

Two differently dimensioned plane wave resonant cavities were built to measure the self consistency in the method of plane wave resonant reciprocity calibration. Since the calibrations occurred at frequencies corresponding to longitudinal resonances, the first cavity was made one third the length of the second. Thus, the frequency of every third longitudinal resonance in the "long" tube matched the frequency of a longitudinal resonance in the "short" tube.

For each plane wave resonant calibration, three microphones were required. In the final calibration configuration, only two different size microphones were used, although each right circular cylindrical cavity was made of brass with ports constructed for the mounting of three different sizes of microphones. Two, one inch diameter reciprocal W.E.640AA condenser microphones were mounted in the opposite ends of the cavity while a one eighteenth inch (1.41 mm) diameter comparison microphone was mounted in one end (for the long tube) or in the side of the cylinder wall (for the short tube). The comparison microphone was a Knowles type BT-1751 subminiature transducer which had a small preamplifier built into the transducer

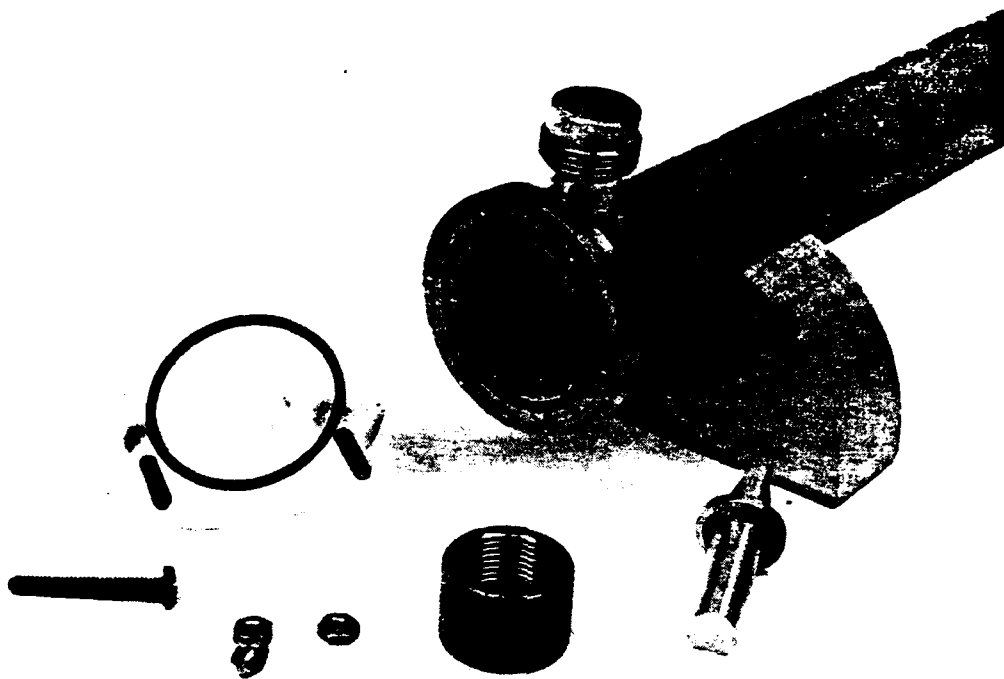
case. These brass tubes and the mounting ports for the various microphones are shown in the following photographs.



Photograph 3.1 The 70.12 cm brass tube used as a plane wave resonant cavity.

In this photograph, the left mount for the WE640AA microphone is dismantled and is shown in front of the tube. The tube itself is placed upon two wooden supports used for stability on the lab table. The rubber O-ring seal is easily seen in the dismantled mount and was provided for eventual calibrations in different gas media. The small pipe inlet in the center of the tube is intended for the

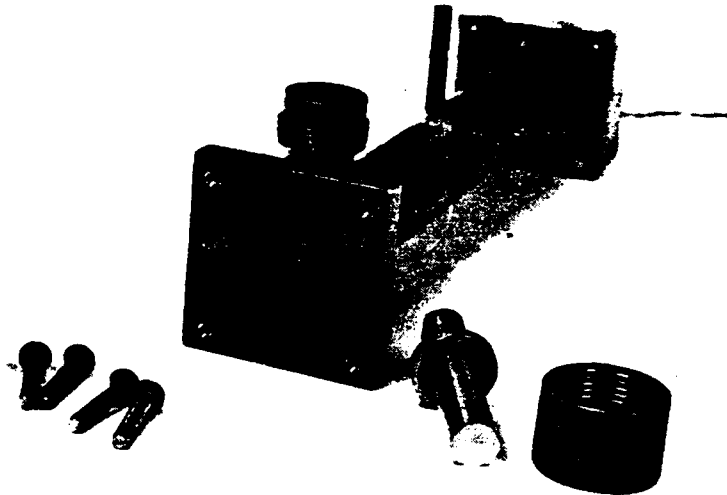
introduction of these different gases into the cavity. Since this capability was not employed in this experiment, the small hole intended as a gasport at the base of the center inlet pipe (radius $\sim .0004$ meters) served only to increase the acoustic losses during resonance measurements. The large ports for the 1/2 inch comparison microphones are easily seen towards each end of the tube and are shown closed with the brass plugs shown in greater detail in photograph 3.2.



Photograph 3.2 Mounting ports - end view

Here, one of the plexiglass mounts for the WE640AA 1 inch condenser microphone is shown dismantled. The port for the 1/2 inch comparison microphone is also shown in a dismantled state. The nuts and bolts used to fasten the mount and WE640AA to the end are nonconductive nylon. The O-ring seal and groove are easily seen. The markings shown inside the O-ring groove were used as reference marks for diameter measurements made using a calipers. In the final calibration configuration, the 1/2 inch microphone ports were sealed with the plug shown in the lower right

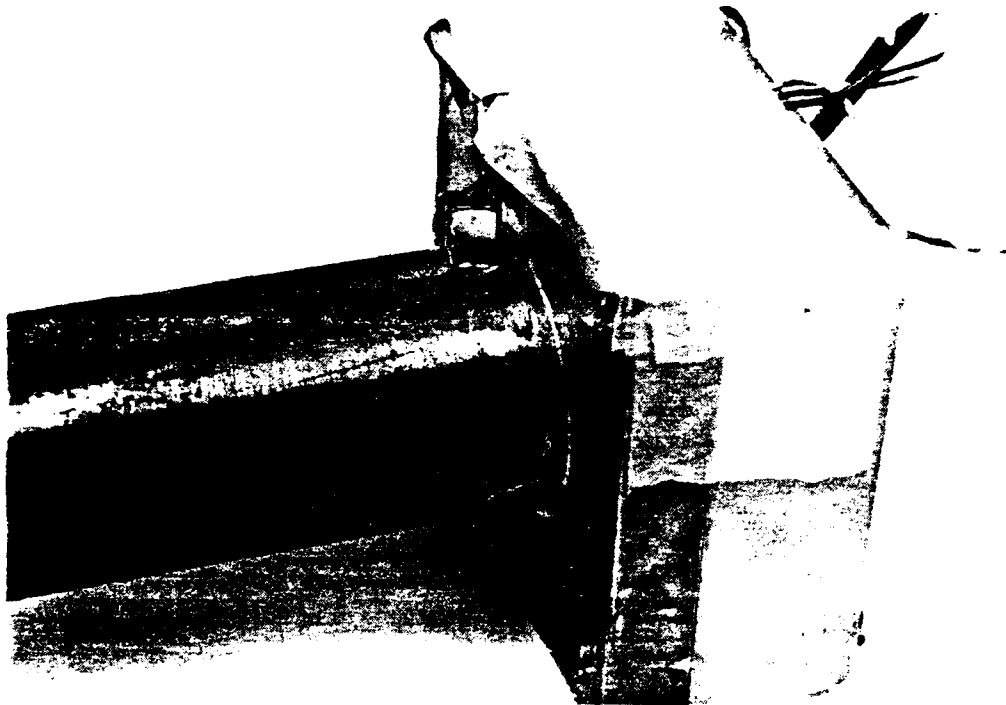
foreground of photograph 3.2 and a Knowles type BT-1751 subminiature transducer was mounted in the end, alongside the WE640AA condenser microphone.



Photograph 3.3 The "short" tube.

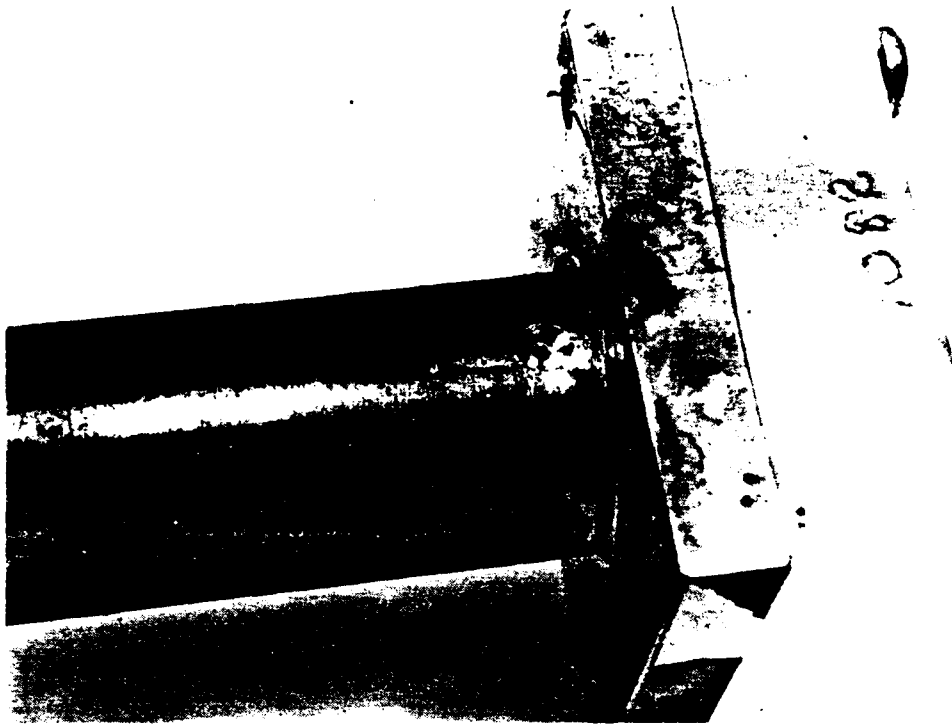
Here is an end view of the short plane wave resonant cavity. Both the 1 inch plexiglass mount and the 1/2 inch microphone mounts are removed. A gasport is placed in the center of the tube as it was with the long tube. During the final calibrations, the 1/2 inch microphone port was again plugged and the Knowles type BT-1751 subminiature transducer was mounted in the wall of the cylinder. Slightly out of focus, the Knowles subminiature can be seen at the far end

of the above photograph. The markings on the near end were used as references when the major and minor axes of each end were measured with a calipers.



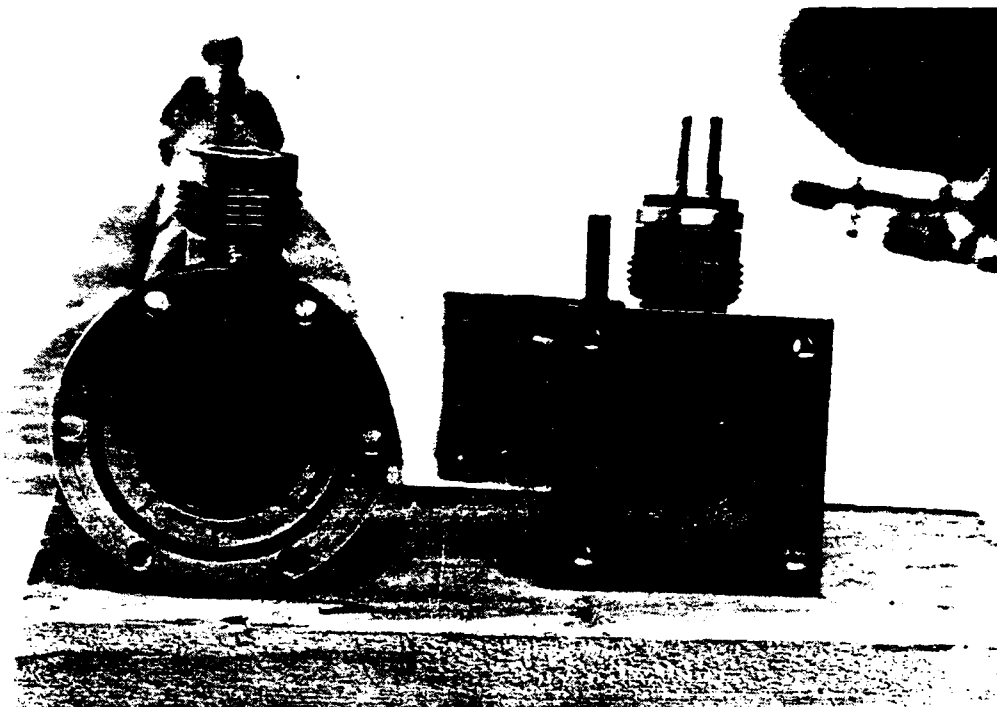
Photograph 3.4 A closeup of the comparison microphone mounted in the wall of the short tube.

Here the Knowles subminiature transducer is shown mounted in the wall of the short tube. Most of the casing shown houses the preamplifier that is an integral part of this type BT-1751 subminiature transducer. The microphone is held in place only by the tape holding down the signal and power leads to the preamplifier.



Photograph 3.5 The microphone port in the wall of the short tube.

This hole in the wall of the cylinder was machined so as to just allow the microphone opening to be flush with the inner wall of the cylinder with the casing of the preamplifier providing contact support. This is illustrated in the previous photograph. Notice that each microphone had its own plastic mount, the one shown in the photograph being designated "1082" which is for the WE640AA microphone of this serial number.



Photograph 3.6 A comparison photograph showing the physical differences in the end microphone mounts between the short and the long tubes.

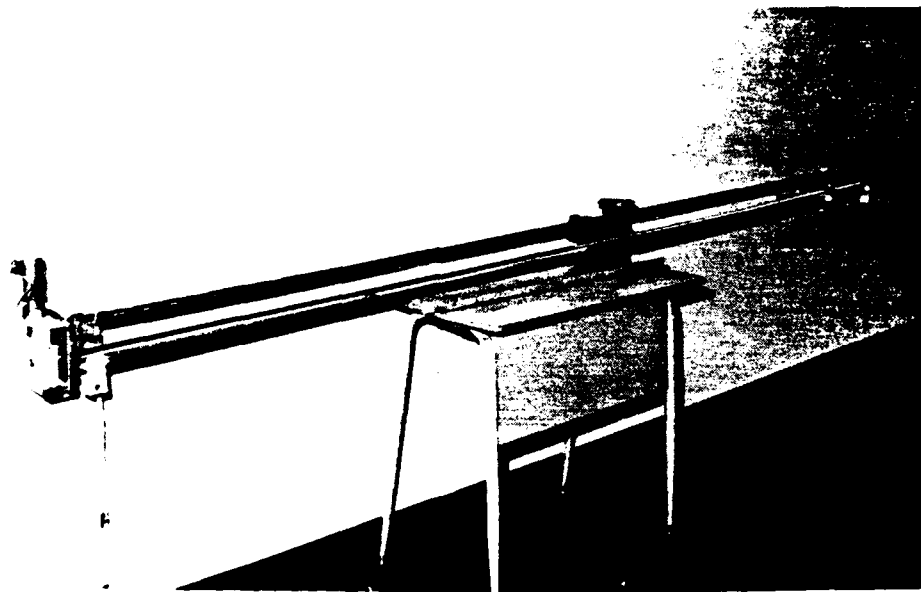
Here the end views are shown for both the short and the long tubes. In the long tube, sufficient room at the end of the cavity remained for the Knowles type BT-1751 subminiature transducer to be mounted alongside the 1 inch WE640AA whereas in the short tube, no such room existed and the Knowles was mounted in the wall of the cylinder.

2. The Microphone Translator for Free Field Calibrations

Two experimental difficulties are hidden in the theory developed for the free field reciprocity calibration derived in chapter one. First, the free field theory requires that the source transducer appear as a point source in the far field of the receiving microphone. This does not appear to require more than one measurement of separation distance between source and receiver [Refer to equation 1.84]. Secondly, it is assumed that the reciprocal microphone will have sufficient strength to project sound at an adequate signal to noise level in the far field. These experimental facts are related as outlined below.

In the first case, free field reciprocity theory requires a point source so that the acoustic pressure amplitude falls off as $1/R$ where R is the "distance" between the source and the receiver. Experimentally, after anechoic conditions are obtained in the laboratory, the measured separation distance between the source face and the receiver diaphragm does not normally vary as $1/R$! For a given operating frequency, a small difference is found between the physical separation distance and what is called the "acoustical separation distance", R' . The received pressure amplitude does fall off as $1/R'$. Experimentally, this requires a correction to the measured physical separation distance that is unique to a source/receiver pair and varies

as a function of frequency. The theoretical and experimental necessity of obtaining this $1/R'$ dependence requires the measurement of several received signals at different distances. A least squares error fit to the measured signal voltage versus the measured separation distance will yield the correction to the measured separation so that the acoustical separation distance may be calculated. The computer controlled microphone translator was constructed to increase the precision in the experimental measurement of the acoustical separation distance.



Photograph 3.7 The microphone translator.

Notice the meter stick on the table next to the translator. The total length of the translator was just over three

reference. Since the greatest range over which measurements are required was 200 degrees, there was more than sufficient resolution in actual translation, and kept the drive motor and motor shaft encoder about three meters away from the sound source. The circuit used to control this translator is shown below:

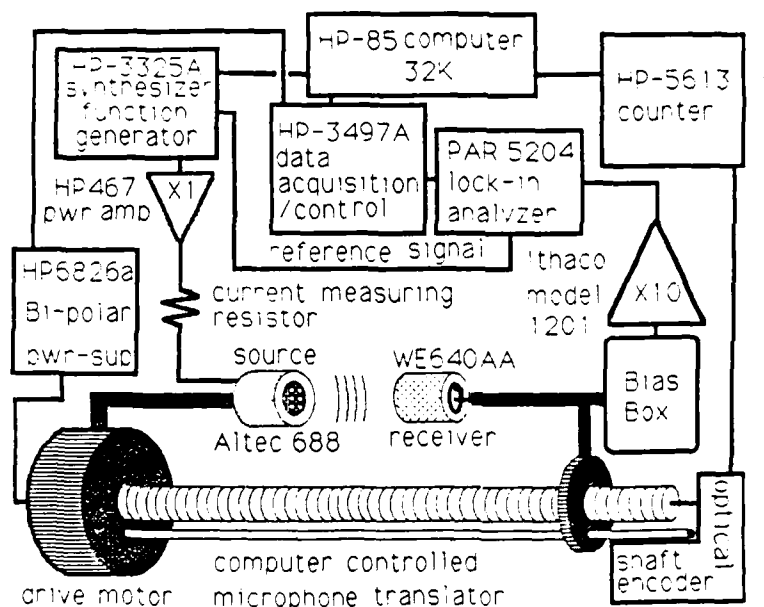
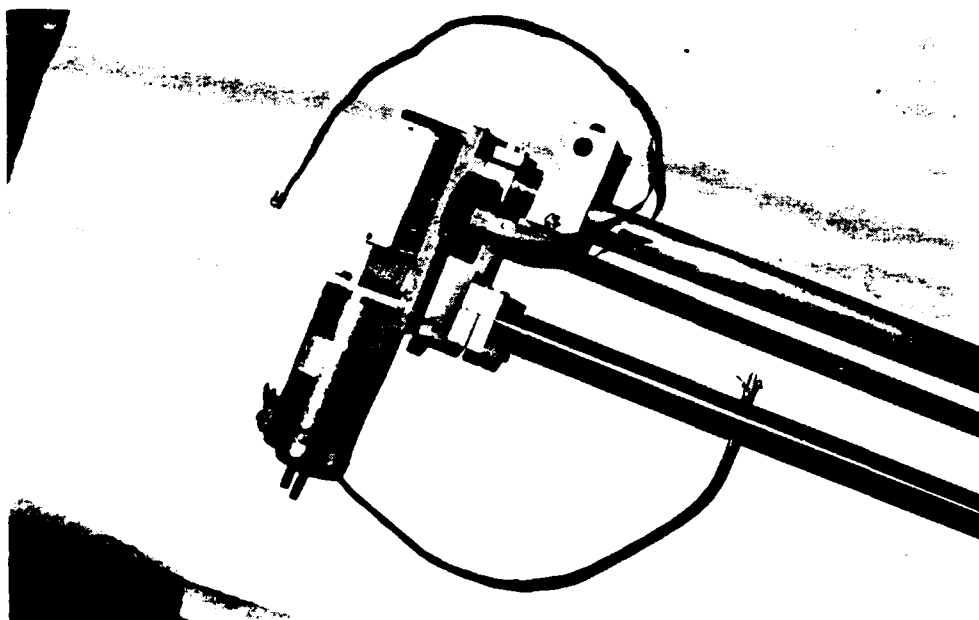


Figure 3.1 Computer control of the microphone translator.

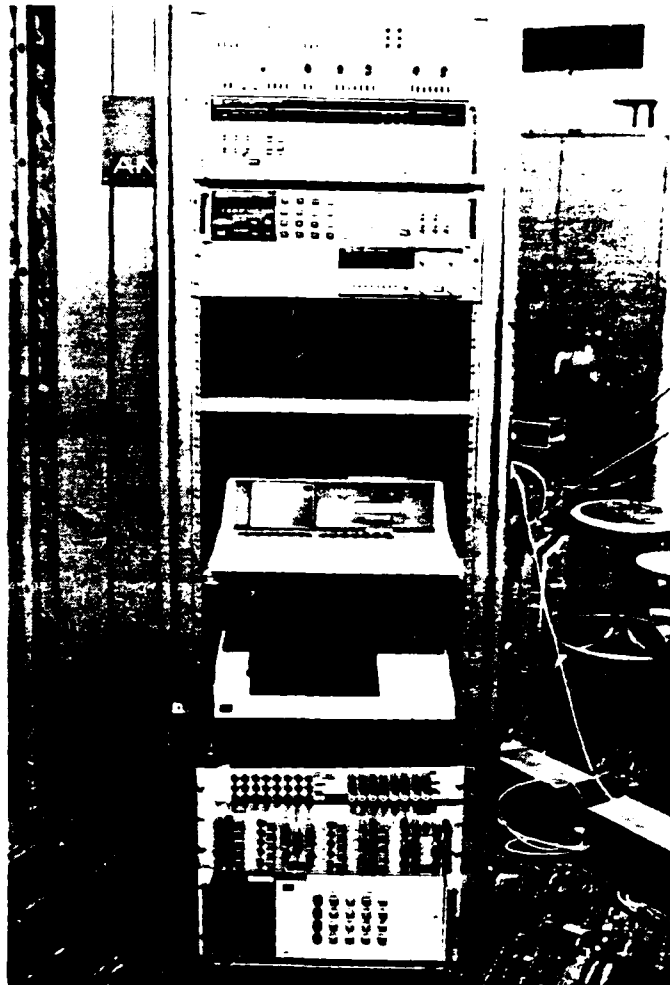
Here, the HP-85 computer controls the drive voltage to the screw motor, which turns the threaded translator shaft. The total angle through which the shaft is turned during an entire interval is monitored via the optical shaft encoder.

This device provides an electronic pulse to the HP-5613 counter for each burst of light from an LED source that shines through a disk containing 1000 slits or "spokes". This provides a "count" measuring the total angular rotation between successive calibration measurements where each "count" represents 1/1000 of a revolution. Measurement of the initial and final positions during any series of calibration stops allows each position to be precisely located after the fact. While the drive motor and the optical shaft encoder are shown in the schematic to be on opposite ends, they were actually both located on the same end as is shown in the next photograph.



Photograph 3.8 The mounting of the drive motor and the optical shaft encoder.

The drive motor had a screw drive and is shown (on the bottom) mounted orthogonal to the threaded (13 threads/inch, 60 degree pitch, 1/2 inch diameter, 10 feet long) translator shaft. The gear box used to couple the screw motor to the shaft can just be seen through its housing. The Hewlett Packard HEDS-6000 incremental optical shaft encoder appears as a small black disc with a lead of computer ribbon cable looped over the top. The center shaft is the threaded translator shaft with precision ground stainless steel upper and lower shafts used to guide and support the moving microphone mounted on a precision ball carriage. The equipment rack with the equipment used in the previous schematic is shown in the next photograph.



Photograph 3.9 The equipment setup at the entrance to the anechoic chamber.

The mobile rack was used to conveniently transport the equipment between the anechoic chamber and the resonant reciprocity laboratory. Missing in this photograph is the VHF switch used in resonant reciprocity to digitally switch equipments allowing the previous reciprocal source to become the receiver and vice versa. From top to bottom, the equipments shown are:

Princeton Applied Research Model 5204 lock-in analyzer
HP-3325-A synthesizer/function generator
HP-3456A digital voltmeter
HP-5316A universal counter
[blank space where HP-98307A VHF switch was normally located]
HP-85 computer
HP-7470A graphics plotter
Interface wiring for the HP-3497A [two panels]
HP-3497A data acquisition and control unit

On the floor to the right of the rack are two HP-467 power amplifiers used to amplify the HP-3325A signal for the Altec electrodynamic source.

The correction to the measured separation distance in free field reciprocity is illustrated in figure 3.31 where the measured separation distances and the acoustical separation distances are both plotted for the 490 Hz microphone calibration measurement. This necessity to vary the range between source and receiver to determine the acoustic separation distance is the indirect cause of the second experimental problem.

When the received microphone signal voltage is measured at increasing ranges, the low source level of the WEA404A condenser microphone results in a very low signal to noise ratio in this far field. This low signal to noise level can introduce significant measurement errors in the calibration procedure. The use of a different reciprocal sound source with an increased acoustic output solves the problem of a low signal to noise ratio in the received signal. In this experiment an Altec 588 electrodynamic microphone was

selected as the reciprocal source since its acoustic output is significantly greater than that obtained for the condenser microphone. The schematic diagram of the setup within the anechoic chamber used to obtain the comparison calibration between the Altec and WE640AA microphones is shown below.

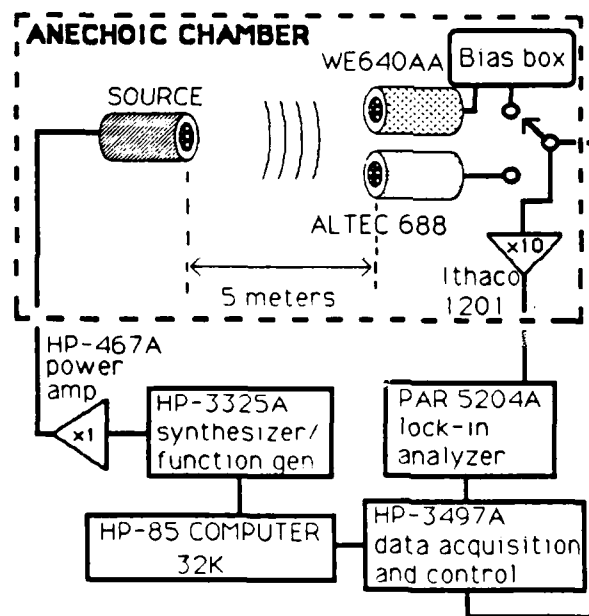


Figure 3.2 The comparison calibration between the Altec and WE640AA microphones.

The experimental results obtained with the above setup will be discussed later in the error analysis of the free field comparison calibration.

C. SIGNALFLOW AND COMPUTER CONTROL WITH PLANE WAVE
 RESONANT RECIPROCITY

The schematic diagram shown below illustrates the signal paths used for computer control of data acquisition. The basic data so acquired was then used to compute a plane wave resonant reciprocity calibration of the microphone open circuit voltage receiving sensitivity.

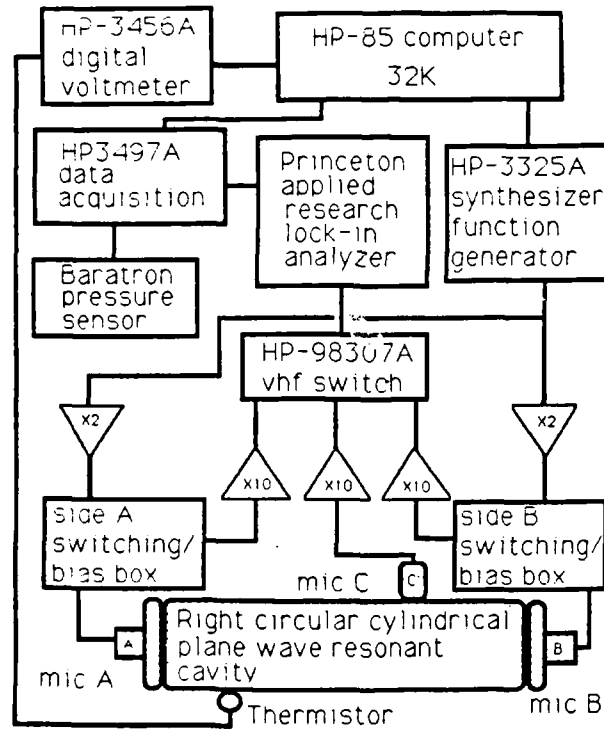


Figure 3.3. Schematic diagram of the signal flow for the plane wave resonant reciprocity calibration

The controlling computer software was written to make the experiment entirely automated after the initial data is given to the computer. The following is a discussion of this procedure:

The computer program (see appendix B), written to control the plane wave reciprocity experiment, performs the following steps beginning sequentially with the highest mode of interest and ending with the lowest mode of interest. Each of these steps (except for the initial input) are performed at each mode.

The initial input is obtained by operator responses to program questions. The program asks for the following data:

- the relative length of tube used (short or long tube)
- the starting relative humidity (assumed to remain constant)
- the highest mode of interest
- the lowest mode of interest
- the initial frequency band to search. This will be around the highest mode.
- the time constant for the PAR 5204 lock in analyzer.
- the voltage scale for the PAR 5204 lock in analyzer.

After this initial input, the computer begins the following sequence of equipment configuration and data acquisition subroutines:

Step 1. Set all equipment to the proper drive voltage and frequency. Then switch microphone "A" to transmit and microphone "B" to receive.

Step 2. Perform a preliminary selection of the drive voltage amplitude so that the mid frequency range initial amplitude is approximately twenty percent of the lock in analyzer's full scale deflection.

Step 3. Sample 26 data points over the initial input frequency band. This band must bracket the center frequency of the mode of interest. Store the frequency and amplitude data and then analyze the data for the resonant frequency, F_9 , the peak amplitude, P_1 , and the quality factor of the resonance, Q_1 . These preliminary values are used as initial inputs to the least square error "Ravine" fit to a Rayleigh line shape. (Most initial values were found to be within approximately one or two percent of the final value.)

Step 4. Computing the "bandwidth" as the initial value for the resonant frequency divided by the initial value of the quality factor, adjust the frequency band of interest to include only plus or minus one "bandwidth" around the initial resonant frequency. Adjust the drive voltage so that the lock in analyzer is operating at ninety percent of max scale at the modal resonance. Again sample 26 data points and store the data both in a memory array and on magnetic tape. Store both the average temperature and average atmospheric pressure found during the 26 point sample.

Step 5. Select microphone "B" to transmit and microphone "A" to receive. Perform steps 2, 3, and 4 for this configuration.

Step 6. Perform a ravine search [Ref 26: p.207], to find the least square error optimum values for F_9 , P_1 , and Q_1 for both sets of data. Store these values on magnetic tape and in a memory array.

Step 7. Select microphone "A" to transmit using the previously obtained value for resonant frequency and the drive voltage selected when "A" transmitted earlier. Select microphone "C" to receive. Measure the comparison voltage V_{ca} and store it.

Step 8. Select microphone "B" to transmit using the ravined value previously obtained for resonant frequency and the drive voltage selected when "B" transmitted earlier. Leave microphone "C" in receive and measure the comparison voltage V_{cb} and store it.

Step 9. Using the equations developed for the six way round robin self consistency check, compute the six different open circuit receiving sensitivities. Store these values on magnetic tape and print these values for operator viewing.

Step 10. Compute the frequencies of interest for the next lower mode and begin anew at step 1 until all the modes of interest have been sampled.

When these logical routines are completed, the computer automatically switches all experimental equipment into the standby mode and awaits the next "initial" input of the operator. If the operator elects to stop data acquisition at this point, printouts of the experimental measurements and computations just completed are immediately available. The magnetic tape data base is available for future analysis and/or comparison when such a need develops.

The magnitude of the improvement in experimental precision using computer control as compared to manual measurements is illustrated in the table shown on the next page. Using measurements obtained for the 735 Hz. resonance (as a comparison sample), the percent relative change in the source amplitude, resonant frequency, and computed quality factor were computed from one run to the next. The time required for the manual measurements (per resonance) averaged 25 minutes. The time required for the computer controlled measurements (per resonance) was slightly less than 4 minutes.

percent relative change
from one run to the next
in measured data.

parameter used to measure the relative change	manual measurement	computer measurement	/	ratio of manual to/ computer results	/
[source amplitude]	.037	.004	/	9.25	/
[measured resonant frequency(mode 3)]	.275	.022	/	12.5	/
[calculated quality factor]	1.92	.026	/	73.8	/

Table 3.1 Percent relative change from run to run
under manual control as compared to computer control for a
selected sample.

It is apparent that a rough *improvement in precision of*
from one to two orders of magnitude occurred due to the
computer control of measurements. This was the typical
result of using computer control of data acquisition.

D. THE CALCULATION OF EXPERIMENTAL ERROR

1. Introduction

When equation 2.27 for a plane wave resonant reciprocity calibration for the open circuit receiving sensitivity is examined, seven experimental variables exist and need to be measured. The method of their measurement and their place in the analytical formulae will determine their individual effect upon the total experimental error. Using the equation developed as the plane wave resonant reciprocity solution for M_A as an illustration,

$$M_A = \left(\frac{e_1 V_{CA} \pi V_0 f_N}{i_1 V_{CB} \rho_0 \gamma_E Q_N} \right)^{1/2} \quad \text{Equation 3.1}$$

straightforward error analysis [Ref. 26], yields for the relative error,

$$\frac{\delta M_A}{M_A} = \frac{1}{2} \left\{ \left[\frac{\delta(e_1/i_1)}{(e_1/i_1)} \right]^2 + \left[\frac{\delta V_{CA}}{V_{CA}} \right]^2 + \left[\frac{\delta V_0}{V_0} \right]^2 + \left[\frac{\delta f_N}{f_N} \right]^2 + \left[\frac{\delta \rho_0}{\rho_0} \right]^2 + \left[\frac{\delta \gamma_E}{\gamma_E} \right]^2 + \left[\frac{\delta Q_N}{Q_N} \right]^2 \right\}^{1/2} \quad \text{Equation 3.2}$$

The variables are,

e_1/i_1 - The ratio of the received signal voltage found across microphone "A" when it is used as a receiver

to the current driving microphone "A" when it is used as a source.

- V_{ca}/V_{cb} - The ratio of the received comparison voltages seen by comparison microphone "C".
- V_0 - The product of the effective cross-sectional area of cylindrical cavity times its length.
- P_0 - Atmospheric pressure within the cavity.
- γ_e - gamma, the effective ratio of specific heats for the gas within the cavity, (accounting for the relative humidity and the non-adiabatic conditions at the boundary of the resonant cavity.)
- Q_n - The quality factor of the Nth resonance.
- F_n - The frequency of the Nth resonance.

These values and their individual probable errors must be determined and included in the calculation of the probable error for M_a .

The necessity of obtaining absolute measurements of e_1 and i_1 prior to computing their ratio was avoided by using the lock-in detector to measure both e_1 and (indirectly), i_1 . Experimentally, the ratio e_1/i_1 was calculated as $e_1/(2\pi f C v_1)$. The variable C is the capacitance of the condenser microphone, v_1 is the voltage drop measured across the condenser microphone when it is acting as a source, and e_1 is the voltage across the condenser microphone when it is acting as a receiver. In this chapter, the term "condenser microphone" is used in the sense that includes the BNC electrical connection between the microphone cartridge and the external electronics. The frequency transfer

characteristics of the lock-in analyzer will cancel out in the ratio of the measured voltages. Any error involved will result from nonlinearity in the lock-in analyzer and the inability to exactly measure capacitance and frequency.

The methods used in measuring these parameters and the determination of their individual contribution to the overall experimental error is presented next. A summary of the individual contributions to the probable error in the plane wave resonant reciprocity calibration is shown later in this chapter (in section D, part 5).

2. Measuring the Ratio e_1/i_1

a. The Electrical Circuit

Figure 3.4 illustrates the signal flow involved in the determination of e_1 , and figure 3.5 is the schematic of the circuit used to measure e_1 .

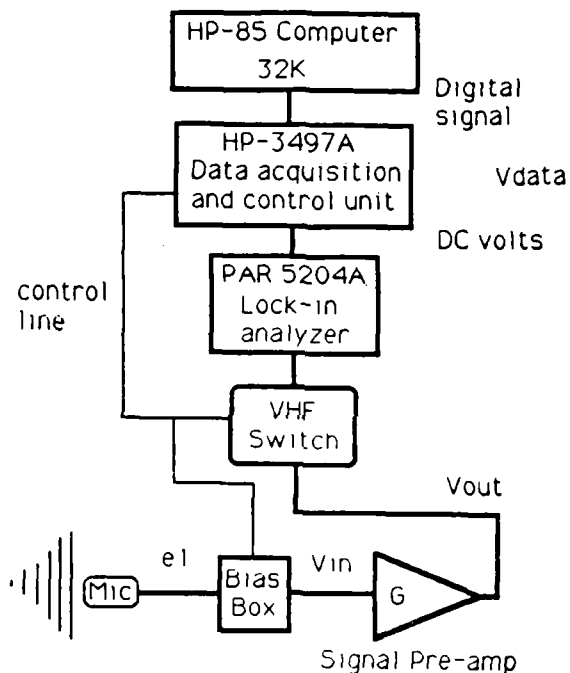


Figure 3.4 Receiving Signal Flow Chart.

Here we see the signal path from the received signal to the measured voltage. In electrical terms the input circuit is:

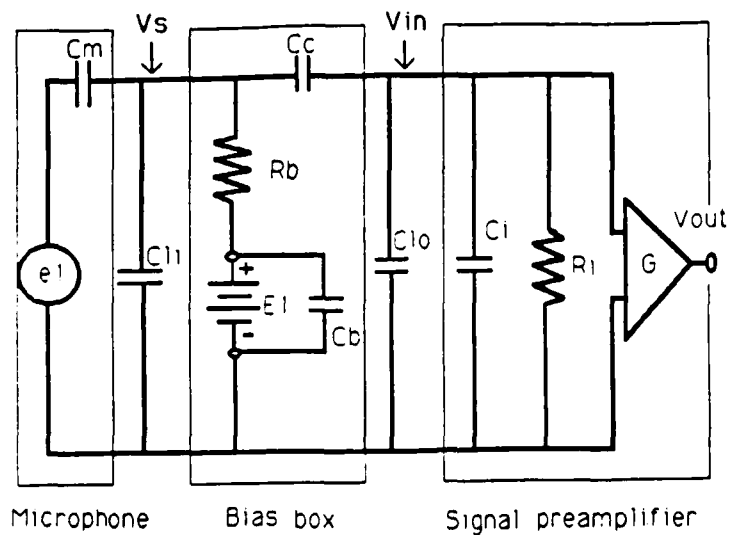


Figure 3.5 Receiving Signal Input Circuit

The circuit elements (with approximate values) and the parameters of interest found in this circuit are:

- e_1 - Signal voltage desired.
- V_{out} - Output voltage of the Signal Preamplifier.
- R_b - Current limiting resistor in the Bias Voltage Supply. (~ 10 megohm)
- C_c - D.C. Blocking capacitor in the Bias Voltage Supply. ($\sim .01\mu f$)
- C_b - Battery bypass for battery noise. ($\sim .01\mu f$)
- C_{li} - Connecting cable capacitance. (~ 40 pf)
- C_{lo} - Connecting cable capacitance. (~ 80 pf)
- C_i - Preamplifier input capacitance. (~ 20 pf)
- E_1 - Bias voltage (~ 116 volts)
- R_1 - Preamplifier input resistance. (~ 10 Megohm)
- V_{in} - Input voltage to the preamplifier.
- G - Gain of the preamplifier. (~ 10)

Figure 3.5 is an abstract electrical model of the real physical system used to process the electrical signal generated by the condenser microphone. It represents a compromise between conflicting factors of simplicity and accuracy that must be addressed from both the experimental and the theoretical standpoint. Numerically, using available computer software, it is possible to determine the "transfer function" of such a lumped parameter circuit with relative ease. The difficulty arises when accurate modeling is attempted and every stray capacitance, resistance, and inductance is measured and included in the model. Experimentally, such an approach is difficult to apply and is not necessary in every case.

The circuit analysis is simplified when the relatively small drop in signal voltage across the blocking capacitor, C_c , in figure 3.5, is accounted for by a one time correction to the final microphone sensitivity. To see how this is done, refer to figure 3.5 and consider the signal voltage that would be measured on each side of the D.C. blocking capacitor, C_c . The effect of the blocking capacitor impedance on the magnitude of " V_{in} " depends upon the magnitude of the input impedance of the signal preamplifier formed by the parallel combination of " C_{10} ", " C_1 ", and " R_1 ". By simple voltage division, using the lumped parameter values given for these devices under figure 3.5, the ratio

of V_s/V_{in} remains constant to within $\sim .01$ dB over the frequency range used in this experiment. The dB signal loss across the blocking capacitor C_c is calculated in Appendix E and shows an approximate $\sim .03$ dB loss across the entire frequency range used. This means that the blocking capacitor C_c may be ignored in the circuit analysis if a one time correction to the open circuit voltage receiving sensitivity of $+ .03$ dB is made at the end. Thus, by measuring the bias box input capacitance (when it is disconnected from the circuit), the cable capacitances, and the input capacitance of the signal preamplifier, the circuit model can be simplified as shown in figure 3.6 below.

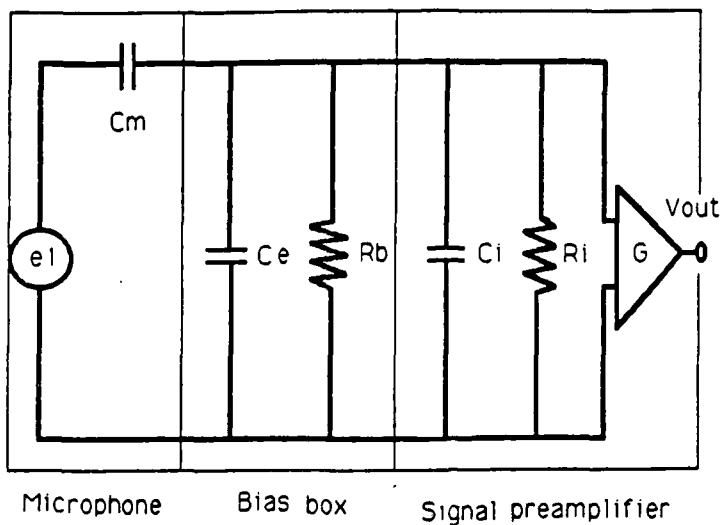


Figure 3.6 Simplified input circuit for acoustic signal

Here, the measured capacitances of the connecting cables, the bias box, and the input of the signal preamplifier can be combined. The capacitances of the connecting cables and the bias boxes were measured directly with a General Radio Type 1615A capacitance bridge in turn calibrated with reference to a General Radio type 1404 reference standard capacitor serial #2507. This reference capacitor had a specification of 10 picofarads (to 20 ppm) for 1Khz at 23(+/-) deg C. In addition, the zero bias voltage capacitance values for the different W.E.640AA

laboratory standard microphones were measured with a Hewlett Packard 4192A LF Impedance analyzer calibrated to the same reference. The results of these measurements are listed in table 3.2 below.

		precision [sample sigma (pf)]
Bias box "A" plus the cable capacitance (BTAR Ct).....	151.900 pf	.028 (n=6)
Bias box "B" plus the cable capacitance (ATBR Ct).....	150.070 pf	.012 (n=5)
W.E.640AA Serial #1248..... (with the "#1248" BNC connector)	52.160 pf	.002 (n=13)
W.E.640AA Serial #1082..... (with the "#1082" BNC connector)	51.974 pf	.002 (n=13)
W.E.640AA Serial #0815..... (with the "#0815" BNC connector)	49.984 pf	.008 (n=13)

Table 3.2 Measured capacitances of bias boxes and microphones.

Since the input capacitance of the signal preamplifier will vary from amplifier to amplifier, the following method was used to calculate the input capacitance for each preamplifier used in the experiment.

b. Measuring The Input Capacitance of Preamplifiers

The specifications of the preamplifiers used in this experiment gave the input capacitance as a nominal 20 to 30 picofarads. Since the capacitance of the W.E.640AA condenser microphone was approximately 50 picofarads, any error in the determination of the preamplifier input capacitance on the order of 1/10 picofarad was significant and the rough value given in the equipment specifications was grossly inadequate. Refer to the circuit shown below.

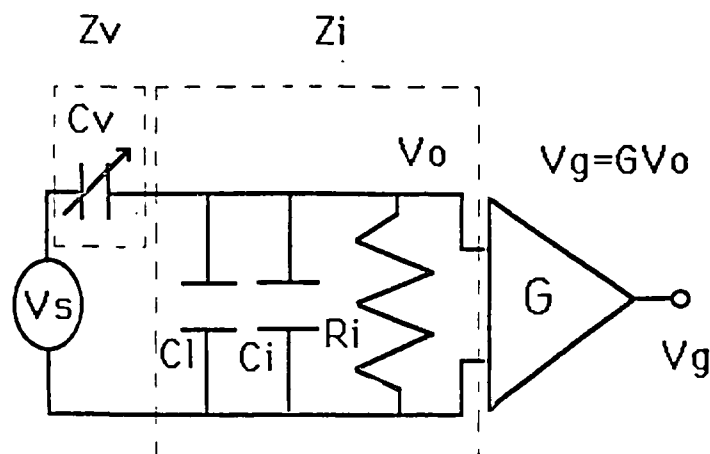


Figure 3.7 Circuit used to measure the input capacitance of signal preamplifiers.

Straightforward voltage division will yield a solution for V_o . When this solution is combined with the gain, $V_g = Z_i * V_s * G / [Z_i + Z_v]$. When this solution is inverted,

$$\left[\frac{1}{V_g} \right] = \left[\frac{1}{j\omega Z_i V_s G} \right] \left[\frac{1}{C_v} \right] + \left[\frac{1}{V_s G} \right] \quad \text{Equation 3.3}$$

Z_v is the impedance of the variable capacitor in the input ($1/[j\omega C_v]$), and Z_i is the input impedance of the cable and preamplifier combination ($R_i/[1 + R_i*j\omega*(C_i+C_1)]$). Typical circuit parameters used for this circuit were:

frequency = 1000 Hz.

$C_1 \sim 4$ pf

$C_i \sim 25$ pf

$G \sim 10$

$C_v \sim 4 - 60$ pf [see table 3.3]

$V_g \sim$ variable

$V_s \sim$ variable, on the order of 10 millivolts.

$R_i \sim 10$ megohm, uncertainty estimated at 1%.

This is the form of the equation for a straight line, $Y=aX+b$. If individual values of $1/V_g$ and $1/C_v$ are fit by the least squares error method to a straight line, the values of "a" and "b" can be calculated. The resultant absolute value of the ratio of a/b equals the magnitude of $1/[j\omega Z_i]$. Individual "boxes" with different values of C_v were constructed and calibrated so that as large a range of values as possible would be available for the least square error analysis. The following table lists the capacitance values measured for these individual boxes using the same General Radio Type 1615A capacitance bridge previously used to obtain the bias box capacitances.

Box #	capacitance(pf) (average)	Precision (Sigma using two samples)
1	3.6128	.001
2	9.7036	.0005
3	11.0215	.0031
4	11.9826	.0005
5	13.9351	.002
6	Not used due to thermal instability.	
7	14.9932	.0005
8	20.3958	.003
9	22.5042	.0005
10	61.4590	.0005

Table 3.3 Measured values of capacitance boxes used as "Cv" in the determination of preamplifier input capacitance.

The capacitors listed above were selected for their thermal stability and were observed to remain stable to within the precision obtained above for the laboratory temperature range of 19-22 degrees centigrade.

When the values for "a" and "b" are obtained via least square error analysis, the solution for the total input capacitance is given by:

$$C_T = \left[\left(\frac{a}{b} \right)^2 - \left(\frac{1}{\omega R_i} \right)^2 \right]^{1/2} \quad \text{Equation 3.4}$$

The uncertainty in the result obtained for C_t is given by
 [Ref. 28: Eqn. 3-2]:

$$\delta C_T = \left\{ \frac{\left(\frac{a}{b}\right)^2 \left(\delta \frac{a}{b}\right)^2}{\left(\frac{a}{b}\right)^2 - \frac{1}{\omega^2 R_i^2}} + \frac{(\delta R_i)^2}{(\omega^4 R_i^6) \left[\left(\frac{a}{b}\right)^2 - \frac{1}{\omega^2 R_i^2} \right]} \right\}^{1/2} \quad \text{Equation 3.5}$$

The results obtained with the least square error linear fit using the method described above are given in the tables below. The ultimate uncertainties in C_t are due largely to the 1% estimated uncertainty in R_i .

The following data have
 ~ 3 significant figures
 and are in picofarads.

	data run #1	data run #2
Ithaco 1201 Ser.#63594 (X10 setting, $R_i \sim 100$ Mohms)		
chan "A"	[a/b]= 22.9081	22.9463
chan "B"	[a/b]= 24.6444	24.6597
Ithaco 1201 Ser.#61783 (X10 setting, $R_i \sim 100$ Mohms)		
chan "A"	[a/b]= 23.6920	23.6938
chan "B"	[a/b]= 26.0170	26.0228
Hewlett Packard Type 465A Lab Serial # 95 (lab B side X10 setting)	[a/b]= 29.6300	29.6302
Hewlett Packard Type 465A Lab Serial # 93 (lab A side X10 setting)	[a/b]= 28.9561	29.0806

Note: The value of the "cable" capacitance, $C_1 = 1.926$ Pf.

Table 3.4 Measured ratios for [a/b]

With the experimentally determined values for $[a/b]$, the value of the preamplifier input capacitance, C_i can be determined.

 Signal Preamplifier/ C_i (pf)/ σ (pf)/"standard σ "/P.E.(ppm)

values of C_i have ~ 3 significant figures

Ithaco 1201 Ser.#63594				
(X10 setting)				
chan A	20.946	.088	20 ppm	~ 4201
chan B	22.675	.088	20 ppm	~ 3880
Ithaco 1201 Ser.#61783				
(X10 setting)				
chan A	21.793	.088	20 ppm	~ 4038
chan B	24.045	.088	20 ppm	~ 3660
Hewlett Packard				
Type 465A Lab Serial #95				
(lab B side X10 setting)	23.067	.148	20 ppm	~ 6416
Hewlett Packard				
Type 465A Lab Serial #93				
(lab A side X10 setting)	22.338	.145	20 ppm	~ 6491

Average probable error for the input capacitance ~ 4780 ppm

Table 3.5 Calculated input capacitances for signal preamplifiers used in experiment.

When the signal preamplifier input capacitances so determined are included in the circuit analysis, the circuit can be further simplified as shown in the following section.

c. The Calculation of e_1

Referring back to figure 3.6, the total input resistance and the total input capacitance can be combined in a complex impedance, Z_T . The value of Z_T is given by,

$$Z_T = \frac{R_T}{1 + j\omega R_T C_T}$$

Equation 3.6

The values for R_T and C_T are given by,

$$R_T = \frac{R_b R_i}{R_b + R_i} \quad ; \quad C_T = C_e + C_i$$

Equation 3.7

Now the circuit becomes,

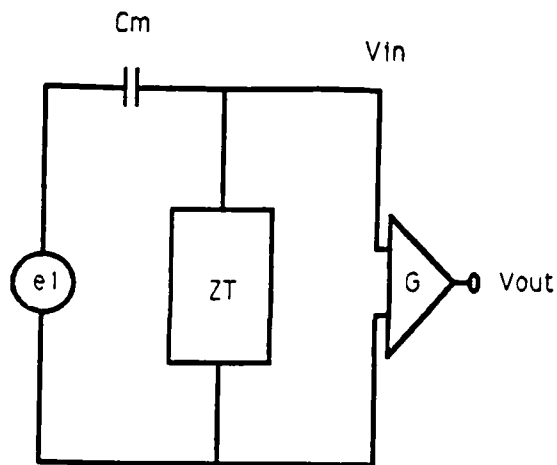


Figure 3.8 Simplified circuit for measuring the acoustic signal

The solution for the ratio of V_{in}/e_1 is given by:

$$\frac{V_{in}}{e_1} = \frac{1}{\{\text{REAL}\} + j \{\text{IMAGINARY}\}}$$

Equation 3.3

The real part is given by,

$$\{\text{REAL}\} = 1 + \frac{C_T}{C_m} \quad \text{Equation 3.9}$$

and the imaginary part is,

$$\{\text{IMAGINARY}\} = \frac{-1}{\omega R_T C_m} \quad \text{Equation 3.10}$$

The solution for the magnitude of e_1 for this circuit is,

$$e_1 = V_{in} \left(\left[1 + \frac{C_T}{C_m} \right]^2 + \left[\frac{1}{\omega R_T C_m} \right]^2 \right)^{1/2} \quad \text{Equation 3.11}$$

Nominal values for the parameters in this equation were:

- $C_t \sim 170$ pf.
- $C_m \sim 50$ pf.
- $R_i \sim 10$ Megohms.

Refer ahead to figure 3.9 to relate the signal amplifier input to the final "voltage" sent via the "Hewlett Packard Interface Bus" (HPIB) to the HP-85 computer. The output of the signal amplifier is equal to the input multiplied by the amplifier gain. This same amplifier output voltage, V_{out} , is then the analog input voltage to the 5204 lock in

analyzer where it is scaled by the gain setting of the PAR 5204 lock-in analyzer, "B", and sent to the data acquisition system. Due to the design of the lock-in analyzer, the gain setting of "B" is selected so that the acquisition input has a range of values of from 0 to 1.15 volts. This data acquisition system is HP-IB compatible and is in turn sampled to provide the digitized output, V_{data} , to the HP-85 computer.

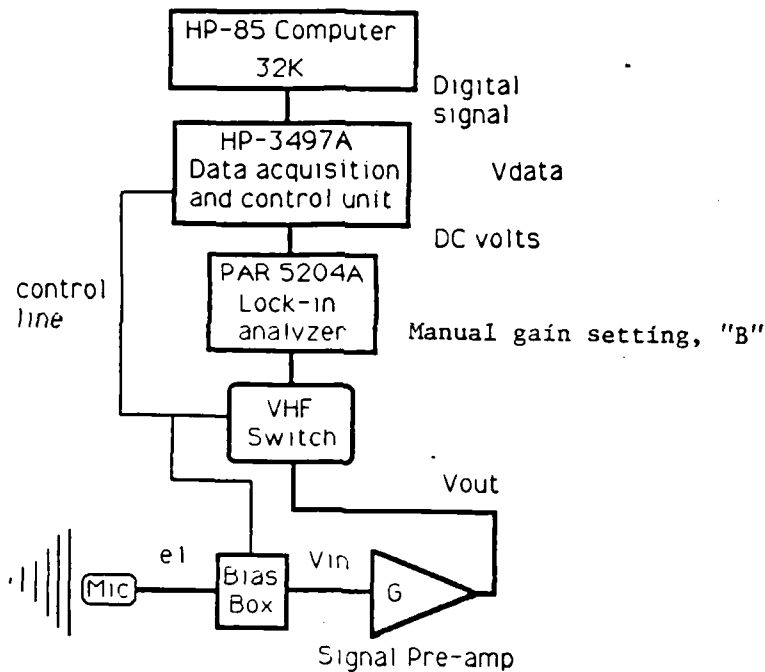


Figure 3.9 Analog to digital signal flow chart.

The inverse of this path gain is computed to determine the value of V_{in} when V_{data} is known. Thus, the analog voltage " $G \cdot V_{in}$ " is obtained by multiplying " V_{data} " by the gain setting, "B".

$$[G][V_{in}] = [B][V_{data}]$$

Equation 3.12

Solving for V_{in} and substituting into equation 3.11 we obtain the received signal voltage in terms of experimentally measured parameters:

$$e_1 = \left[\frac{B V_{data}}{G} \right] \left(\left[1 + \frac{C_I}{C_m} \right]^2 + \left[\frac{-1}{\omega R_T C_m} \right]^2 \right)^{1/2}$$

Equation 3.13

Prior to computing the ratio e_1/i_1 , we must next discuss the calculation of the transmitting current, i_1 .

d. The Calculation of i_1

The drive current for the source microphone is estimated from a knowledge of the microphone capacitance, the bias voltage, and the drive voltage seen across the source terminals.

$$i_1 = j \omega C_{mic} V_{drive}$$

Equation 3.14

Using a constant value of capacitance to model the microphone neglects the effect of the motional impedance on the ratio of $[e_1/i_1]$ for the condenser microphone. (After the fact, it was determined that the value of i_1 should have been experimentally measured and not calculated. However, the following explains what was actually done.)

The drive voltage across the source microphone's terminals that is used for the computation of i_1 is not the drive voltage that the computer program "asks" for but rather is a resultant of the "asked" for voltage and the signal path transfer function between the signal function generator and the microphone. This discrepancy is corrected by using an experimentally determined least squares fit to "ask" vs "get" data. The circuit shown below is the circuit used to obtain the "ask" vs "get" data needed.

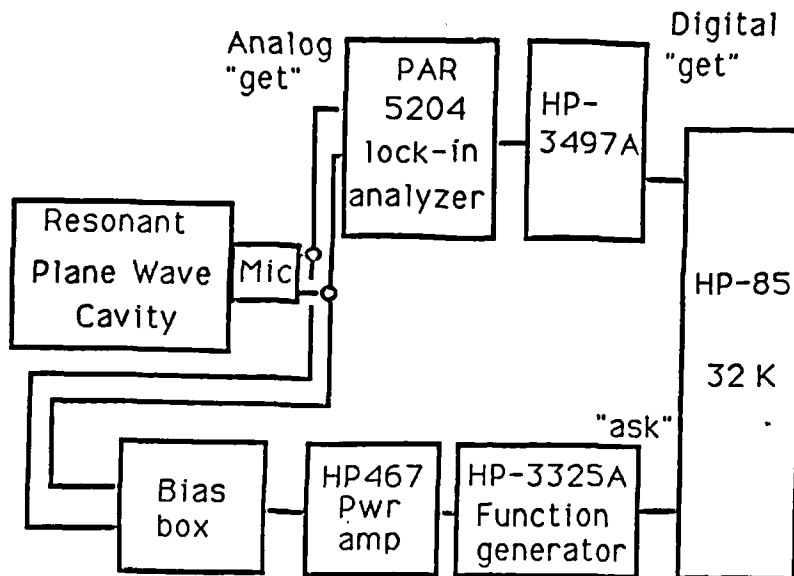


Figure 3.10 Circuit used to measure voltage across microphone when the magnitude of the source voltage is under computer control.

Using the data experimentally measured in this fashion, we have a series of estimates of "Vget" that use acceptable straight line approximations to the transfer function for short segments of frequency.

Equation form:	$V_{get} = [K(f)] * V_{ask}$
0 hz < f < 520 hz	$V_{get} = [.9278 + 4.979E-5 * f] * V_{ask}$ (probable error ~ 450 ppm)
520 hz < f < 1020 hz	$V_{get} = [.9516 + 4.163E-6 * f] * V_{ask}$ (probable error ~ 310 ppm)
1020 hz < f < 1510 hz	$V_{get} = [.9541 + 1.714E-6 * f] * V_{ask}$ (probable error ~ 410 ppm)
1510 hz < f < 2500 hz	$V_{get} = [.9558 + 6.122E-7 * f] * V_{ask}$ (probable error ~ 386 ppm)
2500 hz < f < 9999 hz	$V_{get} = [.9568 + 2.224E-7 * f] * V_{ask}$ (probable error ~ 269 ppm)

Equations 3.13

The next correction we must include in order to accurately calculate the drive current is the observed increase in capacitance of the source microphone which occurs with an increase in bias voltage.

While the capacitance of the source microphone is primarily a function of its dimensions, the electrostatic force between the backplate and the diaphragm of the condenser microphone as a result of the applied bias voltage, will cause a displacement of the microphone diaphragm away from the unbiased equilibrium position. This change in the separation between the diaphragm and the backplate will cause a slight increase in microphone capacitance relative to the "no bias" capacitance. This slight change (~.3%) is easily measured and is tabulated below. The data were obtained using the internal bias supply voltage and the standard functions available on the Hewlett Packard HP-4192A LF impedance analyzer.

Approximate solutions for M_0 are obtained for the W.E.640AA microphones using the change in capacitance vs bias voltage data. The theory and results of such a calculation are shown in Appendix F.

 For W.E.640AA TYPE "L" laboratory standard microphones.
 Measured values are uncorrected HP-4192A readings.

Bias (volts D.C.)	Measured C/delta C (all values in Pf.)			Bias ² (volts ²)
	W.E.640AA Serial #'s			
	#1082	#1248	#0815	
-35	56.790/.030	56.990/.045	54.842/.072	1225
-30	56.785/.025	56.980/.035	54.820/.050	900
-25	56.780/.020	56.970/.025	54.805/.035	625
-20	56.770/.010	56.960/.015	54.790/.020	400
-15	56.765/.005	56.955/.010	54.785/.015	225
-10	56.763/.003	56.950/.005	54.775/.005	100
0	56.760/.000	56.945/.000	54.770/.000	
+10	56.763/.003	56.950/.005	54.775/.005	100
+15	56.765/.005	56.955/.010	54.788/.018	225
+20	56.770/.010	56.958/.013	54.793/.023	400
+25	56.775/.015	56.970/.025	54.808/.038	625
+30	56.780/.020	56.980/.035	54.823/.053	900
+35	56.790/.030	56.990/.045	54.842/.075	1225
	correction for mounting bracket = -4.794 (pf)			
	correction for calibration of HP-4192A = +0.008 (pf)			
	Total correction required = -4.786 (pf)			

Table 3.6 Measured change in capacitance due to application of a bias voltage to a condenser microphone

Due to the possibility of damaging the HP-4192A LF impedance analyzer, it was impractical to measure the change in capacitance due to the applied bias when the W.E.640AA microphones were biased at their experimental bias of 115 volts. A linear least squares fit to the data shown above was used to extrapolate an estimate of the change in microphone capacitance which resulted from the applied bias voltage. The equations so obtained had the form,

$$\Delta C_m = a [V_{bias}]^2 + b$$

Equation 3.16

Individual correlation coefficients of .985, .996, and .999 were obtained for the bias voltage capacitance correction equations given below for W.E.640AA microphones with serial numbers #1082, #1248, and #0815 respectively. The uncertainties in the slopes and intercepts so obtained are given as "delta a" and "delta b" respectively.

$$\begin{aligned} \text{delta C1} &= [2.4731 \text{ E-5}] * V^2 + 3.1668 \text{ E-4} \quad (\text{pf}) \\ (\#1082) \quad \text{delta "a"} &\sim 1.2\text{E-6}, \text{delta "b"} \sim 8.03\text{E-4} \end{aligned}$$

$$\begin{aligned} \text{delta C2} &= [3.6615 \text{ E-5}] * V^2 + 1.0404 \text{ E-3} \quad (\text{pf}) \quad \text{Equations 3.17} \\ (\#1248) \quad \text{delta "a"} &\sim 1.6\text{E-6}, \text{delta "b"} \sim 1.1\text{E-4} \end{aligned}$$

$$\begin{aligned} \text{delta C3} &= [5.9254 \text{ E-5}] * V^2 + 2.3190 \text{ E-4} \quad (\text{pf}) \\ (\#0815) \quad \text{delta "a"} &\sim 8.2\text{E-7}, \text{delta "b"} \sim 5.5\text{E-4} \end{aligned}$$

At a nominal bias voltage of ~ 117 volts, the capacitance corrections expected due to the bias voltage are on the order of one percent and are significant to the overall calibration.

Thus, we can calculate the value of i_1 as,

$$i_1 = (2\pi f_N) [K(f) V_{ASK}] [C_{om} + \Delta C_m]$$

Equation 3.18

and the equation for e_1/i_1 becomes,

$$\frac{e_1}{i_1} = \frac{\left[\frac{B V_{DATA}}{G} \right] \left[\left(1 + \frac{C_T}{C_m} \right)^2 + \left(\frac{-1}{\omega_N R_T C_m} \right)^2 \right]^{1/2}}{\left[2\pi f_N \right] \left[K(f) V_{ASK} \right] \left[C_{om} + \Delta C_m \right]} \quad \text{Equation 3.19}$$

The probable error in the ratio e_1/i_1 may now be calculated provided the probable errors associated with the preamplifier gain, G , the measured resonant frequency, f_n , and the non-linearity in e_1/v_1 due to the lock-in analyzer are available. An analysis of these probable errors will be included in the next four sections.

e. Measuring The Signal Preamplifier Gain, G

Two different signal preamplifiers were available for use in this experiment. These were the Hewlett Packard type 465A amplifier and the Ithaco model 1201 low noise preamplifier. Both amplifiers were used at a nominal gain of "10" but were experimentally observed to have different gain stability characteristics. Since the duration of a typical experimental "run" averaged eight hours, it was of paramount importance that the drift in the signal gain be minimized over this time period. Both amplifiers had experimental advantages; the HP-465A had the lowest drift rate and was selected for use in the plane wave resonant reciprocity experiment. The Ithaco 1201 had an internal battery power supply which greatly reduced cross talk and 60 cycle hum during the later free field reciprocity calibrations. The circuit used to measure the gain experimentally was controlled by the HP-85 computer and is shown below.

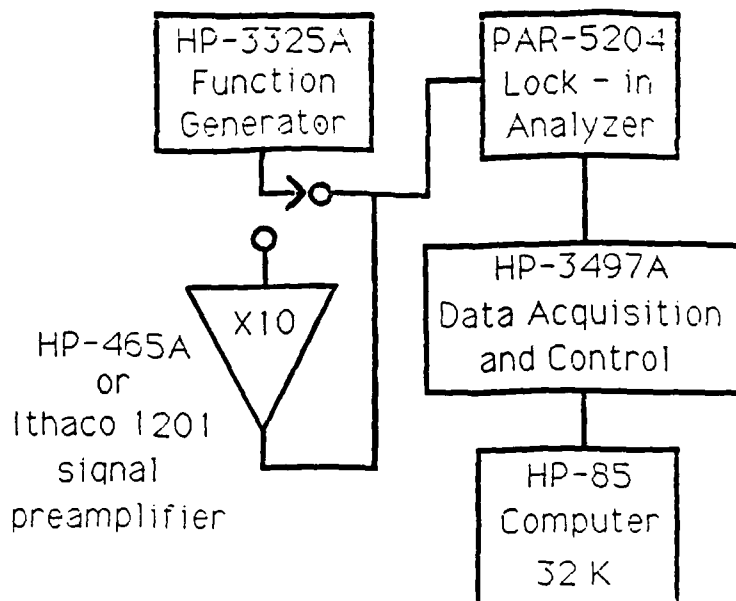


Figure 3.11 Circuit used to measure amplifier gain.

In the above circuit, after establishing a constant rms voltage output, the function generator was directed by computer to step through the frequency range of interest (200-6000Hz) at intervals of 100 Hz. At each frequency the output voltage was measured by the lock-in analyzer/data acquisition and control unit and stored in a computer array. Next, the amplifier was included in the circuit and the procedure was repeated. The entire procedure was repeated several times to obtain an estimate of precision for the array data. The gain of HP-465A amplifiers was calculated by comparing the two arrays and the results are shown in figures 3.12 and 3.13 below.

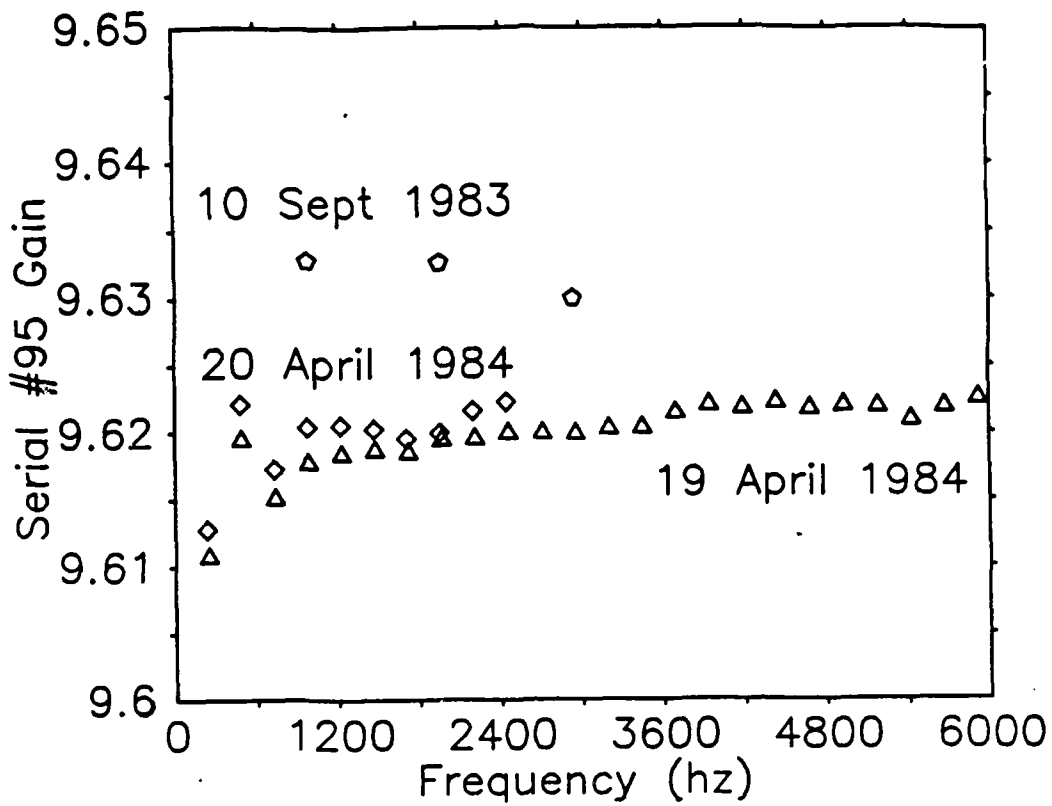


Figure 3.12 Measured gain for HP-465A serial #95

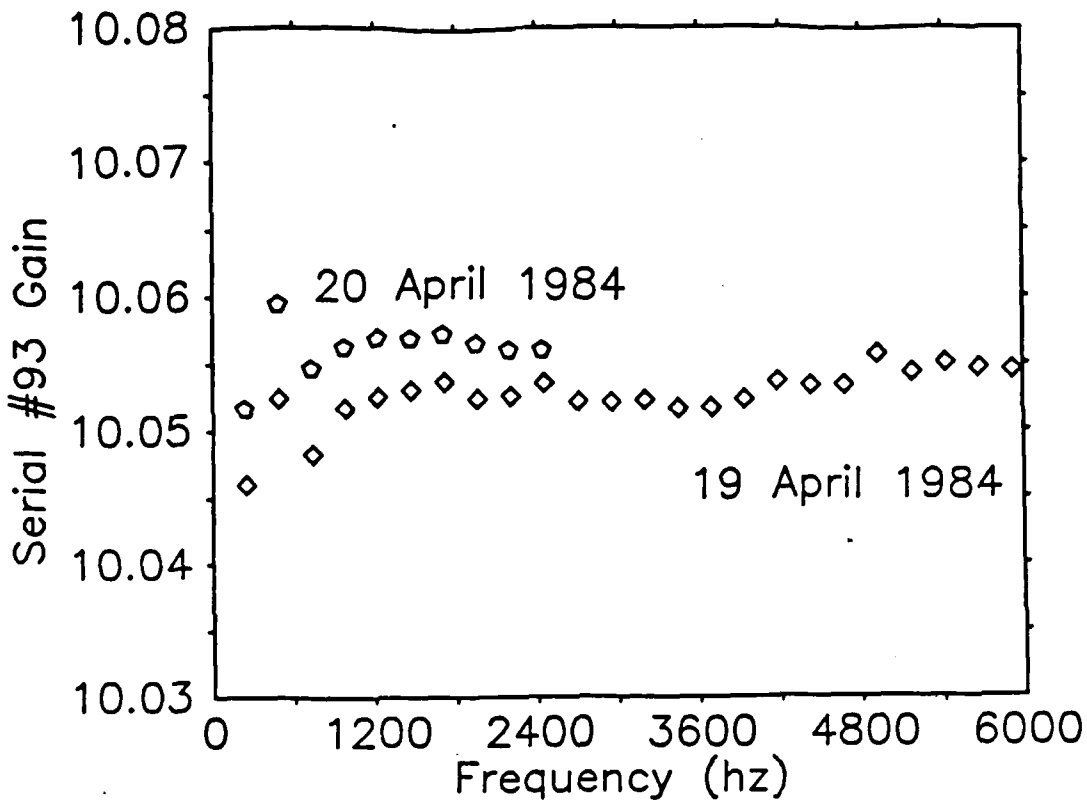


Figure 3.13 Measured gain for HP-465A serial #93

Since the drift of measured values over a single day is roughly 1/5 the drift observed over an eight month period, the latter is used as the worst case estimate of uncertainty in G, while the former is used as the best case estimate. Thus, the range of precision in this data is from ~260ppm to ~1300 ppm. Since the computer controlled circuit measures the relative gain, the systematic error included in any one measurement is cancelled out and the precision of the data is used as the estimate for probable error in this parameter. The gain analysis for the Ithaco amplifiers will

be included later when the free field reciprocity experiment is discussed.

Next, the non-linearities associated with the lock-in detector signal path will be discussed.

f. Measuring Non-Linearity in The Lock-in Detector

The non-linearity in the lock-in detector was measured using the circuit shown in figure 3.14 below.

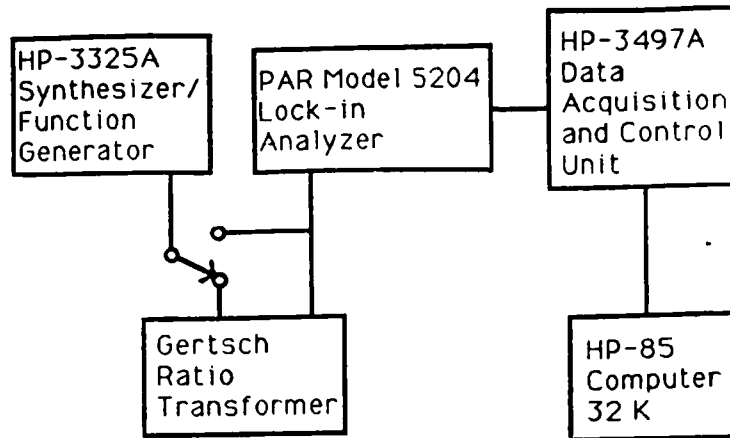


Figure 3.14 Circuit used to determine non-linearity in the lock-in detector.

Experimental determination of the linearity of the lock-in detector found that the fractional error varied as a function of what portion of the scale was used to measure the data. Since the computer program dynamically sought to run the source until the receiver was at $\sim 90\%$ of full scale, the linearity at that scale position was measured and used in the error calculations. Two different ratio transformers were used to determine the linearity of the

system and the measured results are shown in the following tables.

All data was obtained at 1000 hz, so that the limits of the ratio transformers would not be exceeded.

Transformer serial# 304

transformer ratio	voltage ratio	fractional error(ppm)
.1	.097117	- 29700
.2	.206257	+ 30300
.3	.307339	+ 23900
.4	.398773	- 3080
.5	.497208	- 5620
.6	.597665	- 3910
.7	.698417	- 2270
.8	.800050	+ 063
.9	.900181	+ 201

Table 3.7 Linearity data obtained using ratio transformer serial # 304

As shown on the next page, a different ratio transformer was used to obtain a comparison.

All data was obtained at a frequency of 1000 hz so that the limits of the ratio transformer would not be exceeded.

Transformer serial# 572

transformer ratio	voltage ratio	fractional error (ppm)
.1	.096869	- 32300
.2	.199362	- 3200
.3	.300154	+ 3000
.4	.399208	- 1980
.5	.499039	- 1926
.6	.598614	- 2315
.7	.700138	+ 197
.8	.798215	- 2236
.9	.898320	- 1870

Table 3.8 Linearity data obtained using ratio transformer serial # 572

Since the linearity of these ratio transformers nominally is on the order of 10 ppm, the fractional error due to nonlinearity in the signal flow through the lock-in detector is from ~200 to ~1800 ppm depending upon which ratio transformer is accurate. An estimate of 1400 ppm will be used for the probable error in the linearity of the system near full scale and ~ 3700 ppm near half scale.

g. Computation of The Probable Error in e_1/i_1

For the purpose of error analysis, the effect of the $[wRtC_m]$ term in equation 3.19 is relatively small since the neglected term is at worst one order of magnitude smaller and normally two orders of magnitude smaller than the $[1 + C_t/C_m]$ term. As a result, its contribution to the overall error will also be smaller. Equation 3.19 is therefore rewritten for the purpose of error analysis as:

$$\frac{e_1}{i_1} \cong \frac{\left(\frac{B}{G}\right) \left(\frac{V_{DATA}}{K(f) V_{ASK}}\right) \left(1 + \frac{C_T}{C_M}\right)}{2\pi f_N C_M} \quad \text{Equation 3.20}$$

The relative error in e_1/i_1 can now be more easily computed as:

$$\frac{\delta\left(\frac{e_1}{i_1}\right)}{\frac{e_1}{i_1}} = \left\{ \left(\frac{\delta B}{B}\right)^2 + \left(\frac{\delta\left(\frac{V_{DATA}}{V_{GET}}\right)}{\frac{V_{DATA}}{V_{GET}}}\right)^2 + \left(\frac{\delta f_N}{f_N}\right)^2 + \left(\frac{\delta G}{G}\right)^2 + \left(\frac{\delta [C_m^{-1} + C_T C_m^{-2}]}{[C_m^{-1} + C_T C_m^{-2}]}\right)^2 \right\}^{1/2} \quad \text{Equation 3.21}$$

When it is noted that the contribution to the error due to the resonant frequency will not apply to the total error in the open circuit receiving voltage sensitivity, M_o , due to a cancellation from the resonant frequency in the numerator of J_o , we can exclude the relative error due to the resonant frequency, note that the scale factor B is a constant, and

rewrite the relative uncertainty in $[e1/i1]$ as,

$$\frac{\delta\left(\frac{e1}{i1}\right)}{\left(\frac{e1}{i1}\right)} = \left\{ \left(\frac{\delta\left(\frac{V_{data}}{V_{get}}\right)}{\left(\frac{V_{data}}{V_{get}}\right)} \right)^2 + \left(\frac{\delta G}{G} \right)^2 + \left(\frac{\delta(C_m^{-1} + C_T C_m^{-2})}{(C_m^{-1} + C_T C_m^{-2})} \right)^2 \right\}^{1/2} \quad \text{Equation 3.22}$$

The error in the voltage ratio will come from two sources; the uncertainty in V_{get} , as a result of the inexactness of $K(f) \cdot V_{ask}$, and the uncertainty due to the nonlinearity in the voltage ratio resulting from the non-linearity in the lock-in analyzer. Using the results from the previous section and the experimental determination of the inexactness found for $K(f) \cdot V_{ask}$ (shown in equations 3.15), we have,

$$\frac{\delta\left(\frac{V_{data}}{V_{get}}\right)}{\left(\frac{V_{data}}{V_{get}}\right)} = \left([1400 \text{ ppm}]^2 + [365 \text{ ppm}]^2 \right)^{1/2} = 1447 \text{ ppm} \quad \text{Equation 3.23}$$

The uncertainties due the capacitance terms are computed next. Let the result, W , be defined as:

$$W = C_m^{-1} + C_T C_m^{-2} \quad \text{Equation 3.24}$$

Straightforward error analysis yields,

$$\delta W = \left\{ \left(\frac{\partial W}{\partial C_m} \delta C_m \right)^2 + \left(\frac{\partial W}{\partial C_T} \delta C_T \right)^2 \right\}^{1/2} \quad \text{Equation 3.25}$$

with,

$$\frac{\partial W}{\partial C_m} = -C_m^{-2} - 2C_T C_m^{-3} \quad \text{Equation 3.26}$$

and,

$$\frac{\partial W}{\partial C_T} = C_m^{-2} \quad \text{Equation 3.27}$$

Substitution of equations 3.26 and 3.27 into equation 3.25 and subsequent division by equation 3.24, the fractional uncertainty due to capacitance terms is obtained.

$$\frac{\delta W}{W} = \frac{\left\{ \left[(-C_m^{-2} - 2C_T C_m^{-3}) (\delta C_m) \right]^2 + \left[\frac{\delta C_T}{C_m^2} \right]^2 \right\}^{1/2}}{(C_m^{-1} + C_T C_m^{-2})} \quad \text{Equation 3.28}$$

With nominal values of C_i , C_m , ΔC_i and ΔC_m taken from the combination of data within tables 3.2 and 3.4 we obtain,

$C_T \sim 178$ pf (total of C_{i0} , C_{i1} , and C_m ref. figure 3.5)
 $C_m \sim 52$ pf
 $\Delta C_T \sim .15$ pf
 $\Delta C_m \sim .002$ pf

Upon substitution into the equation for the relative uncertainty due to the capacitance terms, these figures yield:

$$\frac{\Delta W}{W} \cong 660 \text{ ppm}$$

Equation 3.29

Calculating the uncertainty in e_1/i_1 due to uncertainty in capacitance, uncertainty in the voltage ratio and uncertainty in the preamplifier gain, we obtain,

$$\frac{\Delta \left(\frac{e_1}{i_1} \right)}{\left(\frac{e_1}{i_1} \right)} = \left[(660)^2 + (1447)^2 + (780)^2 \right]^{1/2} = 1770 \text{ ppm}$$

Equation 3.30

Next we will consider the measurement of the voltage ratio V_{ca}/V_{cb} .

3. The Measurement of V_{ca}/V_{cb}

Refer to the comparison voltage signal flowpath shown in figure 3.3 and reproduced below.

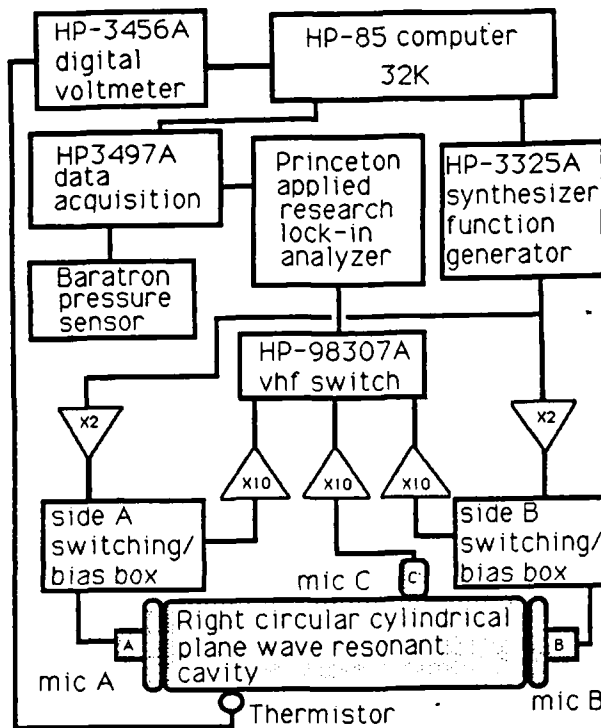


Figure 3.3 Signalflow path for comparison voltages

Since the signal path for the measurement of both " V_{ca} " and " V_{cb} " is *identical*, only the ratio of these measured voltages is important. As such, the non-linearity of the lock in analyzer will determine the error contributed by this ratio. When the non-linearities measured using the Gertsch ratio transformers are examined in table 3.7 and

table 3.8, the average non-linearity is much worse than that obtained at a scale reading of 0.9. The previous use of the non-linearity associated with a 0.9 scale reading for the ratio of V_{data}/V_{get} in the calculation of e_1/i_1 was possible only because the controlling program dynamically adjusted the transmitting sources until the receiving microphone gave an output in this scale region. No such dynamic adjustment was achieved for the comparison voltages V_{ca} or V_{cb} and they typically were at half scale. Since the probable error due to non-linearity in the system at half scale is ~ 3770 ppm, this is the value of probable error used for the ratio V_{ca}/V_{cb} .

4. Calculating The Reciprocity Factor "J"

Refer to equation 2.40 which is reproduced immediately below.

$$J_0 = \frac{\pi V_0 f_N}{P_0 \gamma_E Q_N}$$

Equation 2.40

Experimental calculation of the reciprocity factor, J_0 , required the measurement of five experimental parameters. These are the atmospheric pressure, the resonant frequency, the quality factor of each modal resonance, the ratio of specific heats for the gas within the cavity, and the cavity volume. Two other experimental parameters varied over the course of the experiment and required measurement in real time. These parameters were the temperature and the relative humidity. The relative humidity and temperature will cause a change in the ratio of specific heats [Ref.25], and any temperature change affects the speed of sound and hence the resonant frequency obtained. A discussion of the means used to measure all of these parameters will be presented next.

a. Measuring Atmospheric Pressure

Changes in the ambient pressure were monitored using a high precision MKS Baratron pressure head sensor, model 270 with a HS6-1500 purifying diffusion pump, type 162 all of which then was calibrated by comparison to the ambient pressure at the experimental altitude. The absolute reference was provided as data determined by the Meteorological Department at the Naval Postgraduate School. The data was available at 15 minute intervals and was compared over roughly one weeks time. The correction so determined was applied to the output of the Baratron's associated electronics signal as measured by the Hewlett Packard 3456A digital voltmeter. Refer to figure 3.15 below for a sketch of the pressure sensor signal path.

AD-A164 149

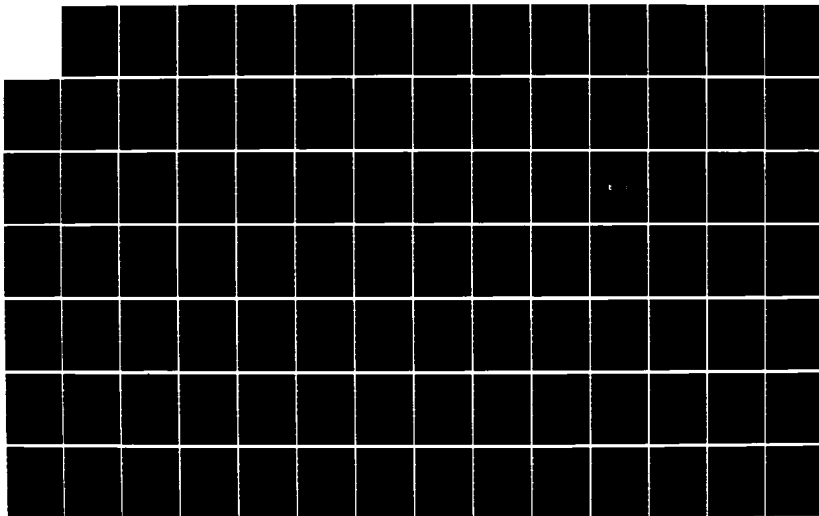
RECIPROCITY CALIBRATION IN A PLANE WAVE RESONATOR(U)
NAVAL POSTGRADUATE SCHOOL MONTEREY CA C L BURNASTER
DEC 85 NPS61-86-006

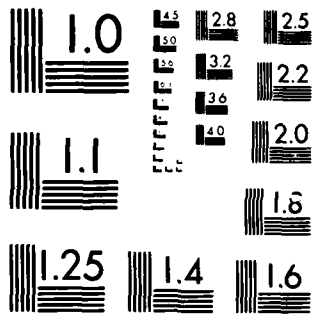
3/3

UNCLASSIFIED

F/G 14/2

NL





MICROCOPY RESOLUTION TEST CHART
NATIONAL BUREAU OF STANDARDS 1963-A

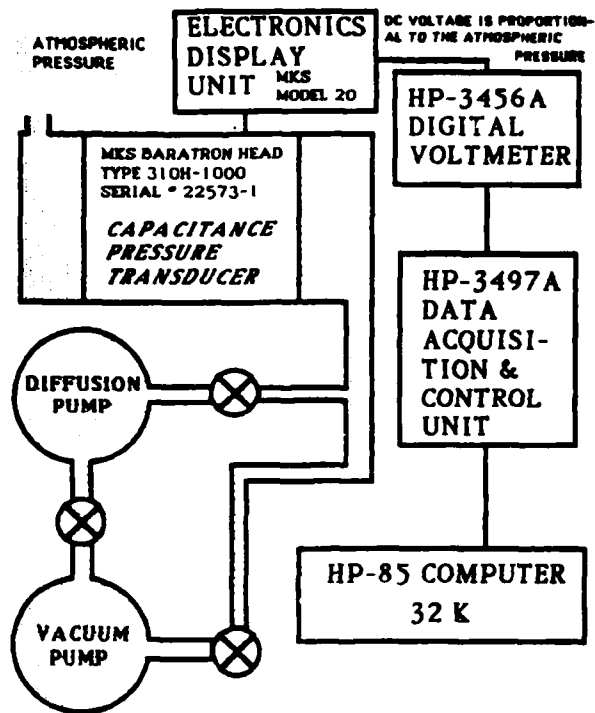


Figure 3.15 The pressure sensor signal path.

The data used to obtain the calibration for the output of the baratron pressure head is plotted in figure 3.16 and is a plot of the output of the Baratron system over approximately one weeks time. The output of the MKS baratron pressure head is scaled to indicate mmHg (Torr) so that the correction calibration of +5.68 mbar becomes +4.26 mmHg in the software implementation of this calibration.

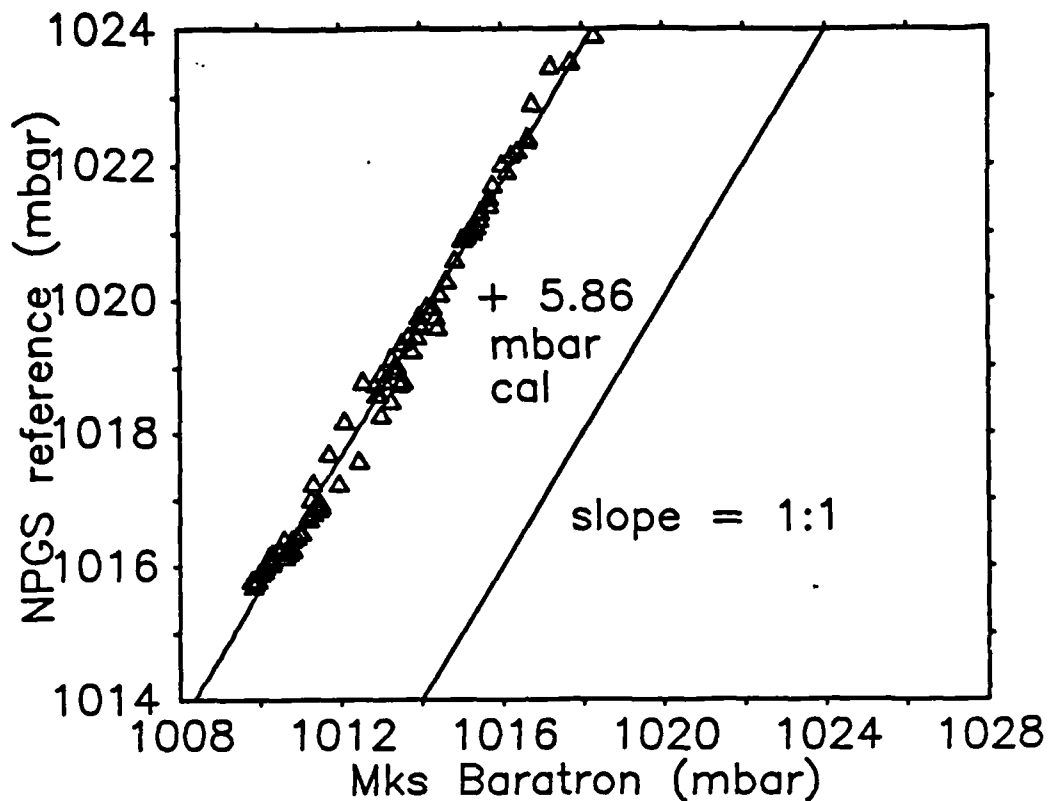


Figure 3.16 Pressure sensor vs. pressure reference

The precision of this pressure reading is observed as deviations from the least square fit to a straight line. The deviations range from $\sim .1$ mbar to ~ 1.2 mbar and the average value is $\sim .25$ mbar. If the systematic error is taken as the claimed accuracy of the Naval Postgraduate School reference, ($\sim .2$ mbar) the probable error in pressure is ~ 319 ppm.

b. Uncertainty in Resonant Frequency and Quality Factor

Plane wave longitudinal resonances in the "short" cylindrical cavity were sampled and analyzed using the least square error ravine process referred to in step 6 of part C in this chapter. The inaccuracies found in measuring the quality factor generally increase with the sharpness of the resonance. Since the short tube had higher Q's for its modal resonances, it was selected for this experimental determination of the precision of F_n and Q_n . As such, the fractional error in Q_n found using the short tube will be the upper bound on the determination of the fractional error in Q_n for the experimental calibration. There is no experimental reason to expect any difference in the precision found for F_n determined in the long tube compared with that determined in the short tube. It must be noted, however, that the fractional error in the determination of resonant frequency does not enter into the calculation for the open circuit receiving voltage sensitivity shown in equation 3.1 since the resonant frequency in the denominator of the ratio found for e_1/i_1 is cancelled by the resonant frequency found in the numerator of the reciprocity factor, J. The analysis that follows for the probable error in F_n is included only for completeness. The transducers used as source and receiver for these measurements were type W.E.640AA condenser microphones mounted in the ends of the plane wave resonant cavity.

Normally, the computer program that controlled the experiment caused first one condenser microphone to act as a source and the other as a receiver and then switched the roles of source and receiver so that reciprocity data could be obtained. To determine the precision of the numerical algorithm that obtained a least mean square error fit to a Rayleigh line shape, two such sets of data were still obtained but the program was not allowed to switch roles between source and receiver after the first data set was sampled. See figure 3.17 below for an illustration of how the Rayleigh line shape was sampled around resonance.

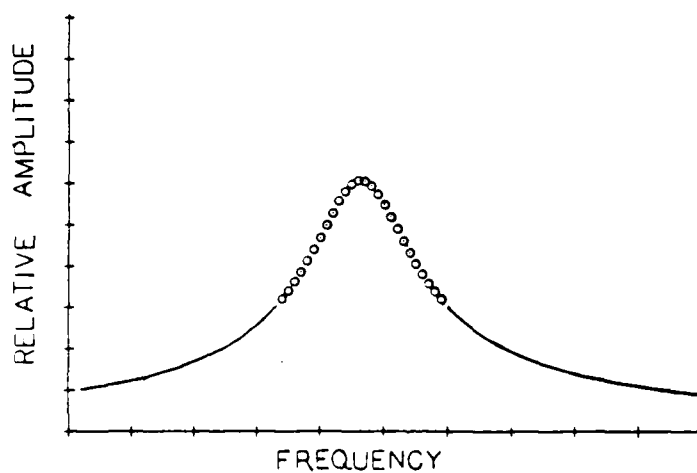


Figure 3.17 Data sample of a modal resonance from which a ravine F_n , Q_n , and amplitude are obtained.

With no change in the source or receiver, two such data sets were obtained one after the other. After both data

sets were ravined, an immediate comparison in resonant frequency and quality factor for the mode under inspection was made. When several modes were sampled many times, sufficient data was available to determine the precision of the ravine technique by direct comparison. Since the *relative humidity* varied within the laboratory on a time scale of hours while the *temperature* within the laboratory changed noticeably every few minutes, only the change in average temperature as measured by the thermistor shown in figure 3.3, was important for comparison purposes as the mean time between data set 1 and data set 2 was approximately 45 seconds. The fact that the speed of sound in an ideal gas is proportional to the square root of the absolute temperature was used to normalize all the ravined resonant frequencies to a common temperature of 20 degrees celsius for comparison purposes. These normalized resonant frequencies and the associated quality factors for three selected modes are given in table 3.9 below.

	Data set 1		Data set 2	
	Fn1 (Hz)	Qn1	Fn2 (hz)	Qn2
Mode 6	4418.3168	136.0039	4418.3753	136.0080
	4418.3466	135.9561	4418.3059	135.9890
	4418.2921	135.9326	4418.2692	135.9356
	4418.2725	135.8651	4418.2368	135.8540
	4418.2727	135.9193	4418.2463	135.9010
	4418.2624	135.9017	4418.2475	135.8697
Mode 10	7371.1629	127.7876	7371.3382	127.7575
	7371.4691	127.7841	7371.4724	127.7953
	7371.5582	127.8270	7371.5235	127.8268
	7371.5865	127.8205	7371.5533	127.8211
	7371.6375	127.8591	7371.6006	127.8483
	7371.6222	127.8077	7371.5953	127.8442
	7371.6297	127.8777	7371.5867	127.8813
	7371.6051	127.8772	7371.5731	127.8668
	7371.6250	127.9132	7371.5900	127.9086
	7371.6005	127.8899	7371.5709	127.9129
	7371.6039	127.8869	7371.5771	127.8824
	7371.6055	127.9279	7371.5650	127.9199
	7371.6589	127.8962	7371.6269	127.7822
	7371.6643	127.7987	7371.6503	127.8922
	7371.6897	127.9481	7371.6636	127.9464
Mode 22	16164.2490	184.8521	16164.6214	184.8147
	16165.1969	184.2745	16165.2196	184.2566
	16165.4770	184.2353	16165.4558	184.2680
	16165.6858	184.6545	16165.6152	184.7035
	16165.7553	185.2799	16165.7331	185.3310
	16165.8517	185.9562	16165.8137	186.0090
	16165.8158	186.3843	16165.6702	186.4248
	16165.8549	186.9020	16165.7844	186.8726
	16165.9372	187.4353	16165.6821	187.3151
	16165.9394	187.9696	16165.8735	188.0011

Table 3.9 Temperature normalized resonance frequencies and the associated quality factors for three different modes.

In the following two graphs of the fractional error found between data set 1 and data set 2, the vertical axis is in parts per million (ppm) fractional error and the

horizontal axis is taken from gaussian probability paper [Ref. 28: p.67] and is plotted as the percent of readings at or below the value found on the vertical scale. Such a plot illustrates the distribution of a data set with a gaussian distribution as a straight line. By calculating the correlation coefficient of the *plotted data* as a function of an arbitrary linear horizontal scale, the correlation to a straight line is determined.

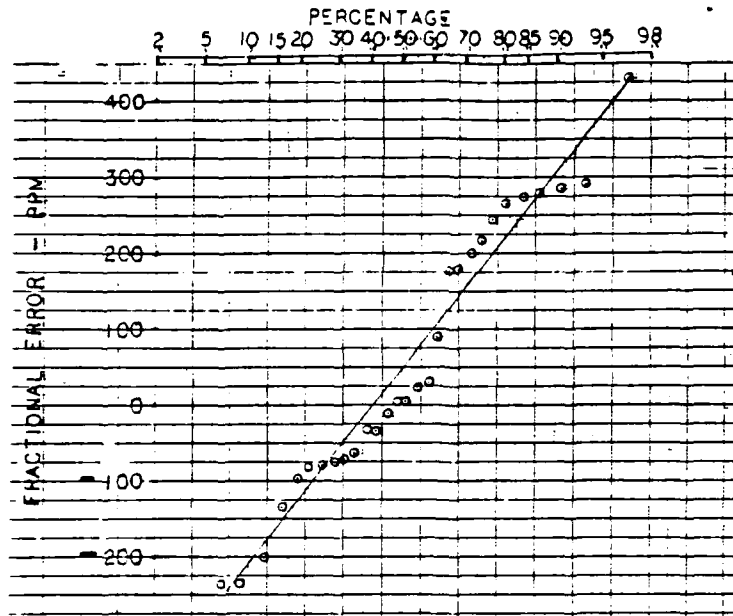


Figure 3.18 Fractional error in quality factor
plotted on probability paper. The linear correlation coefficient
is equal to .98

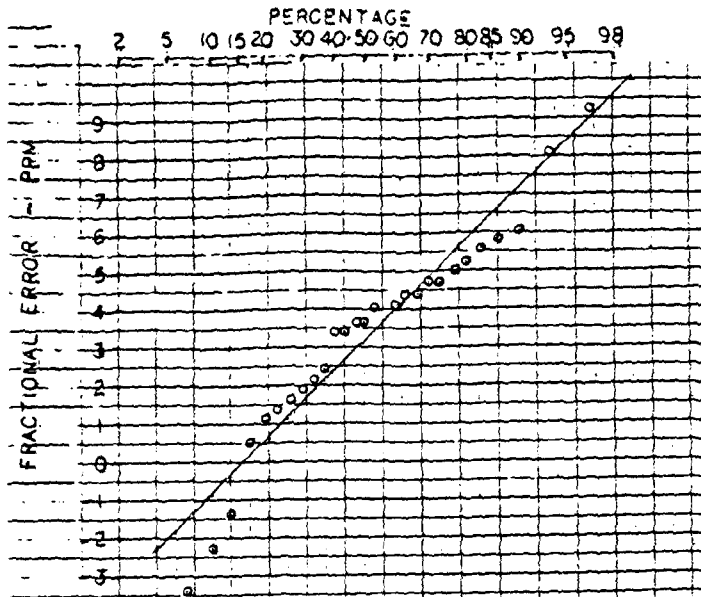


Figure 3.19 Fractional error in resonant frequency
plotted on probability paper. The linear correlation coefficient
is equal to .97

All the data shown in table 3.9 was used. Since both of the probability plots seem to roughly fit a straight line, the conclusion is that the data sets have roughly a gaussian distribution and as such, the standard deviation is taken as a measure of the precision of the technique. For the quality factor, the probable error is then ~ 180 ppm. For the resonant frequency, the above results show a probable error of ~ 7 ppm.

c. Calculating The Effect of The Non-adiabatic Boundary Conditions Upon The Stiffness of The Gas Within The Resonant Cavity

In chapter one, two methods of calculating the bulk modulus of elasticity of the gas within the plane wave resonant cavity are shown in equation 1.81. The starting point of this analysis is the adiabatic form of the bulk modulus of elasticity given as the product of the atmospheric pressure and the ratio of specific heats of the gas within the cavity. It will be shown that the effective ratio of specific heats of the gas within the plane wave resonant cavity will be determined by the gas content, the thermal properties of the physical boundaries, and the ratio of volume to surface area for the physical cavity.

The temperature and relative humidity change the ratio of specific heats in an empirical equation determined by Wong and Embleton [Ref.25]. Their result is given below. The relative humidity (the mole fraction of water vapor in humid air divided by the mole fraction of water vapor in saturated humid air) is given by "h" and the temperature in degrees centigrade is given by "t".

$$j_H = 1.39984 - A(h + 0.125)$$
$$A = 5.2 \times 10^{-4} + 4 \times 10^{-5} t + 7.5 \times 10^{-7} t^2 + 4.5 \times 10^{-8} t^3 \quad \text{Equation 3.31}$$

This equation will provide the value for gamma (the ratio of specific heats, c_p/c_v) for free field reciprocity calculations.

In order to consider the effect of the non-adiabatic conditions along the boundary of the plane wave resonant cavity, the influence of the thin layer of air in contact with the wall upon the stiffness of the gas within the cavity must be examined. Since the wall of the cavity is made of brass, with a thermal conductivity four orders of magnitude greater than air, and the heat capacity of the brass tube is four orders of magnitude greater than the heat capacity of the air contained within, the condition along the thin layer of air next to the wall is approximately isothermal. The stiffness of this small layer is therefore slightly less than that of the remainder of the air volume within the cavity. The overall bulk modulus must therefore be reduced slightly to account for this effect.

Since the ratio of specific heats given by Wong and Embleton is valid many thermal layer depths away from the wall and the ratio of specific heats for the isothermal case is equal to one, the effective gamma is first approximated by volume weighting the thermal layer with a gamma of one and the remaining air column with the value of gamma given in equation 3.31. To first order in thermal layer depth, this yields an effective gamma as shown below,

$$\gamma_E \cong \gamma_H - 2(\gamma_H - 1) \frac{\delta_T}{r_0}$$

Equation 3.32

Here, the thermal layer depth is given by [Ref. 27: pp. 225-6],

$$\delta_T = \left\{ \frac{2K}{\rho \omega c_p} \right\}^{1/2}$$

Equation 3.33

Where,

- K = thermal conductivity [J/sec*M*degK]
- ρ = air density [Kg/M³]
- c_p = specific heat at constant pressure [J/Kg*degK]
- ω = 2π *frequency [rad/sec]

thus,

$$\begin{aligned} \delta_T &\sim (2.5E-3)/\text{sqr}\{f\} \text{ [meters]} \\ r_0 &= 1.256E-2 \text{ M (short tube)}, 1.718E-2 \text{ M (long tube)} \end{aligned}$$

If the end effects are not neglected, equation 3.32 must be modified as shown below where "L" is the length of the cavity.

$$\gamma_E \cong \gamma_H - 2(\gamma_H - 1) \left(\frac{\delta_T}{r_0} + \frac{\delta_T}{L} \right) + \left(\frac{\delta_T}{L} \right)$$

$$r_0 < L, \quad \delta_T \ll L$$

Equation 3.34

When the ends are accounted for to first order in thermal layer depth, the relative change in the corrected value of gamma over that which is calculated when the ends are neglected is .003 percent and .01 percent for the long and short tubes respectively. Since the simple model used to obtain equation 3.32 yields an approximate correction to gamma on the order of 0.5 percent, the ends are neglected in the following analysis.

To verify that the preceding analysis is correct to first order in thermal layer depth, a more precise analysis is required. When the change from adiabatic to isothermal is modeled as an exponential change following the known thermal characteristics within the right circular cylinder [Ref. 28], and when the boundary value for gamma is matched both at the wall of the cylinder and within the volume, then the volume weighting of the adiabatic bulk modulus is reflected in an effective value of gamma given by,

$$\gamma_E = \frac{2\pi}{\text{END AREA}} \int_{r=0}^{r_0} r \left[\gamma_H - (\gamma_H - 1) e^{-\frac{r_0 - r}{\delta_T}} \right] dr \quad \text{Equation 3.35}$$

And to second order in thermal layer depth, the solution is,

$$\gamma_E = \gamma_H - 2(\gamma_H - 1) \frac{\delta_T}{r_0} + 2(\gamma_H - 1) \left(\frac{\delta_T}{r_0}\right)^2$$

Equation 3.36

This solution agrees with that of equation 3.32 to first order in thermal layer depth. This correction is shown below as a function of frequency in figure 3.20.

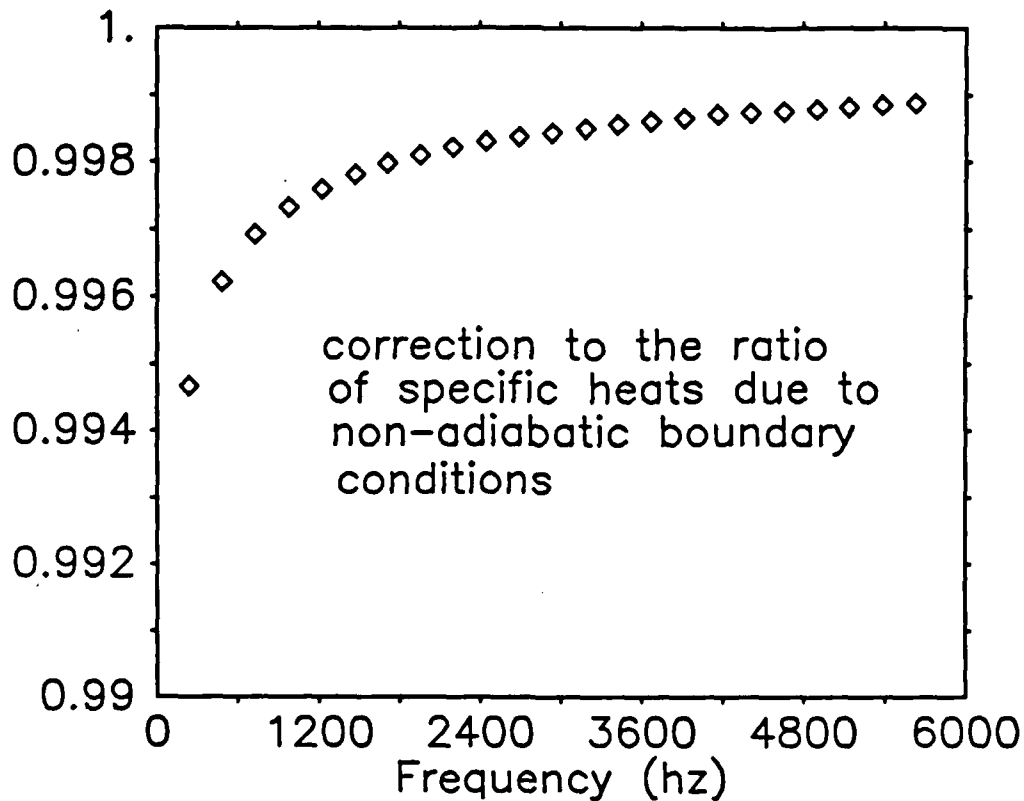


Figure 3.20 Correction to the ratio of specific heats due to the non-adiabatic boundary conditions within a right circular brass cavity 70.1 cm long and 1.73 cm radius, filled with air.

This correction, applied to the value of gamma and used with ambient pressure to calculate the adiabatic bulk modulus, provides the correction to the adiabatic bulk modulus of elasticity due to the non-adiabatic boundary conditions within a specific (the "long" tube) right circular plane wave resonant cavity.

When the restrictions given for equation 3.34 apply, the effective ratio of specific heats, valid to first order in thermal layer depth, can be put in a more general form:

$$\gamma_E = \gamma_H + (1 - \gamma_H) \left\{ \left[\frac{\kappa}{\pi \rho c} \right]^{1/2} \left[\frac{\text{Surface Area}}{\sqrt{f} \text{ Volume}} \right] \right\} \text{Equation 3.37}$$

In general, the independent parameter used to plot the magnitude of this correction to the open circuit voltage receiving sensitivity is given as "B", where:

$$B = \left\{ \left[\frac{\kappa}{\pi \rho c} \right]^{1/2} \left[\frac{\text{Surface Area}}{\sqrt{f} \text{ Volume}} \right] \right\} \text{Equation 3.38}$$

The correction described by equation 3.37 in terms of "B" is shown in the figure below.

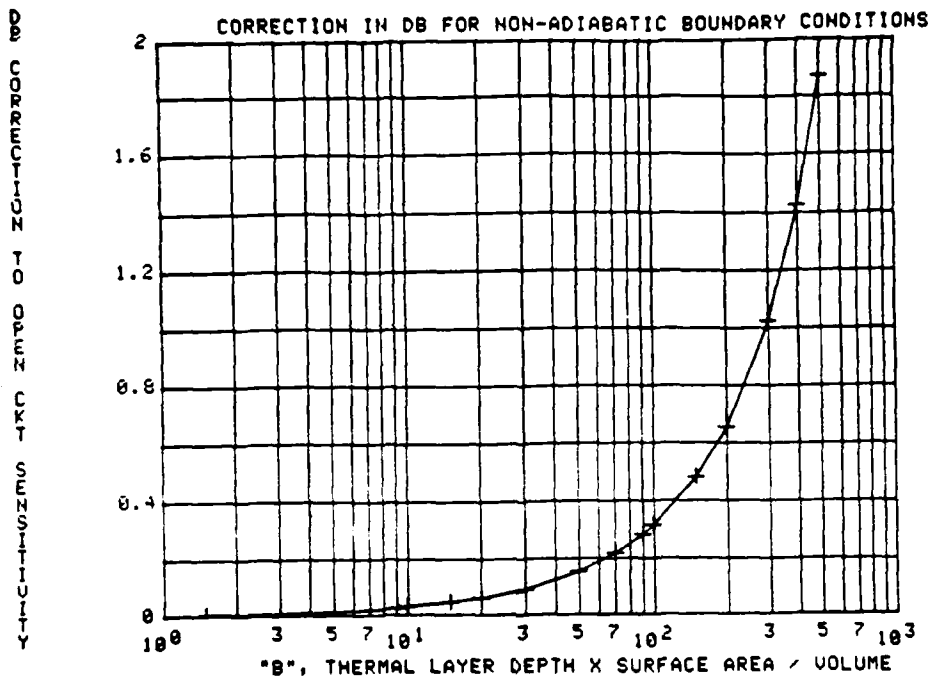


Figure 3.21 The correction to Mo due to the change in stiffness of the gas within the cavity caused by the non-adiabatic boundary conditions.

The correction shown above does not correct for heat conduction losses at the boundary of the tube. Heat conduction losses, as well as any acoustical loss, will be determined in the *experimental measure of Qn* which is then directly employed in the calculation of the acoustical transfer admittance, Jo.

Since the paper of Wong and Embleton was not available when the computer program controlling the experiment was

written, a correction to the preliminary experimental results is needed. The experimental data that was obtained using the program in appendix B, used a less accurate correction to the ratio of specific heats to account for the effects of changes in temperature, humidity, and the effect of the non-adiabatic boundary layer (See appendix B, lines 3770-3810). This approximate solution for the ratio of specific heats must be corrected to that obtained by Wong and Embleton and the associated correction to the open circuit receiving sensitivity must also be made. Analytically, when the range of experimental temperatures is varied from 19 to 21 degrees centigrade and the range of experimental relative humidities is varied from 40% to 65%, the experimental result for the absolute value of the open circuit voltage receiving sensitivity, M_o , must be corrected by $+.007\text{dB}$ throughout the frequency range used as a result of using the ratio of specific heats in equation 3.31. When this correction is used, the experimental uncertainty in the ratio of specific heats is that obtained by Wong and Embleton and is given as 400ppm [Ref. 25].

d. Volume Measurements in The Plane Wave Resonant Cavities

Two different right cylindrical cavity resonators were used in the plane wave resonant reciprocity calibrations. The lengths were selected so that the resonant fundamental in the long tube was one third the resonant fundamental in the short tube. This allowed direct comparison of experimental results obtained with two different resonant cavities at every third modal resonance of the long tube.

The actual experimental volume was measured in a straightforward way with a slight negative correction necessary due to the small protrusion of the W.E.640AA type microphones into the cavity. The microphones were adjusted in position so that the longitudinal equilibrium positions of the diaphragms were flush with the plane of the physical end of the cylinder. Since there were three different microphone pairs each with their own volumetric protrusion into the main volume, three different experimental corrections were measured and applied to the basic volume found for each resonant cavity. The results obtained using two different gauge calipers (one Peacock caliper and one Kanon caliper) are shown below in table 3.10.

Long Cylindrical Cavity vs. Short Cylindrical Cavity

End area shape ~ Circular ~ Elliptical
 average eccentricity e < .033 e ~ .094

The following data have four significant digits:

End area	9.2758E-4 M ²	4.9577E-4 M ²
Length	7.0120E-1 M	2.3372E-1 M
Basic volumes	6.5042E-4 M ³	1.1587E-4 M ³

Individual microphone volumetric protrusions.

W.E.640AA Serial - protrusion

1248	3.407E-7 M ²
1082	3.084E-7 M ²
0815	3.370E-7 M ²

Serial pair W.E.640AA's	Long tube volume corrected value	Short tube volume corrected value
1248 - 1082	6.4977E-4 M ³	1.1522E-4 M ³
1248 - 0815	6.4974E-4 M ³	1.1519E-4 M ³
1082 - 0815	6.4977E-4 M ³	1.1523E-4 M ³

Table 3.10 Volume measurements obtained for the
plane wave cavity resonators

When the relative error in each of these volumes is calculated, the values obtained depend essentially upon which resonant cavity is being used. Since the thermal expansion coefficient for brass is $\sim 1.9E-5/\text{deg C}$ and the temperature range in the laboratory was from 19 to 22 degrees centigrade, the fractional error in length due to thermal effects was ~ 30 ppm. Since the uncertainties in

measuring the length of the long tube at least one order of magnitude greater, the thermal effects were neglected for calculations of volume.

For the long cavity, refer to equation 3.39.

$$\frac{SV_0}{V_0} = \left\{ \left(\frac{2SD_d}{\text{Dia.}} \right)^2 + \left(\frac{SL}{L} \right)^2 \right\}^{1/2} \quad \text{Equation 3.39}$$

The uncertainties in the individual measurements were found to be,

The average length of long tube = 7.012 E-1 M

The standard deviation in length = 2.08E-4 M, based on three measurements made with a Kanon vernier calipers ser.#5K014 from the USNPGS Mechanical Engineering Dept.

The average diameter of long tube = 3.437E-2 M

The standard deviation in diameter = 2.85E-5 M, based on eight measurements made with a Peacock vernier calipers from the USNPGS Physics Dept.

Next, use is made of the fact that with a random distribution of error in the measurements, the standard deviation divided by the square root of the number of samples is the standard deviation in the estimate of the sample mean. With these considerations and including the systematic error involved in neglecting the effects of thermal expansion, the uncertainty in the volume measured for the large tube was found to be ~ 612 ppm.

When careful measurements of the dimensions of the small cavity were made, the model used to calculate the end area had to be that of an ellipse since definite major and minor axis were measured at each end of the tube. Using equation 3.40, the uncertainty in the volume was calculated. The semi-major axis is given by "a" and the semi-minor axis is given by "b".

$$\frac{\delta V_0}{V_0} = \left\{ \left(\frac{\delta a}{a}\right)^2 + \left(\frac{\delta b}{b}\right)^2 + \left(\frac{\delta L}{L}\right)^2 \right\}^{1/2} \quad \text{Equation 3.40}$$

The data used to calculate the experimental uncertainty in the volume of the small tube was measured exclusively with the Peacock gauge calipers and is shown below.

The average length of the small tube = 2.337 E-1 M

The standard deviation in length = 5.63 E-5 M, based upon twelve measurements made using the Peacock calipers.

The average semi-major axis of the end = 1.259 E-2 M, based upon twelve measurements made using the Peacock calipers.

The standard deviation in the semi-major axis = 4.85 E-5 M

The average semi-minor axis of the end = 1.254 E-2 M, based upon fourteen measurements made using the Peacock calipers.

The standard deviation in the semi-minor axis = 5.18E-5M, based upon fourteen measurements made using the Peacock calipers.

Using the above values, the uncertainty found for the small tube is calculated using equation 3.40. As expected, the relative error was greater with the smaller volume and the uncertainty in the volume measured for the small tube (including the systematic error involved in ignoring thermal expansion) was calculated as ~ 1569 ppm.

e. Measuring Temperature and Relative Humidity

Since both the temperature and the relative humidity found within the lab directly affected the ratio of specific heats as shown by equation 3.31 and the temperature change affected the thermal expansion of the brass cylinder, these experimental parameters were also measured.

The measure of temperature occurred under program control before and after each basic 26 point data set was obtained. The two values were averaged and this value was stored with the acoustic data. Since the two temperature samples were obtained symmetric in time around the sample obtained for the center frequency of the modal resonance, the average value obtained is the estimate of temperature associated with that modal resonance. The equipment used to automate this measurement of temperature was a HP-3456A digital voltmeter sampling the output of HP0837-1064 thermistor \pm directed by the HP-85 computer. The equipment could easily track relative temperature changes on the order of .001 degree centigrade. The useful temperature range for this setup was -80 to 130 degrees centigrade, well beyond the normal range of 19 to 22 degrees centigrade found in the laboratory. The thermistor was sealed and placed into a bath of icewater where its output was observed to be +.20 degrees centigrade which was then calibrated to the triple point of water (.01 degrees centigrade at 1 atmosphere) by subtracting .19 degrees. Thus, the fractional error in

absolute temperature sampled by the system is estimated to be $(\pm) .01$ degrees absolute or ~ 34 ppm for a standard laboratory absolute temperature of 293 degrees.

The percent relative humidity was sampled only at the beginning of each program run and was assumed to be constant for the duration of each run. A Durotherm relative humidity gauge built by Sussp Co. of West Germany was used to observe the value of relative humidity to $\sim 1\%$. This observed value was then manually input to the computer where it was used for all the calculations. During the course of several months, the range of relative humidities within the laboratory was observed to vary from 40 to 65 percent relative humidity. An average daily variation of $\sim (\pm) 5\%$ occurred during those portions of the day that experimental data was normally obtained. Over the course of any one program run, the largest change in relative humidity observed was 4 %, with an average change of 1%. When the largest change is considered using equation 3.71, the fractional error introduced into the open circuit receiving sensitivity by considering the relative humidity to be a known but constant value for the duration of the experiment was 28 ppm.

5. A Summary of Experimental Uncertainty For The Plane Wave Resonant Reciprocity Experiment

In addition to the sources of error previously discussed, two more sources were considered. First, the open circuit receiving sensitivity is directly proportional to the bias voltage used to bias the condenser microphones. The battery power supplies built to bias the condenser microphones provided an approximate D.C. voltage of ~ 120 volts. Since the battery voltage depended greatly upon the temperature, real time sampling of the bias voltage was done with each basic 26 point data set using the HP-3456A digital voltmeter. The specifications of the digital voltmeter claim a measurement accuracy of 40 ppm traceable to the National Bureau of Standards and this is the probable error used for the bias voltage.

Second, since the frequency of longitudinal resonance will vary linearly with the square root of absolute temperature, slight differences in the calibration frequency of the "Nth" mode were observed due to temperature variations within the laboratory from one day to the next. The range of temperatures in the lab was from ~ 19 to ~ 22 degrees centigrade which results in a potential 0.5% maximum shift in the calibration frequency associated with a particular mode. The average slope of the open circuit voltage receiving sensitivity versus frequency for the highest 10 modes was $\sim -.00024$ dB/Hz. For comparison

purposes, this corresponds to roughly a .007 dB difference in sensitivity over a 28 Hz maximum frequency shift at the 23rd mode. This temperature dependent systematic error is neglected during measurements of experimental precision since this possible shift is roughly an order of magnitude smaller than other observed uncertainties.

A summary of the probable error found in experimental parameters is shown below in table 3.11. Equation 3.2 has been modified by deleting F_n and adding the uncertainty caused by the bias voltage to calculate the overall probable error. The result shows the relative uncertainty in the open circuit voltage receiving sensitivity and is given in equation 3.41.

$$\frac{\Delta M_A}{M_A} = \frac{1}{2} \left\{ \left[\frac{\Delta \left(\frac{e_i}{i_i} \right)}{\left(\frac{e_i}{i_i} \right)} \right]^2 + \left[\frac{\Delta \left(\frac{V_{CA}}{V_{CB}} \right)}{\left(\frac{V_{CA}}{V_{CB}} \right)} \right]^2 + \left[\frac{\Delta V_0}{V_0} \right]^2 + \right. \\ \left. \left[2 \frac{\Delta E_{bias}}{E_{bias}} \right]^2 + \left[\frac{\Delta P_0}{P_0} \right]^2 + \left[\frac{\Delta \gamma_E}{\gamma_E} \right]^2 + \left[\frac{\Delta Q_N}{Q_N} \right]^2 \right\}^{\frac{1}{2}} \quad \text{Equation 3.41}$$

parameter	probable error (ppm)	
	expected	vs. range
1. ratio V_{ca}/V_{cb} (scale \sim .5) (non-linearity)	3800	(1900-5600)
2. ratio e_1/i_1 a. ratio (V_{data}/V_{get}); 1450 ppm b. system capacitance; 660 ppm c. preamplifier gain; 780 ppm	1800	(900-2500)
3. atmospheric pressure	320	(220-1200)
4. quality factor, Q_n	180	(80-310)
5. resonant frequency, f_n	7	(5-9)
6. ratio of specific heats	400	N.A.
7. cavity volume, long tube	1200	(610-1700)
8. cavity volume, small tube	3600	(1600-5700)
9. bias voltage	60	(40-80)

Table 3.11 Summary of probable error in experimental parameters

With these probable errors, the *expected uncertainty* in the "long tube" plane wave resonant reciprocity calibration is roughly 2200 ppm or $\sim .02$ dB re 1 V/ubar with a range of up to 3300 ppm or $\sim .03$ dB re 1 V/ubar. In the short tube, the *expected uncertainty* in the plane wave resonant reciprocity calibration is roughly 2780 ppm or (rounding up) $\sim .03$ dB re 1 V/ubar with a range of up to 4200 ppm or $\sim .04$ dB re 1 V/ubar. When the precision of the preliminary experimental results is presented and discussed in chapter

IV, it will be seen that this expected experimental uncertainty is of the same order of magnitude as the precision observed in the experimental results.

The absolute accuracy of the final calibration will still require corrections to the raw program output to account for:

- the compliance of the microphones,
- the motional impedance of the microphones,
- the non-standard definition of the capacitance of the WE640AA microphone which includes the capacitance of the BNC electrical connector extending the microphone cartridge,
- the change of stiffness of the gas within the cavity due to non-adiabatic boundary conditions, and
- the corrections associated with accurate measurements of capacitance for the cables, the bias circuits, and the microphones (opposed to the approximate values used in the computer program).

In the next section, the experimental procedure and associated uncertainty in the comparison calibration will be examined.

SIGNAL FLOW AND COMPUTER CONTROL FOR THE FREE FIELD
COMPARISON CALIBRATION

1. Introduction

The intent of this portion of the experiment was to obtain an accurate low frequency free field calibration for the W.E.640AA condenser microphone as a check on the absolute accuracy of the resonant reciprocity calibration. At very low frequencies, the diffraction correction goes to zero [Ref. 3: p.33, Fig. A2] and the free field results are useful for comparison with the plane wave resonant reciprocity calibration and the standard pressure coupler calibration. Since the W.E.640AA condenser microphone had such a low acoustical output in the frequency range of interest, a free field reciprocity calibration for this microphone was not obtained. Instead, sufficient data was obtained to compute a free field reciprocity calibration for an Altec type 688 electrodynamic microphone which was then used to compute a free field comparison calibration for the W.E.640AA condenser microphone.

2. Experimental Considerations for a Free Field Comparison Calibration

The free field reciprocity equations developed in chapter one are difficult to use directly with a condenser microphone when used as a speaker at low frequency due to the low acoustic output of a condenser microphone. The Altec type 688 electrodynamic microphone performs well in this frequency range when used as a speaker. Using this feature to advantage, a free field comparison calibration for the W.E.640AA condenser microphone is more easily obtained.

Starting with equations 1.30 and 1.84, we have,

$$\frac{V_A}{M_A} = \frac{V_B}{M_B}$$

Equation 1.30

and,

$$M_A = \left\{ \frac{e_4 V_A 2 \lambda r}{i 1 V_B e_0 c} \right\}^{1/2}$$

Equation 1.84

Let "Ma" refer to the Altec type 688 electrodynamic microphone and "Mb" to the W.E.640AA condenser microphone. Then, solving equation 1.30 for Mb and substituting the solution for Ma into the result, we obtain,

$$M_B = \left\{ \frac{e^4 V_B a r}{i_1 V_A f \rho_0} \right\}^{1/2}$$

Equation 3.42

When the standard relationship between density, atmospheric pressure and temperature [Ref. 9: p.40] is substituted into equation 3.42, we are able to obtain the form of the equation used in the experiment to obtain the free field comparison calibration for the W.E.640AA condenser microphone. The equation used in the computer program in appendix D differs only in the scale factor necessary for the units used.

$$M_B = \left\{ \left(\frac{e^4}{i_1} \right) \left(\frac{V_B}{V_A} \right) \left(\frac{T_K r}{\rho f} \right) \left(\frac{2 \rho_0}{\rho_0 T_0} \right)_{STP} \right\}^{1/2}$$

Equation 3.43

Here we have, in addition to the definitions used from chapter 1:

- T_K = temperature in degrees kelvin.
- T₀ = standard temperature. (273 deg K)
- P = atmospheric pressure.
- P₀ = standard atmospheric pressure. 1 Atmos: 101350 Pa
- ρ = density of air at standard pressure and temperature.
(1.29305 kg/m³)
- r = separation in meters between source and microphone.

The above calibration was accomplished in two separate steps. First, a separate acoustic source was used to provide the same pressure field within an anechoic chamber for each of the frequencies of interest for the later comparison calibration. The program that facilitated the measurement of these ratios was called "VRATIO" and is listed in appendix C. These comparisons were stored in an array used in a subsequent computer program called "N28" that controlled the translation of the W.E.640AA condenser microphone while the 688 electrodynamic microphone performed as a stationary source. Program "N28" is listed in appendix D. The second step then consisted of running program "N28" at each frequency of interest. The next sections describe the operation of these two programs.

3. Measurement of The Sensitivity Ratio, M(640R)/M(688R)

The ratio of the W.E.640AA open circuit voltage receiving sensitivity to the Altec type 688A open circuit voltage receiving sensitivity (M(640R)/M(688R)) was measured using the circuit shown in figure 3.22 in the first part of a two step experiment to obtain the comparison calibration of the W.E.640AA condenser microphone. The figure shown below illustrates the the signal flowpath for the electrical equipment involved.

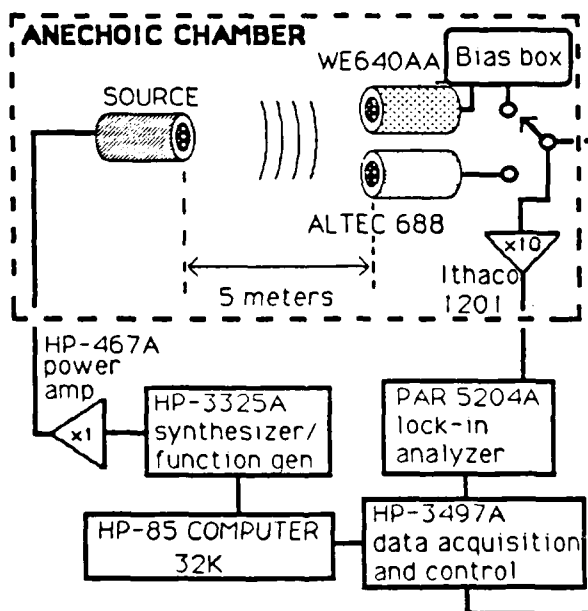


Figure 3.22 Signal flow used in measuring V_b/V_a inside the anechoic chamber.

The requirement that a free field calibration be carried out in a space that is free from surfaces which cause appreciable reflection of sound and free from background noise which may obscure the received signal [Ref 3: p.19] was met by using the anechoic chamber located at the Naval Postgraduate School, Monterey, California. It was found to satisfy the dimensional requirements [Ref.3: p.19] for a measurement error of less than ~ 0.1 dB. As will later be shown, a variation of calibration sensitivity due to suspected reflections from apparatus in the anechoic chamber were observed to be on the order of ~ 0.08 dB.

Each receiving microphone was hung at the same spatial location with a three wire support referenced to the front face of the microphones about five meters from the sound source. This was roughly three and one half wavelengths separation at the lowest frequency of interest. The nearest surface within the anechoic chamber was roughly two meters away from the three wire mounting point.

Program "VRATIO" worked as follows:

Step 1. The first microphone was mounted in position in the anechoic chamber and all visible motion was allowed to subside.

Step 2. Program "VRATIO" was set into operation. A separate speaker source is turned on by the computer program. The program samples the received signal and averages twenty five data points per frequency of interest. These average values are stored in an array labeled $A(1,M)$.

Step 3. When the program has completed sampling the first microphone, it pauses and asks the operator to mount the second microphone. When the first microphone is removed and the second mounted, and all swaying stops, the operator indicates that the microphone exchange is complete by pressing CONT.

Step 4. The program samples and averages twenty five data points per frequency of interest and stores the average values in the array A(2,M).

Step 5. The program calculates and prints the ratio $A(1,M)/A(2,M)$ and stores the result in array R(i). The standard deviation for each ratio is printed as "SQR(S)" and the program run is complete.

The results of the first step are given below.

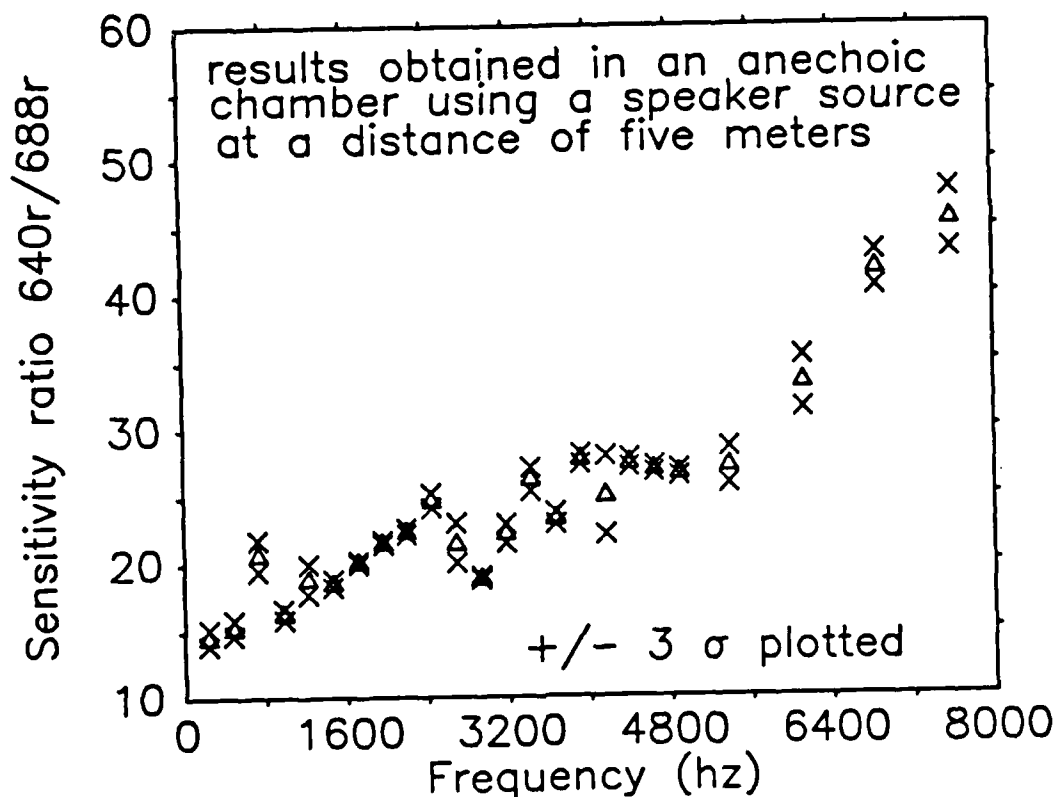


Figure 3.27 The sensitivity ratio obtained for 640R/688R.

To check the above results, consider the known sensitivity levels for type W.E.640AA and Altec type 68BA microphones, shown below.

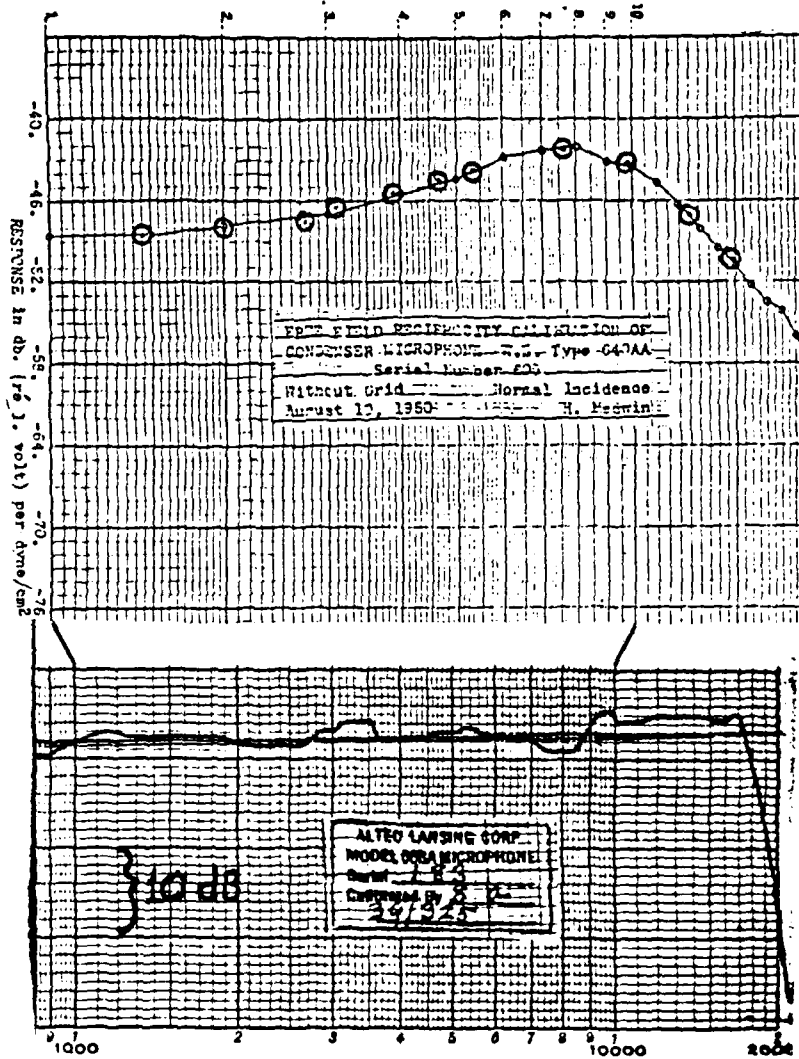


Figure 3.24 Mo for the W.E.640AA serial #'s 1248 & 609 (top) and the Altec type 68BA (bottom).

When the response of the 688 electrodynamic microphone is

divided point by point into the response of the 640 condenser microphone, quantitative agreement with the experimentally determined ratios shown in figure 3.23 is obtained. The values so obtained *did* result in the expected response for the condenser microphone. The actual free field calibrations obtained for the W.E.640AA serial#1248 condenser microphone are shown as the larger circles in the W.E.640AA sensitivity plot)

4. Free Field Reciprocity Measurements

A sketch of the experimental equipment used to make the final free field reciprocity measurements is given in the figure below.

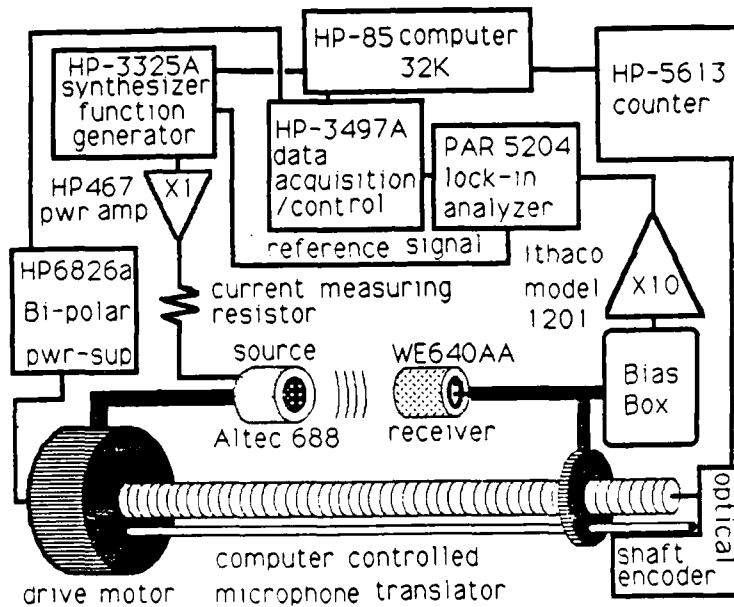


Figure 3.25 Signal flow in the free field comparison calibration based upon free field reciprocity.

A description of the operation of this final step in the free field comparison calibration is given below in the description of the operation of the controlling program.

The third computer program given in appendix D, was written to control the second half of the free field

comparison calibration based upon a reciprocity calibration. After the initial operator inputs are made, the data is sampled, analyzed and stored on magnetic tape. Separate computer runs are required for each frequency of interest. The operator must remain present during each data run to respond to interactive computer inputs.

The initial operator inputs are:

- insert comparison ratios for each frequency of interest into the program. (See Appendix C for the program used to obtain these ratios.)
- input the plane wave tube modal number of the resonance frequency desired. This will allow later comparison with the plane wave pressure calibration results after the diffraction effects of the free field calibration are subtracted out.
- input the driving voltage to be used by the synthesizer/ function generator.
- input the 5204 lock in analyzer's sensitivity scale.
- input the 5204 lock in analyzer's time constant.
- measure and enter the starting separation distance (cm) between the source and the receiver.
- measure and enter the 4 - wire current limiting resistor used in the driving circuit. (ohms)

The computer program will then perform the following steps;

Step 1. The function generator/synthesizer is set to the proper drive voltage and frequency. The source is turned on and the receiver output is monitored.

Step 2. The program samples the peripheral equipment for atmospheric pressure, ambient temperature, and the receiver bias voltage. These are temporarily stored in computer memory.

Step 3. The counters for the optical revolution counter are initialized. (The resolution is 1000 "counts" per 1 complete turn. One complete turn of the threaded drive shaft moves the receiving microphone about 1/8 of a centimeter.)

Step 4. The driving voltage for the main drive motor is turned on for exactly six seconds and then removed.

Step 5. The system waits fifteen seconds for all transverse motion to damp out. Then the program then takes thirty sequential samples (at intervals of three electronic time constants) of the received voltage. After averaging, the data is temporarily stored.

Step 6. When the eighth drive interval is complete, and the sequential sampling is complete for that interval, the program asks the operator to enter the anechoic chamber and measure and input to the program the separation between source and receiver. This will allow a spot check on the relative error of the measuring technique used by the operator.

Step 7. Return to step 4 and continue until twenty separation distances have been sampled. At the end of twenty intervals, the source is turned off, the bias voltage, ambient temperature, and atmospheric pressure are sampled and averages are obtained with the data obtained in step 2. These averages are then stored on magnetic tape.

Step 8. The program asks the operator to enter the anechoic chamber and measure the final separation and enter it into the computer.

Step 9. The initial and final operator entered distances allow the program to scale the counter registers. Arrays containing scaled values of received voltages and scaled values of the related separation distances are displayed to the operator and stored on magnetic tape.

Step 10. The program then performs a least squares fit of the received data to $\{ V(r) = E0/[r + a] \}$ r is the computer measured distance corresponding to $V(r)$, and "a" is correction to the separation distance needed to obtain spherical spreading.

Step 11. The values for $E0$ and "a" obtained by the least squares fit are printed for operator use and stored on magnetic tape.

Step 12. The program prints a plot of $V(r)$ vs r for operator viewing.

Step 13. The program prints a plot of $\log[V(r)]$ vs $\log[r]$ for operator viewing. Here a straight line indicates the region in the data array where $[1/r]$ spherical spreading occurred.

Step 14. The program calculates, prints and stores on magnetic tape the receiving sensitivity for this particular frequency as a function of range.

Step 15. The program shuts down awaiting a new set of initial operator inputs to go to the next frequency of interest.

The following three figures illustrate the output available to the operator as the above program is run. The data shown below was obtained for the 735 hz comparison calibration for W.E.640AA serial #1248. The 4-wire resistance measurement obtained previously for the calculation of the source current, i_1 , is output just before the raw data is printed. The parameters, "V0", "a", and the correlation coefficient, "R" refer to the least squares fit to $V0/(r+a)$ for this data used by the program. "N" is the number associated with a particular distance; "RUN" refers to the distance in cm. travelled since the last measurement; "R(CM)" refers to the separation distance in cm. between source and receiver for a particular measurement; and "VOLTS" refers to output voltage measured across the microphone at a particular distance.

PROGRAM OUTPUT

(COMMENTS)

633A TRANS,640AA RCV

configuration of microphones

633A TRANS,640AA RCV

value of 4-wire resistance

4WIRES-R(OHMS)=

66.939

TIME=

9.4899275

date = 22, May 1984

DATE=

522

N	RUN	R(CM)	VOLTS
1	1.562	16.052	2.10241E-004
2	1.558	17.620	1.89975E-004
3	1.558	19.178	1.73354E-004
4	1.554	20.732	1.59739E-004
5	1.548	22.280	1.48260E-004
6	1.548	23.828	1.38481E-004
7	1.550	25.378	1.29801E-004
8	1.551	26.928	1.21991E-004
9	1.557	28.485	1.15030E-004
10	1.558	30.043	1.08835E-004
11	1.559	31.602	1.03422E-004
12	1.554	33.156	9.86840E-005
13	1.557	34.714	9.40276E-005
14	1.558	36.272	8.91893E-005
15	1.566	37.838	8.46141E-005
16	1.561	39.399	8.03322E-005
17	1.554	40.953	7.64400E-005
18	1.554	42.507	7.29783E-005
19	1.547	44.053	7.00997E-005
20	1.547	45.600	6.76076E-005

main data

N = number of run

RUN = dist in cm for interval since last measurement

R(CM) = total separation in cm.

VOLTS = open ckt. received voltage

$V_0 =$ (VOLTS)

2.96750147274E-3

$a =$ (CM)

-2.40925074952

R =

.99677305408

Results of least square error analysis for $V(r) = V_0/(r+a)$

Figure 3.26 Raw data output from "N28"

PROGRAM OUTPUT

(COMMENTS)

```

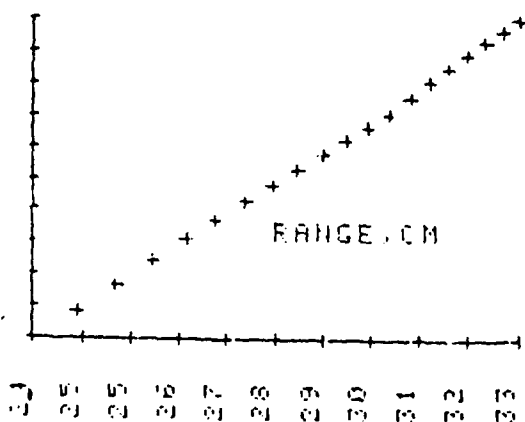
# OF MEASUREMENTS= 20
MEAS CHECK(CM)= 26.75
CALC DIST (CM)= 26.9282586845
DIST ^ERROR=
.666387505607
START DIST(CM)= 14.5
END DIST(CM)= 45.5
5204 SENS = .001
717 MVOLTS= 1200
TOTAL COUNT= 163164
FREQ (HZ) = 735
    
```

Eighth interval "spot" check on total separation.

percent fractional error for measured separation vs. calculated separation at the eighth interval.

5204 sens = scale selected on the PAR 5204 lock-in analyzer

717 MVOLTS = driving voltage output from the function generator in millivolts



At this point a log/-log plot is shown of the data. If the far field is a straight line with slope equal to +1, then the data is OK. That is to say, the spreading loss goes as $[1/r]$ (spherical spreading). If the line varies about a "straight" line, then standing waves or some other difficulty is being encountered and further experimental adjustment in the apparatus is required prior to taking data.

Figure 3.27. Quality control output from "N28"

PROGRAM OUTPUT

(COMMENTS)

```

33.156 2.0499E-002
DB RE 1V/UB0200VBIAS=
-49.0305189366
34.714 2.0510E-002
DB RE 1V/UB0200VBIAS=
-49.0250671534
36.272 2.0453E-002
DB RE 1V/UB0200VBIAS=
-49.0505545224

```

```

37.838 2.0375E-002
DB RE 1V/UB0200VBIAS=
-49.083064092

```

Here the last nine calibration measurements are shown with:

```

39.399 2.0288E-002
DB RE 1V/UB0200VBIAS=
-49.121353334
40.953 2.0200E-002
DB RE 1V/UB0200VBIAS=
-49.1582737186
42.507 2.0131E-002
DB RE 1V/UB0200VBIAS=
-49.1879232478
44.053 2.0107E-002
DB RE 1V/UB0200VBIAS=
-49.1983365912
45.600 2.0109E-002
DB RE 1V/UB0200VBIAS=
-49.1971631044

```

distance(cm)-sensitivity
(at ~ 116 V bias)
and sensitivity level in
dB re 1 V/ubar (at 200 V bias).

```

I1=
3.53087269409E-3
V0=
P9=
(MO)=
3.02593557046E-3
AVGDB 1V/UB0200VBIAS=
-49.1327049904
SIGMA=
1.59812697439E-4
<PRATIO=

```

I1 = the measured transmitting current

.236 V0 = least square error
65.839 reference voltage determined earlier.

average ratio determined with program VRATIO.

20.71

Figure 3.28 A sample of the final distance versus Mo calculated by program "N28"

At each frequency there were twenty measured values of M_0 corresponding to the twenty different measurement distances. The statistics shown at the end were computed using all twenty data points although the last figure only shows the last nine calibrations.

Before the final results can be plotted and interpreted, error analysis and potential corrections need to be considered. This will be done next.

F. EXPERIMENTAL ERROR FOR THE FREE FIELD COMPARISON CALIBRATION

1. Introduction

The equation used for the receiving sensitivity based upon a free field reciprocity calibration is derived in the previous section and is given in equation 3.43 which is reproduced below.

$$M_B = \left\{ \frac{e_4 V_B T_K r 2 \rho_0}{i_1 V_A \rho f \rho_0 T_0} \right\}^{1/2} \quad \text{Equation 3.43}$$

The source current, i_1 , is not directly measured but is determined from the voltage drop across a resistor in the speaker circuit and a four wire measurement of the resistance of this resistor. When the ratio $V(\text{drop})/R_4$ is substituted for i_1 , we have,

$$M_B = \left\{ \frac{(4.303) e_4 R_4 V_B T_K r}{V_{\text{drop}} V_A \rho f} \right\}^{1/2} \quad \text{Equation 3.44}$$

The expected probable error based upon this equation will be somewhat different than the probable error found for plane wave reciprocity.

$$\frac{SM_B}{m_0} = \frac{1}{2} \left\{ \left(\frac{\delta e_4}{e_4} \right)^2 + \left(\frac{\delta V_{drop}}{V_{drop}} \right)^2 + \left(\frac{\delta \left(\frac{V_B}{V_A} \right)}{\left(\frac{V_B}{V_A} \right)} \right)^2 + \left(\frac{\delta E_{bias}}{E_{bias}} \right)^2 + \left(\frac{\delta T_K}{T_K} \right)^2 + \left(\frac{\delta r}{r} \right)^2 + \left(\frac{\delta \rho}{\rho} \right)^2 + \left(\frac{\delta f}{f} \right)^2 \right\}^{1/2} \text{Equation 3.45}$$

The variables in equation 3.45 are defined as:

- e4 - the received voltage measured with the PAR 5204 lock-in analyzer.
- Vdrop - the voltage drop across the current limiting resistor found in the driving circuit. Used to measure the driving current. This was measured with an HP-3438A digital multimeter.
- R4 - The current limiting resistor used in the speaker circuit. This was measured with a 4-wire resistance measurement using the HP-3456A digital voltmeter.
- Vb/Va - Comparison voltage ratio measured by the program "VRATIO" described previously. Both of these voltages were measured on the PAR 5204 lock-in analyzer.
- T - Temperature in degrees centigrade. The HP-3456A digital voltmeter was used in conjunction with a thermistor (accessory No. 44414A) to sample temperature.
- r - The measured separation distance corrected for acoustic centers.
- P0 - Atmospheric pressure (mmHG) monitored and averaged during the data run. This parameter was obtained using the same experimental setup as was used and described in the previous section for plane wave resonant reciprocity.
- f - The frequency (hz) of the source signal. These frequencies were selected as multiples of 245 Hz for ease of comparison with the plane wave resonant reciprocity calibrations.
- Ebias - The bias voltage used for the W.E. 840AA condenser microphone.

These parameters and their calculated probable errors must be measured and included in the calculation for "Mb". The error analysis for the value of the atmospheric pressure, the temperature, and the frequency are the same as previously done in the case of the plane wave resonant calibration. The experimental methods used to measure the remainder of these parameters is presented next.

2. Measuring The Open Circuit Receiving Voltage, e4

a. Analysis of The Electrical Circuit Used to Measure e4

The received microphone voltage was measured in the manner shown in figure 3.25. The simplified circuit shown in figure 3.6 still applies to the analysis of the received signal. However, due to the different cables and cable capacitances involved, the values obtained for the transfer function will be slightly different. Equation 3.11 is still used to calculate magnitude of the received voltage. The value "e1" has been replaced with "e4" to conform to the notation used in the free field experiment.

$$e_4 = \left(\frac{B}{G}\right)(V_{data}) \left\{ \left(1 + \frac{C_T}{C_m}\right)^2 + \left(\frac{1}{\omega R C_m}\right)^2 \right\}^{1/2} \quad \text{Equation 3.11}$$

Since the $[\omega * R * C_m]$ term in the calculation of e4 is negligible for the purpose of error analysis, it will be neglected. The error analysis for e4 is given below.

$$\frac{\delta e_4}{e_4} = \left\{ \left[\frac{\delta [B V_{data}]}{B V_{data}} \right]^2 + \left[\frac{\delta G}{G} \right]^2 + \left[\frac{\delta \left(1 + \frac{C_T}{C_m}\right)}{1 + \frac{C_T}{C_m}} \right]^2 \right\}^{1/2} \quad \text{Equation 3.46}$$

Since the fractional uncertainty in the capacitance term may be calculated from previous uncertainty analysis (with $C_t \sim 255$ Pf.), and specifications for the PAR 5204 claim an uncertainty in the $B \cdot V_{in}$ product to be $\sim 1\%$ (although experimental measurement of consistency between attenuators and amplifiers showed a 0.2% accuracy), only the uncertainty in the amplifier gain for the Ithaco 1201 preamplifier remains to be determined prior to calculating the total fractional uncertainty in e_4 .

b. Determination of Gain Uncertainty for The Ithaco
1201 Preamplifier

The Ithaco preamplifier was used in the anechoic chamber because of its self contained battery power supply. In the anechoic chamber, severe electrical noise was preventing experimental progress until the Ithaco preamplifier was employed. Acoustically, the anechoic chamber was quiet. Electrically, it had 60 cycle interference. The following is a plot of the gain characteristics obtained for the Ithaco preamplifier when operated on AC power as compared to operation with the internal battery.

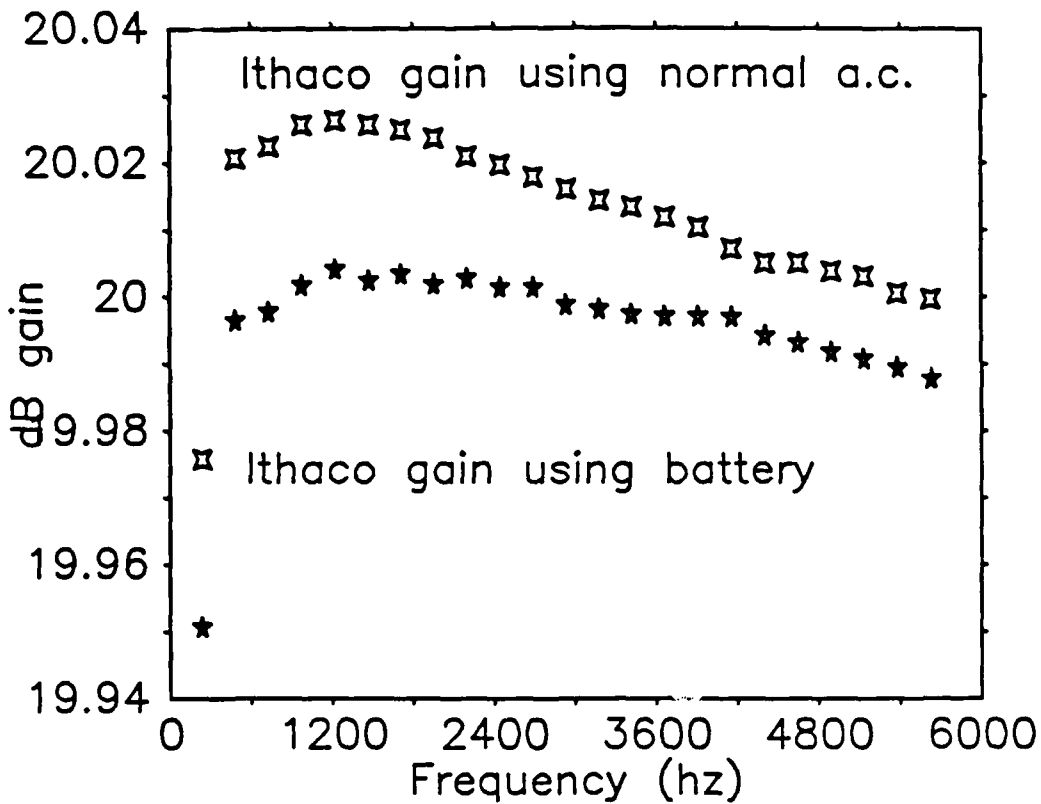


Figure 3.29 Measured gain for the Ithaco preamplifier.

When the battery was fully charged, the gain approximated that obtained using AC power. After several days use, a noticeable drop to the extent shown was observed. The fractional difference between battery power and AC power is seen to be roughly 0.08%. This 800 ppm fractional change is used as an estimate for the uncertainty in the battery powered gain.

c. Computation of The Uncertainty in The Measure of e4

The following are a list of specifications/parameter averages for use in equation 3.46 to estimate the probable error in e4.

- typical value for e4 ~ 1.0 E-4 volts (obtained from figure 3.26)
- preamplifier gain, G ~ 10
- uncertainty in gain, delta G ~ 800 ppm
- scale factor x volts in product, Bvin ~ 6.1 E-5 volts
- total capacitance, Ct ~ 255 pf
- microphone capacitance, Cm ~ 50 pf
- although the PAR 5204 specifications claim an uncertainty in Bvin product to be delta Bvin ~ 1% (if the magnitude option is factory installed), experimental measurement of the consistency found between attenuators and amplifiers shows an accuracy of 0.2%.
- uncertainty in Ct obtained from previous section, delta Ct ~ .15 pf
- uncertainty in Cm obtained from the previous section, delta Cm ~ .002 pf

When these values are used to calculate the components of equation 3.46, an estimate for the probable error in e4 is obtained.

$$\frac{\Delta e_4}{e_4} = \left\{ (2000)^2 + (800)^2 + (525)^2 \right\}^{1/2} \quad \text{Equation 3.47}$$

Thus, the total probable error in e4 is estimated to be ~ 2220 ppm.

Next, the analytical considerations for the experimental determination of the measure of [Vdrop] will be discussed.

3. Analytical Considerations for The Measurement of Vdrop

a. The Measure of Vdrop

The voltage drop across the current limiting resistor was continuously monitored using a HP-3698 digital multimeter included across the circuit. See figure 3.30 below.

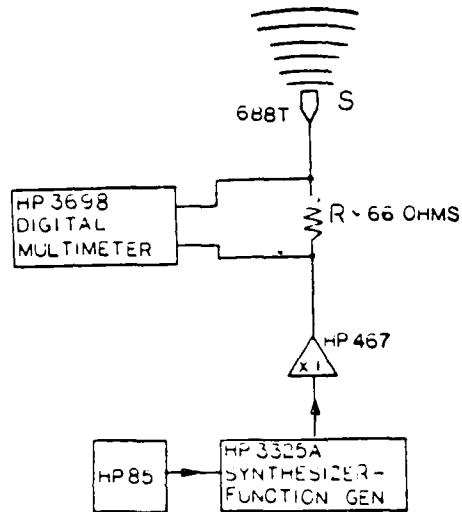


Figure 3.30 Measuring the voltage drop [Vdrop] across the current resistor.

The determination of this voltage drop was straightforward and was done for each frequency of

interest. Unfortunately, unacceptable cross talk occurred when any attempt was made to use the same equipment in both sides of the system under computer control. As a result, the lock in analyzer could not be used in the transmitting circuit as it was already employed in the receiving circuit. To avoid the cross-talk problem, the voltage drop was calculated from a linear least square error fit to experimental measurements of $[V_{drop} = a \cdot V_{ask} + b]$ measured at each frequency of interest. The values of "a" and "b" so found are shown in appendix D in lines 4000 to 4070. The uncertainty in the voltage measured as "Vdrop" was taken from the equipment specifications as $(0.29 \text{ plus } 163/\text{freq})\%$ and is calculated as $\sim 5120 \text{ ppm}$ at 735 Hz.

4. Analytical Considerations Made in The Measurement of

R4

The current limiting resistor was specially chosen for its low temperature coefficient over the temperature range expected within the anechoic chamber. It was mounted in a shielded box with permanent electrical connections wired in to facilitate a four-wire resistance measurement. Based upon the equipment specifications of measurement accuracy of $(.0045 + 4/\text{resistance})\%$ for the four wire resistance measurement obtained using the HP-3658 digital voltmeter, the probable error in R4 was calculated to be ~ 651 ppm. The thermal instability of the resistor used over the temperature range of $17 < T < 22$ degrees centigrade was experimentally measured and the data was fit using the method of least square error. The result is given below where T is measured in degrees centigrade.

$$R4 = \left\{ (5.3282 \times 10^{-4})T + 66.658 \right\} \text{ ohms} \quad \text{Equation 3.48}$$

When the range of temperature from 17 to 21 degrees centigrade is used, the probable error due to the neglect of temperature variation in the value of R4 ~ 160 ppm. Thus the total probable error in R4 is ~ 670 ppm.

5. Measuring The "Acoustic" Separation Distance

a. Introduction

The distance between the faces of the microphones was measured three times during each run of program "N28". The starting distance between the faces of the microphones was the first distance measured and manually input to the computer. A steel tape measure was attached to the source microphone support and could be rotated into position for distance measurements. When the acoustic data was being sampled, the steel tape was positioned behind the source microphone and did not significantly interfere with the acoustic data by introducing additional scattering in the system. The second distance was measured approximately halfway through the computer controlled spatial translation of the W.E.640AA microphone. The program stopped taking acoustical data and requested the operator to enter the anechoic chamber, rotate the steel tape into position, measure the distance, stow the tape, and seal the anechoic chamber. When this distance was manually entered into the computer, the program continued with the translation of the W.E.640AA and the acoustic sampling. The final distance was measured at the end of each translation run and manually entered into the computer. The spot check of measured distance as shown in figure 3.27 normally indicated a small discrepancy between the computer calculated distance which

was based upon the operator entered initial and final distances, and the measured distance at that point. The results usually were on the order of a few tenths of one percent relative error. An average value of this discrepancy was ~ 0.5% . This value is used as the estimate of the precision in the measurement of "acoustic separation".

b. Determination of Spherical Spreading

A direct plot of $V(r)$ versus r does not yield the desired $[1/r]$ spreading loss. When a correction is added to the measured separation distance, r , to obtain the "acoustic" separation distance, r' , a plot of this "acoustic" separation versus $V(r)$ yields a perfect $[1/r']$ plot. The correction, "a", to the measured separation distance is obtained by a linear least square error fit applied to the inverse of $V(r)=V_0/[r+a]$. Here "r" is the measured separation distance and $[r+a]$ is the "acoustic" separation distance. $V(r)$ is the received open circuit signal voltage. The slope of the least square error fit to a straight line equals $[1/V_0]$ and the intercept equals $[a/V_0]$. The correction "a" is obtained by dividing the "intercept" by the "slope". If this correction is not made, the fractional error in the free field calibration will be significantly larger. A plot of $V(r)$ versus both the measured separation distance and the acoustic separation distance is seen in the figure below for data measured at 490 Hz.

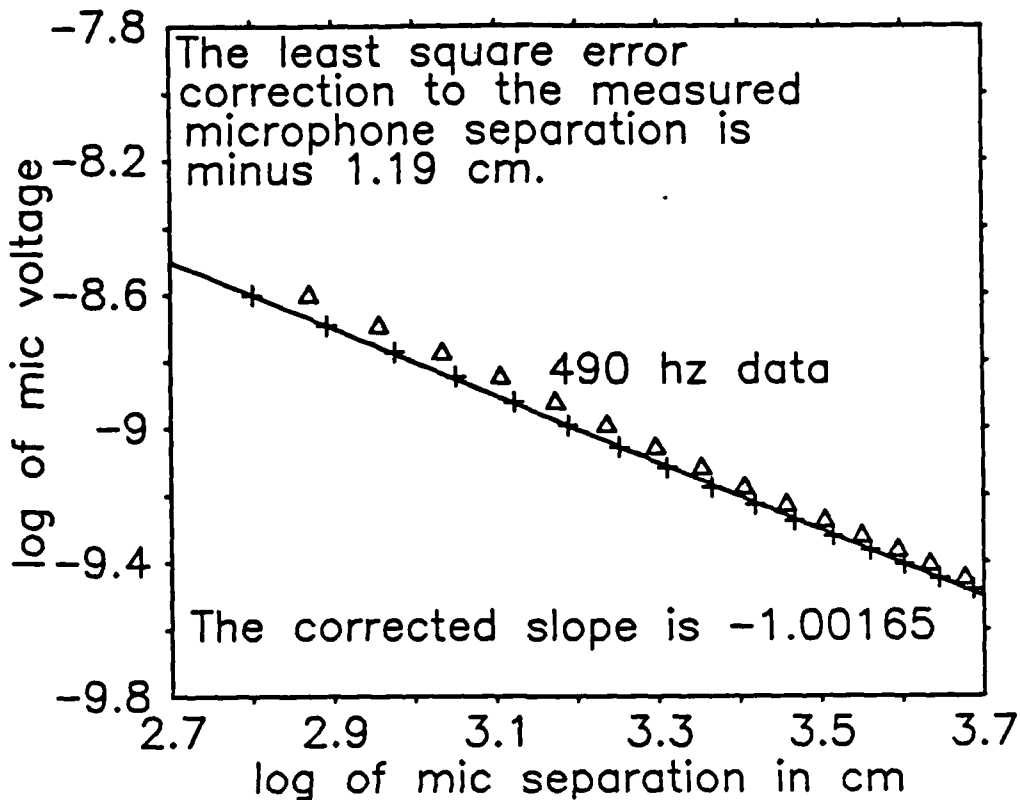


Figure 3.31 A plot showing the correction for the "acoustic" separation distance at 490 Hz.

The uncertainty of the correction applied to the measured distance was found to vary approximately $\sim 5.0\%$ from one run to the next. With a correction magnitude of about ~ 2 cm., this yields an uncertainty in this correction of ~ 0.1 cm. The resolution of the tape measure was estimated to have a systematic error of ~ 0.05 cm. Finally, for a typical distance of 30 cm., the measured precision of

the separation distance of $\sim 0.5\%$ yields a calculated uncertainty of ~ 0.15 cm.

The total probable error for the measure of the separation between microphones is calculated to be the square root of the sum of the squares of the uncertainty in r , the uncertainty in the correction, and the estimate of systematic error.

$$\frac{\delta r'}{r'} = \frac{[(\delta r)^2 + (\delta a)^2 + (\delta_{\text{SYSTEMATIC}})^2]^{1/2}}{r'} \quad \text{Equation 3.49}$$

Thus, the total probable error in the measure of the acoustical separation between microphones at a typical separation of 30 cm. was estimated to be ~ 6240 ppm.

6. Calculating The Uncertainty in The Ratio V_b/V_a

The procedure used to measure this voltage ratio has already been discussed in section C.2. As was seen, the precision of the measure of this ratio varied from frequency to frequency. Figure 3.23 is reproduced below for convenience.

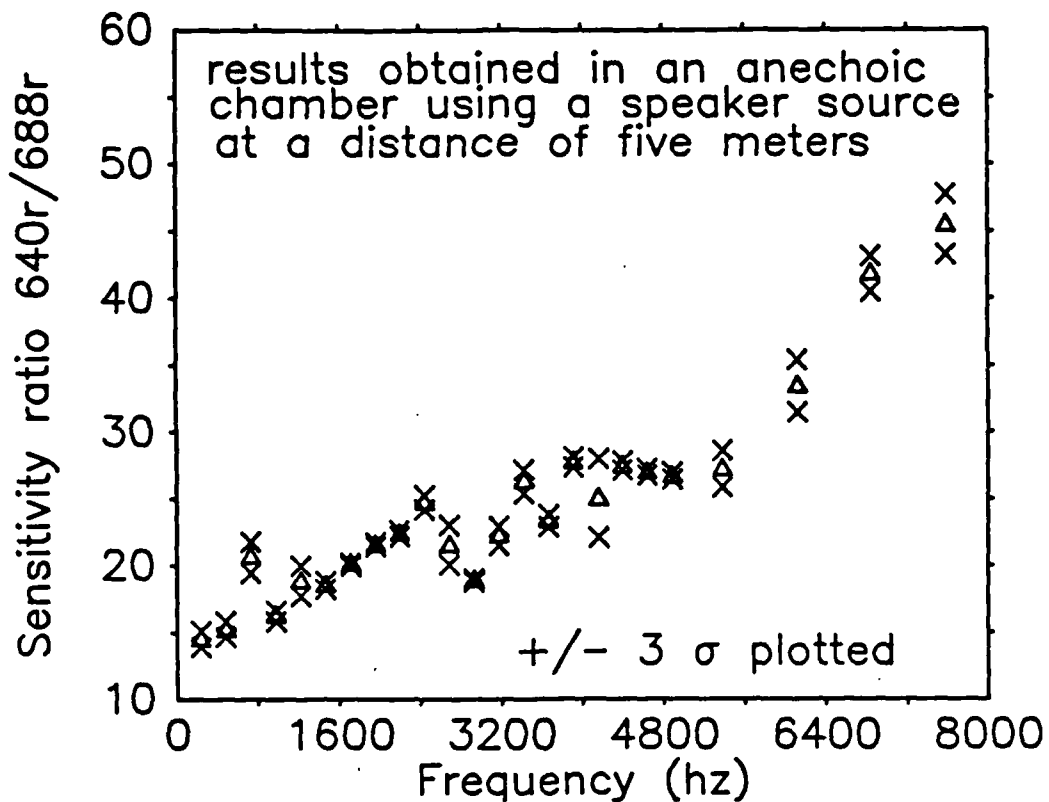


Figure 3.32 The sensitivity ratio obtained for 640R/688R.

The precision of the different values measured for $[V_b/V_a]$ is seen to vary with frequency. When the average of the

different precisions is taken as an estimate of the probable error and the average fractional error is taken to represent the experimental uncertainty, $\Delta [V_b/V_a]$ was calculated as roughly ~ 6300 ppm.

7. A Summary of Experimental Error for The Free Field Comparison Calibration

The probable error for each measured parameter is summarized in the table shown below.

parameter	probable error (in ppm)
* frequency	7
* pressure	320
* temperature	34
* Ebias	60
e4	2220
Vdrop	5120
R4	670
r (acoustic)	6240
Vb/Va	6300

* These probable errors are explained in an earlier chapter on error analysis for plane wave resonant reciprocity.

Table 3.12 A summary of probable error for the free field comparison calibration

The total error in the free field sensitivity calibration is given by the equation shown below. Note that the uncertainty in the bias voltage is included as it was in the previous section for the plane wave resonant reciprocity calibration.

$$\frac{SM_B}{M_B} = \frac{1}{2} \left\{ \left(\frac{\Delta e_4}{e_4} \right)^2 + \left(\frac{\Delta V_d}{V_d} \right)^2 + \left(\frac{\Delta R_4}{R_4} \right)^2 + \left(S \frac{\left(\frac{V_B}{V_A} \right)}{\frac{V_B}{V_A}} \right)^2 + \right. \\ \left. \left(\frac{\Delta T}{T} \right)^2 + \left(\frac{\Delta r'}{r'} \right)^2 + \left(\frac{\Delta \rho}{\rho} \right)^2 + \left(\frac{\Delta f}{f} \right)^2 + \left(2 \frac{\Delta E_{bias}}{E_{bias}} \right)^2 \right\}^{1/2} \text{ Equation 3.50}$$

The total calculated probable error in the free field comparison calibration is taken as one half the square root of the sum of the squares of these individual probable errors and is calculated to be approximately ~ 5,300 ppm. This is on the order of ~0.05 dB re 1 volt/ubar when applied to the sensitivity calibration.

However, one additional experimental uncertainty was observed when the free field sensitivities were plotted with respect to the distance, r.

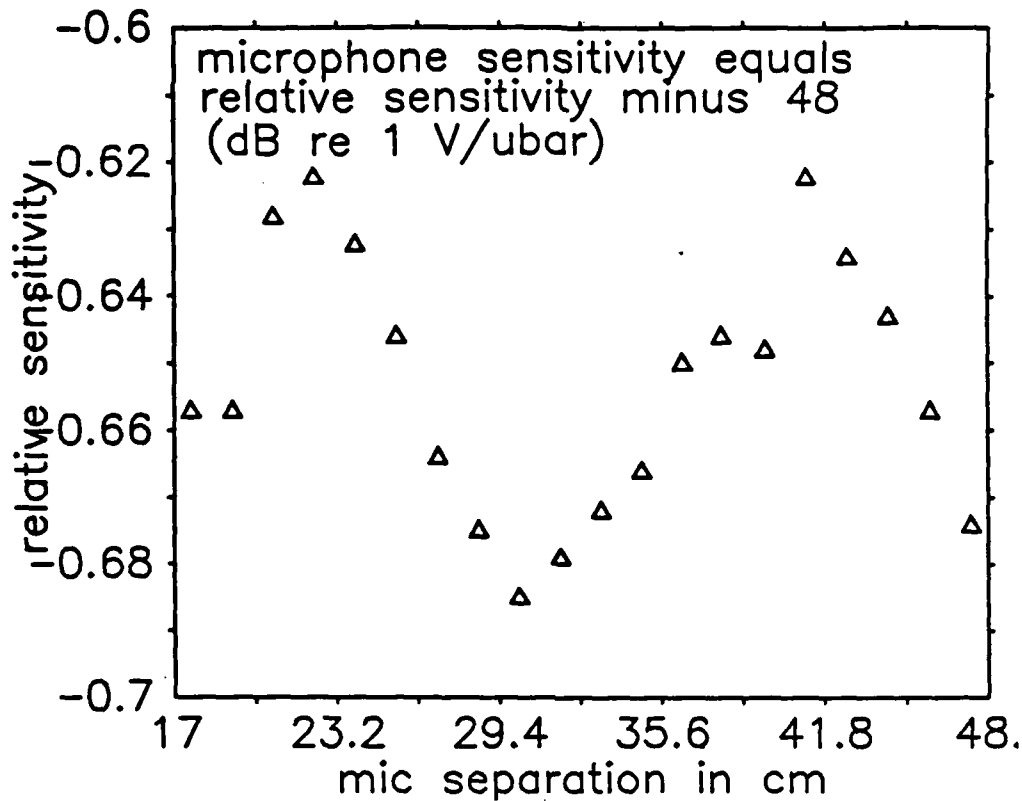


Figure 3.33 The variation of the 490 Hz. microphone sensitivity with separation distance.

The spatial variation observed in this plot is cyclic over roughly ~ 18 cm. This is not explained by standing waves between the source and receiver nor by reflection from any reflecting surface located along the acoustic axis. This suggests a more complex but unknown interference pattern as the source of this variation. When this observed variation of approximately $\sim .035$ dB (roughly 4040 ppm), is included with the 5,300 ppm probable error previously obtained, the overall uncertainty in the free field comparison calibration is calculated to be $\sim 6,700$ ppm or .06 dB re 1 volt/ubar.

IV. SELF CONSISTENCY OF THE PLANE WAVE

RESONANT RECIPROCITY CALIBRATION

A. INTRODUCTION

Three different "experimental calibrations" of the same microphone were examined to experimentally obtain the precision associated with the plane wave resonant reciprocity calibration provided by the output of the computer program listed in appendix B.

First, the external electronics package normally connected to the side "A" microphone was switched with the external electronics package normally connected to the side "B" microphone. The precision associated with this electronics "swap" was then experimentally observed. This exchange is illustrated in the figure below.

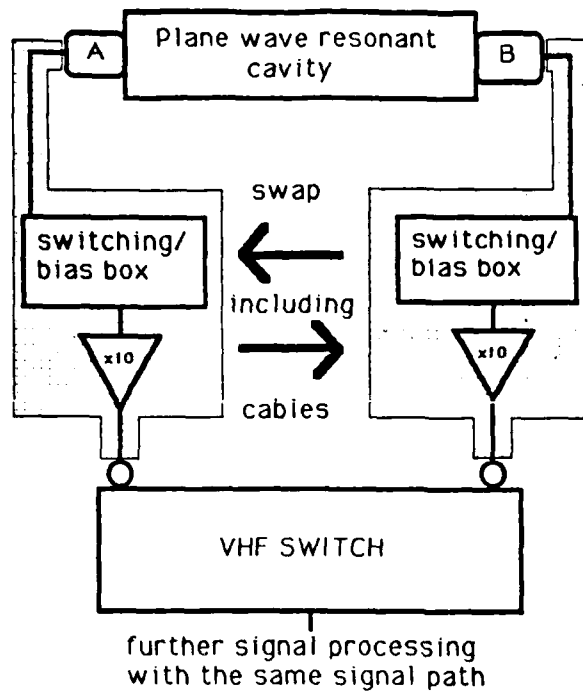
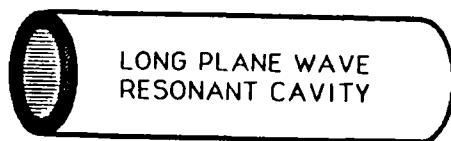


Figure 4.1 An illustration of the "electronics swap"

Second, two *physically different* right circular cylindrical plane wave resonant cavities were each used to calibrate the same microphones. Here the precision associated with the mechanical details of the construction of the cavities and the physical remounting of the microphones was observed. A comparison between these two plane wave resonant cavities is illustrated in the figure below. Note that every third harmonic of the long cavity is matched with the harmonics associated with the short cavity.

$F_0 = 245 \text{ hz}$



length = 70.12 cm
inside diameter = 3.44 cm
material = brass

$F_0 = 735 \text{ hz}$



length = 23.37 cm
inside diameter = 2.51 cm
material = brass

Figure 4.2 The relative sizes of plane wave resonant cavities used in comparing calibrations

Third, the reference microphone was calibrated opposite reciprocal microphones of significantly different sensitivities. In the case of the WE640AA microphones used here, this difference in sensitivity level was roughly 4 dB over the frequency range considered.

Finally, whatever the configuration, each time the plane wave resonant reciprocity calibration was calculated, a six way round robin self consistency check was obtained as described in chapter two. In this procedure, two different calibrations were obtained for each of the three microphones

involved in every plane wave resonant reciprocity calibration. One calibration was based upon the absolute plane wave resonant reciprocity calibration of microphone A and the other calibration was based upon the absolute plane wave resonant reciprocity calibration of microphone B. The entire "set" is listed below:

- Ma - plane wave resonant reciprocity calibration of mic "A".
- Mab - comparison calibration of mic "A" based upon the reciprocity calibration of mic "B".
- Mb - plane wave resonant reciprocity calibration of mic "B".
- Mba - comparison calibration of mic "B" based upon the reciprocity calibration of mic "A".
- Mca - comparison calibration of mic "C" based upon the reciprocity calibration of mic "A".
- Mcb - comparison calibration of mic "C" based upon the reciprocity calibration of mic "B".

Five different electromechanical configurations were necessary to observe the precision of these experimental calibrations. A discussion of these configurations and the results obtained will be given next.

B. THE OBSERVATION OF EXPERIMENTAL PRECISION

The five electromechanical configurations used to determine the experimental precision are shown in the figure below:

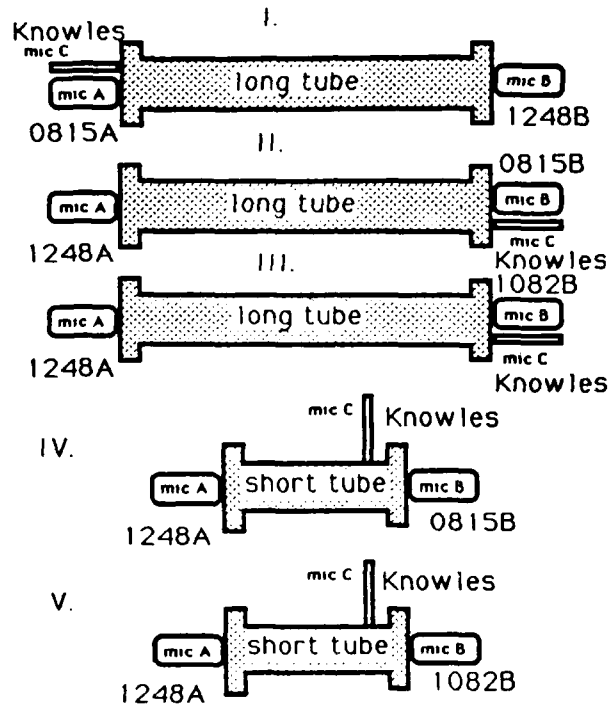


Figure 4.3 Electromechanical configurations used in the plane wave resonant reciprocity calibrations.

The "A" or "B" subscript to the WE640AA condenser microphone serial numbers refers to the external electronics configuration of bias box and preamplifier used for that microphone in a particular calibration run. Throughout the calibrations obtained using the above configurations,

microphone serial #1248 was the "reference" microphone whose plane wave resonant reciprocity calibrations were ultimately compared with a pressure coupler calibration obtained for the same microphone at the National Bureau of Standards. In row I. of figure 4.3 above, the WE640AA microphone serial #1248 was calibrated in the *long tube* using side "B" electronics. In row II. of figure 4.3, the reference microphone was calibrated using side "A" electronics. In row III. of figure 4.3, the reference microphone is paired opposite WE640AA serial #1082 which is approximately four dB less sensitive than the WE640AA serial #815 previously used. In rows IV. & V. of figure 4.3, the *short tube* is used to pair the reference microphone with the serial #815 and serial #1082 microphones, respectively. A compilation of the "raw calibration" program output for these different configurations is tabulated below.

(All calibration values are for WE640AA serial #1248 in dB re 1 volt/ubar.)
 (The frequency of the calibration equals the mode # times 243 Hz)

mode #	Long tube				Short tube		average long-average short
	Configuration/average & sigma	Configuration/average & sigma	Configuration/average & sigma	Configuration/average & sigma	Configuration/average & sigma		
	I.	II.	I.-II.	III.	IV.	V.	
1.	-48.98	-48.93	-.05	-48.89/-48.93 .05			
2.	-48.93	-48.93	.00	-48.93/-48.93 .00			
3.	-48.87	-48.89	+.02	-48.88/-48.88 .01	-48.87	-48.85/-48.88 .01	-.02
4.	-48.90	-48.88	-.02	-48.88/-48.89 .01			
5.	-48.83	-48.87	+.04	-48.86/-48.85 .02			
6.	-48.88	-48.86	-.02	-48.85/-48.86 .02	-48.81	-48.81/-48.81 .00	-.05
7.	-48.77	-48.80	+.03	-48.81/-48.79 .02			
8.	-48.77	-48.74	-.03	-48.73/-48.75 .02			
9.	-48.63	-48.69	+.06	-48.67/-48.66 .03	-48.71	-48.68/-48.70 .02	+.04
10.	-48.71	-48.69	-.02	-48.67/-48.69 .02			
11.	-48.60	-48.66	+.06	-48.64/-48.63 .03			
12.	-48.65	-48.61	-.02	-48.60/-48.61 .02	-48.61	-48.58/-48.60 .02	-.02
13.	-48.53	-48.58	+.05	-48.57/-48.56 .03			
14.	-48.58	-48.58	.00	-48.56/-48.57 .01			
15.	-48.55	-48.58	+.03	-48.56/-48.56 .02	-48.50	-48.57/-48.48 .02	-.08
16.	-48.53	-48.56	+.03	-48.53/-48.54 .02			
17.	-48.54	-48.58	+.04	-48.55/-48.56 .02			
18.	-48.51	-48.56	+.05	-48.53/-48.53 .03	-48.50	-48.41/-48.48 .05	-.07
19.	-48.57	-48.62	+.05	-48.60/-48.59 .03			

20.	-48.55	-48.63	+ .08	-48.59/-48.59				
					.04			
21.*	-49.48*	-48.71	-.77	-48.77/-48.74	-48.70	-48.68/-48.69	-.05	
					.04		.01	
22.	-48.75	-48.78	+ .03	-48.85/-48.79				
					.05			
23.	-48.96	-48.95	-.01	-49.00/-48.97				
					.03			

note 1: The data for mode #21 in column I is ignored in the statistics for that row as bad data.

note 2: The various configurations of microphones and preamplifier systems (I., II., etc,...) are found in figure 4.3.

Table 4.1 WE640AA serial #1248 calibration data.

When the statistics of the above data are determined, the sigma of the average modal calibration level is ~ 0.02 dB for both the long and short tube data. Additionally, with the exception of the data obtained at mode #9 (2205 Hz), the short tube calibrations averaged ~ 0.05 dB greater sensitivity level when compared to the long tube calibrations. This is in the direction expected since the negative correction necessary to account for the finite compliance of the microphone is greater in magnitude (as shown in the next chapter) when the microphone is mounted in the smaller plane wave resonant cavity.

Next, the round-robin precision associated with each modal calibration is discussed.

C. THE PRECISION FOUND FOR THE ROUND-ROBIN COMPARISON

For each of the configurations shown in figure 4.3, the six way round robin self consistency check was obtained by comparing the two different calibrations obtained for any one of the three microphones involved. The following table lists the results obtained for the relative error between these two calibrations. The relative error obtained using configurations II, III, and IV is presented below for comparison. As shown in figure 4.3, configurations II and III used the long tube while configuration IV used the short tube. In each case, the relative error was calculated as,

$$\text{Relative Error (\%)} = \left(\frac{M_A - M_B}{M_A + M_B} \right) (100) \quad \text{Equation 4.1}$$

Mode #	Frequency (hz)	Configuration		
		II.	III.	IV.
1	245	-0.040	+0.001	
2	420	+0.085	+0.006	
3	735	+0.019	+0.013	-0.104
4	980	+0.007	+0.001	
5	1325	+0.011	+0.010	
6	1470	+0.014	+0.064	+0.123
7	1715	+0.083	+0.103	
8	1950	+0.015	+0.013	
9	2295	+0.038	+0.001	+0.037

10	2450	-.009	+.004	
11	2695	-.144	-.000	
12	2940	-.017	-.001	-.070
13	3185	-.006	-.001	
14	3430	-.016	-.009	
15	3675	-.006	+.004	-.023
16	3920	-.017	-.005	
17	4165	-.003	+.055	
18	4410	-.011	-.001	-.022
19	4655	-.011	-.001	
20	4900	+.060	+.058	
21	5145	-.021	-.008	-.010
22	5390	-.012	-.009	
23	5635	-.009	-.065	

Table 4.2 Round robin comparison between Ma and Mab to obtain the "modal" experimental precision.

The worst comparison between Ma and Mab was found for configuration II at mode 11. For this worst case, the fractional error was 0.144 %. This corresponds to a calibration difference of ~ 0.013 dB in the sensitivity levels obtained for Ma and Mab. The average value of $(Ma-Mab)/(Ma+Mab)$ was found to be 0.026 % which corresponds to an average calibration difference in sensitivity levels of ~ 0.002 dB. Thus, the round-robin self consistency check shows an average difference between Ma and Mab of ~ 0.004 dB.

The next examination of experimental precision will deal with that precision found when the external combination of preamplifier and bias boxes on sides "A" and "B" are exchanged,

D. THE PRECISION ASSOCIATED WITH THE SWAP OF SIDE "A" AND SIDE "B" EXTERNAL ELECTRONICS

In table 4.1, a comparison of the results found for configurations I and II will yield an estimate of the experimental uncertainty due to inaccuracies in the electronics systems calibration. From the data so obtained, it is impossible to determine if there was a significant systematic error applied equally to the calibrations of both electronic systems. Any such error will appear in the absolute comparisons which will be given in chapter five. The average difference between configurations I and II was $-.018$ dB. The standard deviation of this quantity was $.035$ dB. This indicates that the experimental limit in the temperature independent calibration of the electronics was reached. Any systematic error introduced as a result of calibration differences existing between the side "A" and side "B" electronics was masked in the standard deviation of $M_a(1248)$ minus $M_b(1248)$.

Next, the precision of the "A" side serial #1248 microphone calibration is determined as the microphone on the "B" side is changed to one of significantly different sensitivity.

E. THE PRECISION OBTAINED BY REPLACING THE SIDE "B" RECIPROCAL MICROPHONE WITH ONE HAVING A SIGNIFICANTLY DIFFERENT SENSITIVITY (4 DB)

When the results obtained with configurations II and III shown in table 4.1 are compared, the experimental uncertainty due to exchanging the side "B" reciprocal microphone is observed. The average difference here was $-.01$ dB with a standard deviation in this difference of $.05$ dB. Again the observable systematic error shown by the average difference was less than the statistical uncertainty in the procedure. This result shows that there was no statistical difference in the calibration of the reference microphone as the sensitivity of the side "B" microphone was changed.

Next, the precision associated with replacing the long tube with the short tube is discussed.

F. THE PRECISION ASSOCIATED WITH REPLACING THE LONG TUBE WITH THE SHORT TUBE AS THE PLANE WAVE RESONANT CAVITY

When the results obtained with the long tube were compared with the results obtained with the short tube, the average absolute difference in calibration was .05 dB with a standard deviation of .03 dB. In six of the seven frequencies used for comparison of the calibration results (configuration II data vs configuration IV data), the sensitivity obtained using the long tube was less than that obtained using the smaller tube. This relative difference in raw sensitivities is expected as shown by the calculated magnitudes of the impressed pressure correction which are provided in chapter five.

In the following section, a summary of the experimental precision found for the plane wave resonant reciprocity method will be presented and the average uncertainty in the experimental precision will be computed.

G. A SUMMARY OF THE EXPERIMENTAL PRECISION FOUND FOR THE PLANE WAVE RESONANT RECIPROCAL CALIBRATION METHOD

The summary of experimental results is shown in the table below. All calibrations values are in dB re 1 volt/ubar and are for W.E.640AA serial #1248.

all dB re 1V/ubar

Observation	Average (dB)	Sigma (dB)
Electronics swap 1248A/815B minus 815A/1248B	-.018	.035
Side "B" exchange of reciprocal microphone 1248A re 815B minus 1248A re 1082B	-.010	.029
Long tube vs. Short tube 1248A/815B re long minus 1248A/815B re short	-.032	.038
Round robin self consistency comparisons for configurations II, III, & IV. $Abs((Ma-Mab)/(Ma+Mab))$.002	.007

Table 4.3 A summary of precision in plane wave resonant reciprocity calibrations

From the data summarized in the above table, it is obvious that the comparison between M_a and M_{ab} in the self consistency check for all the plane wave resonant calibrations is an order of magnitude smaller than the other

observed uncertainties. This suggests that the repositioning of microphones and equipments in the different configurations may be a major source of the uncertainties. Since systematic differences are expected when comparing the long vs short tube results, the sigma for this difference is not a part of the overall uncertainty. The square root of the sum of the squares of the sigmas for the electronics swap and the exchange of side "B" microphones will be the experimental estimate of the overall precision. This estimate of the experimental precision for the method of plane wave resonant reciprocity is $\sim .045$ dB.

In the next chapter, corrections that are necessary for the *absolute comparison* of the plane wave resonant reciprocity calibration to the results of other calibration techniques will be discussed. The microphone used for all these absolute comparisons will be the WE640AA serial #1248 condenser microphone.

V. ABSOLUTE ACCURACY OF EXPERIMENTAL RESULTS

A. INTRODUCTION

With the self consistency of the calibrations using plane wave resonant reciprocity established in chapter four, several corrections to the raw computer output must be made before comparisons can be made between plane wave resonant reciprocity calibrations and NBS pressure coupler comparison calibrations. The raw computer output shown below was obtained using experimental configurations I through V listed in chapter four, figure 4.3. These are plane wave resonant reciprocity calibrations for the W.E.640AA serial #1248 condenser microphone.

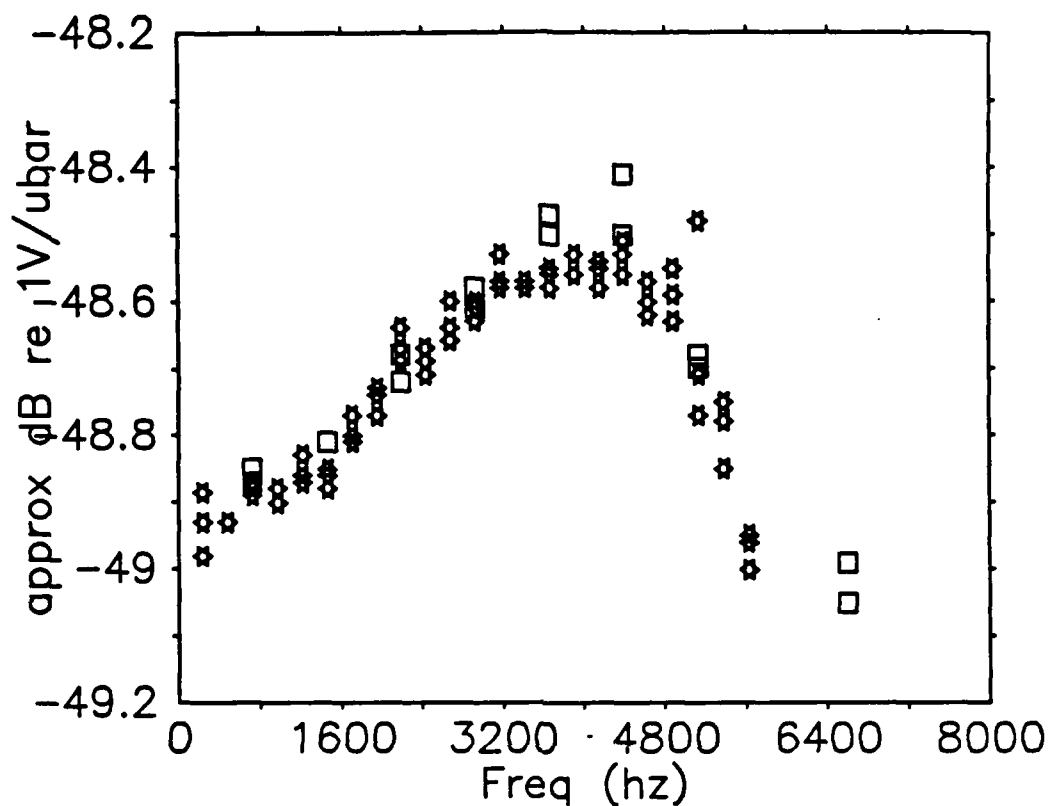


Figure 5.1 Raw data from both the long [star] and short [box] resonant tubes for plane wave resonant reciprocity calibrations.

To obtain the final values for the absolute plane wave resonant reciprocity calibration, four corrections must be made to the "raw" program calculation of M_0 . The first two are general corrections to the "ideal" resonant reciprocity calculations incorporating equation 3.1 into the computer program. The third results from the experimental procedure employed. The fourth has three parts and corrects for

deliberate errors introduced into the program for experimental convenience. All the corrections are summarized below.

1. The impressed pressure correction. The correction due to the finite compliance of the microphone. ($\sim .001$ to $\sim .14$ dB)
2. The correction to the ratio of specific heats. The correction to the bulk modulus of elasticity for the air volume within the cavity due to the non-adiabatic boundary conditions at the walls of the cylindrical brass cavity expressed as a change in the ratio of specific heats. In this case, a correction of $\sim .007$ dB is needed at all frequencies to correct for the inaccurate calculation of this correction that was used in the computer program.
3. The driving point electrical impedance correction. The driving point impedance correction for the Thevenin equivalent circuit used to represent the condenser microphone. (\sim negligible)
4. Corrections to program calculations.
 - a. A standard electrical definition for the microphone must be used prior to comparison with other calibration results. It is therefore necessary to subtract out the capacitance of the BNC electrical connection used as part of the microphone during this experiment. (~ 2.8 pF) A correction to M_0 due to this change in microphone capacitance will result. ($\sim .15$ to $\sim .36$ dB including the correction described next in part 4b.)
 - b. For experimental convenience, the values of the bias box and cable capacitances were fixed early in the writing of the operational computer program and are listed in lines 670-760 of the program in appendix B. Subsequent, more accurate measurements of these capacitances require a correction to M_0 . ($\sim .16$ to $\sim .36$ dB including the correction described above in part 4a.)
 - c. The drop in signal voltage across the D.C. blocking capacitor in the bias box of the microphone preamplifier signal path was temporarily ignored in

chapter three. As shown in Appendix E, this loss is approximately independent of frequency over the range of frequencies employed in this experiment. The correction required for M_0 to account for this "loss" in signal is roughly $\sim + 0.03$ dB.

The effect of the compliance of the microphone on the plane wave resonant reciprocity open circuit voltage receiving sensitivity calibration will be discussed first.

B. CALCULATION OF THE IMPRESSED PRESSURE CORRECTION

Using the standard method of pressure coupler reciprocity calibration [Ref. 3], the equivalent volume correction is required whenever the equivalent volume of the pair of microphones within the cavity exceeds 0.4 percent of the physical volume within the coupler [Ref. 3: p.15]. This accounts for the effect of the acoustic impedance of the microphone on the pressure coupler microphone calibration. This correction *requires the accurate determination of the equivalent volume of the microphone under calibration or the functional equivalent, its acoustic impedance* [Ref. 3: p.8]. The method of plane wave resonant reciprocity calibration requires the determination of the acoustic impedance for any microphone under calibration regardless of the volume of the cavity.

In part C of chapter two, the correction required to account for the finite mechanical impedance of a microphone was derived. This impressed pressure correction accomplishes the same task for plane wave resonant reciprocity as the equivalent volume correction accomplishes in pressure coupler reciprocity. A systematic error in the plane wave resonant reciprocity calibration of condenser microphones on the order of ~ 0.001 to $.14$ dB re $1\text{v}/\text{ubar}$ may result if the impressed pressure correction is ignored.

The correction is shown in equation 2.46 and the acoustic driving point impedance is given in equation 2.49. Both equations are reproduced below.

$$M_A = M_{Ao} \left\{ 1 - \frac{1}{Z_{22} J} \right\}^{\frac{1}{2}} \quad \text{Equation 2.46}$$

$$Z_{22} = \left[Z_{A(\text{mic A})} \left(\frac{A_T}{A_{d(\text{mic A})}} \right) + Z_{A(\text{mic B})} \left(\frac{A_T}{A_{d(\text{mic B})}} \right) \right] \quad \text{Equation 2.49}$$

The acoustic impedances, $Z_{A(\text{mic A})}$ and $Z_{A(\text{mic B})}$, shown in equation 2.49 must be exactly measured if the correction is to be accurately determined. In the absence of an accurate determination of these acoustic impedances, an average value for the acoustic impedance of a WE640AA laboratory standard microphone was obtained from the ANSI standard method for the calibration of microphones [Ref. 3]. This value was used for both $Z_{A(\text{mic A})}$ and $Z_{A(\text{mic B})}$ in the determination of the magnitude of this correction at one frequency when it was illustrated in chapter two. While this will allow an approximation to be made in calculating the impressed pressure correction, no insight is obtained with regard to the possible range of corrections that result from extreme

samples (due to different values of Z_a) of the W.E.640AA microphone population. The "equivalent volumes" of two W.E.640AA microphones that represent such extremes and which will provide such insight are provided below in table 5.1 [Ref. 29]. The term "equivalent volume" is often used in pressure coupler calibrations as a matter of convenience. It is simply another way to express the acoustic impedance of the microphone in a manner which simplifies pressure coupler reciprocity calculations. As such, it will generally have both a real and an imaginary part representing the dissipative and reactive portions of the microphone impedance. The exact relationship [Ref. 3: p.8] between the "equivalent volume" and " Z_a " must be used to derive the final impressed pressure correction as it is shown in equation 5.2.

Equivalent volumes of two condenser microphones [Ref. 29].

W.E.640AA Serial# 646

W.E.640AA Serial# 151

- all units MKS, M³ -

Frequency (Hz) (multiplied by)	Re. volume - {E-7}	Im. volume {E-9}	Re. volume - {E-7}	Im. volume {E-9}
50.0	1.2207	-.93636	.43979	-.24779
100.0	1.2207	-1.8728	.43976	-.49557
200.0	1.2203	-3.7458	.43965	-.99101
300.0	1.2196	-5.6195	.43946	-1.4862
400.0	1.2187	-7.4940	.43919	-1.9809
500.0	1.2176	-9.3697	.43885	-2.4751
600.0	1.2162	-11.247	.43843	-2.9687
700.0	1.2145	-13.125	.43794	-3.4614
800.0	1.2125	-15.006	.43737	-3.9532
900.0	1.2103	-16.889	.43673	-4.4439
1000.0	1.2078	-18.774	.43601	-4.9333
1500.0	1.1909	-28.234	.43131	-7.3576
2000.0	1.1660	-37.751	.42477	-9.7314
2500.0	1.1321	-47.284	.41646	-12.038
3000.0	1.0878	-56.746	.40645	-14.262
4000.0	.96365	-74.797	.38168	-18.400
5000.0	.78900	-89.957	.35134	-22.034
6000.0	.57288	-99.723	.31659	-25.073
7000.0	.34154	-102.28	.27874	-27.454
8000.0	.12923	-97.767	.23925	-29.148
9000.0	-.038557	-88.254	.19954	-30.166
10000.0	-.15406	-76.476	.16094	-30.550
11000.0	-.22358	-64.609	.12456	-30.373
12000.0	-.25897	-53.866	.091201	-29.726
13000.0	-.27171	-44.698	.061398	-28.709
14000.0	-.27059	-37.116	.035386	-27.421
15000.0	-.26157	-30.940	.013165	-25.952
16000.0	-.24846	-25.938	-.0054385	-24.381
17000.0	-.23356	-21.866	-.020718	-22.770
18000.0	-.21825	-18.529	-.033032	-21.167
19000.0	-.20327	-15.902	-.042759	-19.609
20000.0	-.18903	-13.691	-.050276	-18.119

* The above values have only ~ three significant digits. [Ref. 29]

Table 5.1 Equivalent volumes for extreme W.E.640AA
laboratory standard condenser microphones

In addition to these values, the measured acoustical impedances for four particular W.E.640AA laboratory standard type "L" microphones were obtained from the literature [Ref. 30].

W.E.640AA Serial#	Acoustic parameter		
	Stiffness (NM ⁻⁵)	Mass (kgM ⁻⁴)	Resistance (NsecM ⁻⁵)
1087	1.95E+12	584	3.80E+7
1121	1.88E+12	475	3.63E+7
1134	1.67E+12	473	3.12E+7
0904	1.52E+12	434	3.16E+7
*** design parameters [Ref. 30]	1.2 E+12	420	2.63E+7

Table 5.2 Tabulated values of acoustic impedance for four W.E.640AA microphones

When equation 2.24 and equation 2.49 are combined, two analytical forms of the impressed pressure correction for plane wave resonant reciprocity may be computed. Choice between the two equations shown below is strictly a matter of convenience. The first expresses the correction using the acoustic impedance, and the second uses the equivalent volume of the microphone. In each case, it is assumed that identical microphones are mounted in the ends of the plane wave resonant cavity.

$$\text{CORR} \cong \left[1 - \frac{A_d Q_n P_o \gamma_E}{A_T V_o \omega Z_A} \right]^{1/2} \quad \text{Equation 5.1}$$

or,

$$\text{CORR} \cong \left[1 - j \frac{A_d Q_n V_e}{A_T V_o} \right]^{1/2} \quad \text{Equation 5.2}$$

where we define:

- V_e = equivalent volume ; $[\gamma_E P_o] / [j \omega Z_A]$
- γ_E = ratio of specific heats
- f_n = frequency of Nth modal resonance
- Z_A = acoustic driving-point impedance of the microphone
- Q_n = quality factor of Nth modal resonance
- V_o = volume of plane wave resonant cavity
- A_T = area of tube cross section
- A_d = area of microphone diaphragm

Provided the resonant frequencies and modal quality factors are available, the correction factor can be calculated for the case of plane wave resonant reciprocity calibrations.

Using equation 5.2, the range of the impressed pressure corrections can be calculated using experimental data for the quality factor of the modal resonance while the data provided by the National Bureau of Standards is used for the

equivalent volumes of the two extreme samples of the W.E.640AA population. The atmospheric pressure is also provided to facilitate use of equation 5.1.

 All values MKS units; $V_0(\text{short}) \sim 1.159\text{E-}4$, $V_0(\text{long}) \sim 6.504\text{E-}4$,
 $A_d/A_t(\text{short}) \sim .5435$, $A_d/A_t(\text{long}) \sim .2903$

freq (Hz)	* long tube		** short tube		serial#646		serial#151	
	Po	Qn	Po	Qn	real	imag	real	imag
					(E-7)	(E-9)	(E-7)	(E-9)
735	100007	97.5	99843	42.4	1.21	-13.8	.438	-3.63
1470	100027	116.8	99838	76.0	1.19	-27.7	.432	-7.21
2205	100081	153.0	99862	103.0	1.15	-41.7	.421	-10.68
2940	100106	193.7	99872	115.1	1.09	-55.6	.408	-14.00
3675	100076	218.7	99886	117.0	1.00	-68.9	.390	-17.00
4410	100082	229.8	99898	116.1	.892	-81.0	.369	-19.89
5145	100039	239.5	99910	114.0	.758	-91.4	.346	-22.48

* 2 May data tape, records 26-46 (see appendix G)

** 22 Nov data tape, records 24-33 (see appendix G)

freq (Hz)	long tube dB			short tube dB		
	Ref #646	Ref #151	spread	Ref #646	Ref #151	spread
735	-.0013	-.0003	.001	-.0053	-.0015	.0039
1470	-.0031	-.0008	.0023	-.0195	-.0053	.0142
2205	-.0061	-.0016	.0045	-.0406	-.0108	.0298
2940	-.0104	-.0026	.0078	-.0622	-.0159	.0463
3675	-.0146	-.0036	.0110	-.0802	-.0199	.0603
4410	-.0180	-.0044	.0136	-.0951	-.0232	.0719
5145	-.0212	-.0052	.0160	-.1068	-.0259	.0809

 Table 5.3 Tabulated values of the impressed pressure correction obtained using equivalent volumes of extreme samples of the W.E.640AA population and the difference between these corrections.

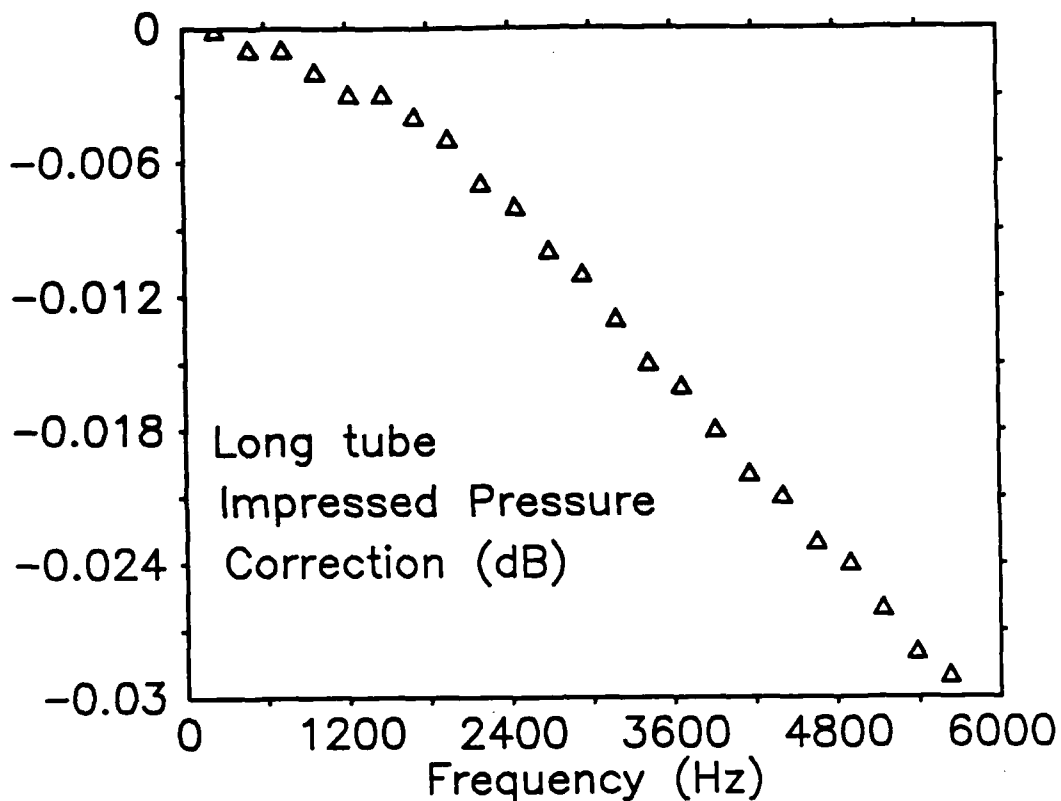


Figure 5.2 Calculated values of the impressed pressure correction applicable to the "long" tube plane wave resonant reciprocity calibration, [3 sigma < .003 dB]

The above corrections are calculated using an average value of Z_a obtained from table 5.2, and experimental data for the other parameters in equation 5.1. When the same procedure is used for corrections to M_0 found using the "small" cavity, both the magnitude and the range of the corrections are slightly larger.

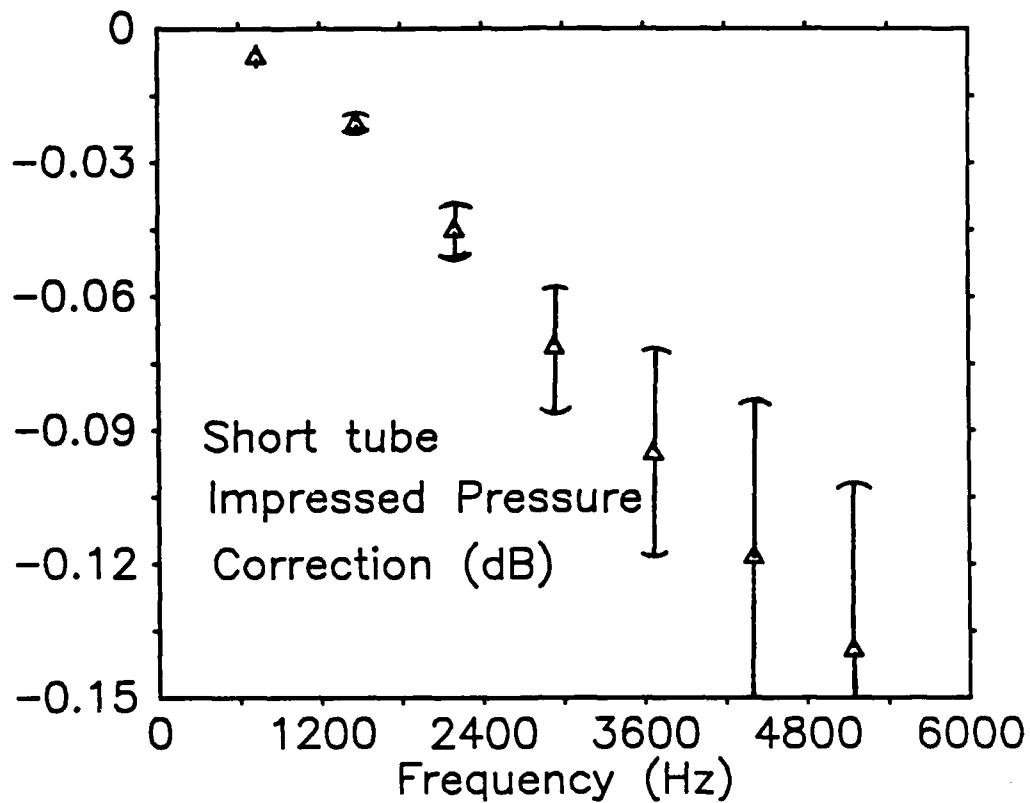


Figure 5.3 Calculated values of the impressed pressure correction applicable to the "short" tube plane wave resonant reciprocity calibration. [3 sigma shown]

The impressed pressure correction for the short tube (figure 5.3) is larger than that obtained for the long tube (figure 5.2). The impact of this difference on the absolute calibration results will be discussed in the next chapter.

The next section will discuss the correction to the bulk modulus of elasticity for the air within the resonant cavity due to the non-adiabatic boundary conditions.

C. THE CORRECTION TO THE BULK MODULUS OF ELASTICITY WITHIN THE PLANE WAVE RESONANT CAVITY DUE TO THE NON-ADIABATIC BOUNDARY CONDITIONS

In chapter three, the form of the adiabatic bulk modulus of elasticity for the air within the resonant cavity was given as the product of the atmospheric pressure and the ratio of specific heats. The general correction to account for the change in stiffness of the volume of air within the resonant cavity due to the non-adiabatic boundary conditions was given in equation 3.37 as a correction to the ratio of specific heats obtained under free field conditions of temperature and humidity. A correction to the sensitivity level that incorporated this correction was given in figure 3.21. In general, to account for effect of the change in stiffness of the volume of air within the resonant cavity due to non-adiabatic boundary conditions, the sensitivity level must be corrected by adding:

$$\text{CORR} = 10 \text{ LOG} \left(\frac{\gamma_H}{\gamma_E} \right) \quad \text{Equation 5.3}$$

When the solution for the effective value of gamma is first obtained using the program solution, and next using equation 3.37, the program solution is found to be ~.007 dB too low

across a percent relative humidity and temperature range of
 $40\% < H < 65\%$ and $19 \text{ deg C.} < T < 21 \text{ deg C.}$

The raw sensitivity levels plotted in figure 5.1 must therefore be increased by $\sim .007$ dB to correct the program results for the fundamentally wrong, but only slightly inaccurate solution for the effective gamma programmed in lines 3770-3810 of the program shown in appendix B.

D. THE ELECTRICAL DRIVING POINT IMPEDANCE CORRECTION

When the electrical model for the W.E.640AA serial #1248 condenser microphone was chosen, the effect of the medium upon the motion of the microphone diaphragm and consequently upon the electrical driving point impedance was assumed to be negligible. Thus, neglecting the electrical resistance of the dielectric in the back volume of the microphone, the electrical model chosen was that of a simple capacitance:

$$Z_{MK} \cong Z_{EB} \cong \frac{1}{j\omega C_{mic.}} \quad \text{Equation 5.4}$$

The validity of such an assumption rests upon two conditions. First, that the length of the tube loading the diaphragm at a plane wave resonance is a multiple of a half wavelength. Second, that the termination at the opposite end of the tube is for all practical measurements, rigid. These conditions illustrate one method used to obtain the blocked electrical impedance (~capacitive) of a condenser microphone. If the termination at the opposite end is *absolutely rigid* and if the system has low dissipation (high Q), then the motion of the diaphragm is effectively blocked [see equation 2.43] and Z_{eb} can be measured [Ref. 29]. Since

AD-R164 149

RECIPROCITY CALIBRATION IN A PLANE WAVE RESONATOR(U)
NAVAL POSTGRADUATE SCHOOL MONTEREY CA C L BURMASTER
DEC 85 NPS61-86-006

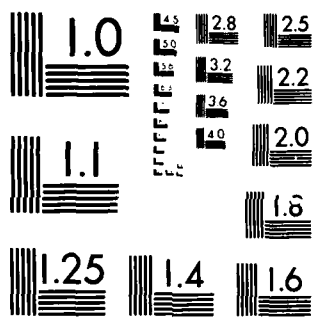
4/5

UNCLASSIFIED

F/G 14/2

NL

The table consists of a grid of 10 columns and 10 rows. The top row contains 10 blacked-out cells. The remaining 9 rows each contain 10 blacked-out cells. The grid is used for data recording in the report.



MICROCOPY RESOLUTION TEST CHART
NATIONAL BUREAU OF STANDARDS 1963-A

the plane wave resonator was anticipated to operate under these conditions, the assumption seemed reasonable. However, even though the system used had low dissipation (high Q), the termination at the opposite end was a finite impedance resulting from the combination of another W.E.640AA and a semi-rigid plastic mount. The desired blocked mechanical conditions provided by an absolutely rigid end were not achieved.

A calculation of the motional impedance of the microphone and an analysis of the required correction (if any) is therefore necessary to examine the validity of the assumption that the experimental termination is essentially rigid.

$$Z_E = Z_{EB} + Z_{MOT} \quad \text{Equation 5.5}$$

where,

- Z_e = electrical driving point impedance.
- Z_{eb} = blocked electrical impedance.
- Z_{mot} = motional impedance

When equation 2.21 was employed to calculate M_a , the value of e_1 was calculated using equation 3.13 which in turn was based upon figure 3.8 and the simple electrical model given in equation 5.4. Using figure 3.8,

$$\frac{V_{OUT}}{G} = \left[\frac{Z_T}{Z_T + Z_{EB}} \right] e_1 \quad \text{Equation 5.6}$$

where,

- G = gain of signal preamplifier
- Z_T = total input impedance at the preamplifier.
- Z_{EB} = blocked electrical impedance (1/jωC).

In terms of Z_T and Z_{EB}, the program solution for e₁ was,

$$|e_1|_{\text{(PROGRAM)}} = \frac{V_{OUT}}{G} \left| \left[1 + \frac{Z_{EB}}{Z_T} \right]^{\frac{1}{2}} \right| \quad \text{Equation 5.7}$$

If the actual electrical driving point impedance had been measured and used in the calculation instead of Z_{EB}, the solution for e₁ would have been:

$$|e_1|_{\text{(CORRECT)}} = \frac{V_{OUT}}{G} \left| \left[1 + \frac{Z_e}{Z_T} \right]^{\frac{1}{2}} \right| \quad \text{Equation 5.8}$$

where Z_e is the electrical driving point impedance and is defined as the ratio of the voltage across the input

terminals of the microphone divided by the input current when the microphone is operating under the load of the plane wave resonant cavity.

The correction to the calculated value of M_A obtained using equation 3.13 which accounts for the effect of the motional impedance upon the computed value of e_1 is:

$$\text{CORR TO } M_A \text{ (due } e_1) = \left| \frac{\left[1 + \frac{Z_e}{Z_T} \right]}{\left[1 + \frac{Z_{EB}}{Z_T} \right]} \right|^{1/2} \quad \text{Equation 5.9}$$

When similar considerations are made for the correct calculation of i_1 using Z_e instead of Z_{EB} (using equation 3.14), the correction to M_A becomes:

$$\text{CORR TO } M_A \text{ (due } I_1) = \left| \frac{Z_e}{Z_{EB}} \right|^{1/2} \quad \text{Equation 5.10}$$

The product of these two corrections yields the total correction:

$$\text{CORR TO } M_A \text{ DUE } Z_{MOT} = \left| \left(\frac{Z_e}{Z_{EB}} \right)^{1/2} \left(\frac{1 + \frac{Z_e}{Z_T}}{1 + \frac{Z_{EB}}{Z_T}} \right)^{1/2} \right| \quad \text{Equation 5.11}$$

If Z_e , Z_{eb} , and Z_t were available, this correction could be calculated. However, only Z_{eb} and Z_t are available. While this does not allow an exact correction to be computed, a close approximation can be determined.

Equation 5.11 can be rewritten slightly to be of the form:

$$\text{CORR TO MA due } Z_{mot} = \left| \left(1 + \frac{Z_{mot}}{Z_{eb}} \right)^{1/2} \left(1 + \frac{\left(\frac{Z_{mot}}{Z_t} \right)^{1/2}}{\left(1 + \frac{Z_{eb}}{Z_t} \right)} \right)^{1/2} \right| \quad \text{Equation 5.12}$$

Since the real part of $[Z_{eb}/Z_t]$ can be computed and can be shown to be very much greater than 1, the correction becomes:

$$\text{CORR TO MA due } Z_{mot} \cong \left| 1 + \frac{Z_{mot}}{Z_{eb}} \right| \quad \text{Equation 5.13}$$

Beginning with equations 2.36 and dividing V_1 by I_1 , the determination of Z_e yields a solution for Z_{mot} . This is the method shown by Hunt [Ref.34:p.96]. The traditional value of Z_{mot} as obtained by Hunt $[-b^2/Z_{22}]$, is seen to be modified

by the square of the impressed pressure correction. When these results are combined with the transduction coefficient previously determined (see the text before equation 2.54), equation 5.13 is of the form:

$$C_{\text{CORR to } M_A \text{ due } Z_{\text{mot}}} \cong \left| 1 + j \left(\frac{2A_T C_0}{w A_d} \right) \left(\frac{C_0 E_0}{\epsilon_0 A_e} \right)^2 \frac{(IMPC)^2}{Z_A} \right| \quad \text{Equation 5.14}$$

Here the term IMPC refers to the impressed pressure correction previously derived. Since the largest magnitude of the impressed pressure correction is ~ 0.98 , it is the magnitude of other terms found in the transduction coefficient and the acoustic impedance which will determine the magnitude of this correction. When the phase of the impressed pressure correction is ignored, the remaining terms yield the value of the maximum possible correction due to Z_{mot} . This worst case magnitude is approximated by substitution of the following values into equation 5.14:

$E_0 \sim 117$ volts
 $C_0 \sim 49.14$ pf
 $A_T/A_d \sim 3.44$
 $A_e \sim 1.29E-4$ M²
 $R_a \sim 3.43 E+7$ NSM⁻⁵
 $M_a \sim 492$ KgM⁻⁴
 $K_a \sim 1.76 E+12$ NM⁻⁵

A straightforward computation shows this correction to be much less than .001 dB and therefore negligible.

E. THE CORRECTION DUE TO REVISED VALUES OF MICROPHONE AND TOTAL BIAS SUPPLY CAPACITANCE

At an early stage in the experiment, it was decided that the electrical definition of the "microphone" would for simplicity include the BNC connector that was fabricated for the electrical connection to the W.E.640AA microphone cartridge. This resulted in the capacitance of the "extender" contributing to a slight increase in the capacitance measured for the "W.E.640AA microphone" and at the same time contributing to an equal decrease in capacitance measured for the external system capacitance. When this "extender" capacitance is taken into account in the sensitivity calculations, a correction results for the open circuit voltage receiving sensitivity for the microphone.

Additionally, a considerable time passed from the first measurement of microphone capacitance and the final result. Consequently, the values of capacitance used for various capacitance terms in the analytical solutions for "Mo" that were programmed on the computer were "frozen" for computational purposes, knowing full well that a later correction would be necessary. These corrections and the "extender" correction were made using equation 5.15 below. Equation 5.15 is obtained from equation 3.11 and the fact that the open circuit voltage receiving sensitivity is

directly proportional to the received signal voltage, e_1 .

$$\frac{M_A(\text{correct})}{M_A(\text{Program})} = \frac{\left[\left(1 + \frac{C_T''}{C_M''} \right)^2 + \left(\frac{1}{\omega R C_M''} \right)^2 \right]^{1/2}}{\left[\left(1 + \frac{C_T}{C_M} \right)^2 + \left(\frac{1}{\omega R C_M} \right)^2 \right]^{1/2}} \quad \text{Equation 5.15}$$

Here we define,

- C_t = program value used for the cable and bias supply capacitance. (BTAR:177.28pf, ATBR:176.053pf)
- C_t' = corrected experimental measure of C_t .
- C_t'' = C_t' corrected to include the "extender" capacitance. (BTAR:173.22pf, ATBR:171.42pf)
- C_m = program value used for the microphone capacitance. (Serial #1248: 52.722pf)
- C_m' = corrected experimental measure of C_m .
- C_m'' = C_m' corrected to exclude the "extender" capacitance. (Serial #1248: 49.41pf) (#1248 BNC Connector = 2.75 pf)
- R = parallel combination of the bias blocking resistor and the input resistance of the signal preamplifier. (BTAR:~5047050ohms, ATBR:~4987470ohms)
- ω = $2\pi \cdot F_n$

Since there were six experimental combinations of microphone-system pairs, there were six different sets of corrections that were calculated. As shown below, the magnitude of the correction required depended primarily upon the correction to the microphone capacitance.

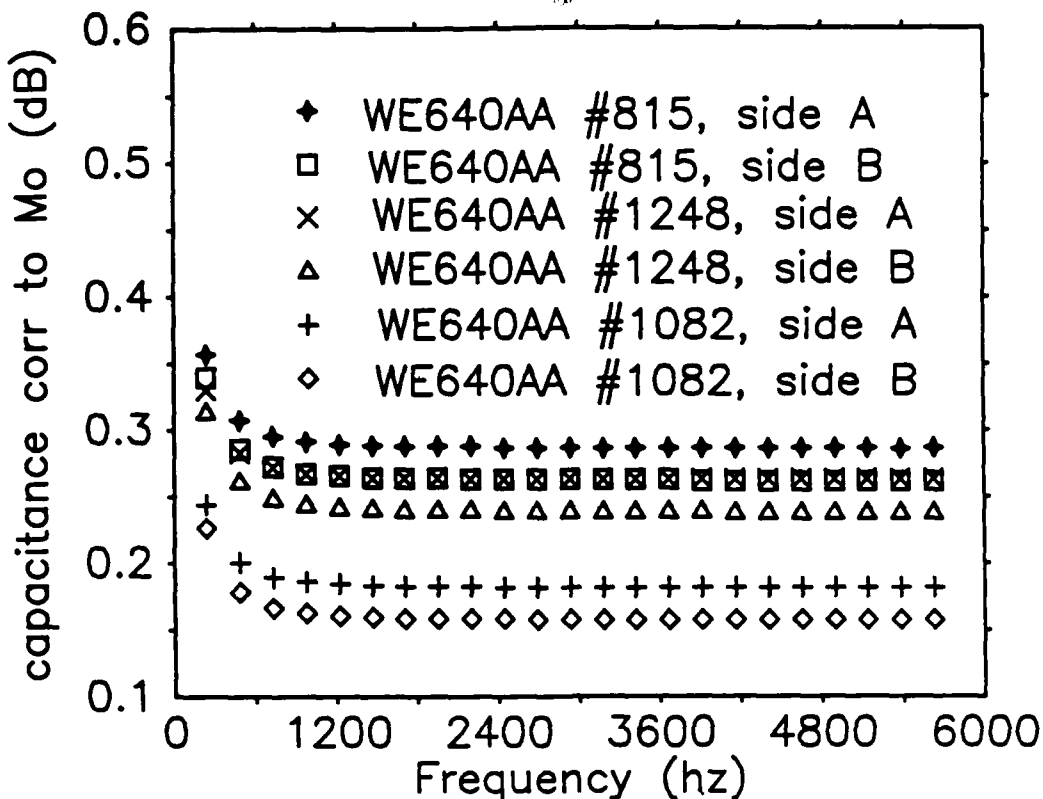


Figure 5.4 The microphone plus bias box capacitance correction plotted for all six experimental combinations.

This correction would be unnecessary for experimental setups where the magnitude of the electrical parameters were well established and properly included in the controlling computer program.

The final correction to be considered is a result of the approximation of the circuit shown in figure 3.3 by the circuit shown in figure 3.4. This coupling capacitance correction is derived in appendix E and will be summarized in the next section.

F. THE COUPLING CAPACITANCE CORRECTION

When preliminary solutions for the received signal transfer function given by equation 3.11 were made, it was convenient to note that the *signal loss* due to the blocking capacitor C_c in the circuit shown in figure 3.3 was roughly *constant* across the frequency range of the resonant reciprocity calibration. The correction for the drop in the signal voltage across the blocking capacitor which was temporarily neglected and must now be included. In Appendix E, the calculation of the magnitude of the required correction was shown to be roughly constant at $\sim +0.03\text{dB}$ for the calibration frequencies used in this experiment. The tabulated corrections are shown in the next table.

Frequency (Hz) correction (dB)

245	.039
490	.032
735	.031
980 - 2695	.030
2940 - 5635	.029

average = .030, sigma = .002

Table 5.4 D.C. Blocking capacitor corrections.

This concludes the descriptions of the corrections necessary to obtain an absolute calibration.

G. THE ABSOLUTE PLANE WAVE RESONANT RECIPROCITY CALIBRATION

1. Introduction

When the values obtained by the computer program for the open circuit voltage receiving sensitivity are corrected as indicated in three of the preceding four sections, the calibration is compared with a National Bureau of Standards pressure coupler calibration obtained for the same microphone. The lower six modal calibrations (below ~ 1500 Hz) obtained using the long tube have an average discrepancy of ~ 0.03 dB when compared with the NBS calibration data. The lower two modal calibrations (below ~ 1500 Hz) obtained using the short tube have an average discrepancy of ~ 0.06 dB when compared with the NBS calibration data. Above the frequencies indicated, the difference between NBS and plane wave resonant reciprocity calibrations are seen to increase beyond the experimental uncertainty of the plane wave resonant reciprocity calibrations.

2. Experimental Results for The Plane Wave Resonant
Reciprocity Calibration Compared With a NBS Pressure Coupler
Comparison Calibration Obtained For The Same Microphone

The previous corrections are applied in the table shown below:

All dB re 1 V/ubar, all corrections in dB.

freq (Hz)	#1248 prog output (sigma)	***** corrections *****					final cal	** NBS
		ratio of specific heats	* extender & Ct corr (.03 range)	IMPC	Cc corr			
245	-48.93(.05)	+.007	+.32	-.000	+.039	-48.56	-48.55	
490	-48.93(.00)	"	+.27	-.001	+.032	-48.62	-48.59	
735	-48.88(.01)	"	+.26	-.001	+.031	-48.58	-48.58	
980	-48.89(.01)	"	+.26	-.002	+.030	-48.60	-48.61	
1225	-48.85(.02)	"	+.25	-.003	"	-48.56	-48.61	
1470	-48.86(.02)	"	"	-.003	"	-48.57	-48.63	
1715	-48.79(.02)	"	"	-.004	"	-48.51	-48.63	
1960	-48.75(.02)	"	"	-.005	"	-48.46	-48.63	
2205	-48.66(.03)	"	"	-.007	"	-48.38	-48.64	
2450	-48.69(.02)	"	"	-.008	"	-48.41	-48.65	
2695	-48.63(.03)	"	"	-.010	"	-48.35	-48.67	
2940	-48.61(.02)	"	"	-.011	+.029	-48.33	-48.67	
3185	-48.56(.03)	"	"	-.013	"	-48.28	-48.70	
3430	-48.57(.01)	"	"	-.015	"	-48.30	-48.73	
3675	-48.56(.02)	"	"	-.016	"	-48.29	-48.76	
3920	-48.54(.02)	"	"	-.018	"	-48.27	-48.79	
4165	-48.56(.02)	"	"	-.020	"	-48.29	-48.84	
4410	-48.53(.03)	"	"	-.021	"	-48.26	-48.90	
4655	-48.60(.03)	"	"	-.023	"	-48.33	-48.96	
4900	-48.59(.04)	"	"	-.024	"	-48.33	-49.02	
5145	-48.74(.04)	"	"	-.026	"	-48.48	-49.10	
5390	-48.79(.05)	"	"	-.028	"	-48.53	-49.20	
5635	-48.97(.03)	"	"	-.029	"	-48.71	-49.30	

* The value of this correction depends upon the configuration used. ** interpolated from original data. See table 5.7.

Table 5.5 Absolute plane wave resonant reciprocity
calibrations obtained using the 70 cm tube compared with the NBS
comparison calibrations.

A similar table showing the corrections applied to the raw program output for the short tube is next.

 All dB re 1 V/ubar, all corrections in dB.

***** Corrections *****							
freq (Hz)	#1248 prog output (sigma)	Ratio of specific heats	* Extender & Ct corr (.03 range)	IMPC	Cc corr	Final cal.	** NBS
735	-48.86(.01)	+0.007	+0.27	-0.006	+0.031	-48.55	-48.58
1470	-48.81(.00)	"	+0.26	-0.021	+0.030	-48.53	-48.63
2205	-48.70(.02)	"	+0.26	-0.045	"	-48.44	-48.64
2940	-48.60(.02)	"	+0.26	-0.071	+0.029	-48.37	-48.67
3675	-48.48(.02)	"	+0.25	-0.095	"	-48.28	-48.76
4410	-48.46(.06)	"	"	-0.118	"	-48.28	-48.90
5145	-48.69(.01)	"	"	-0.139	"	-48.53	-49.10

* The value of this correction depends upon the configuration used. ** interpolated from original data. See table 5.7.

Table 5.6 Absolute plane wave reciprocity

calibrations obtained with the 23 cm tube compared with the NBS comparison calibrations.

When the results of the short tube and long tube are plotted with the NBS data, the agreement between both plane wave resonant reciprocity tubes is apparent.

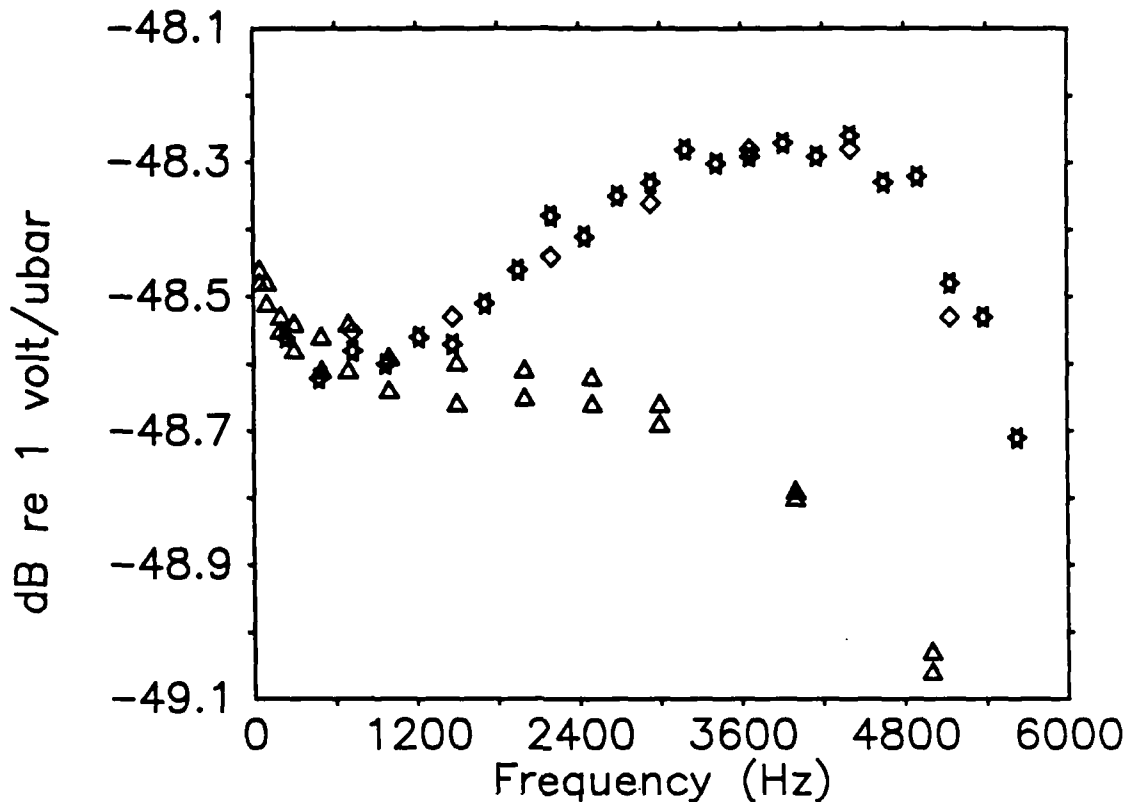


Figure 5.5 Plane wave resonant reciprocity calibration vs NBS comparison pressure coupler calibration of W.E.640AA serial#1248 type L laboratory standard microphone

The triangles plot the NBS pressure coupler comparison calibration, the stars plot the long tube plane wave resonant reciprocity calibration and the diamonds show the short tube resonant reciprocity calibrations. The experimental uncertainties obtained for the data shown in the above figure is tabulated in the next table.

NBS data **			W.E.640AA Serial #1248 data					
freq Hz	run#1	run#2	upper limit (+sigma)	Average resonant reciprocity cal	lower limit (-sigma)			
***** All dB are re 1 Volt/ubar *****			[Long tube data]			[Short tube data]		
50	-48.48	-48.46						
100	-48.51	-48.48						
200	-48.55	-48.53						
245			-48.51	-48.56	-48.61			
300	-48.58	-48.54						
490			-48.61	-48.62	-48.63			
500	-48.61	-48.56						
700	-48.61	-48.54						
735			-48.57	-48.58	-48.59	-48.52	-48.55	-48.58
980			-48.59	-48.60	-48.61			
1000	-48.64	-48.59						
1225			-48.54	-48.56	-48.58			
1470			-48.55	-48.57	-48.59	-48.50	-48.53	-48.56
1500	-48.66	-48.60						
1715			-48.49	-48.51	-48.53			
1960			-48.44	-48.46	-48.48			
2000	-48.65	-48.61						
2205			-48.35	-48.38	-48.41	-48.35	-48.44	-48.53
2450			-48.39	-48.41	-48.43			
2500	-48.66	-48.62						
2695			-48.32	-48.35	-48.38			
2940			-48.31	-48.33	-48.35	-48.24	-48.36	-48.48
3000	-48.69	-48.66						
3195			-48.25	-48.28	-48.31			
3430			-48.29	-48.30	-48.31			
3675			-48.27	-48.29	-48.31	-48.13	-48.28	-48.43
3920			-48.25	-48.27	-48.29			
4000	-48.79	-48.80						
4165			-48.28	-48.29	-48.31			
4410			-48.23	-48.26	-48.29	-48.04	-48.28	-48.52
4655			-48.30	-48.33	-48.36			
4900			-48.28	-48.32	-48.36			
5000	-49.03	-49.06						
5145			-48.44	-48.48	-48.54	-48.38	-48.53	-48.68
5390			-48.49	-48.53	-48.58			
5635			-48.68	-48.71	-48.74			
6000	-49.42	-49.47						

** The certified NBS calibration specified only 3 significant figures. The above data is before the roundoff provided in the formal report and shows the individual comparison calibrations actually obtained as referenced to two separate standard

microphones used for this purpose at the NBS [Ref 29].

Table 5.7 W.E.640AA Serial #1248 calibrations.

The upper bound is one "experimental sigma" above the average sensitivity shown in the center column for both the long and short data sets. The lower bound is one "experimental sigma" below the same average. For each data set at each different calibration frequency, the sigma used is the square root of the sum of the squares of the experimental sigma found for Ma. The long tube results agree with the NBS calibration to within ~ 0.03 dB up to 1470 Hz and the short tube results agree with the NBS calibration to within ~ 0.06 dB up to 1470 Hz. Above this frequency, the resonant reciprocity calibrations disagree with the NBS comparison calibration beyond the experimental uncertainty. However, both resonant reciprocity tubes provide consistent results throughout the range of frequencies used in the experiment.

Since the diaphragm area of the microphone occupies a significant portion of the cross sectional area of the short tube ($\sim 54\%$ as compared to $\sim 29\%$ in the long tube), any deviation from the assumption that $Z_{a(\text{mic A})}$ equals $Z_{a(\text{mic B})}$ will adversely effect the accuracy of the impressed pressure correction in the short tube to a greater extent than the corresponding correction for the impressed pressure

in the long tube. Additionally, the fractional error in the volume of the short tube is greater than that obtained for the long tube (the tube volume is used in calculating "Jo" in the impressed pressure correction). Both of these contributions to increased absolute uncertainty apply for the short tube calibration. For these reasons, the microphone calibrations obtained using the long tube geometry are believed to be the more accurate of the two .

H. THE CORRECTED FREE FIELD COMPARISON CALIBRATION

There were only two corrections to the free field comparison results given by program "N28". The first is calculated using equation 5.15 with a change of value for C_t and C_t'' to 255.0 pF. When this is done the correction is essentially the same for all the frequencies sampled and is equal to +0.54 dB. The second correction is for the diffraction of the microphone and mount and is given in appendix A to reference 3. With both of the corrections applied, the diffraction corrected (pentagon plot) free field (star plot) comparison calibration is superimposed upon the NBS pressure coupler (triangle plot) calibration. In addition, the uncorrected free field results are shown with Professor Medwin's calibration results in figure 3.24. The corrected results are shown on the next page.

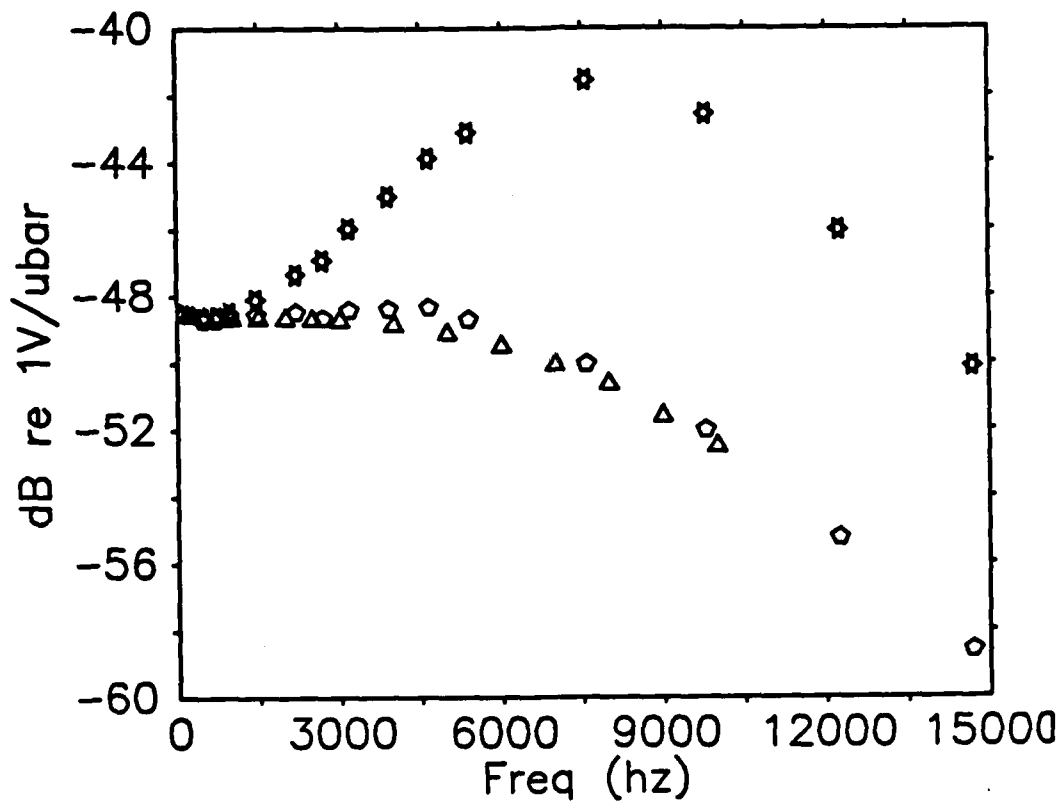


Figure 5.6 The corrected free field comparison calibration for W.E.640AA serial #1248 microphone.

Since the diffraction correction obtained from data in reference A is accurate only for a standard microphone mount and the mount used in this experiment was not standard, the diffraction correction so obtained was only approximate. This is seen in the ~0.5 dB agreement between the NBS pressure coupler results and the diffraction "corrected" results.

In the next plot, the data is "blown-up" so that the low frequency detail is seen.

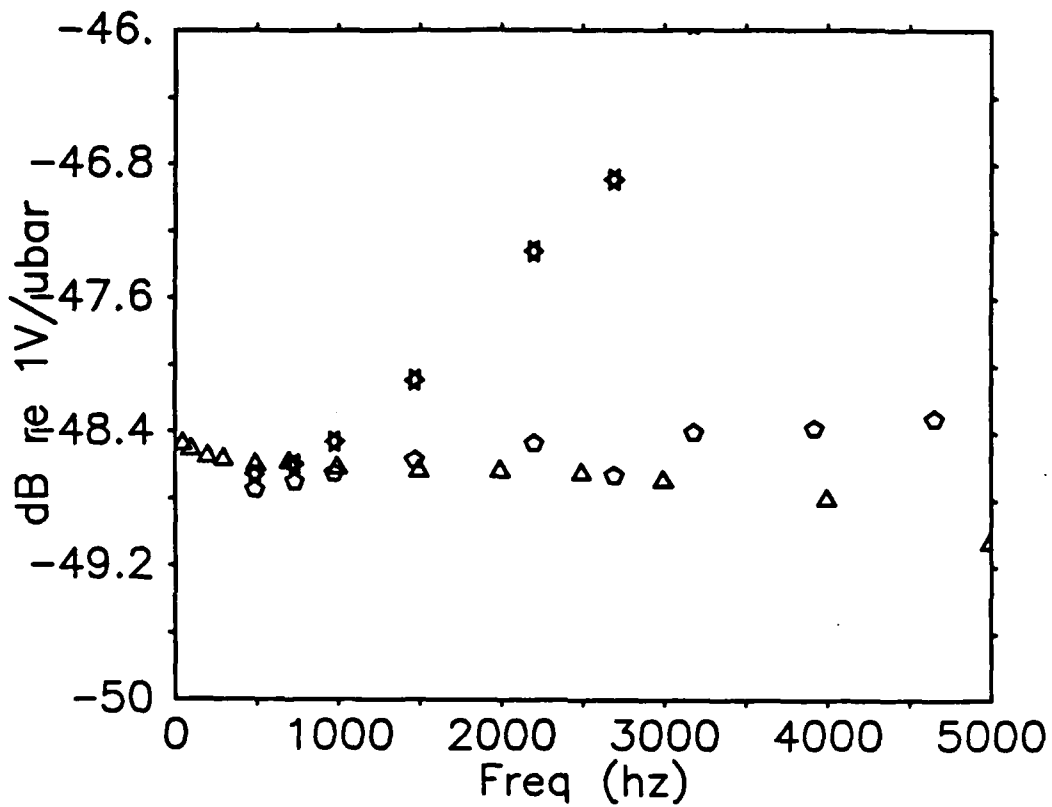


Figure 5.7 Low frequency detail in the corrected free field comparison calibration.

The data plotted in the previous two plots is given in the table below.

 All data in dB re 1 Volt/ubar

NBS data (pressure coupler)			Free field data for Serial #1248				
Freq Hz	run #1	run#2	Free field "raw"	Ct Corr	Free field cal.	diffraction correction*	diffraction corrected calibration
200	-48.55	-48.53					
245			-49.54	0.54	-49.00	.0	-49.54
300	-48.58	-48.54					
490			-49.19	0.54	-48.65	-.1	-48.75
500	-48.61	-48.56					
700	-48.61	-48.54					
735			-49.13	0.54	-48.59	-.11	-48.70
980			-49.00	0.54	-48.46	-.19	-48.65
1000	-48.64	-48.59					
1470			-48.63	0.54	-48.09	-.48	-48.57
1500	-48.66	-48.60					
2000	-48.65	-48.61					
2205			-47.86	0.54	-47.32	-1.15	-48.47
2450			-47.33	0.54	-46.79	-1.44	-48.23
2500	-48.66	-48.62					
2695			-47.42	0.54	-46.88	-1.77	-48.65
3000	-48.69	-48.66					
3185			-46.50	0.54	-45.96	-2.44	-48.40
3920			-45.51	0.54	-44.97	-3.40	-48.37
4000	-48.79	-48.80					
4655			-44.37	0.54	-43.83	-4.48	-48.31
5000	-49.03	-49.06					
5390			-43.63	0.54	-43.09	-5.59	-48.68
6000	-49.42	-49.47					
7000	-49.97	-50.01					
7595			-42.07	0.54	-41.53	-8.48	-50.01
8000	-50.55	-50.55					
9000	-51.48	-51.59					
9800			-43.06	0.54	-42.52	-9.46	-48.52
12250			-46.55	0.54	-46.01	-9.23	-55.24
14700			-50.63	0.54	-50.09	-8.49	-58.58

* L.R. interpolation to data listed in appendix A of Ref. 3

Table 5.8 NBS vs Free field data.

Since the anechoic chamber is designed to be reflection-free for plane waves, the normal specific acoustic impedance of the walls is intended to be the "rho-c" product for air. This is not a perfect impedance match to spherical acoustic waves which have a reactive component. The specific acoustic impedance of a spherical wave is given below.

$$Z_A = \frac{\rho_0 c}{1 - j/kr} \quad \text{Equation 5.16}$$

When the speaker and microphone are "relatively close" to the wall, meaning kr is small, there will be reflections due to the impedance mismatch even in a perfectly anechoic room. These reflections cause an error in the value of M_0 . Additionally, the requirement [Ref. 3:p.19] that at low frequencies the acoustic impedances of the walls be within $2r'/r$ percent of "rho-c" where r' is the microphone separation distance from the surface to the microphone and r is the microphone separation, is not met. The inability to meet these restrictions within the anechoic chamber is seen in the discrepancy in M_0 observed at low frequency.

I. A SUMMARY OF PLANE WAVE RESONANT RECIPROCITY CALIBRATIONS

The plane wave resonant reciprocity calibrations shown so far have been those obtained for the W.E.640AA serial #1248 condenser microphone and were used for comparison with the NBS pressure coupler calibration. Additional calibrations for two more W.E.640AA condenser microphones and one small electret "hearing-aid" subminiature transducer were obtained.

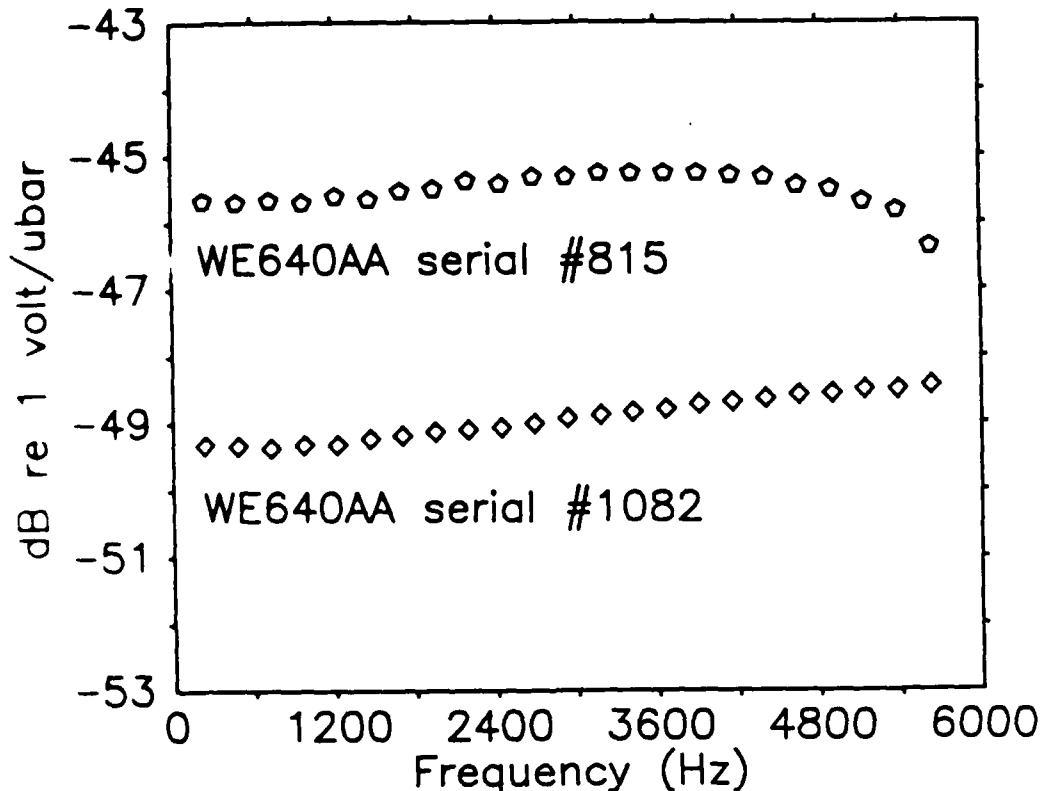


Figure 5.8 Plane wave resonant reciprocity calibrations for W.E.640AA serials #815 and #1082 listed top to bottom.

The absolute experimental uncertainty is essentially the same for all WE640AA microphones, ~ 0.03 dB below 1470 Hz, while above this frequency the difference between the resonant reciprocity calibration and the NBS comparison calibration climbs to a maximum of ~ 0.5 dB.

The theory for resonant reciprocity calibrations has been shown to absolutely agree with standard methods of calibration only for the case of plane wave resonance at low frequency. Experimental results that extend calibration frequencies into the region of radial and azimuthal resonances are expected to fail in accuracy. To illustrate, the calibration data plotted on the next page shows the agreement between short and long tube calibrations out to the 23rd modal resonance in the long tube (~ 5635 Hz) which is the upper limit for plane wave resonances in that tube. The effect on the calibration due to the interference of radial and azimuthal modes with plane wave modes is apparent above the 23rd mode. Here the discrepancy between short and long tube calibration results is seen to sharply increase.

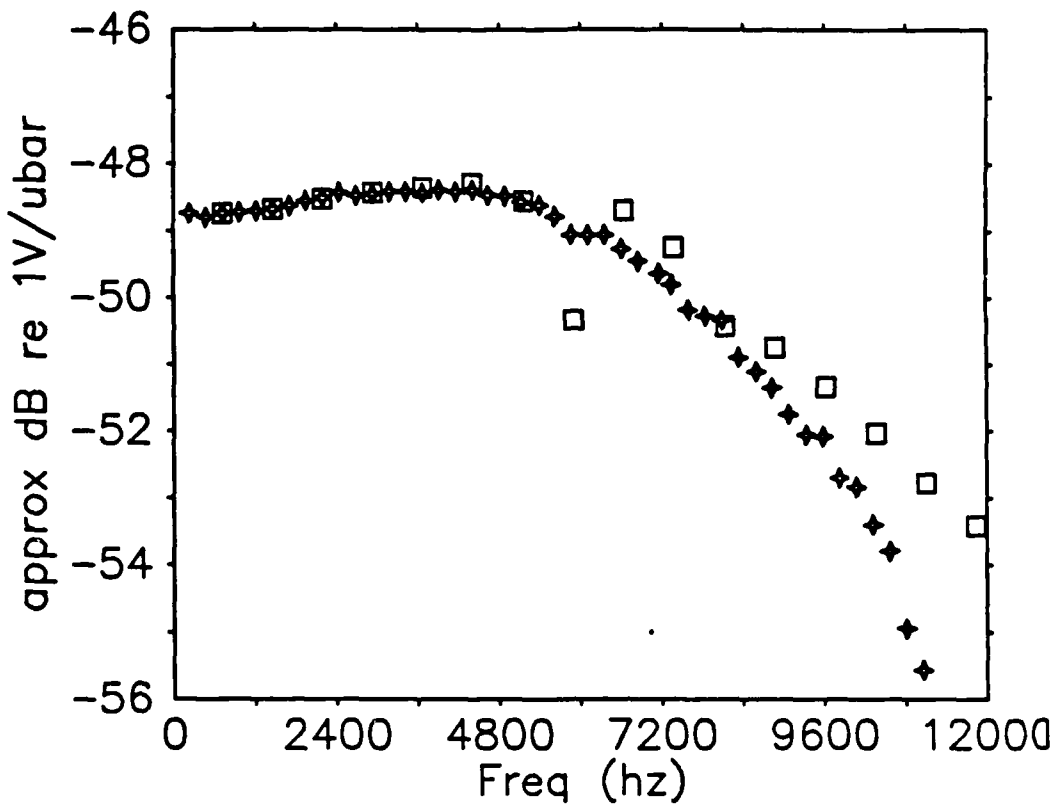


Figure 5.9 The effect of radial and azimuthal modes on the plane wave resonant reciprocity calibration.

These calibrations are listed as approximate since they are the "raw" program output.

The type BT-1751 Knowles subminiature transducer was used as the comparison microphone and the following comparison calibration was obtained:

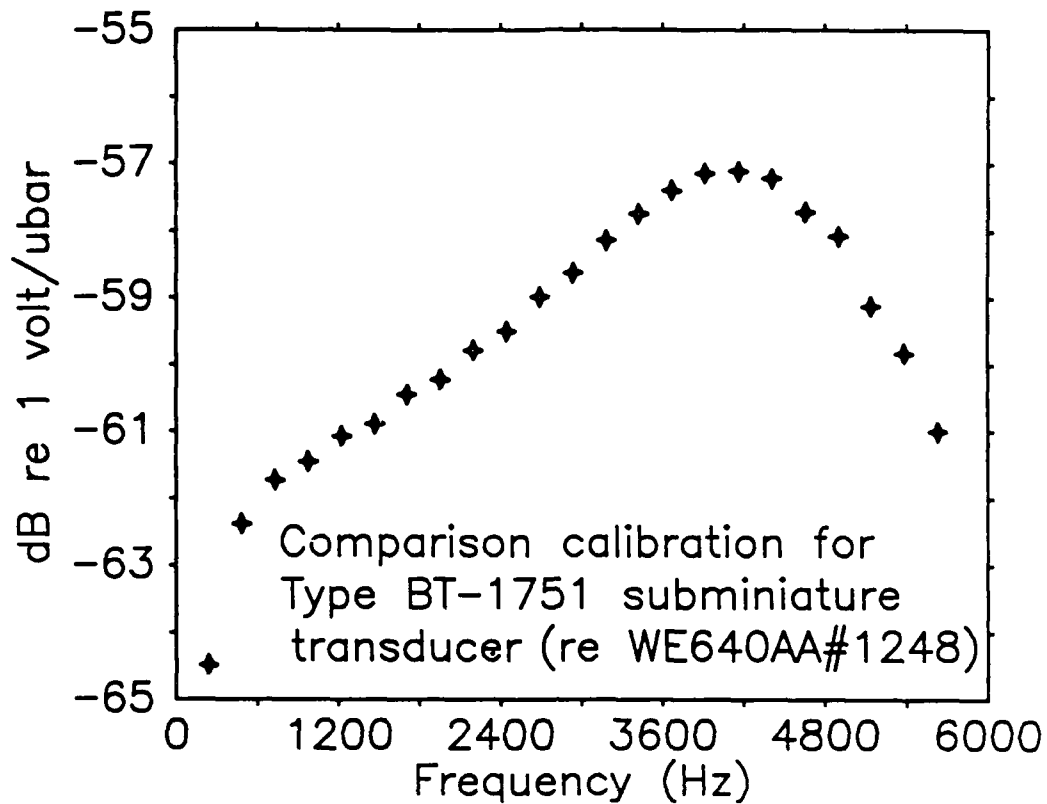


Figure 5.10 Comparison calibration for the type BT-1751 Knowles subminiature transducer.

The sigma of the experimental precision is smaller than the size of the plotting symbols in this calibration. When this calibration is compared with the manufacturer specifications for this device, the sensitivity appears to be about ~ 1.5 dB too low. However, the variations in the D.C. supply voltage for the Type BT-1751 preamplifier were not monitored. From Knowles technical bulletins, a change of just a few tenths of a volt (1.25 Volts to 1.0 volts) can cause roughly a ~ 1.0

dB drop in sensitivity. Since the battery used to power the BT-1751 D.C. supply was not replaced during that portion of the experiment (~12 months), such a drop is probable.

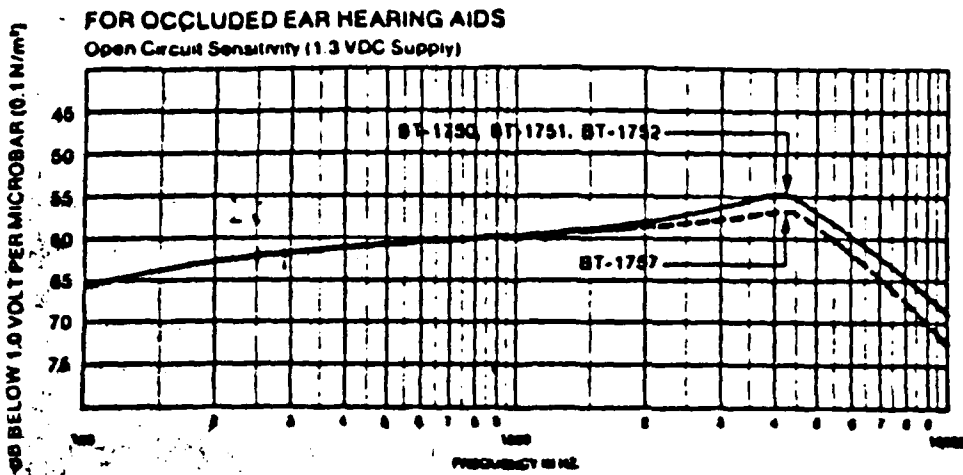


Figure 5.11 Manufacturer's calibration curves for the Type 1751 and Type 1757 Knowles subminiature transducers.

This concludes the free field comparison and the plane wave resonant reciprocity calibration experiments.

VI. CONCLUSION

A. SUMMARY

In chapter I, the general subject of acoustic reciprocity calibrations of electroacoustic transducers is reviewed and the effect of the medium and boundary conditions surrounding the transducer are considered for three different experimental environments. Solutions for the acoustic transfer admittance for a pressure coupler calibration, a free field calibration, and a plane wave resonant reciprocity calibration are shown to differ only by a multiplicative constant. Derivations of the open circuit voltage receiving sensitivities are provided for all three techniques. In chapter II, considerations are made regarding experimental techniques used to implement plane wave resonant reciprocity calibrations. The resulting reciprocity equations provide a six way round robin check on experimental precision (plus or minus .002 dB) and the number of experimental parameters required for the calibration is reduced by one. The derivation of a plane wave resonant reciprocity calibration is extended to include necessary conditions relating the acoustic impedance of the reciprocal microphone, the frequency, the speed of sound

within the gas, the gas density, and the dimensions of the plane wave resonant cavity. An impressed pressure correction is derived from the canonical equations for an electroacoustic transducer by making the reasonable assumption that the diaphragm of a condenser microphone *does* "move" under the influence of an acoustic pressure. This consideration of the finite impedance of the microphone results in a correction to the theoretical sensitivity of an ideal microphone and is shown to depend upon the ratio of the driving point acoustic admittance of the microphone to the transfer acoustic admittance of the medium. In chapter III, the improvement in experimental precision due to computer control of the data acquisition is measured and the probable errors associated with experimental measurements and calculations are determined. In chapter IV the self consistency of the plane wave resonant reciprocity calibrations are obtained and the overall experimental precision is found to be ~ 0.045 dB. In chapter V, calculations necessary to determine and correct for the impressed pressure, the effect of the non-adiabatic boundary conditions on the stiffness of the gas within the resonant cavity, circuit analysis approximations, and corrections to values of program constants in the computer program controlling the plane wave resonant reciprocity calibration are obtained. When the raw experimental calibration data is

corrected as outlined above, the absolute plane wave resonant reciprocity calibrations have close experimental agreement below ~1500 hertz (with an average absolute discrepancy in the long tube of ~.03 dB and in the short tube of ~ .06 dB) with that portion of a pressure coupler comparison calibration performed in air (and hydrogen) on the same microphone by the National Bureau of Standards. Beyond this frequency, the difference (in dB) between the NBS comparison calibration and the resonant reciprocity calibrations increases linearly with frequency with a linear correlation coefficient of $r = 0.991$.

Both the long and the short tube resonant reciprocity calibrations have an average absolute difference of ~ .029 dB (.018 dB sigma) from 735 to 5145 Hz, the common frequency range of both calibrations. Although the average absolute difference in the resonant reciprocity calibrations and the diffraction corrected free field comparison calibrations (from 1470 to 5390 Hz) is ~ 0.12 dB (sigma ~ .09 dB) and the average absolute difference in the NBS comparison calibration and the diffraction corrected free field comparison calibration is ~ 0.32 dB (sigma ~ .22 dB), the failure to use experimentally an exact replica of the standard mounting [Ref.3:p.21] for the WE640AA results in an unknown uncertainty for the diffraction correction and hence calls into question the validity of the absolute agreement

(sigma ~ .09 dB) with the free field results observed from 1470 to 5390 Hz.

In conclusion it can be said that the results of this experiment show that the method of plane wave resonant reciprocity calibration is in absolute agreement with other laboratory standard techniques at low frequency, is under computer control, and has the potential of becoming a fully automated laboratory standard technique of reciprocity calibration for electrostatic transducers.

B. FURTHER EXPERIMENTS AND THEORETICAL INVESTIGATIONS

In the future, the practical convenience of combining under computer control all of the data acquisition necessary to calculate the microphone's acoustical impedance, the driving point electrical impedance, and the plane wave resonant reciprocity calibration is the logical correction to and extension of this experimental method.

A more detailed experimental and theoretical study of the impressed pressure correction is needed with regard to more compliant electrodynamic microphones (and other transducer types), different gas atmospheres, a wider range of length to diameter ratios, and a wider range of diaphragm diameter to tube diameter ratios for the resonant cavities.

Any further experiment may also extend the upper frequency limit of plane wave resonant reciprocity calibrations by examining the selective employment of "clean" plane wave resonances in the region of azimuthal modal resonances and/or the use of highly symmetric mountings of the microphones on precisely machined cylindrical cavities. This suggestion is a result of two experimental observations. First, several higher frequency "short" tube plane wave resonant reciprocity calibrations appear to be asymptotically approaching the correct pressure calibration. The particular modes (twelve through sixteen)

used for these calibrations are seen in figure 1.6. The plane wave resonant reciprocity calibrations which result from the use of these modes are shown in figure 5.9 and tend towards agreement with the NBS pressure coupler comparison calibrations even though they exist in a frequency domain where azimuthal resonances are expected. Secondly, extended plane wave resonances were observed *exclusive* of any observable azimuthal or radial modes up to ~ 50 KHz when highly symmetric electret microphones were used in the early stages of the experiment. In light of the aforementioned experimental indications, these apparently "clean" plane wave resonances may possibly be employed with success.

The application of plane wave resonant reciprocity to a system of transducers coupled through a water filled cylindrical cavity with a "pressure-release" (styrofoam) boundary is another avenue of experimental and theoretical investigation which may be both interesting and significant. A preliminary investigation has already begun [Ref. 35] by applying the method to a "slow wave resonant calibration" where a compliant wall and fluid filled waveguide are used to obtain a low frequency reciprocity calibration in water.

APPENDIX A

HARMONICITY IN PLANE WAVE RESONANT RECIPROCALITY CALIBRATION

When the condenser microphones are mounted in the ends of the brass cylindrical cavity, the acoustical load at the ends is affected by the mechanical impedance of the microphones and the assumption that the microphones are non-compliant must be more carefully examined.

If the microphones were perfectly rigid, the boundary conditions at each end of the cavity require that the gradient of the acoustic pressure be equal to zero. If this is the case, then the resonant frequencies observed for modes greater than the first will simply be multiples of this fundamental resonance ($KL = n\pi$). This appears to be the case when the resonant frequencies are plotted opposite the mode number of the resonance. Since the information plotted below was obtained over a ten hour period, the resonant frequencies were obtained at different laboratory temperatures over a range of roughly 19 degrees centigrade to 22 degrees centigrade. Since the speed of sound in air at normal atmospheric pressure varies as the square root of the absolute temperature, and since the frequency of a plane progressive sound wave varies as the free space sound speed, the frequency of resonance varies also as the square root of

the absolute temperature within the plane wave resonant cavity. For comparison purposes, the temperature dependence of the different resonant frequencies was removed by referencing all the resonances to 20 degrees centigrade using equation A.1 shown below.

$$f(\text{re. } 20^{\circ}\text{C}) = f(\text{re. } T_1) \left(\frac{293.16}{273.16 + T_1} \right)^{1/2} \quad \text{Equation A.1}$$

If this plot of the "corrected" resonant frequency vs. mode number were exactly a straight line, then the modal resonances would be perfect multiples of the fundamental resonance and the ends of the tube would be "rigid" (perfect harmonicity). This appears to be the case when figure A.1 is "eye integrated".

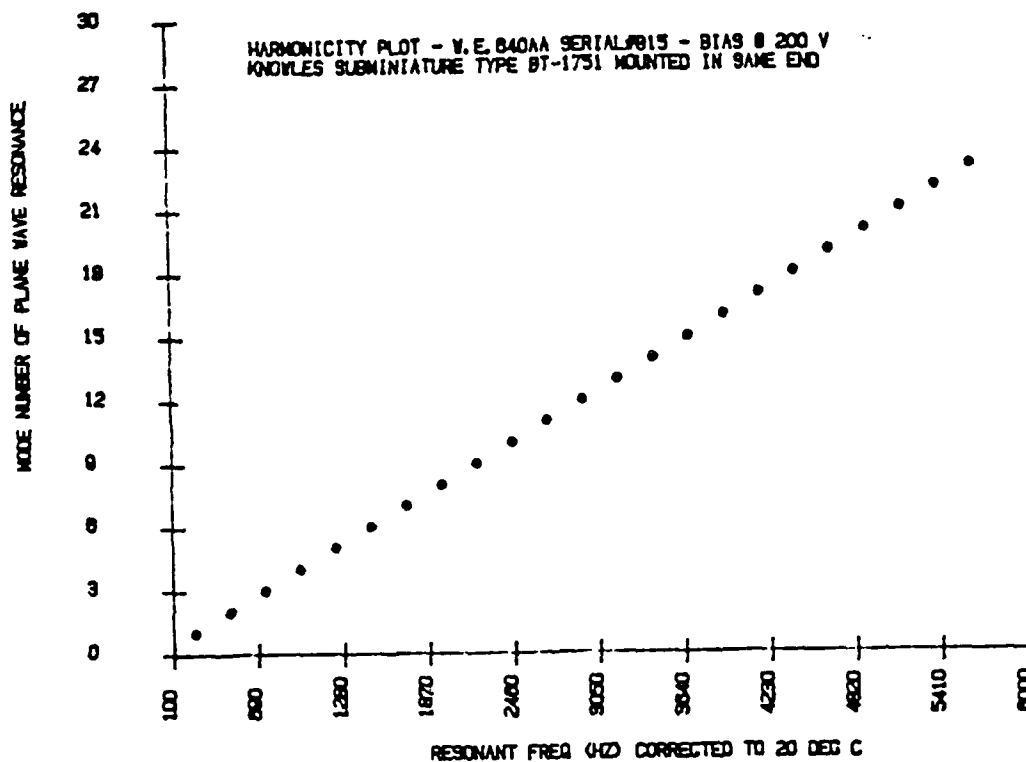


Figure A.1 Resonant frequency re. 20 deg C vs Mode Number

As is seen above, any lack of "harmonicity" or deviation from a straight line is not readily apparent. The terminations in the plane wave resonant cavity appear essentially "rigid" with regard to their influence upon the resonant frequency obtained for the acoustic pressure. If the condenser microphones were *absolutely* noncompliant, then they would not function as microphones as there would be no change in capacitance with impressed acoustic pressure. Functionally, the microphones cannot be "rigid". To see the magnitude of the deviation from true harmonicity, the data

is normalized by dividing all the individual resonance frequencies by the "apparent" fundamental associated with the highest resonant frequency obtained (simulating the rigid limit), the non-harmonicity at the low resonant modes becomes apparent as a deviation from a value of one provided the scale is properly chosen. See figure A.2.

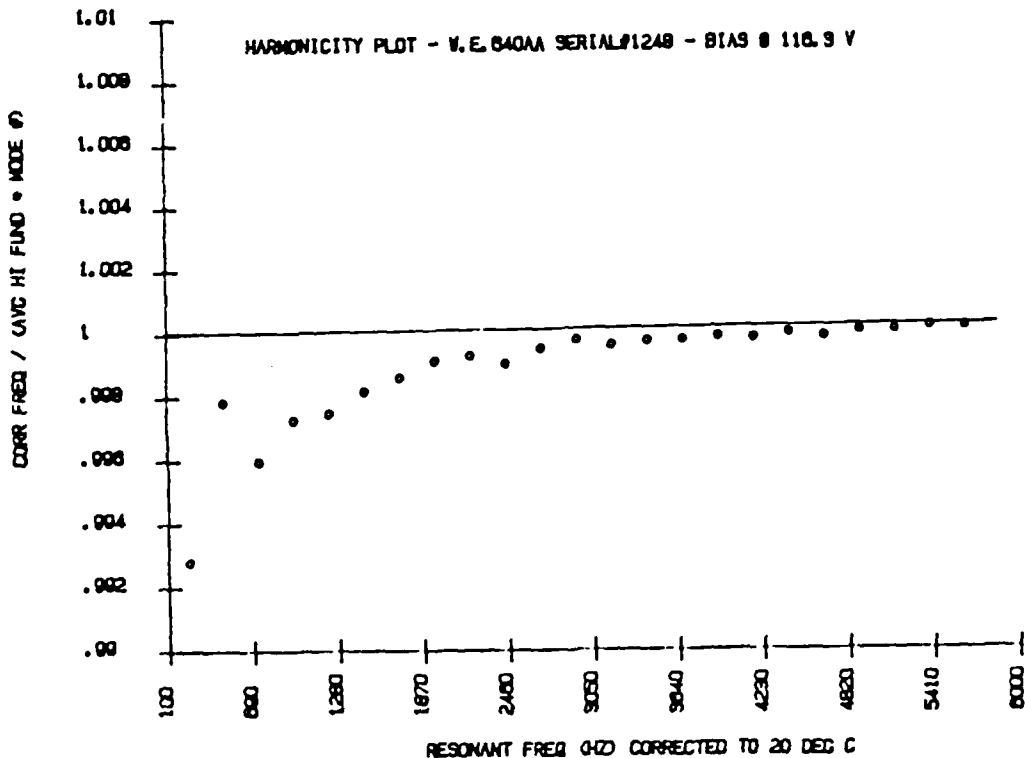


Figure A.2 Harmonicity as measured with data from
Condenser Microphone W.E.640AA Serial#1248

With regard to the effect this measured non-harmonicity has upon the value of the receiving sensitivity in the plane wave reciprocity calibration, recall equation 2.13.

$$\frac{P_2'}{P_3} = \cos(kL) + j \left[\frac{\rho_0 c A_B}{Z_{mb}} \right] \sin(kL) \quad \text{Equation 2.13}$$

Here we see that at modal resonances, for the compliance of the condenser microphones to be a negligible effect, we require that:

$$\begin{aligned} | \rho_0 c A_B \sin(kL) | &\ll | Z_{mb} | \\ \text{AND,} \\ \cos(kL) &\cong 1 \end{aligned} \quad \text{Equations A.2}$$

In figure A.2, the ratio of the resonant frequency for the lowest mode to the normalized resonant frequency found for the highest mode was calculated to be .9927. This represents an estimate of how close the boundary conditions correspond to a value of kL equals π for the fundamental mode (worst case). When we express Equation 2.13 in terms of acoustic impedances, we see that,

$$\frac{P_2'}{P_3} = \cos(kL) + j \left[\frac{Z_A(\text{AIR})}{Z_A(\text{END})} \right] \sin(kL) \quad \text{Equation A.3}$$

Since the ratio of the acoustic impedance of the medium (air) to that of the semi-rigid composite ends (microphone plus rigid mount) is much less than one, we have upon substitution for $\text{Cos}(kl)$ and $\text{Sin}(kl)$ in Equation A.3,

$$\frac{P_2'}{P_3} \cong \text{Cos} [.9927\pi] \cong -.9997 \quad \text{Equation A.4}$$

This justifies the assumption that the microphones are essentially non-compliant with regard to their effect on the pressure distribution within the resonant cavity. Since the ratio of the pressures comes in under the square root in the calculation for the microphone open circuit voltage receiving sensitivity, this assumption will introduce, at the lowest mode, roughly a $20\log(\text{sqr}[\text{Cos}(.9927*\pi)])$ or .001 db re 1V/ubar error. Errors introduced due to this assumption are significantly lower at the higher modal resonances as seen in figure A.2.

APPENDIX B

ONE EXAMPLE OF THE COMPUTER PROGRAM USED FOR PLANE WAVE RESONANT RECIPROCITY CALIBRATIONS

A. INTRODUCTION

The computer program shown on the following pages was written in Hewlett Packard series 80 Basic. It was used on the HP-85 and completed data acquisition and sensitivity calculations for three microphones at one modal resonance roughly every twenty minutes. The most time consuming portion of the program was that part which calculated the three parameter least mean square error fit to a Rayleigh line shape. Actual data acquisition was completed in roughly three minutes.

A careful examination of the particular program shown in part C below shows that it is but one of six almost identical programs used to accommodate the various combinations of preamplifiers and microphones that were experimentally used. The decision to write six "different" programs was made for operational simplicity. Such variables as volumetric protrusion into the main cavity depended upon which two microphones were in place. The

voltage transfer for each "end" of the cylindrical cavity depended upon the amplifier and microphone combination used. Thus slightly different programs were used to accommodate (referencing W.E.640AA serial numbers); 1248-1082, 1248-815, 1082-815, and three more similar microphone setups with the "electronics" reversed. The particular program discussed in this appendix is the one with microphone #1248 with the "A" side electronics and microphone #1082 with the "B" side electronics.

The following pages are separated into three different parts for convenience. First, there is a functional description of the program shown in table B.1. Next, there is the program listing and last there is a list of definitions for the variables used in the program. The functional outline for the program is shown next.

B. FUNCTIONAL DESCRIPTION OF THE PROGRAM

The main program is divided into eight subsections outlined below.

1. Initial setup.
2. A transmit, B receive data. (ATBR)
3. B transmit, A receive data. (BTAR)
4. A transmit, C receive comparison voltage.
5. B transmit, C receive comparison voltage.
6. Numerical analysis of all data.
7. Calculation of six different values of open circuit voltage receiving sensitivity.
8. Subroutines (17)

These eight functional descriptions are more fully described in table B.1 below.

Beginning line number - Functional description

10 Program initialization and preliminary equipment setup.
240 Magnetic tape initialization.
390 Operator inputs for data run.
630 Dimension arrays and input measured capacitances, load resistances and numerical corrections for the side mounted microphones.
2010 Input cavity volumes for different configurations and rearrange data.
2170 Begin program run. Switch system to ATBR.
2350 Search for initial drive voltage for first data sample.
2520 Initial data sample.
2540 Analyze data for rough Q,F,&A.
2570 Obtain receiver bias voltage and calculate the required correction to microphone capacitance.
2630 With the preliminary values of Q,F,&A, obtain the first modal data set with side B receiving. Obtain rough Q,F,&A for this data set.
2870 Switch system to BTAR.
2880 Obtain bias voltage for side A to receive and calculate the required correction to the microphone capacitance.
2940 Sample the modal resonance for side A receiving. Obtain rough Q,F,&A for this data set.
3150 Goto Ravine Subroutine for ATBR data. Store ravined values.
3270 Goto Ravine subroutine for BTAR data. Store ravined values.
3450 Based upon the requested drive voltage, calculate the transmit current used for the "A" microphone in ATBR.

3670 Switch and obtain the ATCR comparison voltage.
 3720 Switch and obtain the BPCR comparison voltage.
 3760 Calculate the effective value for specific heats used to correct the bulk modulus of elasticity for boundary conditions.
 3820 Change atmospheric pressure from mmHg to MKS.
 3860 Calculations for six way round robin determination of M_a (reciprocity), M_b (reciprocity), M_{ab} (comparison), M_{ba} (comparison), M_{ca} (comparison), & M_{cb} (comparison)
 4020 Store results on magnetic tape and print out results for operator.
 4390 Check for end of data runs desired.
 4400 Based upon the quality factor for the (N+1)th mode, calculate the expected bandwidth of Nth resonance to be used in the next computer controlled calibration.
 4530 Subroutine used to ravine the modal data for accurate values of Q, F, & A.
 5470 Subroutine used to calculate the mean square error with regard to the Rayleigh line shape.
 5580 Subroutine used for initial data collection.
 5760 Subroutine used to adjustment the initial drive voltage and control the preliminary data sampling.
 6270 Subroutine used to make a raw data computation of Q, F, & A.
 7020 Subroutine used to sample temperature.
 7120 Subroutine used to sample atmospheric pressure.
 7220 Subroutine used to obtain side A bias voltage.
 7320 Subroutine used to obtain side B bias voltage.
 7410 Subroutine used to select system to ATBR.
 7540 Subroutine used to select system to BTAR.
 7690 Subroutine used to select system to ATCR.
 7810 Subroutine used to select system to BPCR.
 7930 Subroutine used to sample voltage V_{ca} .
 8080 Subroutine used to sample voltage V_{cb} .
 8220 Subroutine used to relate preamplifier gain, 5204 scale, and capacitive voltage division to the signal voltage V_a .
 8310 Subroutine used to relate preamplifier gain, 5204 scale, and capacitive voltage division to the signal voltage V_b .
 4440 End after all desired modes are sampled.

Table B.1 Functional program listing

C. PROGRAM LISTING

```

10 CLEAR ! 1248-"A";1082-"B"
20 ! INPUT TIME IF NOT ALREADY
30 OPTION BASE 1
40 L4=0
50 DIM G2(26),G4(26),B1(30),T1(90),T3(90),T4(90),V1(2),T5(2)
.P5(2),K1(2),G9(2),A7(2),A1(2,48)
60 DIM G5(2,26),F5(2,26),F7(4),C1(5),A2(2),G1(2,50)
70 DIM F(26),A(26),F1(26),B(3,3),X(3),C(3),V(2),Q(2),D(90),K
(3),F2(2),G(90),T(3),V2(2,3),A3(26)
80 DISP "SETTIME H=3600+M=60,MDD;...ONLY IF NECESSARY"
90 ! REVISED 28 APRIL 84
100 ! RECIPROCITY PRG G91A
110 ! PRELIMINARY SETUP
111 ! 1248-1082 SETUP
120 OUTPUT 717 ;"AM",1,"MR"
130 PRINT "PROGRAM G91A OF 27 APRIL 84"
140 PRINTER IS 701,80
150 IMAGE 2A,2X,7A,X,6A,X,7A,X,7A,X,7A,4X,4A,7X,4A,9X,2A,1X,
6A
160 PRINT USING 150 ; "N","Freq HZ","TdegC","QA","QB","<MA>"
,"<MB>","<MC>","%","RECORD"
170 IMAGE 2D,X,DDDD,DD,X,DD,DD,X,DD,DD,X,DD,DD,X,D,DD
E,X,D,DDDE,X,D,DDDE,X,D,DD,X,DD
180 DISP "THIS PRG PERFORMS A RECIPROCITY CAL AT DESIG MODA
L FREQS AND PUTS DATA ON TAPE"
190 BEEP
210 C1=1 ! CAVITY VOL-1248-1082
220 DISP "INPUT DDMYY"
230 INPUT T(3)
240 ! INPUT TAPE STATUS
250 DISP "ENTER 1=ERASE,REWIND &FORMAT; 2=TAPE ALREADY READY
"
260 BEEP
270 INPUT U7
280 IF U7=1 THEN 290 ELSE 400
290 DISP "ARE YOU CERTAIN YOU WANT TO ERASE THE TAPE?????"
300 DISP "1=YES,2=NO"
310 INPUT U7
320 IF U7=1 THEN 330 ELSE 400
330 ERASETAPE @ BEEP
340 ! PREPARE TAPE
350 CREATE "DAT1",100,96
360 CREATE "DAT2",100,96
370 CREATE "DATV",100,800
380 CREATE "DATF",100,800
390 ! ENTER RUN PARAMETERS
400 DISP "SHORT OR LONG TUBE?"
410 DISP "SHORT=1, LONG=2"
420 BEEP
430 INPUT C !
440 DISP "ENTER STARTING RECORD#"
450 INPUT L4 ! INIT RECORD NUMBER
450 DISP "ENTER HIGH MODE # "

```

```

470 INPUT L
480 DISP "ENTER LOW MODE #"
490 INPUT L1
500 DISP "ENTER THE LOW FREQ (HZ) FOR HIGH MODE"
510 INPUT F1
520 DISP "ENTER THE HI FREQ (HZ) FOR HIGH MODE"
530 INPUT F2
540 DISP "ENTER 5204 TIME CONSTANT(SEC)"
550 INPUT T1
560 T1=TT=1000
570 DISP "ENTER THE 5204 SENSITIVITY IN VOLTS"
580 INPUT B
590 M9=15 ! MAX # OF RAVINES
600 DISP "ENTER REL HUMIDITY%"
610 BEEP
620 INPUT R1
630 !
640 ! DIMENSION ARRAYS
650 ! DATA ARRAYS
660 ! .....
670 ! MEASURED CAPACITANCES
675 C1(1)=52.722 ! PF#1248
690 C2=C1(1)
700 C1(2)=177.2802 ! PF BTAR SYS
715 C1(3)=53.123 ! PF#1082
720 C3=C1(3)
730 C1(4)=176.0527 ! PF ATBR SYS
740 C1(5)=50.212 ! PF#815
750 C5=C1(5)
760 !
761 R8=5047050 ! A SIDE R EFF LOAD
762 R9=4987470 ! B SIDE R EFF LOAD
770 ! GEOMETRY CORRECTION
780 ! FOR SHORT TUBE
790 D(1)=.965115 !
800 D(2)=.863218
810 D(3)=.702132
820 D(4)=.494203
830 D(5)=.255249
840 D(6)=.00325317
850 D(7)=.243115
860 D(8)=.466004
870 D(9)=.649799
880 D(10)=.782323
890 D(11)=.855722
900 D(12)=.866966
910 D(13)=.817927
920 D(14)=.715056
930 D(15)=.568673
940 D(16)=.391959
950 D(17)=.139753
960 D(18)=.007256489
970 D(19)=.171237

```

```

980 D(20)=-.323466
990 D(21)=-.440099
1000 D(22)=-.515326
1010 RAD ! CORR FOR SMALL OFFSET
1020 ! GOTD 1070
1030 FOR N=1 TO 22
1040 D(N)=ABS(COS(N*PI*1.46/23.37))
1050 NEXT N
1060 ! LONG TUBE GEO CORR...
1070 G(1)=-.99602
1080 G(2)=-.984117
1090 G(3)=-.964383
1100 G(4)=-.936999
1110 G(5)=-.9022062
1120 G(6)=-.860311
1130 G(7)=-.81158049
1140 G(8)=-.75674208
1150 G(9)=-.6959764
1160 G(10)=-.6299141
1170 G(11)=-.5591307
1180 G(12)=-.4824135
1190 G(13)=-.4058943
1200 G(14)=-.3247655
1210 G(15)=-.2415518
1220 G(16)=-.1569648
1230 G(17)=-.0717239
1240 G(18)=-.01345009
1250 G(19)=-.09784211
1260 G(20)=-.18074880877
1270 G(21)=-.2614853
1280 G(22)=-.3393913
1290 G(23)=-.413837
1300 G(24)=-.48422887
1310 G(25)=-.5500143
1320 G(26)=-.6106872
1330 G(27)=-.66579
1340 G(28)=-.7149249
1350 G(29)=-.7577435
1360 G(30)=-.7939622
1370 G(31)=-.8233586
1380 G(32)=-.8457732
1390 G(33)=-.8611109
1400 G(34)=-.8693409
1410 G(35)=-.8704961
1420 G(36)=-.8646722
1430 G(37)=-.852026
1440 G(38)=-.8327731
1450 G(39)=-.8071849
1460 G(40)=-.7755856
1470 G(41)=-.7383485
1480 G(42)=-.6958912
1490 G(43)=-.6486715
1500 G(44)=-.5971825

```

```

1510 G(45)=-.5419471
1520 G(46)=-.4835125
1530 G(47)=-.4224453
1540 G(48)=-.3593248
1550 G(49)=-.2947382
1560 G(50)=-.2292741
1980 G2=1
1990 A7(1)=-.20134
2000 A7(2)=-.147528
2010 V2(1,1)=-.0001152232 ! METERS^3
2020 V2(1,2)=-.0001151946 ! V2(C,C1)
2025 V2(1,3)=-.0001152269 ! C1-1:1248-1082
2030 V2(2,1)=-.0006498109 ! C1-2:1248-815
2040 V2(2,2)=-.0006497823 ! C1-3:1082-815
2045 V2(2,3)=-.0006497779 ! P-III-60
2050 F9=1
2060 I9=1
2070 FOR M=1 TO 50
2080 G1(2,M)=G(M)
2090 NEXT M
2100 FOR M=1 TO 22
2110 G1(1,M)=D(M)
2120 NEXT M
2130 FOR M=23 TO 50
2140 G1(1,M)=0
2150 NEXT M
2160 !
2170 ! BEGIN PROGRAM
2180 PRINTER IS 2
2190 PRINT "TIME DATE"
2200 IMAGE 2X,2D,2D,4X,4D
2210 FOR R=L TO L1 STEP -1
2220 PRINTER IS 2
2230 PRINT USING 2200 ; TIME/3600,DATE
2240 L=R
2250 PRINT " "
2260 IF C=1 THEN U7=3=L ELSE U7=L
2270 DISP "MODE NUMBER IS",L
2280 DISP "LOW FREQ (HZ) IS",F1
2290 DISP "HI FREQ (HZ) IS",F2
2300 DISP "5204 SCALE SENS(V)IS",B
2310 CLEAR @ BEEP
2320 DISP "SELECT ATBR SWITCHING"
2330 GOSUB 7400 ! SELECT ATBR
2340 BEEP
2350 DISP "GET INITIAL DRIVE VOLTAGE"
2360 ! VOLTAGE
2370 J1=0
2380 A1=5
2390 ! INITIAL SEARCH FOR DRIVE VOLTAGE
2400 OUTPUT 717 ;"FR", (F2+F1)/2,"HZ"
2410 OUTPUT 717 ;"AM",A1,"MR"
2420 WAIT T1=3

```

```

2430 OUTPUT 709 ;"VT3"
2440 ENTER 709 ; Q9
2450 IF Q9>.25 THEN 2470 ELSE A1=A1+25
2460 GOTO 2410
2470 IF Q9<.35 THEN 2490 ELSE A1=A1-20
2480 GOTO 2410
2490 BEEP
2500 DISP "PRELIM DATA SAMPLE"
2510 DISP "USED TO EST BANDWIDTH"
2520 GOSUB 5570 ! INITIAL DATA
                                         COLLECTION

2530 BEEP
2540 DISP "ANALYZE SAMPLE"
2550 GOSUB 6260 ! DATA ANALYSIS
2560 BEEP
2570 DISP "GET 'B' BIAS"
2580 GOSUB 7310 ! GET F2,"B BIAS"
2590 DISP "'B' BIAS=" ,E2
2600 !
2610 C1(3)=C3+.00016584+.000024894*E2^2 ! CORR FOR BIAS ON 1
2620 BEEP
2630 DISP "GET ATBR DATA"
2640 GOSUB 5750 ! GET DATA ATBR
2650 GOSUB 4450 ! VHF TO NEUTRAL
2660 PRINT "ATBR DRIVE(MV)=" ,A1
2670 DISP "ATBR AVG TEMP=" ,T5(1)
2680 DISP "AVG ATMOS PRESS MMHG=" ,P5(1)
2690 DISP "SAVE & SCALE DATA"
2700 A9=A1
2710 A2=A1 ! SAVE ATBR DRIVE
2720 FOR N=1 TO 26
2730 GOSUB 8300 ! GET B2
2740 G5(1,N)=A(N)*B*B2
2750 A(N)=G5(1,N)
2760 NEXT N
2770 BEEP
2780 DISP "ANALYZE ATBR DATA"
2790 GOSUB 6260 ! DATA ANALYSIS
2800 ! SAVE ROUGH VALUES
2810 ! OBTAINED WITH DATA
2820 ! ANALYSIS ROUTINE-11 POINT
                                         FIT
2830 V(1)=P1
2840 Q(1)=Q1
2850 F2(1)=F9
2860 BEEP
2870 DISP "SWITCH TO BTAR"
2880 DISP "GET 'A' BIAS"
2890 GOSUB 7530 ! SWITCH BTAR
2900 GOSUB 7210 ! GET E1,"A BIAS"
2910 DISP "'A' BIAS=" ,E1
2920 C1(1)=C2+.0012485+.000036329*E1^2 ! CORR FOR BIAS ON 12
48

```



```

2930 DISP "GET BTAR DATA"
2940 GOSUB 5750 ! DATA COLLECTION
2950 PRINT "BTAR DRIVE(MV)=",A1
2960 DISP "BTAR AVG TEMP=",T5(2)
2970 DISP "AVG ATMOS PRESS MMHG=",P5(2)
2980 ! SAVE AND SCALE DATA
2990 FOR N=1 TO 26
3000 GOSUB 8210 ! GET B1
3010 G5(2,N)=A(N)*B=B1
3020 A(N)=G5(2,N)
3030 NEXT N
3040 GOSUB 6260 ! DATA ANALYSIS
3050 ! SAVE ROUGH VALUES
3060 V(2)=P1
3070 Q(2)=Q1
3080 F2(2)=F9
3090 ! RECALL ATBR DATA
3100 Q1=Q(1)
3110 F9=F2(1)
3120 P1=V(1)
3130 FOR N=1 TO 26
3140 A(N)=G5(1,N)
3150 NEXT N
3160 DISP " RAVINE ATBR DATA"
3170 Q5=Q1
3180 GOSUB 4510 ! RAVINE DATA
3190 ! SAVE RAVINED ATBR
3200 ! VALUES
3210 Q(1)=Q1
3220 F2(1)=F9
3230 V(1)=P1
3240 GOSUB 5460 ! GET MSE
3250 ! NORMALIZE MSE
3260 K1(1)=K(1)/P1^2 ! END ATBR
E
3270 ! RECALL BTAR DATA
3280 Q1=Q(2)
3290 F9=F2(2)
3300 P1=V(2)
3310 FOR N=1 TO 26
3320 A(N)=G5(2,N)
3330 NEXT N
3340 DISP " RAVINE BTAR DATA"
3350 Q5=Q1
3360 GOSUB 4510 ! RAVINE DATA
3370 ! SAVE RAVINED BTAR
3380 ! VALUES
3390 Q(2)=Q1
3400 F2(2)=F9
3410 V(2)=P1
3420 GOSUB 5460 ! GET MSE
3430 ! NORMALIZE MSE
3440 K1(2)=K(1)/P1^2 ! END BTAR
E

```

RAVIN

RAVIN

```

3450 ! .....
3460 ! GET CORRECT DRIVE
3470 ! CURRENT FOR "A" MIC....
3480 ! HERE FOLLOW A SERIES OF
3490 ! STRAIGHT LINE FITS TO
3500 ! ACTUAL DATA,ASK VS GET.
3510 IF F2(2)<520 THEN 3515 ELSE 3520 ! P-III-80
3515 B6=.92775+.00004979592*F2(2)
3517 GOTO 3550
3520 IF F2(2)<1020 THEN 3525 ELSE 3530
3525 B6=.9516+.000004163265*F2(2)
3527 GOTO 3550
3530 IF F2(2)<1510 THEN 3535 ELSE 3540
3535 B6=.95412+.000001714286*F2(2)
3537 GOTO 3550
3540 IF F2(2)<2500 THEN 3545 ELSE 3549
3545 B6=.95577+6.122449E-7*F2(2)
3547 GOTO 3550
3549 B6=.9568022+.000000222449*F2(2)
3550 A2=A2*B6
3640 I1=2*PI*F2(1)*A2*.001*(C2+.00124885+.0000363329*E1^2)*.
000000000001
3650 DISP "A TRANS CURRENT(A)=",I1
3660 BEEP
3670 DISP "GET ATCR COMPARISON"
3680 GOSUB 7680 ! SWITCH ATCR
3690 GOSUB 7920
3700 DISP "ATCR VOLTAGE=",V1(1)
3710 BEEP
3720 DISP "GET BTRC COMPARISON"
3730 GOSUB 7800 ! SWITCH BTRC
3740 GOSUB 8070
3750 DISP "BTRC VOLTAGE=",V1(2)
3760 ! CALC RATIO OF SPECIFIC HEATS J=1-BTAR,2=ATBR

3770 FOR N=1 TO 2
3780 D=R1/100*.625*10^(23.84-2948/(273.16+T5(N))-5.03*LGT(27
3.16+T5(N)))
3790 G0=(0*1.324+(1000-0)*1.402432)/1000
3800 G9(N)=G0-2*(G0-1)*A7(C)/SQR(F2(N))+2*(G0-1)*A7(C)^2/F2(
N)
3810 NEXT N
3820 ! CHG PRESS TO MKS
3830 FOR N=1 TO 2
3840 P5(N)=P5(N)*101330/760
3850 NEXT N
3860 ! OPEN CIRCUIT SENSITIVITY CALCULATIONS
3870 ! M1=MA (ADJUSTMENT MADE SO REF BIAS IS 200 VOLT
S)
3880 ! M2=MB C=1=SHORT TUBE
3890 ! M3=MCA C=2=LONG TUBE
3900 ! M4=MCB
3910 ! M5=MAB C1=1=1248T/1082R

```

```

3920 ! M6=MBA
3930 M1=SQR(V(2)-V(1)*PI*V2(C,C1)*F2(1)/(I1+V1(2)+G9(1)+PS(
1)*Q(1)))
3940 M2=SQR(V(1)+V(1)*V1(2)*PI*V2(C,C1)*F2(2)/(I1+V(2)+V1(1)
+G9(2)+PS(2)*Q(2)))
3948 G1=G1(C,L)
3950 IF C=2 THEN G1=1 ! LONG TUBE HAS THE REF MIC IN THE END

3960 M3=M1*V1(2)/(V(2)+G1)
3970 M4=M2*V1(1)/(V(1)+G1)
4000 M5=M2*V(2)+V1(1)/(V(1)+V1(2))
4010 M6=M1*V(1)+V1(2)/(V(2)+V1(1))
4020 ! STORE RESULTS ON TAPE
4030 BEEP
4040 BEEP
4050 PRINTER IS 2
4060 PRINT "MODE #=",L
4070 PRINT "FREQ=",F2(1)
4080 PRINT "MA=",M1
4090 PRINT "MAB=",M5
4100 PRINT "MB=",M2
4110 PRINT "MBA=",M6
4120 PRINT "MCA=",M4
4130 PRINT "MCB=",M3
4131 PRINT "E1=",E1
4132 PRINT "E2=",E2
4140 PRINT "K1(1)=",K1(1)
4150 PRINT "K1(2)=",K1(2)
4160 PRINTER IS 701,80
4190 ASSIGN# 1 TO "DAT1"
4200 PRINT# 1,L4 : L,M1,M2,M3,M4,M5,M6,P5(1),P5(2),T5(1),T5(
2),C
4210 ASSIGN# 1 TO "DAT2"
4220 PRINT# 1,L4 : A2,V1(1),V1(2),G9(1),G9(2),V(1),V(2),Q(1)
,Q(2),F2(1),F2(2),C1
4230 ASSIGN# 1 TO "DATV"
4240 PRINT# 1,L4 : GS(.)
4250 ASSIGN# 1 TO "DATF"
4260 PRINT# 1,L4 : F5(.)
4270 U1=(M1+M5)/2
4280 U2=(M2+M6)/2
4290 U3=(M4+M3)/2
4300 U4=(M1-M5)*100/(M1+M5)
4310 PRINT USING 170 : L,F2(2),T5(2),Q(1),Q(2),U1,U2,U3,U4,L
4
4320 !
4330 : ITERATE RECORD# AND
4340 ! CHECK FOR END OF RUN
4350 L4=L4+1
4360 GOTO 4390
4370 ! CHECK FOR LAST MODE
4380 ! OTHERWISE END
4390 IF L=1 THEN 4440 ELSE 4400

```

```

4400 I9=(L-1)*F9/L
4410 F1=I9-2*I9/(Q1+SQR(I9/F9))
4420 F2=I9+2*I9/(Q1+SQR(I9/F9))
4430 NEXT R
4440 END
4450 !
4460 ! PUT VHF SW IN NEUTRAL
4470 !
4480 OUTPUT 716 USING "2A" ; "A3"
4490 OUTPUT 716 USING "2A" ; "B3"
4500 RETURN
4510 ! .....
4520 !
4530 ! RAVINE SUBROUTINE
4540 !
4550 ! RAVINE Q
4560 !
4570 FOR M=1 TO M9
4580 Q4=Q1/200
4590 Q3=Q1+Q4
4600 Q2=Q1
4610 Q1=Q1-Q4
4620 K(1)=0
4630 FOR N=1 TO 26
4640 K1=(F(N)/F9-F9/F(N))^2*Q1*Q1+1
4650 K2=SQR(K1)
4660 K(1)=K(1)+(A(N)-P1/K2)^2
4670 NEXT N
4680 K(2)=0
4690 FOR N=1 TO 26
4700 K1=(F(N)/F9-F9/F(N))^2*Q2*Q2+1
4710 K2=SQR(K1)
4720 K(2)=K(2)+(A(N)-P1/K2)^2
4730 NEXT N
4740 K(3)=0
4750 FOR N=1 TO 26
4760 K1=(F(N)/F9-F9/F(N))^2*Q3*Q3+1
4770 K2=SQR(K1)
4780 K(3)=K(3)+(A(N)-P1/K2)^2
4790 NEXT N
4800 K=Q4*(K(3)-K(1))/(2*(2*K(2)-K(1)-K(3)))
4810 Q1=Q2+K
4820 !
4830 ! RAVINE PEAK AMPLITUDE
4840 !
4850 P4=P1/500
4860 P3=P1+P4
4870 P2=P1
4880 P1=P1-P4
4890 K(1)=0
4900 FOR N=1 TO 26
4910 K1=(F(N)/F9-F9/F(N))^2*Q1*Q1+1
4920 K2=SQR(K1)

```

```

4930 K(1)=K(1)+(A(N)-P1/K2)^2
4940 NEXT N
4950 K(2)=0
4960 FOR N=1 TO 26
4970 K1=(F(N)/F9-F9/F(N))^2*Q1*Q1+1
4980 K2=SQR(K1)
4990 K(2)=K(2)+(A(N)-P2/K2)^2
5000 NEXT N
5010 K(3)=0
5020 FOR N=1 TO 26
5030 K1=(F(N)/F9-F9/F(N))^2*Q1*Q1+1
5040 K2=SQR(K1)
5050 K(3)=K(3)+(A(N)-P3/K2)^2
5060 NEXT N
5070 K=P4*(K(3)-K(1))/(2*(2*K(2)-K(1)-K(3)))
5080 P1=P2+K
5090 !
5100 ! RAVINE FREQ
5110 !
5120 F8=F9/(Q1*2000)
5130 F7=F9+F8
5140 F6=F9
5150 F5=F9-F8
5160 K(1)=0
5170 FOR N=1 TO 26
5180 K1=(F(N)/F5-F5/F(N))^2*Q1*Q1+1
5190 K2=SQR(K1)
5200 K(1)=K(1)+(A(N)-P1/K2)^2
5210 NEXT N
5220 K(2)=0
5230 FOR N=1 TO 26
5240 K1=(F(N)/F6-F6/F(N))^2*Q1*Q1+1
5250 K2=SQR(K1)
5260 K(2)=K(2)+(A(N)-P1/K2)^2
5270 NEXT N
5280 K(3)=0
5290 FOR N=1 TO 26
5300 K1=(F(N)/F7-F7/F(N))^2*Q1*Q1+1
5310 K2=SQR(K1)
5320 K(3)=K(3)+(A(N)-P1/K2)^2
5330 NEXT N
5340 K=F8*(K(3)-K(1))/(2*(2*K(2)-K(1)-K(3)))
5350 F9=F6+K
5360 IF ABS((Q1-Q5)/Q1)>.001 THEN S370 ELSE S410
5370 Q5=Q1
5380 DISP "Q=",Q1
5390 NEXT M
5400 GOTO 5450
5410 !
5420 DISP "SMOOTH Q=",Q1
5430 DISP "SMOOTH F=",F9
5440 DISP "SMOOTH A=",P1
5450 RETURN

```

```

5460 ! .....
5470 ! MSE SUBROUTINE
5480 !
5490 !
5500 K(1)=0 ! SUB TO GET MSE
5510 FOR N=1 TO 26
5520 K1=(F(N)/F9-F9/F(N))^2+Q1+Q1+1
5530 K2=SQR(K1)
5540 K(1)=K(1)+(A(N)-P1/K2)^2
5550 NEXT N
5560 RETURN
5570 ! .....
5580 ! INITIAL DATA COLLECTION
5590 ! SUBROUTINE
5600 !
5610 A5=0
5620 D1=(F2-F1)/25
5630 F=F1
5640 OUTPUT 717 ;"FR",F,"HZ"
5650 OUTPUT 717 ;"AM",A1,"MR"
5660 FOR N=1 TO 26
5670 F(N)=F
5680 OUTPUT 717 ;"FR",F(N),"HZ"
5690 WAIT 4*T1
5700 OUTPUT 709 ;"VT3"
5710 ENTER 709 ; A(N)
5720 F=F+D1
5730 NEXT N
5740 RETURN
5750 ! .....
5760 ! DRIVE ADJUSTMENT
5770 ! AND DATA COLLECTION
5780 ! .....
5790 OUTPUT 717 ;"FR",F9,"HZ"
5800 IF A1>3455 THEN 5810 ELSE 5830
5810 OUTPUT 717 ;"AM",3455,"MR"
5815 A1=3455
5820 GOTO 5910
5830 OUTPUT 717 ;"AM",A1,"MR"
5840 WAIT 8*T1
5850 OUTPUT 709 ;"VT3"
5860 ENTER 709 ; Q9 ! FRACTIONAL VOLTAGE OUTPUT FROM 5204-70
3
5870 IF Q9>.95 THEN 5890 ELSE A1=A1+25
5880 GOTO 5800
5890 IF Q9<.95 THEN 5910 ELSE A1=A1-20
5900 GOTO 5800
5910 DISP "DRIVE VOLTAGE(MV)IS",A1
5920 D1=(F2-F1)/25
5930 PRINT "REQUESTED DRIVE VOLTAGE =" ,A1
5940 F=F1
5950 OUTPUT 717 ;"FR",F,"HZ"
5960 OUTPUT 717 ;"AM",A1,"MR"

```

```

5970 GOSUB 7110 ! GET PRESS=P
5980 P5(J)=P
5990 T8=TIME/3600
6000 GOSUB 7010 ! GET TEMP=T
6010 T5(J)=T
6020 FOR N=1 TO 26
6030 A(N)=0
6040 F(N)=F
6050 F5(J,N)=F
6060 OUTPUT 717 ;"FR",F(N),"HZ"
6070 WAIT 8=T1
6080 FOR Q6=1 TO 16
6090 OUTPUT 709 ;"VT3"
6100 ENTER 709 ; B1(Q6)
6110 A(N)=A(N)+B1(Q6)
6120 NEXT Q6
6130 A(N)=A(N)/16
6140 F=F+D1
6150 NEXT N
6160 OUTPUT 717 ;"AM",T,"MR"
6170 GOSUB 7010 ! GET TEMP=T
6180 T5(J)=(T5(J)+T)/2 ! AVERAGE
TEMP DURING DATA
RUN
6190 T9=TIME/3600
6200 T(J)=(T8+T9)/2
6210 GOSUB 7110 ! GET PRESS=P
6220 P5(J)=(P+P5(J))/2 ! AVERAGE
6230 P5(J)=100*P5(J) ! ADJ=MMHG
6240 P5(J)=P5(J)+4.2646 ! CAL
6250 RETURN
6260 ! .....
6270 ! RAW DATA ANALYSIS
6280 ! SUBROUTINE
6290 !
6300 A5=AMAX(A)
6310 FOR X=1 TO 26
6320 IF A(X)=A5 THEN 6340 ELSE 6330
6330 NEXT X
6340 A6=X
6350 X1=0
6360 X2=0
6370 X3=0
6380 X4=0
6390 Y1=0
6400 Y2=0
6410 Y3=0
6420 FOR N=1 TO 7
6430 F1(N)=F(A6-4+N)-F(A6-3)
6440 A3(N)=A(A6-4+N)-A(A6-3)
6450 NEXT N
6460 FOR I=1 TO 7
6470 X4=X4+F1(I)*4
6480 X3=X3+F1(I)*3

```

```

6490 X2=X2+F1(I)^2
6500 X1=X1+F1(I)
6510 Y1=Y1+A3(I)
6520 Y2=Y2+A3(I)*F1(I)
6530 Y3=Y3+A3(I)*F1(I)^2
6540 NEXT I
6550 B(1,1)=X4
6560 B(1,2)=X3
6570 B(1,3)=X2
6580 B(2,1)=X3
6590 B(2,2)=X2
6600 B(2,3)=X1
6610 B(3,1)=X2
6620 B(3,2)=X1
6630 B(3,3)=7
6640 C(1)=Y3
6650 C(2)=Y2
6660 C(3)=Y1
6670 MAT X=SYS(B,C)
6680 F9=-(X(2)/X(1)*.5)+F(A6-3)
6690 P1=X(3)+A(A6-3)-X(2)^2/(4*X(1))
6700 H7=P1/SQR(2)
6710 FOR I=1 TO A6
6720 IF A(I)<H7 THEN 6730 ELSE 6790
6730 IF H7<A(I+1) THEN 6740 ELSE 6790
6740 F3=F(I)
6750 H3=A(I)
6760 F4=F(I+1)
6770 H4=A(I+1)
6780 GOTO 6800
6790 NEXT I
6800 FOR N=A6 TO 26
6810 IF A(N)>H7 THEN 6820 ELSE 6880
6820 IF H7>A(N+1) THEN 6830 ELSE 6880
6830 F5=F(N)
6840 H5=A(N)
6850 F6=F(N+1)
6860 H6=A(N+1)
6870 GOTO 6890
6880 NEXT N
6890 F7=F3+(H7-H3)*(F4-F3)/(H4-H3)
6900 F8=F5+(H5-H7)*(F6-F5)/(H5-H6)
6910 Q1=F9/(F8-F7)
6920 IF J1=0 THEN 6930 ELSE 6950
6930 F1=F9-F9/Q1
6940 F2=F9+F9/Q1
6950 J1=J1+1
6960 CLEAR @ BEEP
6970 DISP "ROUGH Q=",Q1
6980 DISP "ROUGH F=",F9
6990 DISP "ROUGH A=",P1
7000 RETURN ! END OF RAW ANALYSIS
7010 ! .....H7

```



```

7020 ! SUBROUTINE TO GET TEMP
7030 ! DEGREES CENTIGRADE IN
7040 ! VARIABLE = T
7050 ! .....
7060 OUTPUT 709 ;"D04.1"
7070 OUTPUT 722 ;"F4R1M6T1"
7080 WAIT 5000
7090 ENTER 722 ; T
7100 RETURN
7110 ! .....
7120 ! SUBROUTINE TO GET ATMOS
7130 ! PRESSURE IN MMHG = P
7140 ! .....
7150 OUTPUT 709 ;"D04.1"
7160 OUTPUT 709 ;"D04.2"
7170 OUTPUT 722 ;"F1R1M0T1"
7180 WAIT 1000
7190 ENTER 722 ; P
7200 RETURN
7210 ! .....
7220 ! SUBROUTINE TO GET SIDE
7230 ! "A" BIAS VOLTAGE = E1
7240 ! .....
7250 OUTPUT 709 ;"D04.1,2"
7260 OUTPUT 709 ;"D04.3"
7270 OUTPUT 722 ;"F1R1M0T1"
7280 WAIT 60000
7290 ENTER 722 ; E1
7300 RETURN
7310 ! .....
7320 ! SUBROUTINE TO GET SIDE
7330 ! "B" BIAS VOLTAGE = E2
7340 ! .....
7350 OUTPUT 709 ;"D04.1,2,3"
7360 OUTPUT 722 ;"F1R1M0T1"
7370 WAIT 60000
7380 ENTER 722 ; E2
7390 RETURN
7400 ! .....
7410 ! SELECT
7420 ! ATBR
7430 OUTPUT 709 ;"AR"
7440 OUTPUT 709 ;"D04.7,12,13"
7450 OUTPUT 709 ;"D04.4,10,11"
7460 DISP "A-TRANS, 8-RCV"
7470 OUTPUT 716 USING "2A" ; "A4"
7480 OUTPUT 716 USING "2A" ; "B4"
7490 WAIT 10000 ! ALLOWS

```

TRANSCIENTS TO DIE OUT

```

7500 J-1
7510 OUTPUT 709 ;"AC1"
7520 RETURN
7530 ! .....

```

```

7540 ! BTAR
7550 ! SWITCHING
7560 !
7570 OUTPUT 709 ;"AR"
7580 OUTPUT 709 ;"DO4,4,10,11"
7590 ! SW SOURCE TO B, PWR ON B
7600 OUTPUT 709 ;"DC4,7,12,13"
7610 DISP "B-TRANS,A-RCVR"
7620 OUTPUT 716 USING "2A" ; "A1"
7630 OUTPUT 716 USING "2A" ; "B1"
7640 WAIT 10000
7650 J=2
7660 OUTPUT 709 ;"AC10"
7670 RETURN
7680 ! .....
7690 ! ATCR SWITCHING
7700 !
7710 OUTPUT 709 ;"AR"
7720 OUTPUT 709 ;"DO4,0,7,12,13"
7730 OUTPUT 709 ;"DC4,4,10,11"
7740 OUTPUT 716 USING "2A" ; "A2"
7750 OUTPUT 716 USING "2A" ; "B2"
7760 ! ATCR
7770 OUTPUT 709 ;"AC1"
7780 WAIT 10000
7790 RETURN
7800 ! .....
7810 ! BTCR SWITCHING
7820 !
7830 OUTPUT 709 ;"AR"
7840 OUTPUT 709 ;"DO4,4,10,11"
7850 OUTPUT 709 ;"DC4,7,12,13"
7860 OUTPUT 716 USING "2A" ; "A2"
7870 OUTPUT 716 USING "2A" ; "B2"
7880 ! BTCR
7890 OUTPUT 709 ;"AC10"
7900 WAIT 10000
7910 RETURN
7920 ! .....
7930 ! SUBROUTINE TO GET
7940 ! ATCR-V1(1)
7950 OUTPUT 717 ;"FR",F2(1),"HZ"
7960 OUTPUT 717 ;"AM",A9,"MR"
7970 S5=0
7980 FOR N=1 TO 36
7990 WAIT 8*T1
8000 OUTPUT 709 ;"VT3"
8010 ENTER 709 ; S4
8020 S5=S5+S4
8030 NEXT N
8040 S5=S5-B/G2
8050 V1(1)=S5/36
8060 RETURN

```

IN-OUT RELAY

```

3070 ! .....
8080 ! SUBROUTINE BTCR=V1(2)
8090 OUTPUT 717 : "FR",F2(2),"HZ"
8100 OUTPUT 717 : "AM".A1,"MR"
8110 S7=0
8120 FOR N=1 TO 36
8130 WAIT 8=T1
8140 OUTPUT 709 : "VT3"
8150 ENTER 709 ; S6
8160 S7=S7+S6
8170 NEXT N
8180 S7=S7*B/G2
8190 V1(2)=S7/36
8200 RETURN
8210 ! .....
8220 ! SUBROUTINE TO RELATE
8230 ! MIC "A"1248 RECEIVED VOLTAGE TO 5204 I
      INPUT
8235 IF F5(2,N)<300 THEN 8240 ELSE 8250
8240 B6=10.05431
8245 GOTO 8270
8250 IF F5(2,N)<1200 THEN 8255 ELSE 8265
8255 B6=10.0683817-.00001030612=F5(2,N)
8260 GOTO 8270
8265 IF F5(2,N)<5500 THEN 8266 ELSE 8268
8266 B6=10.062585-.00000262425=F5(2,N)
8267 GOTO 8270
8268 B6=10.071968-.00000457469=F5(2,N)
8270 B3=(C1(2)/C1(1)+1)^2 ! C1(2)=BTAR PF;C1(1)=1248+BIAS PF

8271 B4=(1/(2*PI*F5(2,N)*R8*C1(1)*.000000000001))^2
8272 B5=SQR(B3+B4)
8279 B1=B5/B6
8280 ! B1=A1(1,U7)/B6 ! XTRA
8290 RETURN
8300 ! .....
8310 ! SUBROUTINE TO RELATE
8320 ! MIC "B"1082 RECEIVED VOLTAGE TO 5204 INPUT
8325 IF F5(1,N)<300 THEN 8330 ELSE 8340
8330 D6=9.62515
8335 GOTO 8370
8340 IF F5(1,N)<1100 THEN 8345 ELSE 8355
8345 D6=9.642248-.00001940816=F5(1,N)
8350 GOTO 8370
8355 IF F5(1,N)<5500 THEN 8360 ELSE 8366
8360 D6=9.627574-.000003284514=F5(1,N)
8365 GOTO 8370
8366 D6=9.638486-.000005069388=F5(1,N)
8370 D3=(C1(4)/C1(3)+1)^2 ! C1(4)=ATBR PF;C1(3)=1082+ BIAS P
      F
8371 D4=(1/(2*PI*F5(1,N)*R9*C1(3)*.000000000001))^2
8372 D5=SQR(D3+D4)
8379 B2=D5/D6
8380 ! B2=A1(2,U7)/D6 ! XTRA
8390 RETURN

```

D. VARIABLE DEFINITIONS USED IN THE PROGRAM

- A[] - The microphone signal voltage corrected for the input transfer function to the lock-in analyzer and the analyzer's sensitivity. The argument is the number of one of the 26 data samples seen at each mode.
- A5 - Initialized variable always equal to zero.
- A9 - Temporary storage for drive voltage in millivolts.
- A1 - The drive amplitude desired in millivolts.
- A1[] - not used.
- A1[,]- not used.
- A7[] - An array used in the program correction to the ratio of specific heats. The argument is "C".
- A6 - Temporary variable used in the raw data analysis routine to indicate the data location of the peak signal obtained.
- A3[] - Storage of statistics in raw data analysis routine.
- A2 - Temporary storage for drive voltage in millivolts.
- A2[] - not used.
- B - The PAR 5204 sensitivity in volts.
- B[] - not used.
- B[,]- An array used to store variables used in a least square error fit to a second order polynomial.
- B1[] - A temporary accumulator for the signal averaging associated with each data point in the 26 point sample.
- B1 - A temporary output used in relating the "A side" signal voltage to the PAR 5204 input voltage.
- B6 - Used in the subroutine calculating drive current. B6 multiplied by the "asked for" voltage yields the "get" driving voltage for "BTAR".
- B5 - Used as a temporary variable in the signal transfer function relating the "BTAR" microphone signal to the PAR 5204 input.
- B2 - A temporary output used in relating the "B side" signal voltage to the PAR 5204 input voltage.
- C - A program indicator of short tube (C=1) or long tube (C=2).
- C2 - A dummy variable for microphone #1248 capacitance.
- C[] - Storage of statistics in raw data analysis routine.
- C5 - A dummy variable for microphone #815 capacitance.
- C1 - An indicator of cavity volume 1= 1248-1082
correction with regard to which 2= 1248-815
microphones are mounted in the ends. 3= 1082-815
- C1[] - An array containing measured microphone capacitances and system capacitances. Used later to store the microphone capacitances corrected for bias voltage.
- C7 - A dummy variable for microphone #1082 capacitance.

- D[] - An array containing the geometrical correction for the Knowles subminiature microphone mounted in the wall of the short tube. The array argument is the mode number.
- D5 - Temporary variable used in calculating the "ATBR" signal transfer to the input of the PAR 5204.
- D4 - Temporary variable used in calculating the "ATBR" signal transfer to the input of the PAR 5204.
- D1 - The frequency increment in the initial data sample.
- D6 - "D6" multiplied by the "asked for" voltage yields the "get" driving voltage for "ATBR".
- D3 - Used as a temporary variable in the signal transfer function relating the "ATBR" microphone signal to the PAR 5204 input.
- E1 - "A side" bias voltage.
- E1[] - not used.
- E2 - "B side" bias voltage.
- F - The frequency in the initial data collection routine.
- F[] - Temporary storage used in initial data collection.
- F8 - Upper half power point calculated for the raw data analysis.
- F5 - Temporary variable used in the raw data analysis for the quality factor Q1.
- F5[], - not used.
- F4 - Temporary variable used in the raw data analysis for the quality factor Q1.
- F9 - Current best estimate of resonant frequency. Used also as the unperturbed value of frequency in the Ravine subroutine.
- F1 - The initial estimate of the low frequency boundary of the first modal resonance of interest. Later used as a program calculated estimate for the lower frequency of the initial search band for the the next lower modal resonance.
- F1[] - Storage of statistics in raw data analysis routine.
- F7 - Lower half power point calculated for the raw data analysis.
- F7[] - not used.
- F6 - Unperturbed frequency in the Ravine subroutine.
- F3 - Temporary variable used in the raw data analysis routine.
- F2 - The initial estimate of the high frequency boundary of the first modal resonance of interest. Later used as a program calculated estimate for the higher frequency of the initial search band for the next lower modal resonance.
- F2[] - Storage array for the ravined estimate of frequency for a modal resonance.
- G[] - The geometrical correction for the 1/2 inch diameter microphone mounted in the wall of the long tube. The array argument is the mode number of the microphone.
- G[], - Storage for the signal voltage sampled at each of the points in the vicinity of a mode.

- argument 1 = 1 = ATBF while 0 = BTAR and the second argument is the point number of the data sample (1 to 26).
- G9[] - The effective gamma as calculated by the computer program. The argument is "C".
 - G4[] - not used.
 - G1 - Temporary storage for G1[,] in the calculation of the various microphone sensitivities.
 - G1[,] - A temporary storage for geometrical correction factors. G1[2,m]=G[m] and G1[1,m]=D[m]. M = mode number.
 - G2 - Always equal to one.
 - G2[] - not used.
 - G0 - Temporary variable used in the program correction to the ratio of specific heats.
 - H5 - Used in initial determination of quality factor, Q1, resonant frequency, F9, and peak amplitude for the resonance, P1.
 - H4 - Used in initial determination of quality factor, Q1, resonant frequency, F9, and peak amplitude for the resonance, P1.
 - H7 - Half power amplitude used in the raw data analysis used for the initial determination of quality factor, Q1, resonant frequency, F9, and peak amplitude for the resonance, P1.
 - H6 - Used in initial determination of quality factor, Q1, resonant frequency, F9, and peak amplitude for the resonance, P1.
 - H3 - Used in initial determination of quality factor, Q1, resonant frequency, F9, and peak amplitude for the resonance, P1.
 - I - A program counter.
 - I9 - The center frequency calculated for the next lower modal resonance.
 - I1 - The transmitting current calculated using the capacitive model for the microphone and the driving voltage across the microphone terminals.
 - J - A program flag used in the switching subroutines and later used to indicate BTAR or ATBF in the data.
 - J1 - A flag used to indicate when the initial data sample is complete or not. If J1 > 1, then the initial sample is over.
 - K - Used in the Ravine subroutine as a temporary calculation of the "step" correction to either F1, Q1, or F9 due to the previous perturbation.
 - K[] - Mean square error output by MSE subroutine.
 - K1 - Used in the Ravine subroutine as a temporary calculation.
 - F1[] - Normalized mean square error. Used in Ravine subroutine.
 - K2 - Used in the Ravine subroutine as a temporary calculation.
 - L - The initial high mode number.
 - L4 - A counter used to indicate the highest record mode interest.
 - L1 - The initial low mode number.

- M5 - Comparison calibration of Mic "A" based upon the reciprocity calibration of Mic "B".
- M4 - Comparison calibration of Mic "C" based upon the reciprocity calibration of Mic "B".
- M9 - The maximum number of "ravines" desired in the least square error analysis of F, Q, and A using a Rayleigh line shape.
- M1 - Reciprocity calibration for "A side" microphone.
- M6 - Comparison calibration of Mic "B" based upon the reciprocity calibration of Mic "A".
- M3 - Comparison calibration of Mic "C" based upon the reciprocity calibration of Mic "A".
- M2 - Reciprocity calibration for "B side" microphone.
- N - A program counter.
- O - The mass of water in the atmosphere per unit volume as calculated by reference to the temperature and relative humidity. This is used in the computer correction to the ratio of specific heats due to the non-adiabatic boundary conditions within the resonant cavity.
- P - The output variable in the subroutine used to measure atmospheric pressure.
- P5[] - The average atmospheric pressure obtained over one modal data sample. Used also as the initial pressure obtained before the data sample is obtained.
- P4 - The amount by which the peak voltage is perturbed in the Ravine subroutine.
- PI - ~ 3.14159
- P1 - The best estimate of the peak signal voltage. The lower perturbation in the signal voltage in the Ravine subroutine.
- P3 - The higher perturbation of the peak voltage in the Ravine subroutine.
- P2 - The previous best estimate of the peak voltage and the current unperturbed value for the peak voltage in the Ravine subroutine.
- Q[] - Storage array for the ravined estimate of the quality factor for a modal resonance.
- Q5 - Temporary storage for quality factor used in Ravine subroutine.
- Q4 - The size of the perturbation of "Q" used in the Ravine subroutine.
- Q9 - A sample of output voltage used in the search for the optimum initial drive voltage.
- Q6 - A counter in the signal averaging associated with one point data sample.
- Q1 - The current best estimate of the "Q". The lower perturbation of the value for "Q" in the Ravine subroutine.
- Q3 - The higher perturbation of the value for "Q" in the Ravine subroutine.
- Q2 - The previous best estimate and current unperturbed value

for the value of "Q" in the Ravine subroutine.

R - A program counter for mode number under consideration.

R8 - "A side" effective resistance including the input preamp resistance and the bias blocking resistor.

R9 - "B side" effective resistance including the input preamp resistance and the bias blocking resistor.

R1 - The relative humidity observed at the beginning of the experiment.

S5 - An accumulator in the subroutine obtaining comparison voltages.

S4 - A sample variable in the subroutine obtaining comparison voltages.

S7 - An accumulator in the subroutine obtaining comparison voltages.

S6 - A sample variable in the subroutine obtaining comparison voltages.

T - Temperature variable in the "Get Temp" subroutine. Used as the temporary storage for the value of temperature obtained just after a data sample has been obtained.

T1[] - The average temperature obtained over one modal data sample.

T3[] - not used.

T[] - not used.

T8 - The time in decimal hours at the beginning of a data sample.

T5[] - The value of modal temperature before the data samples are taken. Also used to store the average value of temperature associated with a modal calibration.

T4[] - not used.

T1 - The PAR 5204 time constant (sec.).

T9 - The time in decimal hours at the end of a data sample.

U4 - The percent uncertainty between Ma and Mab.

U1 - The average value of Ma and Mab.

U7 - A program flag; if U7=1, then erase the tape; if U7=0, then do not erase the tape. Later in the program, this is used as a counter (see line 2260) logically related to either the long or short tube as a count of mode number.

U3 - The average value of Mca and Mcb.

U2 - The average value of Mb and Mba.

V[] - Storage array for ravined signal voltage at modal resonance.

V1[] - Storage array for the comparison voltages; 1 = Vca, 2 = Vcb.

V2[] - not used.

V2[,]- An array storing the corrected volumes. The arguments are "C" and "C1".

X[] - Output of matrix function in raw data analysis routine.

X4 - Storage of statistics in raw data analysis routine.

X1 - Storage of statistics in raw data analysis routine.

X3 - Storage of statistics in raw data analysis routine.

- X2 - Storage of statistics in raw data analysis routine.
- Y1 - Storage of statistics in raw data analysis routine.
- Y3 - Storage of statistics in raw data analysis routine.
- Y2 - Storage of statistics in raw data analysis routine.

Note: A number of iterations of this program were written both in its development and to accommodate the five different electroacoustic configurations described in chapter four. As a result, not all the original variables were employed in the final program. Since computer memory was not a problem, the dimension statements for these variables were left unchanged to facilitate returns to older configurations. This is why some of the variables are listed as "not used" in this particular version.

APPENDIX C

DESCRIPTION OF THE PROGRAM USED TO OBTAIN THE COMPARISON RATIO, V_b/V_a IN THE FREE FIELD COMPARISON CALIBRATION

A. INTRODUCTION

The computer program written on the following page was written in Hewlett Packard series 80 basic. It was used on the HP-85 and obtained the comparison voltages for the free field reciprocity calibration.

The following pages are separated into three different parts for convenience. First, there is a functional description of the program shown in table C.1. Next there is the program listing and last there is a list of definitions for the variables used in the program. Figure 3.2 in the beginning of chapter III illustrates the equipment setup controlled by this program.

The functional outline is shown next.

B. FUNCTIONAL DESCRIPTION OF THE PROGRAM

This program is divided into six subsections outlined below:

1. Initial setup using W.E.640AA microphone.
2. Calculation of voltage division for condenser microphone.
3. Speaker transmit, W.E.640AA receive data.
4. Secondary setup using Altec 688A electrodynamic microphone.
5. Speaker transmit, Altec 688A receive data.
6. Calculation of ratio 640R/688R vs. frequency.

These six functional descriptions are more fully described in the table below.

Beginning line number - functional description

10 Program initialization and equipment setup. The condenser microphone must be set up before proceeding with the run.

40 This operator modifiable line dictates the frequencies that will be examined for a signal voltage. In this example, we start with mode 19 and proceed through mode 31. These modes refer to the longitudinal resonances obtained in the long tube with plane wave resonant reciprocity.

52 Here the circuit variables involved in the voltage division associated with the condenser microphone are used to calculate the signal transfer function.

60 Twenty five samples at each frequency of interest are averaged to reduce the error associated with a low signal to noise ratio. The average and standard deviation are calculated and stored.

170 The operator is cued to enter the anechoic chamber to remove the condenser microphone and replace it with the Altec 688A electrodynamic microphone. A three wire support was used to spatially relocate the Altec in the same position.

210 Data sampling for the Altec 688A begins in the same fashion described in line 60 above.

350 The HP-95 begins calculating and printing the results to let the operator know that the procedure is finished. Both the average ratio and the standard deviation of the ratio are computed.

Table C.1 The functional program listing for Vratio.

C. PROGRAM LISTING

```

10 OPTION BASE 1
20 DIM A(2,40),R(40),S(3,40)
30 OUTPUT 717 ;"AM",125,"MR"
40 FOR M=19 TO 31 STEP 3
50 S=0
51 Q=0
52 E1=116.12
53 C=52.722+.0012485+.000036329*E1^2
54 R8=9247663
55 B4=(1/(2*PI+245*M*R8+C*.00000000001))^2
56 G1=SQR((255/C+1)^2+B4)
60 FOR N=1 TO 25
70 OUTPUT 717 ;"FR",M*245,"HZ"
80 WAIT 500
90 OUTPUT 709 ;"VT3"
92 ENTER 709 ; S1
105 S1=S1*.001*G1
110 S=S+S1
115 Q=Q+S1^2
120 NEXT N
130 A(1,M)=S/25
135 S(1,M)=(Q-25*A(1,M)^2)/24
140 PRINT ""
145 PRINT "FREQ=",M*245
150 PRINT "A(1,M)=",A(1,M)
160 NEXT M
170 CLEAR @ BEEP
180 DISP "SET UP NEXT MIC NOW"
190 DISP "PRESS CONT WHEN DONE"
200 PAUSE
210 FOR M=19 TO 31 STEP 3
220 S=0
225 Q=0
230 FOR N=1 TO 25
240 OUTPUT 717 ;"FR",M*245,"HZ"
250 WAIT 500
260 OUTPUT 709 ;"VT3"
270 ENTER 709 ; S1
275 S1=S1*.001
280 S=S+S1
285 Q=Q+S1^2
290 NEXT N
300 A(2,M)=S/25
305 S(2,M)=(Q-25*A(2,M)^2)/24
310 PRINT ""
315 PRINT "FREQ=",M*245
320 PRINT "A(2,M)=",A(2,M)
330 NEXT M
340 PRINT ""
350 PRINT "AVERAGE RATIOS"
360 PRINT ""
370 FOR M=19 TO 31 STEP 3
380 PRINT "FOR",M*245,"HZ. R=",A(1,M)/A(2,M)
390 PRINT ""
395 PRINT "SQR(S)=",SQR(S(1,M)+S(2,M))
400 NEXT M
410 CLEAR @ BEEP
420 DISP "THE END"
430 END

```

D. VARIABLE DEFINITIONS USED IN THE PROGRAM "Vratio"

- A[,] - Storage array used to store the individual values of the ratio. The first argument is 1 = condenser mic; 2 = electrodynamic mic and the second argument is the mode number, "M".
- B4 - Temporary storage for a portion of the transfer function of the input acoustic signal.
- C - The bias voltage corrected value of capacitance for the condenser microphone.
- E1 - This is an operator modifiable value of the measured bias voltage for the condenser microphone.
- G1 - The calculated value of the transfer function at the frequency of interest.
- M - Mode of interest.
- N - Sample counter.
- R8 - Parallel combination of the bias blocking resistor and the input resistance of the signal preamplifier.
- S - Accumulator for sample voltage.
- S1 - Sample voltage.
- SI[,] - Array storage for individual ratio sigmas. The arguments are the same as used for A[,].
- Q - Accumulator for sample voltage squared.

APPENDIX D

DESCRIPTION OF THE PROGRAM USED TO OBTAIN THE FREE FIELD COMPARISON CALIBRATION

A. INTRODUCTION

The computer program shown on the following pages is written in Hewlett Packard series 80 basic. It was used on the HP-85 and completed data acquisition and a comparison sensitivity calibration for the W.E.640AA serial #1248 condenser microphone. The most time consuming portion of the program is that associated with operator interaction. The operator is directed to enter the anechoic chamber and measure the separation distance between the diaphragm of the condenser microphone and the shielded front end of the Altec 688A electrodynamic speaker microphone at the beginning of the run, at a check point in the middle of the run, and at the end of the run. After these operator measured distances and a few other parameters are entered into the computer, the program does the rest.

At the end of each series of measurements at ever increasing separations, a "quality control" plot of the data is provided for operator viewing. Two plots are provided to the operator. The first is a simple plot of signal voltage

vs range and appears as a $1/r$ type plot. The second plots the $\log(v)$ vs $-\log(r)$. If the slope of the log/-log plot is exactly one, the spreading is spherical. Of course, the slope is never exactly one, but variations due to standing waves and other difficulties are easily seen and prompt experimental repair prior to taking additional data.

The following pages are separated into three different parts for convenience. First, there is a functional description of the program which is listed in table D.1. Next, there is the program listing and last there is a list of definitions for the variables used in the program.

The functional listing for the program is next.

B. FUNCTIONAL DESCRIPTION OF THE PROGRAM

The main program is divided into seven subsections as outlined below:

1. Initial program setup with operator inputs. The W.E.640AA is the microphone and the Altec 688A is the speaker.
2. Motor drive activation and sequential sampling at intervals of separation begins.
3. Program stops and cues operator to enter the anechoic chamber to obtain a "check" distance.
4. Motor drive is activated and sequential sampling at intervals of separations continues to the end of the data run. Total time is ~ 45 minutes per freq.
5. The operator is again cued to enter the chamber and obtain the final distance.
6. After the operator enters the final distance, the program enters the calculation phase and outputs the "check" plot.
7. If the operator observes an absence of obvious standing waves and desires to use the sampled data, then he answers a query regarding the type of electrodynamic microphone used (either 688A or 633), inputs a check value for the current measuring resistor, and the program calculates the comparison calibration for the W.E.640AA. A sample of this output is shown in figures 3.26, 3.27, and 3.28.

These seven functional descriptions are more fully outlined in the table below.

Beginning line number	- Functional description
10	Program initialization and equipment setup begins.
40	The counter is reset to prepare for the new run.
50	The computer control is directed to send a "motor off" command.
60	The operator is asked to set in the time if it is the first run of the day.
110	The arrays are dimensioned.
180	The subroutine to set up the recording magnetic tape is run.
190	The subroutine storing the preamplifier gain is run loading this info into the array A[].
195	The least square error fit solutions relating "asked for" driving voltage to "measured" drive current through the current measuring resistor are read into the proper arrays.
200	The operator is asked to enter the initial "record" number where the data will be stored on the magnetic tape.
220	The first "run" prior to the first data sample (N=1) is begun. Note: regardless of what setup existed, the program printed "633 Trans, 640AA receive" due to the fixed value of R1 finally adopted in line 315. A later query actually determines the value for "Vratio" which will be used.
540	Bias voltage is obtained.
552	Operator is asked to enter desired mode number and driving voltage to be used.
560	Operator is asked to enter the desired driving voltage for the speaker.
575	Operator is asked to enter the voltage drop across the current measuring resistor.
578	Subroutine entering the values of V_b/V_a determined in the program "Vratio" initializes the necessary arrays.
580	Operator is asked to enter the PAR 5204 sensitivity in volts.
600	Operator is asked to enter the PAR 5214 time constant.
630	Operator is asked to enter the initial separation between the diaphragm of the condenser microphone and the electrodynamic microphone.
701	Operator is asked to measure the value of the initial current through the current measuring resistor. Since a "line" measurement is used and a later measurement is made, the average value is eventually used to compensate for any slight temperature dependent changes found in the resistance.

800 The bias voltage is sampled. (holdover from previous version)
 810 The tabulated frequency dependent gain for the preamplifier is read into an array.
 820 The "counter" output from the optical shaft encoder is initialized.
 830 The temperature is sampled.
 840 The atmospheric pressure is sampled.
 870 The bias voltage is sampled.
 910 Data sampling loop begins. The drive motor is activated, allowed to run T1 milliseconds, and turned off. A delay of fifteen seconds is observed to allow swaying to cease.
 970 Thirty data readings are sampled at this separation.
 1120 At the eighth interval, the operator is asked to enter the anechoic chamber and obtain a comparison separation measurement. After this is entered in the program, the remaining separation measurements are made by the computer.
 1180 After all data has been measured, the bias voltage is again sampled.
 1190 Again the atmospheric pressure is sampled.
 1200 Again the temperature is sampled.
 1210 The averages are stored for the bias, pressure, and temperature.
 1254 The operator is asked to measure and enter the 4-wire current measuring resistor and the final distance.
 1450 The data is printed for operator viewing and stored on magnetic tape.
 1760 An ordinary data plot is provided for operator evaluation.
 1790 Details of operator measurements are printed.
 2010 A log/log plot is provided for operator evaluation.
 2040 The operator is asked to decide if the run was good or if it must be repeated.
 2080 Calibration sensitivities are printed out vs each range with statistics included. (Sigma is in V/PA)
 2420 The final form of the sensitivity calibrations are stored on tape.
 2500 Subroutine to get least squares fit for 1/n data.
 2760 Subroutine to get temperature.
 2830 Subroutine to get atmospheric pressure.
 2920 Subroutine to get bias voltage.
 3000 Subroutine to get plot of data.
 3430 Subroutine to get array with preamp gain.
 3690 Subroutine to get voltage division for W.E. 8412A.
 3770 Subroutine to setup magnetic tape.
 4000 Subroutine to get coefficients used to calculate β .
 5000 Subroutine to get arrays with "Oratio" output data.

Table D.1 Functional program listing for free
field comparison calibration.

This program was initially written to control data acquisition for *three* separate free field reciprocity calculations. In this final version, two different comparison calibrations based upon the data necessary for one reciprocity calibration are possible. The final comparison calibration is based upon either the Altec 688A electrodynamic microphone or an older "633 type saltshaker" electrodynamic microphone. The comparison calibration results finally used are referenced to the Altec 688A.

The program listing is next.

C. PROGRAM LISTING

```
10 ! REV 19 MAY 84
20 ! PROG N28-INVERSE R DATA COLLECTION. CPU CONTROLS MOTOR
RUN
30 ! AND DATA STORAGE/PLOT
40 OUTPUT 720 ;"RE" ! RESETS COUNTER
50 OUTPUT 709 ;"DO4,14,15" ! MAKES SURE VOLTS TO MOTOR ARE 0
FF
60 CLEAR
61 DISP "SETTIME?? H=3600+M*60.MDD"
62 DISP "PRESS CONT IF OK"
63 PAUSE
70 DISP "HOOK UP MOTOR VOLTS"
80 BEEP
90 BEEP
100 BEEP
110 OPTION BASE 1
120 DIM B(20),V(20),C(20),M0(20),A(40),E1(2),T1(3),P1(3)
130 DIM B1(20),V1(20),B8(20)
140 DIM B7(20),V7(20),V8(20)
150 DIM S4(9),E3(20),E4(20),A2(40),B2(40),R5(40),R6(40)
160 ! B WILL STORE RANGE
170 ! C WILL STORE DELTA RANGE
180 GOSUB 3770 ! TAPE SETUP
190 GOSUB 3430 ! PREAMP GAIN
195 GOSUB 4000 ! INITIALIZE I1
200 DISP "ENTER BEGINNING RECORD NUMBER FOR 'DAT1' STUFF"
210 INPUT L4
220 FOR N=1 TO 20
230 M0(N)=0
240 B1(N)=0
250 V1(N)=0
260 B7(N)=0
270 V7(N)=0
280 B8(N)=0
290 V8(N)=0
300 NEXT N
310 ! FOR R1=1 TO 3
315 R1=1
320 ! R1=1: 633T640R
330 ! R1=2: 688T640R
340 ! R1=3: 688T633R
350 OUTPUT 720 ;"RE" ! RESETS COUNTER
360 OUTPUT 709 ;"DO4,14,15" ! MAKES SURE VOLTS TO MOTOR ARE
OFF
370 IF R1=1 THEN GOTO 400 ! 633T640R
380 IF R1=2 THEN GOTO 440 ! 688T640R
390 IF R1=3 THEN GOTO 480 ! 688T633R
400 PRINT "633A TRANS,640AA RCV"
410 PRINT ""
420 DISP "633A TRANS,640AA RCV"
430 GOTO 510
440 PRINT "688 TRANS,640AA RCV"
450 PRINT ""
```

```

460 DISP "688 TRANS,640AA RCV"
470 GOTO 510
480 PRINT "688 TRANS, 633A RCV"
490 PRINT ""
500 DISP "688 TRANS, 633A RCV"
510 C1=52.722 ! PF #1248
520 R8=9247663 ! OHMS
540 GOSUB 2920 ! GET BIAS
550 C2=255 ! PF
552 DISP "LONG TUBE PLANE WAVE MODE NUMBER FOR FREQ"
554 INPUT F
556 F9=F
558 F=F*245 ! FOR LATER COMPARISON WITH TUBE RECIPROCIDY DAT
A"
560 DISP "INPUT DRIVING MV"
570 INPUT A0 ! ASKED FOR DRIVING VOLTAGE IN MV
571 IF R1=1 THEN V2=A0
575 ! V0=A2(F9)*V2+B2(F9)
576 DISP "INPUT V DROP"
577 INPUT V0
578 GOSUB 5000
580 DISP "ENTER 5204 SENS IN VOLTS"
590 INPUT B0
600 DISP "ENTER 5204 TIME CONSTANT"
610 INPUT T2
620 T2=T2*1000
630 DISP "MEASURE AND ENTER THE START DISTANCE FOR MIC B.MIC
A TO MIC B FACE(CM)"
640 INPUT D1
630 T1=10000 ! INTERVAL OF DRIVE(MOTOR) TIME IN MILLISEC
700 M1=20 ! #POINTS,MAX=20"
710 !
720 !
730 OUTPUT 717 : "FR",F,"HZ"
740 OUTPUT 717 : "AM",A0,"MR"
750 IF R1=1 THEN 760 ELSE 800
760 DISP "MEASURE/ENTER 633 4-WIRE CURRENT LIMITING RESISTAN
CE"
770 INPUT R9(1)
780 ! R9=74.705 ! OHMS
790 PRINT "4WIRE-R(OHMS)=",R9(1)
800 IF R1<3 THEN GOSUB 2920 ! GET BIAS
810 GOSUB 3690 ! GET G1
820 T=0 ! INITIALIZE TOTAL COUNT
830 GOSUB 2760 ! GET T3
840 GOSUB 2830 ! GET P
860 IF R1=3 THEN 890 ELSE 870
870 GOSUB 2920 ! GET BIAS
880 E1(R1)=E1
890 P1(R1)=P
900 T1(R1)=T3
910 FOR N=1 TO M1 ! GET DATA

```

```

920 OUTPUT 720 ;"FN12"
930 OUTPUT 709 ;"DC4,14,15"
940 WAIT T1
950 OUTPUT 709 ;"DO4,14,15"
960 WAIT 15000 ! STOP SWAYING
970 ENTER 720 ; A1 ! COUNT THIS RUN
980 V(N)=0 ! INITIALIZE VOLTS
990 T=T+A1
1000 FOR M=1 TO 30 ! AVG 30 READINGS
1010 OUTPUT 709 ;"VT3"
1020 WAIT 3=T2 ! WAIT THREE 5204 TIME CONSTANTS
1030 ENTER 709 ; E
1040 V(N)=V(N)+E
1050 NEXT M
1060 V(N)=V(N)/30
1070 B(N)=T ! CUMULATIVE COUNT
1080 C(N)=A1 ! COUNT NTH RUN
1090 DISP A1,T,N,V(N)
1100 BEEP
1110 OUTPUT 720 ;"RE"
1120 IF N=INT(M/2.3) THEN 1130 ELSE 1160
1130 BEEP 50,505
1140 DISP "MEAS&ENTER DIST(CM)"
1150 INPUT D7 ! CHECK DIST.
1160 NEXT N ! END OF GET DATA
1161 PRINT "TIME=",TIME/3600
1162 PRINT "DATE=",DATE
1170 IF R1=3 THEN 1180 ELSE 1190
1180 GOSUB 2920 ! GET BIAS
1190 GOSUB 2830 ! GET P
1200 GOSUB 2760 ! GET T3
1210 IF R1<3 THEN E1(R1)=(E1(R1)+E1)/2
1220 P1(R1)=(P1(R1)+P)/2
1230 T1(R1)=(T1(R1)+T3)/2
1240 BEEP 50,505
1250 OUTPUT 717 ;"AM",1,"MR"
1253 IF R1=1 THEN 1254 ELSE 1260
1254 DISP "MEASURE/ENTER 633 4-WIRE CURRENT LIMITING RESISTANCE"
1255 INPUT R9(2)
1256 PRINT "WIRE RESISTANCE=",R9(2)
1257 R9=(R9(1)+R9(2))/2
1258 PRINT "AVG 4-WIRE OHMS=",R9
1260 DISP "MEASURE AND ENTER THE FINAL DIST(CM) "
1270 INPUT D2 ! FINAL DIST
1280 L=ABS(D2-D1) ! TOTAL DIST(CM)
1290 FOR N=1 TO M1 ! SCALE DATA
1300 V(N)=V(N)*B0/G1
1310 IF D1>D2 THEN 1320 ELSE 1340
1320 B(N)=D1-B(N)*L/T
1330 GOTO 1350
1340 B(N)=D1+B(N)*L/T
1350 C(N)=C(N)*L/T

```

```

1360 NEXT N ! END OF SCALE DATA
1370 IMAGE 2D,1X,3D.DDD,1X,4D.DDD,1X,D.DDDDE
1380 PRINT " N RUN R(CM) VOLTS"
1390 FOR N=1 TO M1 ! PRINT DATA
1400 PRINT USING 1370 ; N,C(N),B(N),V(N)
1410 NEXT N ! END OF PRINT DATA
1420 GOSUB 2500 ! GET L^2 FIT
1430 ASSIGN# 1 TO "DAT1"
1440 IF R1<3 THEN 1450 ELSE 1480
1450 PRINT# 1,L4 ; V(),B(),E1(R1),P1(R1),T1(R1),V0,R9,F,A,B,
M1
1460 L4=L4+1
1470 GOTO 1500
1480 PRINT# 1,L4 ; V(),B(),E1(2),P1(R1),T1(R1),V0,R9,F,A,B,M
1
1490 L4=L4+1
1500 !
1510 IF R1=1 THEN 1540 ! STOREDATA
1520 IF R1=2 THEN 1610
1530 IF R1=3 THEN 1680
1540 FOR N=1 TO M1 ! 633T-640R
1550 B1(N)=B(N)
1560 V1(N)=V(N)
1570 NEXT N
1580 V6=1/A
1590 A6=B/A
1600 GOTO 1750
1610 FOR N=1 TO M1 ! 688T-640R
1620 B7(N)=B(N)
1630 V7(N)=V(N)
1640 NEXT N
1650 V7=1/A
1660 A7=B/A
1670 GOTO 1750
1680 FOR N=1 TO M1 ! 688T-633R
1690 B8(N)=B(N)
1700 V8(N)=V(N)
1710 NEXT N
1720 V8=1/A
1730 A8=B/A
1740 ! END STORE DATA
1750 !
1760 GOSUB 3000 ! PLOT DATA
1770 COPY ! END PLOT 1/R DATA
1780 PRINT ""
1790 PRINT "" ! RECORD DETAILS
1800 PRINT "# OF MEASUREMENTS=",M1
1810 PRINT "MEAS CHECK(CM)=",D7
1820 PRINT "CALC DIST (CM)=",B(INT(M1/2.3))
1830 PRINT "....."
1840 PRINT "DIST %ERROR=", (B(INT(M1/2.3))-D7)*100/D7
1850 PRINT "....."
1860 PRINT "START DIST(CM)=",D1

```



```

1870 PRINT "END DIST(CM)=",D2
1880 PRINT "5204 SENS =",B0
1890 PRINT "717 MVOLTS=",A0
1900 PRINT "TOTAL COUNT=",T
1910 PRINT "FREQ (HZ) =",F
1920 PRINT "" ! END RECORD DETAILS
1930 FOR N=1 TO M1 ! SWAP LOG DATA
1940 E3(N)=1/B(N)
1950 E4(N)=V(N)
1960 NEXT N
1970 FOR N=1 TO M1
1980 B(N)=ABS(20=LGT(E3(N)))
1990 V(N)=ABS(20=LGT(E4(N)))
2000 NEXT N
2010 GOSUB 3000 ! PLOT SUBROUTINE
2020 COPY ! END PLOT LOG DATA
2030 GCLEAR @ BEEP
2040 DISP "RERUN LAST DATA ? ENTER 1= RERUN, 2=NO, CONTINUE"

2050 INPUT Z9
2060 IF Z9=1 THEN R1=R1-1
2070 ! NEXT R1
2075 R1=1
2080 PRINT "M0(640) VS RNG(CM)"
2090 PRINT ""
2100 IMAGE 3D,DDD,1X,D,DDDDE
2110 PRINT " RANGE(CM) M0(640)"
2120 M9=0 ! SUM M0
2130 R3=0 ! SUM R
2140 R4=0 ! SUM R^2
2150 K9=0 ! COUNTER
2160 M8=0 ! SUM M0^2
2170 ! FOR M=INT(M1/2) TO M1
2180 ! V4=1/(B1(M)/V7+A7/V7)
2190 ! V3=1/(B1(M)/V8+A8/V8)
2200 ! R3=R3+V4/V3
2210 ! R4=R4+(V4/V3)^2
2220 ! K9=K9+1
2225 ! PRINT "RATIO=",V4/V3
2230 ! NEXT M
2240 ! R5=R3/K9 ! AVG R + SIGMA
2250 ! R6=SQR(ABS(R4-K9*R5^2)/(K9-1))
2254 BEEP
2255 DISP "INPUT V DROP IN VOLTS"
2256 INPUT V0
2257 DISP "INPUT 1=640R+633T"
2258 DISP "INPUT 2=640R+688T"
2259 INPUT N
2260 IF N=1 THEN R5=R5(F9) ELSE R5=R6(F9)
2265 FOR N=1 TO M1
2270 E4=V1(N)
2280 ! I1=(A2(F9)+V2+B2(F9))/R9
2284 I1=V0/R9

```

```

2290 Z1=E4*R5*4.303561*(273.16+T1(1))*(B1(N)+A6)
2300 Z2=I1*P1(1)*100=F
2310 M0(N)=SQR(Z1/Z2)
2320 PRINT USING 2100 ; B1(N),M0(N)
2325 PRINT "DB RE 1V/UB@200VBIAS=",20*LGT(200*M0(N)/E1(1))-2
0
2330 M9=M9+M0(N) ! FORM STATISTICS
2340 M8=M8+M0(N)^2 ! OF M0(N)
2350 NEXT N
2355 PRINT "I1=",I1
2356 PRINT "V0=",V0
2357 PRINT "R9=",R9
2360 M7=M9/M1 ! <M0(N)>
2370 PRINT "<M0>=",M7
2375 PRINT "AVGDB 1V/UB@200VBIAS=",20*LGT(200*M7/E1(1))-20
2380 M6=SQR(ABS(M8-M1*M7^2)/(M1-1))
2390 PRINT "SIGMA=",M6
2400 PRINT "<RATIO>=",R5
2405 ! PRINT "PROG RATIO=",R5(F9)
2410 ! PRINT "SIGMA R=",R6
2411 GOSUB 2420
2417 DISP "END"
2418 BEEP
2419 END
2420 ASSIGN# 1 TO "DAT2"
2430 PRINT# 1,L4 ; F,M0(),M7,M6
2440 ASSIGN# 1 TO *
2450 PRINT ""
2460 RETURN
2490 ! .....
2500 ! SUBROUTINE TO GET LEAST SQUARES FIT (1/V)=(R/V)+(C^D/V)
)
2510 X1=0 ! SX
2520 X2=0 ! SX^2
2530 X3=0 ! SXY
2540 Y1=0 ! SY
2550 Y2=0 ! SY^2
2560 Y3=0 ! N
2570 FOR N=1 TO M1
2580 X1=X1+B(N)
2590 X2=X2+B(N)*B(N)
2600 X3=X3+B(N)/V(N)
2610 Y1=Y1+1/V(N)
2620 Y2=Y2+1/(V(N)*V(N))
2630 Y3=Y3+1
2640 NEXT N
2650 A=(Y3*X3-X1*Y1)/(Y3*X2-X1*X1)
2660 B=(Y1*X2-X1*X3)/(Y3*X2-X1*X1)
2670 Q5=Y3*X3-X1*Y1
2680 Q6=SQR(Y3*X2-X1^2)
2690 Q7=SQR(Y3*Y2-Y1^2)
2700 R=Q5/(Q6*Q7)

```

```

2710 PRINT "V0=(VOLTS)",1/A
2720 PRINT "a=(CM)",B/A
2730 PRINT "R=",R
2740 RETURN
2750 ! .....
2760 ! SUBROUTINE TO GET TEMP
2770 OUTPUT 709 ;"DO4,1"
2780 OUTPUT 722 ;"F4R1M6T1"
2790 WAIT 5000
2800 ENTER 722 ; T3 ! TEMP DEG C
2810 RETURN
2820 ! .....
2830 ! SUBROUTINE TO GET PRESS
2840 OUTPUT 709 ;"DC4,1"
2850 OUTPUT 709 ;"DO4,2"
2860 OUTPUT 722 ;"F1R1M0T1"
2870 WAIT 5000
2880 ENTER 722 ; P ! PRESS
2890 P=100*P+4.2646 ! SCALE + CAL MMHG
2900 RETURN
2910 ! .....
2920 ! SUBROUTINE TO GET BIAS
2930 OUTPUT 709 ;"DC4,1,2"
2940 OUTPUT 709 ;"DO4,3"
2950 OUTPUT 722 ;"F1R1M0T1"
2960 WAIT 5000
2970 ENTER 722 ; E1 ! BIAS FOR 640
2980 RETURN
2990 ! .....
3000 GCLEAR ! PLOT 1/R DATA
3010 V=0 ! V WILL BE MAX VOLTAGE
3020 FOR N=1 TO M1
3030 IF V>V(N) THEN 3050 ELSE 3040
3040 V=V(N)
3050 NEXT N
3060 Z=100000000000
3070 FOR N=1 TO M1
3080 IF Z<V(N) THEN 3100 ELSE 3090
3090 Z=V(N) ! Z WILL BE MIN VOLT
3100 NEXT N
3110 L1=ABS(B(M1)-B(1))/10
3120 IF B(1)<B(M1) THEN 3140 ELSE 3130
3130 PRINT "PLOT IS BACKWARDS"
3140 SCALE B(1)-2*L1,B(M1)+2*L1,Z-2*(V-Z)/5,V+(V-Z)/5
3150 L1=ABS(B(M1)-B(1))/10
3160 XAXIS Z,L1,B(1),B(M1)
3170 YAXIS B(1),(V-Z)/10,Z,V
3180 MOVE B(1)+L1*5,Z+3*(V-Z)/10
3190 LDIR 0
3200 LABEL "RANGE,CM"
3210 MOVE B(M1)-5*L1,V+(V-Z)/10

```

PLOT SUBROUTINE

```

3220 LABEL "VMAX=",V
3230 PENUP
3240 MOVE B(1),V(1)
3250 V1=ABS((V-Z)/30)/2
3260 H1=ABS((B(M1)-B(1))/40)/2
3270 FOR I=1 TO M1
3280 MOVE B(I),V(I)
3290 IDRAW H1,0
3300 IDRAW -(2*H1),0
3310 IDRAW H1,0
3320 IDRAW 0,V1
3330 IDRAW 0,-(2*V1)
3340 NEXT I
3350 LDIR 90
3360 FOR X=B(1) TO B(M1) STEP L1
3370 MOVE X,Z-2.5*(V-Z)/10
3380 LABEL VALS(INT(X))
3390 NEXT X
3400 LDIR 0
3410 RETURN
3420 ! .....
3430 ! PREAMP GAIN
3440 A(1)=9.94366
3450 A(2)=9.99608
3460 A(3)=9.99776
3470 A(4)=10.00223
3480 A(5)=10.0051
3490 A(6)=10.00272
3500 A(7)=10.00388
3510 A(8)=10.00242
3520 A(9)=10.00343 ! ?????
3530 A(10)=10.00181
3540 A(11)=10.00178
3550 A(12)=9.99894
3560 A(13)=9.99823
3570 A(14)=9.99744
3580 A(15)=9.997
3590 A(16)=9.99744 ! ???
3600 A(17)=9.99681
3610 A(18)=9.99361
3620 A(19)=9.99248
3630 A(20)=9.99084
3640 A(21)=9.9896
3650 A(22)=9.98785
3651 A(23)=9.98611
3652 A(24)=9.98511
3653 A(25)=9.98411
3654 A(26)=9.98311
3655 A(27)=9.983
3656 A(28)=9.9825
3657 A(29)=9.982

```

```

3658 A(30)=9.9815
3659 A(31)=9.98125
3660 A(32)=9.981
3661 A(33)=9.98075
3662 A(34)=9.9805
3663 A(35)=9.98025
3664 A(36)=9.98005
3665 A(37)=9.97995
3670 RETURN
3680 ! .....
3690 ! VOLTAGE DIVISION FOR 640
3700 C=C1+.0012485+.000036329+E1^2
3710 B3=(C2/C+1)^2
3720 B4=(1/(2*PI*F*R8+C*.000000000001))^2
3730 B5=SQR(B3+B4)
3740 IF R1=3 THEN G1=1/A(F9) ELSE G1=B5/A(F9)
3750 RETURN
3760 ! .....
3770 DISP "ENTER 1= ERASETAPE,2=OK TAPE"
3780 INPUT U7
3790 IF U7=1 THEN 3800 ELSE 3870
3800 DISP "ARE U CERTAIN U WANT TO ERASE THE TAPE?????"
3810 DISP "1=YES,2=NO"
3820 INPUT U7
3830 IF U7=1 THEN 3840 ELSE 3870
3840 ERASETAPE @ BEEP
3850 CREATE "DAT1",92,480
3860 CREATE "DAT2",31,184
3870 RETURN
4000 ! SUBROUTINE TO SETUP COEFFICIENTS USED TO CALC I1
4010 A2(2)=.0007352517
4011 A2(6)=.0007374895
4012 A2(14)=.0007321923
4013 A2(18)=.0007241014
4015 A2(9)=.0007159909
4016 B2(9)=.00055091
4017 A2(8)=.0007169636
4018 B2(8)=.0003581818
4019 A2(11)=.0007124636
4020 A2(10)=.0007133881
4021 B2(11)=.0002854545
4022 A2(12)=.0007128545
4023 B2(12)=.000672727
4030 A2(23)=0
4040 B2(2)=.000713636
4041 B2(6)=.0001151515
4042 B2(14)=.0002686667
4043 B2(18)=.0003575758
4050 B2(10)=.0001727273
4060 B2(23)=0
4070 RETURN

```

```

5000 ! SUBROUTINE FOR RATIOS
5001 !
5002 ! 640R/633R
5003 !
5010 R5(5)=47.04
5020 R5(6)=52.556
5030 R5(7)=50.03
5040 R5(8)=52.59
5050 R5(9)=49.6
5060 R5(10)=42.76
5070 R5(11)=39.24
5080 R5(12)=37.92
5090 R5(13)=38.18
5100 R5(14)=34.83
5110 R5(15)=32.17
5120 R5(16)=28.92
5130 R5(17)=27.25
5140 R5(18)=28.83
5150 R5(19)=21.33
5151 R5(20)=18.38
5152 !
5153 ! 640R/688R
5154 !
5160 R6(1)=14.57
5161 R6(2)=15.3
5162 R6(3)=20.71
5163 R6(4)=16.3
5164 R6(5)=18.9
5170 ! R6(5)=17.603
5180 ! R6(6)=16.889
5181 R6(6)=18.16
5190 R6(7)=20.158
5200 R6(8)=21.659
5210 R6(9)=22.463
5220 R6(10)=24.728
5230 R6(11)=21.587
5240 R6(12)=18.96
5250 R6(13)=22.276
5260 R6(14)=26.309
5270 R6(15)=23.404
5280 R6(16)=27.752
5290 R6(17)=25.069
5300 R6(18)=27.495
5310 ! R6(19)=26.237
5320 R6(20)=26.742
5321 R6(19)=27.03
5322 R6(22)=27.23
5323 R6(25)=33.42
5324 R6(28)=41.82
5325 R6(31)=45.51
5330 RETURN

```

D. VARIABLE DEFINITIONS USED IN THE PROGRAM

- A - "A" coefficient obtained using the least square error data fit to $[1/V]$ plotted vs "r"; $[1/V(r)] = [r/V_0] + [D/V_0]$; "A" = $1/V_0$, "B" = D/V_0 .
- A[] - Storage array for the previously measured preamplifier gain as a function of mode number. (multiples of 245Hz)
- A8 - Not used.
- A1 - Sample count during an individual run. Output from the optical shaft encoder via the electronic counter and the HP1B.
- A7 - Not used.
- A6 - Temporary storage for the ratio "B/A" obtained with the least square error fit to the measured data.
- A2[] - Storage array for the coefficients used to calculate the source current I_1 .
- A0 - The "asked for" driving voltage in millivolts.
- B[] - Variable used in the plotting routine equal to the total distance travelled at a particular calibration point.
- B - Least square error determined "Y" intercept as described under "A" description. Equal to D/V_0 where "D" is the correction to the measured separation applied to obtain the acoustic separation and V_0 is the least square error voltage when the separation has magnitude of one.
- B8[] - Not used.
- B7[] - Not used.
- B3 - Variable used in the voltage division calculation for the condenser microphone.
- B4 - Variable used in the voltage division calculation for the condenser microphone.
- B5 - Variable used in the voltage division calculation for the condenser microphone.
- B2[] - Storage array for the coefficients used to calculate the source current.
- B0 - FAR 5204 scale sensitivity in volts.
- C[] - Storage array for the individual run distances. The distance travelled between individual calibration measurements.
- C - Variable used in the voltage division calculation for the condenser microphone.
- C1 - The program value of the W.E.540AA microphone capacitance in picofarads. This value includes the BNC "extender" used in the experiment.
- C2 - The measured system capacitance for the acoustic signal input for the condenser microphone.
- D1 - The starting separation distance between the condenser microphone's diaphragm and the face of the Altec speaker.
- D7 - The operator measured "check" distance.

- D2 - The final distance the operator measures and enters into the program. (cm)
- E - Temporary storage for one sample of signal voltage. Thirty such readings are obtained before any individual "data" point is considered complete.
- E4 - Temporary storage for the signal voltage used in the calculation of Mo.
- E4[] - Temporary storage array used prior to plotting data.
- E1 - Sample storage for bias voltage.
- E1[] - Array storage for values of bias voltage.
- E3[] - Temporary storage array used prior to plotting data.
- F - The mode number (multiple of 245 Hz) desired for a particular experimental run. Program modified to be the actual frequency of the former mode number.
- F9 - Temporary storage for "F", the mode number (multiple of 245 Hz) desired for a particular experimental run.
- G1 - Numerical value obtained by subroutine calculation for magnitude of the voltage division transfer function for the condenser microphone input circuit.
- H1 - Variable used in the plotting routine.
- I - A counter used in the plotting routine.
- I1 - Computer calculated value of driving current used in the calculation of Mo.
- K9 - A counter used in the statistical analysis of Mo.
- L4 - The operator entered "record number" used to identify where on the magnetic tape storage is desired.
- L - The total distance between the beginning position and end for a particular data run. (cm)
- L1 - One tenth the total distance travelled in a particular calibration run.
- M8 - Used in the statistical analysis of Mo: the sum of the squares of individual values of Mo.
- M - A counter.
- M8 - Used in the statistical analysis of Mo: the sum of individual values of Mo.
- M1 - The number of "different separation" calibration measurements desired. Normally set at 20.
- M7 - Temporary storage for the open circuit voltage receiving sensitivity calculated in volts/pascals.
- M6 - Sigma for "M7" over the sequence of calibrations at one particular frequency.
- M0[] - Array storage for the individual values of "M7".
- N - A counter for Do loops.
- P1[] - Array storage for the final value of the atmospheric pressure used in a particular calibration calculation.
- P - Sample value for atmospheric pressure.
- Q5 - Temporary variable used in least square error subroutine.
- Q7 - Temporary variable used in least square error subroutine.
- Q6 - Temporary variable used in least square error subroutine.
- Q9 - The parallel combination of the input resistance of the Ithaco 1201 preamplifier (200 Megohms) and the bias

- blocking resistor (~10 Megohms).
- R5[] - Storage array for the previously measured values of "Vratio" obtained for 640R/633R.
- R4 - Used in the statistical analysis of Mo.
- R9 - Temporary storage for the average value of the current measuring resistor.
- R9[] - Storage array for the beginning and ending values of 4-wire resistance measurements obtained for the current measuring resistor.
- R - The linear correlation coefficient for the least square error data fit of $[1/V(r)]$ plotted vs range, r.
- R1 - Originally used to distinguish which part of the three way reciprocity calibration was in use. Set = 1 for the comparison calibrations.
- R5 - Not used.
- R6 - Not used.
- R6[] - Storage array for the previously measured values of "Vratio" obtained for 640R/688R.
- R3 - Used in the statistical analysis of Mo.
- T1 - The interval of drive motor "on" time in millisecc.
- T1[] - Array storage for the average temperature observed during a particular data run.
- T3 - Storage for temperature obtained before a data run.
- T - Accumulator for total count from optical shaft encoder.
- T2 - PAR 5204 time constant, entered in seconds with program conversion to milliseconds.
- U7 - Operator entered cue; if U7 = 1, the magnetic tape is erased. Otherwise it is not erased.
- V - Variable used in the plotting routine. The max signal voltage measured in a particular data run.
- V[] - Variable used in the plotting routine.
- V8 - Not used.
- V8[] - Not used.
- V1 - A variable used in the plotting routine.
- V1[] - Not used.
- V7 - Not used.
- V7[] - Not used.
- V6 - Temporary variable used to store "1/A" from the linear regression analysis.
- V2 - Temporary storage for the "asked for" driving voltage in millivolts.
- V0 - Operator entered voltage drop across the current measuring resistor.
- X - Variable used in the plotting routine.
- X1 - Used in the statistics calculations for the least squares fit of data to a $1/r$ plot. The sum of X values.
- X3 - Used in the statistics calculations for the least squares fit of data to a $1/r$ plot. The sum of XY products.
- X2 - Used in the statistics calculations for the least squares fit of data to a $1/r$ plot. The sum of X squared values.
- A counter.

- Y1 - Used in the statistics calculations for the least squares fit of data to a $1/r$ plot. The sum of Y values.
- Y3 - Used in the statistics calculations for the least squares fit of data to a $1/r$ plot. The counter.
- Y2 - Used in the statistics calculations for the least squares fit of data to a $1/r$ plot. The sum of Y squared values.
- Z9 - Operator entered decision variable; if = 1, then data run must be redone.
- Z1 - Temporary variable used in the calculation of Mo.
- Z2 - Temporary variable used in the calculation of Mo.
- Z - Variable used in the plotting routine. Equal to the minimum signal voltage measured in a particular data run.

APPENDIX E

THE D.C. BLOCKING CAPACITOR CORRECTION

Calculation of the signal loss due to the D.C. blocking capacitor C_c shown below and in figure 3.3, was accomplished by comparing two different numerical solutions for the ratio $[e_1/V_{in}]$. These solutions were obtained for the two different circuits using circuit analysis software. The first numerical solution used a homegrown circuits solution on the HP-15C hand held calculator using the complex mode. The significance of the complex mode on this particular hand held calculator is that complex numbers can be directly employed in the impedance calculations. The second solution was obtained on an IBM XT microprocessor using the "Pspice" circuit analysis software made available by the Electrical Engineering Department at the United States Naval Academy. Both solutions were in substantial agreement with an average discrepancy of .001 dB. The input circuit for the acoustic signal is shown below:

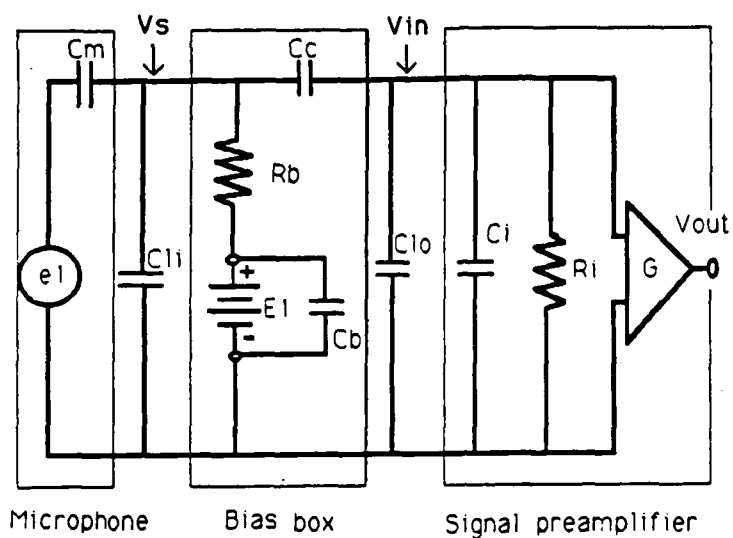


Figure E.1 The input circuit for the acoustic signal.

For comparison purposes, the first circuit analysis neglects both C_c and C_b . In the second analysis both of these 2.014 μ Farad capacitors are included.

The first solution for the signal voltage $e1'$ is given as a function of the "observed" voltage, V_{in} , using the signal transfer obtained for the circuit shown above neglecting C_c and C_b . This analysis parallels the solution used in the computer program. In the second computation,

both C_c and C_b are included and the signal voltage is given by e_1'' .

The correction to the program solution for M_o is given below in equation E.1

$$\text{CORRECTION TO } M_o \text{ due } C_c, C_b = 20 \text{ LOG} \left(\frac{e_1''}{e_1'} \right) \quad \text{Equation E.1}$$

If we define individual impedance terms as follows:

- Z_m - microphone impedance, $1/j\omega C_m$
- Z_c - coupling capacitor impedance, $1/j\omega C_c$
- Z_l - load impedance consisting of C_i , C_{lo} , and R_i .
- Z_b - bias impedance consisting of R_b , C_b , and C_{li} .
- Z_l' - modified load impedance consisting of R_i , R_b , C_i , C_{lo} , and C_{li} .
- Z_t - $(Z_l + Z_c)$ in parallel with Z_b .

Then the correction may be rewritten as:

$$\text{CORRECTION TO } M_o \text{ due } C_c, C_b = 20 \text{ LOG} \left\{ \frac{\left(1 + \frac{Z_m}{Z_t} \right) \left(1 + \frac{Z_c}{Z_l} \right)}{\left(1 + \frac{Z_m}{Z_l'} \right)} \right\} \quad \text{Equation E.2}$$

This correction is solved numerically with the program listed in table E.1.

Register usage

Program Listing
for HP-15c hand-held
scientific calculator

Variable - number	register	(read top to bottom, left to right)			
Ct (140pF) - .0		F LBL B	RCL .3	+	STO 1
*Wo - .2		RCL .2	F[[]]	F[[]]	R/S
Cb (.014uF)- .3		X	1/X	0	GSB 2
Rb (10Mohm)- .4		STO 0	+	RCL .9	RCL 1
Clo+Ci (40pF) - .5		RCL 0	0	F[[]]	g CF 8
Cc (.014uF)- .6		STO X .0	RCL .5	X	g RTN
Cl1 (100pF) - .7		RCL 0	F[[]]	STO 5	F LBL 1
Ri (10Mohm)- .8		STO X .5	+	RE:IM	RCL 0
Cm (50pF) - .9		RCL 0	0	STO 6	X
w (mode*Wo)- 0		STO X .7	RCL .9	1	CHS
re{Zm/Zt} - 1		RCL .3	F[[]]	RCL 1	1/X
im{Zm/Zt} - 2		GSB 1	X	+	g RTN
re{Zc/Zl} - 3		STO .3	STO 1	RCL 2	F LBL 2
im{Zc/Zl} - 4		RCL .6	RE:IM	F[[]]	RCL 0
re{Zm/Zl'} - 5		GSB 1	STO 2	1	STO / .0
im{Zm/Zl'} - 6		STO .6	RCL .8	RCL 3	RCL 0
Ri*Rb/(Ri+Rb)- 9		RCL .9	1/X	+	STO / .5
		GSB 1	RCL .7	RCL 4	RCL 0
		STO .9	F[[]]	F[[]]	STO / .7
* Wo = 245*pi*2		RCL .8	0	X	RCL .3
~ 1539.3804		1/X	RCL .6	1	GSB 1
		RCL .7	F[[]]	RCL 5	STO .3
		F[[]]	X	+	RCL .6
		1/X	STO 3	RCL 6	GSB 1
		0	RE:IM	F[[]]	STO .6
		RCL .6	STO 4	/	RCL .9
		F[[]]	RCL 9	R/S	GSB 1
		+	1/X	RE:IM	STO .9
		1/X	RCL .5	R/S	g RTN
		RCL .4	RCL .7	g ABS	

** program instructions are described in the HP-15C owners handbook. The entering argument in the "x" register is the mode number of the longitudinal resonance desired. The output gives: the real component, the imaginary component, and finally the magnitude. From the magnitude, the correction in dB is obtained.

Table E.1 Program listing for Cc correction

A comparison of the correction obtained using the above program was made with a numerical solution obtained using the IBM XT microprocessor and the "Pspice" circuit analysis software made available by the Electrical Engineering Department at the United States Naval Academy. The parameter variables were the same as listed in table E.1 with the exception that Cc and Cb were given values of .01 uF for simplicity. The tabulated comparison of results is given in table E.2.

Mode #	HP-15c corr solution (dB)	IBM-XT corr solution (dB)	discrepancy (dB)
1	.054	.056	-.002
2	.045	.045	0
3	.043	.044	-.001
4	.042	.044	-.002
5	.042	.044	-.002
6	.042	.043	-.001
7	.041	.040	+.001
8	.041	.040	+.001
9	.041	.040	+.001
10	.041	.040	+.001
***** no further change through mode #23 *****			

Table E.2 Comparison calculations between the HP-15c and the IBM-XT with Cb and Cc = .01uF.

A plot of the proper correction is shown in figure E.2. The correction due to the temporary neglect of Cc in the analytical solution for $[e1/Vin]$ is constant to within a value less than .01 dB.

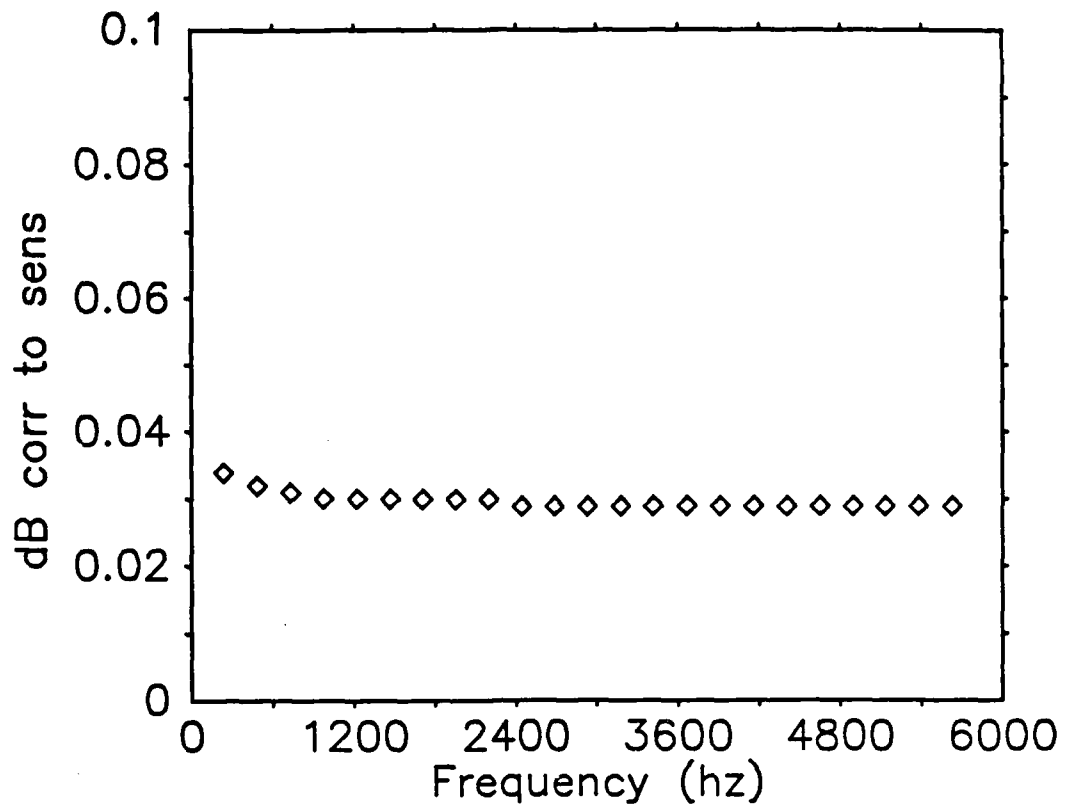


Figure E.2 The bias voltage blocking capacitor
correction

This concludes the calculation for the correction to account for the acoustic signal dropped across the d.c. blocking capacitor. The correction is so almost constant +.03 dB.

AD-A164 149

RECIPROCIY CALIBRATION IN A PLANE WAVE RESONATOR(U)
NAVAL POSTGRADUATE SCHOOL MONTEREY CA C L BURMASTER
DEC 85 NPS61-86-006

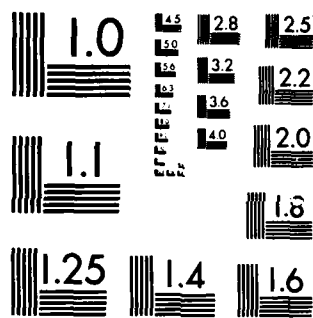
5/3

UNCLASSIFIED

F/G 14/2

NL

										END			
										FILED			
										+			
										DEC			



MICROCOPY RESOLUTION TEST CHART
NATIONAL BUREAU OF STANDARDS-1963-A

APPENDIX F

THE OPEN CIRCUIT VOLTAGE SENSITIVITY CALIBRATION OBTAINED FROM OBSERVING A CHANGE IN MICROPHONE CAPACITANCE WITH A CHANGE IN BIAS VOLTAGE

When the received signal voltage from a condenser microphone is simulated by a small change in the bias voltage and when the definition of the microphone open circuit voltage sensitivity is considered,

$$M_o = \frac{\delta V}{\delta P} = \frac{\partial V}{\partial C} \frac{\partial C}{\partial P} = \frac{\partial V}{\partial C} \frac{\partial C}{\partial V^2} \frac{\partial V^2}{\partial P} \quad \text{Equation F.1}$$

Next, the force on a parallel plate capacitor due to the charge on the plates is given by [Ref. 36]:

$$F = \frac{Q^2}{2 \epsilon_0 A} \quad \text{Equation F.2}$$

The electrostatic pressure is simply the force divided by the effective backplate area. This electrostatic pressure

is used to simulate the acoustic pressure.

$$p \sim \frac{F}{A_{(\text{backplate})}} = \frac{Q^2}{2 \epsilon_0 A^2_{(\text{backplate})}} \quad \text{Equation F.3}$$

The electrostatic pressure shown here only acts on a small portion of the microphone diaphragm; where the charge is concentrated opposite the backplate. Since it is an acoustic pressure that is being simulated, an interpretation of the "area" in the above equation is necessary. If the electrostatic pressure were applied equally to the entire diaphragm, this would be a proper simulation of the acoustic pressure. Since the electrostatic pressure is only applied to a portion of the diaphragm, the use of the diaphragm area in the above equation results in a low estimate for the simulated acoustic pressure. Similarly, since the acoustic pressure is actually applied to an area greater than the backplate area, use of the backplate area in the above equation results in a high estimate for the simulated acoustic pressure. As an initial estimate, the average of the two areas is used with the appropriate uncertainty to simulate the acoustic pressure.

When the definition of capacitance as $C=Q/V$ is substituted into equation F.3, we obtain,

$$\rho = \frac{C_0^2 V_0^2}{2 \epsilon_0 A e^2}$$

Equation F.4

When $C = Q/V$ is differentiated, we obtain,

$$\frac{\partial V}{\partial C} = - \frac{V_0}{C_0}$$

Equation F.5

Solving equation F.4 for the square of the bias voltage,

$$V_0^2 = \frac{2 \epsilon_0 A e^2}{C_0^2} \rho$$

Equation F.6

The partial derivative of V^2 re P is given by:

$$\frac{\partial V^2}{\partial P} = \frac{2 \epsilon_0 A e^2}{C_0^2}$$

Equation F.7

The slope of the experimental straight line fit obtained in equations 3.17 yields the magnitude of the partial

derivative of C with respect to the square of the bias voltage. Thus, the magnitude of the open circuit voltage receiving sensitivity for a condenser microphone is given by combining equation F.1, equation F.5, the experimental slope, and equation F.7.

$$M_0 \sim \frac{V_0}{C_0^3} \left(\frac{\Delta C}{\Delta V^2} \right) (2 \epsilon_0 A e^2)$$

↑
 EXPERIMENTAL
 SLOPE FROM
 MEASURED
 DATA

Equation F.8

The fractional uncertainty in this sensitivity will be:

$$\frac{\delta M_0}{M_0} = \left\{ \left(\frac{\delta V_0}{V_0} \right)^2 + \left(3 \frac{\delta C_0}{C_0} \right)^2 + \left(\frac{\delta \text{SLOPE}}{\text{SLOPE}} \right)^2 + \left(2 \frac{\delta A e^2}{A e^2} \right)^2 \right\}^{\frac{1}{2}}$$

Equation F.9

Table F.1, shown below, gives the computer program used to evaluate the above equation.

 Register usage HP-15c scientific hand-held
 calculator program *

.0 - Vo (200volts)	F LBL A	X	g LOG
.1 - Co **	RCL .1	RCL .2	2
.2 - Eo (8.85E-12F/M)	3	x	0
.3 - Ae ***	y^x	RCL .3	X
.4 -dC/dV^2 **	1/X	g X^2	2
	RCL .0	X	0
	X	RCL .4	-
	2	X	g RTN

* Program instructions are described in the HP-15c owners handbook.

** The W.E.640AA microphones had the following basic capacitances (excluding the BNC connectors) and measured values of [dC/dV^2] (see equations 3.17):

Mic. "Co" w/o extender	-	[dC/dV^2]	sigma []
Serial #1082	-	49.37 Pf	2.47E-17 1.2E-18
Serial #1248	-	49.41 Pf	3.66E-17 1.6E-18
Serial #815	-	46.48 Pf	5.92E-17 8.2E-19

*** Ae is the effective area estimated by obtaining the average of the backplate area and the diaphragm area. The average fractional uncertainties in the above variables are: Ae ~.38, slope ~ .04, Co ~ <.01, Vo assumed exact.

 Table F.1 HP-15c program for Mo calculation

The values of Mo that result from the above equation are:

W.E.640AA	[dC/dV^2]	Mo	245 Hz ~ Mo
			[figure 5.8]
Serial #1082	-----	-55< ~ -50 <-45 dB	~ -49.5 dB
Serial #1248	-----	-52< ~ -47 <-42 dB	~ -48.6 dB
Serial #815	-----	-46< ~ -41 <-36 dB	~ -45.7 dB

These rough calculations are seen to be in agreement with more accurate calibrations shown above as obtained from figure 5.8.

APPENDIX G

A PRINTOUT OF RAW DATA FOR THE PLANE WAVE RESONANT RECIPROCIITY CALIBRATION IN BOTH A LONG AND A SHORT TUBE

After data acquisition, the computer program listed in appendix B stored data on a magnetic tape. The data so stored is printed in this appendix without consideration of significant figures.

The format used in the different data sets is given below:

- L7 - The mode number of the longitudinal resonance.
- M1 - Reciprocity calibration for the side A microphone (V/pa).
- M2 - Reciprocity calibration for the side B microphone (V/pa).
- M3 - Comparison calibration of "C" microphone based upon M1 (V/pa).
- M4 - Comparison calibration of "C" microphone based upon M2 (V/pa).
- M5 - Comparison calibration of the side A microphone based upon M2 (V/pa).
- M6 - Comparison calibration of the side B microphone based upon M1 (V/pa).
- PS[1,N] - Atmospheric pressure (pa) for midtime of side A data.
- PS[2,N] - Atmospheric pressure (pa) for midtime of side B data.
- TS[1,N] - Temperature (deg C) for midtime of side A data.
- TS[2,N] - Temperature (deg C) for midtime of side B data.
- C - (long tube data) System identifier used in program.
- C - (short tube data) A side bias voltage (Volts).
- A2 - Drive voltage in RMS millivolts.
- V1[1,N] - Comparison voltage, Vca (Volts).
- V1[2,N] - Comparison voltage, Vcb (Volts).
- G9[1,N] - Calculated effective gamma at midtime of A side data.
- G9[2,N] - Calculated effective gamma at midtime of B side data.
- V[1,N] - Ravined signal voltage, A side receive (RMS Volts).
- V[2,N] - Ravined signal voltage, B side receive (RMS Volts).

Q[1,N] - Ravined quality factor, A side receive.
Q[2,N] - Ravined quality factor, B side receive.
F2[1,N] - Ravined resonant frequency (hz), A side receive.
F2[2,N] - Ravined resonant frequency (hz), B side receive.
C1 - {long tube data} System identifier used in program.
C1 - {short tube data} B side bias voltage (Volts).

The data that follow are grouped in seven sets. The first five sets list "long tube data" and the last two list "short tube data". At the beginning of each data set, the following library data is provided:

[NAME OF STORAGE TAPE] [ARRAY LOCATION ON TAPE]
[LONG OR SHORT TUBE] [MODE NUMBERS OF DATA IN SET]
[SERIAL # OF SIDE A MIC] [SERIAL # OF SIDE B MIC]
*{SIDE A BIAS VOLTAGE} {SIGMA SIDE A BIAS VOLTAGE}
*{SIDE B BIAS VOLTAGE} {SIGMA SIDE B BIAS VOLTAGE}

* This format is included only for the long tube data.

2 MAY DATA TAPE, ARRAY STORAGE 1 to 23
 LONG TUBE MODES 1 TO 23
 A SIDE = 815 w/ET, B SIDE = 1248
 A SIDE BIAS = 116.334 VOLTS, SIGMA = .001 VOLTS
 B SIDE BIAS = 118.464 VOLTS, SIGMA = .007 VOLTS

L7= 3
 M1= 2.83573873337E-2
 M2= 2.13248930072E-2
 M3= 7.94898356556E-3
 M4= 7.94775872626E-3
 M5= 2.83530178137E-2
 M6= 2.13281794138E-2
 P5(1, 21) = 100083.387675
 P5(2, 21) = 100080.387774
 T5(1, 21) = 21.877
 T5(2, 21) = 21.8625
 C= 2

R2= 2988.07298552
 V1(1, 21) = 1.44938055556E-3
 V1(2, 21) = 1.14653888889E-3
 G9(1, 21) = 1.39735156029
 G9(2, 21) = 1.39735203145
 U(1, 21) = 3.8988806692E-3
 U(2, 21) = 4.09018927983E-3
 Q(1, 21) = 97.9008984344
 Q(2, 21) = 97.9264520258
 F2(1, 21) = 734.073086471
 F2(2, 21) = 734.01667125
 C1= 2

L7= 2
 M1= 2.84040902187E-2
 M2= 2.11778958768E-2
 M3= 7.34137111396E-3
 M4= 7.34252404945E-3
 M5= 2.84085509773E-2
 M6= 2.11745704879E-2
 P5(1, 22) = 100068.188175
 P5(2, 22) = 100068.521497
 T5(1, 22) = 21.8285
 T5(2, 22) = 21.8225
 C= 2

R2= 3289.72986279
 V1(1, 22) = 1.18949638889E-3
 V1(2, 22) = 9.29853611111E-4
 G9(1, 22) = 1.39638713741
 G9(2, 22) = 1.39638763786
 U(1, 22) = 3.4308407436E-3
 U(2, 22) = 3.59764483367E-3
 Q(1, 22) = 78.9557673213
 Q(2, 22) = 78.9377946821
 F2(1, 22) = 490.255804847
 F2(2, 22) = 490.299979984
 C1= 2

L7= 1
 M1= .028518020669
 M2= 2.10292166786E-2
 M3= 5.74570023414E-3
 M4= 5.73084879508E-3
 M5= .028446287875
 M6= .021082245899
 P5(1, 23) = 100028.189491
 P5(2, 23) = 100022.523011
 T5(1, 23) = 21.779
 T5(2, 23) = 21.7735
 C= 2

R2= 3247.32380583
 V1(1, 23) = 7.25259444444E-4
 V1(2, 23) = 5.69087777778E-4
 G9(1, 23) = 1.39418845558
 G9(2, 23) = 1.39418796276
 U(1, 23) = 2.56132270293E-3
 U(2, 23) = 2.82478832223E-3
 Q(1, 23) = 62.1917484365
 Q(2, 23) = 62.4970851541
 F2(1, 23) = 243.865388871
 F2(2, 23) = 243.817485753
 C1= 2

L7= 7
M1= 2.89139897899E-2
M2= 2.15715403913E-2
M3= 9.20818244816E-3
M4= 9.20627313686E-3
M5= 2.89079944909E-2
M6= 2.15760141654E-2
P5(1, 17) = 100095.38728
P5(2, 17) = 100089.920793
T5(1, 17) = 22.0965
T5(2, 17) = 22.085
C= 2

L7= 6
M1= 2.88917579899E-2
M2= 2.13067761447E-2
M3= 8.73809776344E-3
M4= 8.73738972942E-3
M5= 2.88894169371E-2
M6= 2.13085027384E-2
P5(1, 18) = 100120.1198
P5(2, 18) = 100123.853011
T5(1, 18) = 22.048
T5(2, 18) = 22.0335
C= 2

L7= 5
M1= 2.85011736857E-2
M2= .021424296476
M3= 8.56808064812E-3
M4= 8.56617784289E-3
M5= 2.84948441254E-2
M6= 2.14290554553E-2
P5(1, 19) = 100094.653971
P5(2, 19) = 100098.187188
T5(1, 19) = 21.986
T5(2, 19) = 21.977
C= 2

L7= 4
M1= 2.85525910307E-2
M2= 2.12502938119E-2
M3= 8.19332377736E-3
M4= 8.19398398886E-3
M5= 2.85598921786E-2
M6= 2.12485816182E-2
P5(1, 20) = 100089.920793
P5(2, 20) = 100084.787629
T5(1, 20) = 21.927
T5(2, 20) = 21.918
C= 2

A2= 2253.31523138
V1(1, 17) = .001637175
V1(2, 17) = 1.28130833333E-3
G9(1, 17) = 1.39884317379
G9(2, 17) = 1.39884363516
V(1, 17) = 3.83612196978E-3
V(2, 17) = 4.02334948033E-3
Q(1, 17) = 124.007903055
Q(2, 17) = 124.061526956
F2(1, 17) = 1717.92839615
F2(2, 17) = 1717.86535535
C1= 2

A2= 2420.30701372
V1(1, 18) = 1.57981388889E-3
V1(2, 18) = 1.22537222222E-3
G9(1, 18) = 1.39861713728
G9(2, 18) = 1.39861782378
V(1, 18) = 3.8524939282E-3
V(2, 18) = 4.05158635785E-3
Q(1, 18) = 117.480419287
Q(2, 18) = 117.498178043
F2(1, 18) = 1471.7617945
F2(2, 18) = 1471.80133572
C1= 2

A2= 2514.86063706
V1(1, 19) = .00153615
V1(2, 19) = 1.21258055556E-3
G9(1, 19) = 1.39832609872
G9(2, 19) = 1.39832640124
V(1, 19) = 3.9419623822E-3
V(2, 19) = 4.03357186297E-3
Q(1, 19) = 113.709070321
Q(2, 19) = 113.749015418
F2(1, 19) = 1225.52203759
F2(2, 19) = 1225.45161399
C1= 2

A2= 2728.46839697
V1(1, 20) = 1.48949722222E-3
V1(2, 20) = 1.16455333333E-3
G9(1, 20) = 1.39793209953
G9(2, 20) = 1.39793257259
V(1, 20) = 3.86286495644E-3
V(2, 20) = 4.05901667387E-3
Q(1, 20) = 106.09713418
Q(2, 20) = 106.089726407
F2(1, 20) = 980.128501844
F2(2, 20) = 980.168080589
C1= 2

L7= 11
M1= 2.96731998474E-2
M2= 2.20105596773E-2
M3= 1.09269960678E-2
M4= .01092486924
M5= 2.96674242632E-2
M6= 2.20148446412E-2
P5(1, 13)= 100114.253326
P5(2, 13)= 100106.986899
T5(1, 13)= 21.984
T5(2, 13)= 21.988
C= 2

L7= 10
M1= 2.96292218898E-2
M2= 2.17399490607E-2
M3= 1.02680157664E-2
M4= 1.02675524251E-2
M5= 2.96278848796E-2
M6= 2.17409301138E-2
P5(1, 14)= 100076.187912
P5(2, 14)= 100079.121149
T5(1, 14)= 22.033
T5(2, 14)= 22.0345
C= 2

L7= 9
M1= 2.93010479805E-2
M2= 2.19265528484E-2
M3= 9.94252570853E-3
M4= 9.94815796177E-3
M5= 2.93176464714E-2
M6= 2.19141389022E-2
P5(1, 15)= 100107.786872
P5(2, 15)= 100102.587043
T5(1, 15)= 22.047
T5(2, 15)= 22.07
C= 2

L7= 8
M1= 2.93550285021E-2
M2= 2.15725106156E-2
M3= 9.43700194776E-3
M4= 9.43519157294E-3
M5= 2.93493659881E-2
M6= 2.15766727035E-2
P5(1, 16)= 100119.786478
P5(2, 16)= 100105.186958
T5(1, 16)= 22.1255
T5(2, 16)= 22.1235
C= 2

A2= 1440.99162153
V1(1, 13)= 1.90711111111E-3
V1(2, 13)= .001483875
G9(1, 13)= 1.3994235428
G9(2, 13)= 1.39942338225
V(1, 13)= 3.84229614104E-3
V(2, 13)= 4.02959048857E-3
Q(1, 13)= 185.385432342
Q(2, 13)= 185.473935026
F2(1, 13)= 2701.12073709
F2(2, 13)= 2701.16197878
C1= 2

A2= 1680.01385241
V1(1, 14)= 1.80147777778E-3
V1(2, 14)= 1.39241111111E-3
G9(1, 14)= 1.39931023153
G9(2, 14)= 1.39931019348
V(1, 14)= 3.81434966206E-3
V(2, 14)= 4.01791920772E-3
Q(1, 14)= 160.14219529
Q(2, 14)= 160.1558398
F2(1, 14)= 2454.59613366
F2(2, 14)= 2454.65560873
C1= 2

A2= 1775.46321055
V1(1, 15)= 1.74693055556E-3
V1(2, 15)= 1.36948611111E-3
G9(1, 15)= 1.39918144366
G9(2, 15)= 1.3991804244
V(1, 15)= 3.85037765747E-3
V(2, 15)= 4.03593407014E-3
Q(1, 15)= 153.420535912
Q(2, 15)= 153.255761567
F2(1, 15)= 2209.92819076
F2(2, 15)= 2209.94009724
C1= 2

A2= 2038.35184057
V1(1, 16)= 1.66890277778E-3
V1(2, 16)= 1.29143611111E-3
G9(1, 16)= 1.39902595884
G9(2, 16)= 1.39902609303
V(1, 16)= 3.81576365137E-3
V(2, 16)= 4.01718088649E-3
Q(1, 16)= 134.255157767
Q(2, 16)= 134.331062269
F2(1, 16)= 1964.3358954
F2(2, 16)= 1964.40199164
C1= 2

L7= 15
M1= 3.02223122172E-2
M2= 2.21300555083E-2
M3= 1.31237708052E-2
M4= 1.31179550475E-2
M5= .030208919295
M6= 2.21398667203E-2
P5(1, 9) = 100075.387938
P5(2, 9) = 100081.254412
T5(1, 9) = 21.8205
T5(2, 9) = 21.824
C= 2

L7= 14
M1= 3.02004094951E-2
M2= 2.20504051353E-2
M3= 1.25304079626E-2
M4= 1.25778517109E-2
M5= 3.01942729813E-2
M6= 2.20540865352E-2
P5(1, 10) = 100090.920761
P5(2, 10) = 100092.987359
T5(1, 10) = 21.8255
T5(2, 10) = 21.8335
C= 2

L7= 13
M1= 2.99548494721E-2
M2= 2.21801110171E-2
M3= 1.20257920824E-2
M4= 1.20242964513E-2
M5= 2.99511240289E-2
M6= 2.21828698699E-2
P5(1, 11) = 100103.253688
P5(2, 11) = 100100.387116
T5(1, 11) = 21.895
T5(2, 11) = 21.9135
C= 2

L7= 12
M1= 3.00245630586E-2
M2= 2.19348349784E-2
M3= 1.13759278296E-2
M4= 1.13735946377E-2
M5= 3.00104050497E-2
M6= 2.19397347149E-2
P5(1, 12) = 100115.986603
P5(2, 12) = 100114.586649
T5(1, 12) = 21.9655
T5(2, 12) = 21.959
C= 2

R2= 1201.81509816
V1(1, 9) = 2.29795555556E-3
V1(2, 9) = .001766125
G9(1, 9) = 1.39975669961
G9(2, 9) = 1.39975654545
W(1, 9) = 3.87666246879E-3
W(2, 9) = 4.06715279907E-3
Q(1, 9) = 218.966475391
Q(2, 9) = 219.147905622
F2(1, 9) = 3683.5047849
F2(2, 9) = 3683.50570898
C1= 2

R2= 1249.62487442
V1(1, 10) = 2.20627222222E-3
V1(2, 10) = 1.69646944444E-3
G9(1, 10) = 1.39968825088
G9(2, 10) = 1.39968790535
W(1, 10) = 3.86784623137E-3
W(2, 10) = 4.07252865491E-3
Q(1, 10) = 211.050445008
Q(2, 10) = 211.133499315
F2(1, 10) = 3437.8572222
F2(2, 10) = 3437.88274335
C1= 2

R2= 1273.49134268
V1(1, 11) = 2.07049166667E-3
V1(2, 11) = .001608125
G9(1, 11) = 1.39960917622
G9(2, 11) = 1.39960839115
W(1, 11) = 3.81924507706E-3
W(2, 11) = 4.00565234931E-3
Q(1, 11) = 204.966312997
Q(2, 11) = 205.03003518
F2(1, 11) = 3192.03220346
F2(2, 11) = 3192.13719912
C1= 2

R2= 1369.16474919
V1(1, 12) = 2.00508055556E-3
V1(2, 12) = 1.54249722222E-3
G9(1, 12) = 1.39952119947
G9(2, 12) = 1.39952150226
W(1, 12) = 3.86694906101E-3
W(2, 12) = 4.07112332376E-3
Q(1, 12) = 194.702127762
Q(2, 12) = 194.787222018
F2(1, 12) = 2947.45346339
F2(2, 12) = 2947.49162057
C1= 2

L7= 19
M1= 3.01641979712E-2
M2= 2.20735582868E-2
M3= .012813051034
M4= 1.27940498205E-2
M5= 3.01194657396E-2
M6= 2.21063410568E-2
P5(1, 5) = 100129.852913
P5(2, 5) = 100128.519524
T5(1, 5) = 21.127
T5(2, 5) = 21.1595
C= 2

R2= 1106.30395691
V1(1, 5) = 2.21220833333E-3
V1(2, 5) = 1.70330555556E-3
G9(1, 5) = 1.40000241921
G9(2, 5) = 1.40000109154
V(1, 5) = 3.81672029368E-3
V(2, 5) = 4.00988381666E-3
Q(1, 5) = 234.828428378
Q(2, 5) = 235.545019298
F2(1, 5) = 4660.20006043
F2(2, 5) = 4660.50076278
C1= 2

L7= 18
M1= 3.02559023602E-2
M2= 2.22333921491E-2
M3= 1.34360338982E-2
M4= 1.34298493532E-2
M5= 3.02419757066E-2
M6= 2.22436307907E-2
P5(1, 6) = 100129.052839
P5(2, 6) = 100120.786445
T5(1, 6) = 21.283
T5(2, 6) = 21.3115
C= 2

R2= 1130.1859669
V1(1, 6) = 2.32498333333E-3
V1(2, 6) = .0018008
G9(1, 6) = 1.39994872128
G9(2, 6) = 1.39994754351
V(1, 6) = 3.84905778394E-3
V(2, 6) = 4.05512738232E-3
Q(1, 6) = 229.695268876
Q(2, 6) = 229.937779421
F2(1, 6) = 4416.5969346
F2(2, 6) = 4416.82232224
C1= 2

L7= 17
M1= 3.03183916027E-2
M2= 2.21529600077E-2
M3= 1.35447960087E-2
M4= 1.35261157434E-2
M5= 3.02765790829E-2
M6= 2.21835543908E-2
P5(1, 7) = 100096.320583
P5(2, 7) = 100085.387609
T5(1, 7) = 21.4115
T5(2, 7) = 21.4375
C= 2

R2= 1130.12162035
V1(1, 7) = 2.32761388889E-3
V1(2, 7) = 1.78875555556E-3
G9(1, 7) = 1.39989177449
G9(2, 7) = 1.3998906927
V(1, 7) = 3.81214669251E-3
V(2, 7) = 4.00391348676E-3
Q(1, 7) = 227.735053394
Q(2, 7) = 228.400006821
F2(1, 7) = 4171.4937225
F2(2, 7) = 4171.6831117
C1= 2

L7= 16
M1= 3.03948295154E-2
M2= 2.21747806086E-2
M3= 1.35141459287E-2
M4= 1.35100741307E-2
M5= 3.03856715851E-2
M6= 2.21814638604E-2
P5(1, 8) = 100070.988083
P5(2, 8) = 100058.521826
T5(1, 8) = 21.5225
T5(2, 8) = 21.5495
C=

R2= 1153.99936942
V1(1, 8) = .00231775
V1(2, 8) = 1.78168333333E-3
G9(1, 8) = 1.39983100342
G9(2, 8) = 1.39982986271
V(1, 8) = 3.80424246814E-3
V(2, 8) = 4.00720559425E-3
Q(1, 8) = 222.087420882
Q(2, 8) = 222.256864186
F2(1, 8) = 3927.16996571
F2(2, 8) = 3927.30577465
C1= 2

L7= 23
M1= 2.90996999243E-2
M2= 2.11154951639E-2
M3= 9.63430711913E-3
M4= 6.62958614652E-3
M5= 2.90837891056E-2
M6= 2.11270467888E-2
P5(1, 1) = 100130.186136
P5(2, 1) = 100125.452958
T5(1, 1) = 20.9405
T5(2, 1) = 20.9205
C= 2

L7= 22
M1= 2.91815123592E-2
M2= 2.16335030389E-2
M3= 9.96202464095E-3
M4= 9.95909006911E-3
M5= 2.91729161904E-2
M6= 2.16398776242E-2
P5(1, 2) = 100121.786412
P5(2, 2) = 100137.919675
T5(1, 2) = 20.898
T5(2, 2) = 20.795
C= 2

L7= 21
M1= 3.25036205687E-2
M2= 1.98828210651E-2
M3= 1.00664380616E-2
M4= 1.0069127013E-2
M5= 3.25123029444E-2
M6= 1.98775113789E-2
P5(1, 3) = 100132.386063
P5(2, 3) = 100131.719418
T5(1, 3) = 20.714
T5(2, 3) = 20.725
C= 2

L7= 20
M1= 2.98466906902E-2
M2= 2.21096732068E-2
M3= .012152891997
M4= 1.21356612172E-2
M5= 2.98043730465E-2
M6= 2.21410655554E-2
P5(1, 4) = 100136.052609
P5(2, 4) = 100134.585991
T5(1, 4) = 20.9355
T5(2, 4) = 20.9805
C= 2

A2= 1178.41041527
V1(1, 1) = 1.58903055556E-3
V1(2, 1) = 1.21223333333E-3
G9(1, 1) = 1.40016795388
G9(2, 1) = 1.40016879168
V(1, 1) = 3.88815482475E-3
V(2, 1) = 4.08551905224E-3
Q(1, 1) = 243.562616681
Q(2, 1) = 243.839245121
F2(1, 1) = 5641.98967503
F2(2, 1) = 5641.9592321
C1= 2

A2= 1130.44291511
V1(1, 2) = 1.75589722222E-3
V1(2, 2) = 1.37153611111E-3
G9(1, 2) = 1.40013807529
G9(2, 2) = 1.40013858673
V(1, 2) = 3.81422475641E-3
V(2, 2) = 4.01760680383E-3
Q(1, 2) = 242.511154852
Q(2, 2) = 242.639154503
F2(1, 2) = 5395.92587741
F2(2, 2) = 5395.71060223
C1= 2

A2= 1130.37818047
V1(1, 3) = .001962375
V1(2, 3) = 1.26023055556E-3
G9(1, 3) = 1.40010394676
G9(2, 3) = 1.40010346822
V(1, 3) = 3.87496859914E-3
V(2, 3) = 4.06917079863E-3
Q(1, 3) = 240.797461398
Q(2, 3) = 240.664490891
F2(1, 3) = 5149.22262136
F2(2, 3) = 5149.09290547
C1= 2

A2= 1130.31414809
V1(1, 4) = 2.13141666667E-3
V1(2, 4) = 1.66653888889E-3
G9(1, 4) = 1.4000541889
G9(2, 4) = 1.40005234895
V(1, 4) = 3.88317744898E-3
V(2, 4) = 4.09290815325E-3
Q(1, 4) = 235.935890517
Q(2, 4) = 236.626102682
F2(1, 4) = 4904.81940533
F2(2, 4) = 4905.15054914
C1= 2

2 MAY DATA TAPE, ARRAY STORAGE 24 to 46
 LONG TUBE MODES 1 TO 23
 A SIDE = 1248, B SIDE = 815 w/ET
 A SIDE BIAS = 116.307 VOLTS, SIGMA = UNK.
 B SIDE BIAS = 118.495 VOLTS, SIGMA = UNK.

L7= 3
 M1= 2.09042127291E-2
 M2= 2.89921237497E-2
 M3= 7.9337301316E-3
 M4= 7.93068766195E-3
 M5= 2.08961962688E-2
 M6= .029003246071
 P5(1, 44)= 100007.256846
 P5(2, 44)= 100006.856859
 T5(1, 44)= 22.6785
 T5(2, 44)= 22.679
 C= 2

R2= 2964.2195776
 V1(1, 44)= 1.09761722222E-3
 V1(2, 44)= .0014767
 G9(1, 44)= 1.39730470459
 G9(2, 44)= 1.39730456126
 V(1, 44)= 4.01254666592E-3
 V(2, 44)= 3.89088744198E-3
 Q(1, 44)= 97.5462869633
 Q(2, 44)= 97.6161281057
 F2(1, 44)= 734.984958859
 F2(2, 44)= 734.944170726
 C1= 2

L7= 2
 M1= 2.08100398667E-2
 M2= 2.89518038063E-2
 M3= 7.3684614715E-3
 M4= 7.35601854107E-3
 M5= 2.07748984903E-2
 M6= 2.90007766682E-2
 P5(1, 45)= 99964.7915763
 P5(2, 45)= 99967.2581618
 T5(1, 45)= 22.712
 T5(2, 45)= 22.718
 C= 2

R2= 3289.84882065
 V1(1, 45)= 9.06248611111E-4
 V1(2, 45)= 1.22400277778E-3
 G9(1, 45)= 1.39633769907
 G9(2, 45)= 1.39633770773
 V(1, 45)= 3.56681156282E-3
 V(2, 45)= 3.45683379103E-3
 Q(1, 45)= 78.5756676004
 Q(2, 45)= 78.8484008156
 F2(1, 45)= 490.937688613
 F2(2, 45)= 490.991414937
 C1= 2

L7= 1
 M1= 2.08015514549E-2
 M2= 2.88826893266E-2
 M3= 5.73279017959E-3
 M4= 5.73741576655E-3
 M5= 2.08183354994E-2
 M6= 2.88594036829E-2
 P5(1, 46)= 99987.3908329
 P5(2, 46)= 99982.5243263
 T5(1, 46)= 22.7285
 T5(2, 46)= 22.733
 C= 2

R2= 3247.38802543
 V1(1, 46)= 5.52054166667E-4
 V1(2, 46)= 7.48126944444E-4
 G9(1, 46)= 1.39413835471
 G9(2, 46)= 1.39413747889
 V(1, 46)= 2.77909247579E-3
 V(2, 46)= 2.71459457695E-3
 Q(1, 46)= 62.4364846
 Q(2, 46)= 62.3277525457
 F2(1, 46)= 244.234526313
 F2(2, 46)= 244.190758033
 C1= 2

L7= 7
M1= 2.11258578137E-2
M2= 2.96091779439E-2
M3= 9.19050002337E-3
M4= 9.17434857798E-3
M5= 2.10887310918E-2
M6= 2.96613049169E-2
P5(1, 40) = 100037.855839
P5(2, 40) = 100038.589149
T5(1, 40) = 22.5275
T5(2, 40) = 22.533
C= 2

L7= 6
M1= 2.09829232204E-2
M2= 2.93904660383E-2
M3= 8.76362993335E-3
M4= 8.76291585243E-3
M5= 2.09812134832E-2
M6= 2.93928610369E-2
P5(1, 41) = 100027.456182
P5(2, 41) = 100022.389682
T5(1, 41) = 22.568
T5(2, 41) = 22.576
C= 2

L7= 5
M1= 2.09568323338E-2
M2= 2.91920729207E-2
M3= 8.54489853636E-3
M4= 8.54304760576E-3
M5= 2.09522920249E-2
M6= 2.91983576456E-2
P5(1, 42) = 100014.856596
P5(2, 42) = 100010.056754
T5(1, 42) = 22.604
T5(2, 42) = 22.61
C= 2

L7= 4
M1= 2.09074443568E-2
M2= 2.91058156694E-2
M3= 8.21422216433E-3
M4= 8.21305891398E-3
M5= 2.09044835662E-2
M6= 2.91099380494E-2
P5(1, 43) = 100018.7898
P5(2, 43) = 100022.856333
T5(1, 43) = 22.642
T5(2, 43) = 22.6495
C= 2

A2= 2229.39634934
V1(1, 40) = 1.22211944444E-3
V1(2, 40) = 1.65974166667E-3
G9(1, 40) = 1.39881117756
G9(2, 40) = 1.39881089802
V(1, 40) = 3.94425302151E-3
V(2, 40) = 3.81518593856E-3
Q(1, 40) = 123.183802767
Q(2, 40) = 123.614970089
F2(1, 40) = 1719.05898422
F2(2, 40) = 1719.03029107
C1= 2

A2= 2396.39616084
V1(1, 41) = 1.17918055556E-3
V1(2, 41) = 1.60018055556E-3
G9(1, 41) = 1.39858141163
G9(2, 41) = 1.39858111401
V(1, 41) = 3.95492398362E-3
V(2, 41) = 3.83134226245E-3
Q(1, 41) = 116.780092196
Q(2, 41) = 116.810795597
F2(1, 41) = 1472.94567161
F2(2, 41) = 1473.01791456
C1= 2

A2= 2490.96042749
V1(1, 42) = 1.15738722222E-3
V1(2, 42) = 1.56031388889E-3
G9(1, 42) = 1.3982863133
G9(2, 42) = 1.39828598802
V(1, 42) = 3.95485164688E-3
V(2, 42) = 3.82675539311E-3
Q(1, 42) = 113.2720568
Q(2, 42) = 113.323541936
F2(1, 42) = 1226.67383845
F2(2, 42) = 1226.64062842
C1= 2

A2= 2704.58925842
V1(1, 43) = 1.12335194444E-3
V1(2, 43) = 1.51391666667E-3
G9(1, 43) = 1.39788845262
G9(2, 43) = 1.39788821182
V(1, 43) = 3.9809862524E-3
V(2, 43) = 3.85333240762E-3
Q(1, 43) = 105.60805642
Q(2, 43) = 105.639864703
F2(1, 43) = 981.203892849
F2(2, 43) = 981.261179811
C1= 2

L7= 11
M1= 02142981727
M2= 3.04908169926E-2
M3= 1.08901462196E-2
M4= 1.09216504233E-2
M5= 2.14918117845E-2
M6= 3.04028642683E-2
P5(1, 36)= 100112.720043
P5(2, 36)= 100098.853833
T5(1, 36)= 22.431
T5(2, 36)= 22.45
C= 2

L7= 10
M1= 021379729615
M2= 3.01189246009E-2
M3= 1.02747261267E-2
M4= 1.02765067982E-2
M5= 2.13834348499E-2
M6= 3.01137057157E-2
P5(1, 37)= 100079.054484
P5(2, 37)= 100087.987524
T5(1, 37)= 22.4095
T5(2, 37)= 22.392
C= 2

L7= 9
M1= 2.13897679752E-2
M2= 3.00621730156E-2
M3= 9.92684844121E-3
M4= 9.92799004118E-3
M5= 2.13922278253E-2
M6= 3.00587162257E-2
P5(1, 38)= 100081.454405
P5(2, 38)= 100072.988017
T5(1, 38)= 22.4405
T5(2, 38)= 22.4475
C= 2

L7= 8
M1= 021256024143
M2= 2.98595838279E-2
M3= 9.45765105991E-3
M4= 9.45617172699E-3
M5= 2.12526993495E-2
M6= 2.98642550909E-2
P5(1, 39)= 100058.655155
P5(2, 39)= 100059.3218
T5(1, 39)= 22.489
T5(2, 39)= 22.494
C= 2

A2= 1440.8923621
V1(1, 36)= 1.43269166667E-3
V1(2, 36)= 1.95700833333E-3
G9(1, 36)= 1.39939098723
G9(2, 36)= 1.3993900961
V(1, 36)= 3.99975623851E-3
V(2, 36)= 3.85103469993E-3
Q(1, 36)= 185.671412738
Q(2, 36)= 184.625819045
F2(1, 36)= 2703.3984521
F2(2, 36)= 2703.37405933
C1= 2

A2= 1680.01566161
V1(1, 37)= 1.35546388889E-3
V1(2, 37)= 1.84958333333E-3
G9(1, 37)= 1.39928075872
G9(2, 37)= 1.39928155952
V(1, 37)= 3.97266459027E-3
V(2, 37)= 3.84862730931E-3
Q(1, 37)= 160.124713248
Q(2, 37)= 160.053685161
F2(1, 37)= 2456.35723168
F2(2, 37)= 2456.33937859
C1= 2

A2= 1751.53678314
V1(1, 38)= 1.30481944444E-3
V1(2, 38)= 1.76941666667E-3
G9(1, 38)= 1.39915115823
G9(2, 38)= 1.39915083247
V(1, 38)= 3.95102208304E-3
V(2, 38)= 3.81263118659E-3
Q(1, 38)= 152.967705481
Q(2, 38)= 152.945337891
F2(1, 38)= 2211.41355737
F2(2, 38)= 2211.41117555
C1= 2

A2= 2014.42906637
V1(1, 39)= 1.24700555556E-3
V1(2, 39)= 1.69603055556E-3
G9(1, 39)= 1.39899690558
G9(2, 39)= 1.39899672177
V(1, 39)= 3.93764707274E-3
V(2, 39)= 3.81182031435E-3
Q(1, 39)= 134.302430612
Q(2, 39)= 134.348475149
F2(1, 39)= 1965.52773857
F2(2, 39)= 1965.59939715
C1= 2

L7= 15
M1= 2.16479012927E-2
M2= 3.09436742726E-2
M3= 1.31307099314E-2
M4= 1.31321628027E-2
M5= 2.16502965641E-2
M6= 3.09402508323E-2
P5(1, 32) = 100076.45457
P5(2, 32) = 100075.987918
T5(1, 32) = 22.3485
T5(2, 32) = 22.3555
C= 2

L7= 14
M1= 2.16449638636E-2
M2= 3.08150201742E-2
M3= 1.25957931979E-2
M4= 1.25998528341E-2
M5= 2.16519400561E-2
M6= 3.08050916638E-2
P5(1, 33) = 100088.920826
P5(2, 33) = 100088.720833
T5(1, 33) = 22.378
T5(2, 33) = 22.381
C= 2

L7= 13
M1= 2.16469193028E-2
M2= 3.06757935254E-2
M3= .012026989736
M4= 1.20284190423E-2
M5= 2.16493918446E-2
M6= 3.06721483992E-2
P5(1, 34) = 100105.52028
P5(2, 34) = 100102.98703
T5(1, 34) = 22.399
T5(2, 34) = 22.4015
C= 2

L7= 12
M1= 2.15625892132E-2
M2= 3.05959473142E-2
M3= 1.13930381705E-2
M4= 1.13976554425E-2
M5= 2.15698133169E-2
M6= 3.05857002021E-2
P5(1, 35) = 100106.453583
P5(2, 35) = 100103.187024
T5(1, 35) = 22.425
T5(2, 35) = 22.4295
C= 2

A2= 1177.87549672
V1(1, 32) = .001679775
V1(2, 32) = 2.31394444444E-3
G9(1, 32) = 1.3997206294
G9(2, 32) = 1.39972031649
V(1, 32) = 3.95809976105E-3
V(2, 32) = 3.81487681868E-3
Q(1, 32) = 218.664849973
Q(2, 32) = 218.619873435
F2(1, 32) = 3686.89584035
F2(2, 32) = 3686.93524108
C1= 2

A2= 1225.68664151
V1(1, 33) = 1.61733333333E-3
V1(2, 33) = 2.22663888889E-3
G9(1, 33) = 1.39965111119
G9(2, 33) = 1.39965098525
V(1, 33) = 3.95545566692E-3
V(2, 33) = 3.82631863909E-3
Q(1, 33) = 210.9290525
Q(2, 33) = 210.796278059
F2(1, 33) = 3441.14351279
F2(2, 33) = 3441.18734394
C1= 2

A2= 1273.49220524
V1(1, 34) = 1.56221388889E-3
V1(2, 34) = 2.13391666667E-3
G9(1, 34) = 1.39957416425
G9(2, 34) = 1.39957405381
V(1, 34) = 3.98407725317E-3
V(2, 34) = 3.84073733365E-3
Q(1, 34) = 205.325852391
Q(2, 34) = 205.283309133
F2(1, 34) = 3195.03649329
F2(2, 34) = 3195.05267226
C1= 2

A2= 1345.22906563
V1(1, 35) = 1.46932222222E-3
V1(2, 35) = 2.01694444444E-3
G9(1, 35) = 1.39948803181
G9(2, 35) = 1.39948784036
V(1, 35) = 3.94425902111E-3
V(2, 35) = 3.81702319012E-3
Q(1, 35) = 193.741630115
Q(2, 35) = 193.621269909
F2(1, 35) = 2949.88680225
F2(2, 35) = 2949.93324786
C1= 2

L7= 19
M1= 2.15502298586E-2
M2= 3.07635884749E-2
M3= .012844078404
M4= 1.28467788478E-2
M5= 2.15547607548E-2
M6= 3.07571218466E-2
P5(1, 28) = 100053.855313
P5(2, 28) = 100066.188241
T5(1, 28) = 22.2055
T5(2, 28) = 22.225
C= 2

L7= 18
M1= 2.17005962135E-2
M2= 3.09022219504E-2
M3= 1.34193668548E-2
M4= 1.34223414692E-2
M5= 2.17054064931E-2
M6= 3.08953735033E-2
P5(1, 29) = 100082.72103
P5(2, 29) = 100075.587932
T5(1, 29) = 22.2765
T5(2, 29) = 22.28
C= 2

L7= 17
M1= 2.16484526223E-2
M2= 3.09997457473E-2
M3= 1.35907287716E-2
M4= 1.35914622803E-2
M5= 2.16496210164E-2
M6= 3.09980727424E-2
P5(1, 30) = 100059.92178
P5(2, 30) = 100055.721918
T5(1, 30) = 22.2955
T5(2, 30) = 22.2985
C= 2

L7= 16
M1= 2.17074127441E-2
M2= 3.10242524661E-2
M3= 1.35082198857E-2
M4= 1.35127986798E-2
M5= 2.17147707659E-2
M6= 3.10137399387E-2
P5(1, 31) = 100083.521004
P5(2, 31) = 100075.054616
T5(1, 31) = 22.325
T5(2, 31) = 22.3275
C= 2

A2= 1106.3062692
V1(1, 28) = 1.65452777778E-3
V1(2, 28) = 2.27393888889E-3
G9(1, 28) = 1.39994365514
G9(2, 28) = 1.39994279627
V(1, 28) = 3.96202131902E-3
V(2, 28) = 3.81529170086E-3
Q(1, 28) = 235.50738316
Q(2, 28) = 235.389245916
F2(1, 28) = 4669.3074373
F2(2, 28) = 4669.50046784
C1= 2

A2= 1130.18803411
V1(1, 29) = 1.73523055556E-3
V1(2, 29) = 2.38693055556E-3
G9(1, 29) = 1.39989329209
G9(2, 29) = 1.39989314313
V(1, 29) = 3.99501680731E-3
V(2, 29) = 3.85992996066E-3
Q(1, 29) = 229.748996147
Q(2, 29) = 229.666704901
F2(1, 29) = 4424.63728158
F2(2, 29) = 4424.69771542
C1= 2

A2= 1130.12336889
V1(1, 30) = 1.73719722222E-3
V1(2, 30) = 2.39621388889E-3
G9(1, 30) = 1.39984088867
G9(2, 30) = 1.39984075255
V(1, 30) = 3.96224269995E-3
V(2, 30) = 3.81689044923E-3
Q(1, 30) = 227.729646924
Q(2, 30) = 227.717159974
F2(1, 30) = 4178.29834292
F2(2, 30) = 4178.34447102
C1= 2

A2= 1154.00088222
V1(1, 31) = 1.72411388889E-3
V1(2, 31) = 2.38127222222E-3
G9(1, 31) = 1.39978344854
G9(2, 31) = 1.39978334322
V(1, 31) = 3.95842088945E-3
V(2, 31) = 3.82665217337E-3
Q(1, 31) = 222.041838965
Q(2, 31) = 221.912531889
F2(1, 31) = 3932.90774768
F2(2, 31) = 3932.94949997
C1= 2

L7= 23
M1= .920752113469
M2= 2.95593024368E-2
M3= 8.70011958897E-3
M4= 8.70161677855E-3
M5= 2.07556846669E-2
M6= 2.95542164991E-2
P5(1, 24)= 99978.3911289
P5(2, 24)= 99978.7911158
T5(1, 24)= 21.7425
T5(2, 24)= 21.74
C= 2

L7= 22
M1= 2.11653942419E-2
M2= 2.98136061213E-2
M3= 9.90182545478E-3
M4= 9.90416089633E-3
M5= 2.11703863053E-2
M6= 2.98065759513E-2
P5(1, 25)= 100013.656636
P5(2, 25)= 100024.856267
T5(1, 25)= 21.807
T5(2, 25)= 21.829
C= 2

L7= 21
M1= 2.13288121677E-2
M2= 3.02639040477E-2
M3= 1.10186940291E-2
M4= 1.10232143878E-2
M5= 2.13375621958E-2
M6= 3.02514935385E-2
P5(1, 26)= 100039.189129
P5(2, 26)= 100044.322293
T5(1, 26)= 21.927
T5(2, 26)= 21.95
C= 2

L7= 20
M1= 2.15447612704E-2
M2= 3.04653608654E-2
M3= 1.21405224578E-2
M4= 1.21260170217E-2
M5= 2.15190196962E-2
M6= 3.05018042701E-2
P5(1, 27)= 100031.122729
P5(2, 27)= 100034.455951
T5(1, 27)= 22.1065
T5(2, 27)= 22.1195
C= 2

R2= 1154.46104323
V1(1, 24)= 1.16439638889E-3
V1(2, 24)= 1.59583055556E-3
G9(1, 24)= 1.40012160888
G9(2, 24)= 1.40012173892
V(1, 24)= 3.95544252194E-3
V(2, 24)= 3.80648293712E-3
Q(1, 24)= 243.650919769
Q(2, 24)= 243.571713981
F2(1, 24)= 5649.51063903
F2(2, 24)= 5649.64119488
C1= 2

R2= 1130.44525713
V1(1, 25)= .00131405
V1(2, 25)= 1.78586944444E-3
G9(1, 25)= 1.40008351037
G9(2, 25)= 1.40008254191
V(1, 25)= 7.95556670916E-3
V(2, 25)= 3.81733964396E-3
Q(1, 25)= 241.831716762
Q(2, 25)= 241.696810496
F2(1, 25)= 5404.49815415
F2(2, 25)= 5404.63294035
C1= 2

R2= 1130.38093167
V1(1, 26)= 1.45979444444E-3
V1(2, 26)= 1.99241666667E-3
G9(1, 26)= 1.40004039822
G9(2, 26)= 1.40003939679
V(1, 26)= 4.00782180602E-3
V(2, 26)= 3.85670758541E-3
Q(1, 26)= 239.532771819
Q(2, 26)= 239.335471192
F2(1, 26)= 5159.33216106
F2(2, 26)= 5159.57407125
C1= 2

R2= 1106.36942378
V1(1, 27)= 1.56541111111E-3
V1(2, 27)= 2.14190833333E-3
G9(1, 27)= 1.39999191569
G9(2, 27)= 1.39999136104
V(1, 27)= 3.93293315666E-3
V(2, 27)= 3.80106406994E-3
Q(1, 27)= 235.827172982
Q(2, 27)= 236.394760082
F2(1, 27)= 4915.08131044
F2(2, 27)= 4915.30646211
C1= 2

2 MAY DATA TAPE, ARRAY STORAGE 47 to 69
 LONG TUBE MODES 1 TO 23
 A SIDE = 1248, B SIDE = 1082 w/ET
 A SIDE BIAS = 116.333 VOLTS, SIGMA = .002 VOLTS
 B SIDE BIAS = 118.513 VOLTS, SIGMA = .003 VOLTS

L7= 3
 M1= 2 09325171977E-2
 M2= 1.97108282253E-2
 M3= 7.92414903113E-3
 M4= 7.92214867006E-3
 M5= 2.09272330225E-2
 M6= 1.97159052555E-2
 P5(1, 67) = 99935.7925303
 P5(2, 67) = 99929.0594184
 T5(1, 67) = 22.745
 T5(2, 67) = 22.7285
 C= 2

L7= 2
 M1= 2.08067914419E-2
 M2= 1.97298747116E-2
 M3= 7.35976568207E-3
 M4= 7.35884596944E-3
 M5= 2.08041913226E-2
 M6= 1.97323405623E-2
 P5(1, 68) = 99922.1929776
 P5(2, 68) = 99921.6596618
 T5(1, 68) = 22.6505
 T5(2, 68) = 22.6385
 C= 2

L7= 1
 M1= 2.09135921231E-2
 M2= 019539342351
 M3= 5.71965228007E-3
 M4= 5.71959394804E-3
 M5= 2.09133789353E-2
 M6= 1.95395416256E-2
 P5(1, 69) = 99940.7257013
 P5(2, 69) = 99938.9257605
 T5(1, 69) = 22.574
 T5(2, 69) = 22.5615
 C= 2

A2= 3298.35294718
 V1(1, 67) = 1.23136388889E-3
 V1(2, 67) = 1.17574388889E-3
 G9(1, 67) = 1.39731598881
 G9(2, 67) = 1.39731652428
 V(1, 67) = 3.06371454356E-3
 V(2, 67) = 3.10585768612E-3
 Q(1, 67) = 99.4060016179
 Q(2, 67) = 98.4520957501
 F2(1, 67) = 735.260284804
 F2(2, 67) = 735.184089101
 C1= 1

A2= 3289.86544006
 V1(1, 68) = 9.10175277778E-4
 V1(2, 68) = 8.71214722222E-4
 G9(1, 68) = 1.39635452414
 G9(2, 68) = 1.39635539688
 V(1, 68) = 2.44027993938E-3
 V(2, 68) = 2.46301089049E-3
 Q(1, 68) = 79.0573399567
 Q(2, 68) = 79.0871987842
 F2(1, 68) = 491.027635377
 F2(2, 68) = 491.088014183
 C1= 1

A2= 3247.38358845
 V1(1, 69) = 5.54873611111E-4
 V1(2, 69) = 5.31316666667E-4
 G9(1, 69) = 1.39415879139
 G9(2, 69) = 1.39415834817
 V(1, 69) = 1.89556558516E-3
 V(2, 69) = 1.94272999665E-3
 Q(1, 69) = 62.5935503854
 Q(2, 69) = 62.5790018719
 F2(1, 69) = 244.231190194
 F2(2, 69) = 244.164968402
 C1= 1

L7= 7
M1= 2.10956729572E-2
M2= .020172984493
M3= 9.16536170493E-3
M4= 9.18526417411E-3
M5= 2.11414819493E-2
M6= 2.01292740243E-2
P5(1, 63) = 99871.9946289
P5(2, 63) = 99857.1284513
T5(1, 63) = 22.907
T5(2, 63) = 22.917
C= 2

A2= 3090.53879651
V1(1, 63) = 1.74226944444E-3
V1(2, 63) = 1.67639444444E-3
G9(1, 63) = 1.39880805598
G9(2, 63) = 1.3988075591
V(1, 63) = 3.82643044545E-3
V(2, 63) = 3.95851318101E-3
Q(1, 63) = 127.426135131
Q(2, 63) = 126.890724969
F2(1, 63) = 1720.19316764
F2(2, 63) = 1720.156126
C1= 1

L7= 6
M1= 2.10084540478E-2
M2= 1.99926212585E-2
M3= 8.75087716307E-3
M4= 8.76552059786E-3
M5= 2.10436089153E-2
M6= 1.99592221418E-2
P5(1, 64) = 99890.3273592
P5(2, 64) = 99890.2606947
T5(1, 64) = 22.97
T5(2, 64) = 22.9745
C= 2

A2= 3305.21561991
V1(1, 64) = 1.66404444444E-3
V1(2, 64) = 1.60081666667E-3
G9(1, 64) = 1.39857741296
G9(2, 64) = 1.39857731419
V(1, 64) = 3.79539469032E-3
V(2, 64) = 3.84312140989E-3
Q(1, 64) = 119.682769732
Q(2, 64) = 119.292007801
F2(1, 64) = 1474.01532273
F2(2, 64) = 1474.12274979
C1= 1

L7= 5
M1= 2.09735500571E-2
M2= .019825859598
M3= 8.52818097802E-3
M4= 8.5264096101E-3
M5= 2.09693707667E-2
M6= 1.98298109815E-2
P5(1, 65) = 99934.3925763
P5(2, 65) = 99938.7257671
T5(1, 65) = 22.9145
T5(2, 65) = 22.9
C= 2

A2= 3303.75460628
V1(1, 65) = 1.56276388889E-3
V1(2, 65) = 1.49401111111E-3
G9(1, 65) = 1.39828664159
G9(2, 65) = 1.39828720734
V(1, 65) = 3.6337506832E-3
V(2, 65) = 3.67425216602E-3
Q(1, 65) = 115.549415323
Q(2, 65) = 115.582883933
F2(1, 65) = 1227.52903
F2(2, 65) = 1227.44899816
C1= 1

L7= 4
M1= 2.09243222831E-2
M2= 1.97727029432E-2
M3= 8.2012611551E-3
M4= 8.20106015741E-3
M5= 2.09238094668E-2
M6= 1.97731875473E-2
P5(1, 66) = 99935.7258658
P5(2, 66) = 99932.4593066
T5(1, 66) = 22.827
T5(2, 66) = 22.8195
C= 2

A2= 3301.90034744
V1(1, 66) = 1.38849166667E-3
V1(2, 66) = 1.32770833333E-3
G9(1, 66) = 1.39789449398
G9(2, 66) = 1.39789493993
V(1, 66) = 3.3476444188E-3
V(2, 66) = 3.38745426334E-3
Q(1, 66) = 107.096215965
Q(2, 66) = 107.110572762
F2(1, 66) = 981.752270152
F2(2, 66) = 981.803971708
C1= 1

L7= 11
M1= .02151640578
M2= 2.06109238964E-2
M3= .010875330287
M4= 1.08754087834E-2
M5= 2.15165610818E-2
M6= 2.06107751313E-2
P5(1, 59)= 99854.12855
P5(2, 59)= 99851.1953132
T5(1, 59)= 22.645
T5(2, 59)= 22.6565
C= 2

L7= 10
M1= 2.14419891302E-2
M2= 2.04225234024E-2
M3= 1.02680885162E-2
M4= 1.02673034967E-2
M5= 2.14402498474E-2
M6= 2.04240848715E-2
P5(1, 60)= 99841.8622868
P5(2, 60)= 99832.3959316
T5(1, 60)= 22.706
T5(2, 60)= 22.7215
C= 2

L7= 9
M1= 2.14376144163E-2
M2= 2.03992076501E-2
M3= 9.92074149494E-3
M4= 9.92064193104E-3
M5= 2.14373992698E-2
M6= 2.03994123773E-2
P5(1, 61)= 99846.6621289
P5(2, 61)= 99853.7285632
T5(1, 61)= 22.782
T5(2, 61)= 22.7915
C= 2

L7= 8
M1= 2.12948996459E-2
M2= 2.02420957708E-2
M3= 9.44093457698E-3
M4= 9.43812293439E-3
M5= 2.12885573166E-2
M6= 2.02481258606E-2
P5(1, 62)= 99861.4616421
P5(2, 62)= 99855.9951553
T5(1, 62)= 22.8595
T5(2, 62)= 22.8695
C= 2

R2= 1967.46469036
V1(1, 59)= 2.02602777778E-3
V1(2, 59)= 1.95821111111E-3
G9(1, 59)= 1.39939490927
G9(2, 59)= 1.39939438673
V(1, 59)= 3.83969974569E-3
V(2, 59)= 3.87424232253E-3
Q(1, 59)= 192.28372262
Q(2, 59)= 192.287879218
F2(1, 59)= 2704.16353928
F2(2, 59)= 2704.18058459
C1= 1

R2= 2302.24542615
V1(1, 60)= 1.91124722222E-3
V1(2, 60)= 1.84527222222E-3
G9(1, 60)= 1.39928107023
G9(2, 60)= 1.39928039847
V(1, 60)= 3.80163020758E-3
V(2, 60)= 3.85330943939E-3
Q(1, 60)= 164.784920786
Q(2, 60)= 164.831979241
F2(1, 60)= 2457.43052845
F2(2, 60)= 2457.52225536
C1= 1

R2= 2421.52534513
V1(1, 61)= 1.86343055556E-3
V1(2, 61)= 1.78963888889E-3
G9(1, 61)= 1.39914953117
G9(2, 61)= 1.39914909135
V(1, 61)= 3.83165798228E-3
V(2, 61)= 3.86720977096E-3
Q(1, 61)= 158.135118042
Q(2, 61)= 158.127231427
F2(1, 61)= 2212.58136017
F2(2, 61)= 2212.58248896
C1= 1

R2= 2780.01000145
V1(1, 62)= .001770625
V1(2, 62)= 1.70641388889E-3
G9(1, 62)= 1.39899407955
G9(2, 62)= 1.39899368471
V(1, 62)= 3.79748823716E-3
V(2, 62)= 3.8489741006E-3
Q(1, 62)= 139.451673862
Q(2, 62)= 139.549159459
F2(1, 62)= 1966.72763274
F2(2, 62)= 1966.83213238
C1= 1

L7= 15
M1= 2.17027163555E-2
M2= 2.11592046764E-2
M3= 1.31234868507E-2
M4= 1.31224426399E-2
M5= 2.17009895118E-2
M6= .021160888408
P5(1, 55) = 99831.8626158
P5(2, 55) = 99828.8627145
T5(1, 55) = 22.3965
T5(2, 55) = 22.407
C= 2

L7= 14
M1= 2.17042159824E-2
M2= 2.09655136694E-2
M3= 1.25766052484E-2
M4= 1.25787522921E-2
M5= 2.17079212668E-2
M6= 2.09619351051E-2
P5(1, 56) = 99831.3959645
P5(2, 56) = 99821.0629711
T5(1, 56) = 22.4665
T5(2, 56) = 22.4825
C= 2

L7= 13
M1= 2.16954711763E-2
M2= 2.09023110123E-2
M3= 1.20215941537E-2
M4= 1.20219212065E-2
M5= 2.16960615558E-2
M6= 2.09017422319E-2
P5(1, 57) = 99829.8626816
P5(2, 57) = 99830.6626553
T5(1, 57) = 22.533
T5(2, 57) = 22.55
C= 2

L7= 12
M1= 2.16181869459E-2
M2= 2.07744671271E-2
M3= 1.13771655727E-2
M4= 1.13773808876E-2
M5= 2.16185960738E-2
M6= 2.07740739741E-2
P5(1, 58) = 99834.8625171
P5(2, 58) = 99839.7956882
T5(1, 58) = 22.5905
T5(2, 58) = 22.6
C= 2

R2= 1584.86501378
V1(1, 55) = .002364425
V1(2, 55) = 2.32522777778E-3
G9(1, 55) = 1.39973179225
G9(2, 55) = 1.3997313369
V(1, 55) = 3.81250304459E-3
V(2, 55) = 3.84530113812E-3
Q(1, 55) = 228.864767296
Q(2, 55) = 228.913404907
F2(1, 55) = 3686.89442119
F2(2, 55) = 3686.97913381
C1= 1

R2= 1680.53145067
V1(1, 56) = 2.29839444444E-3
V1(2, 56) = 2.24910833333E-3
G9(1, 56) = 1.39966054575
G9(2, 56) = 1.39965984616
V(1, 56) = 3.83082670075E-3
V(2, 56) = 3.88142364894E-3
Q(1, 56) = 218.929041069
Q(2, 56) = 218.883827991
F2(1, 56) = 3441.48338037
F2(2, 56) = 3441.58956932
C1= 1

R2= 1728.31106103
V1(1, 57) = 2.19436111111E-3
V1(2, 57) = 2.13262222222E-3
G9(1, 57) = 1.3995815898
G9(2, 57) = 1.39958082715
V(1, 57) = 3.81529851381E-3
V(2, 57) = 3.84876110112E-3
Q(1, 57) = 212.725299059
Q(2, 57) = 212.715443314
F2(1, 57) = 3195.52859466
F2(2, 57) = 3195.57831732
C1= 1

R2= 1847.89504013
V1(1, 58) = 2.09772222222E-3
V1(2, 58) = 2.04271944444E-3
G9(1, 58) = 1.39949411184
G9(2, 58) = 1.39949370823
V(1, 58) = 3.83032455167E-3
V(2, 58) = 3.88144925427E-3
Q(1, 58) = 201.691102906
Q(2, 58) = 201.679656053
F2(1, 58) = 2950.56475895
F2(2, 58) = 2950.65391957
C1= 1

L7= 19
M1= 2.16167662545E-2
M2= .021689203042
M3= 1.28397291515E-2
M4= 1.28399818086E-2
M5= 2.16171916239E-2
M6= 2.16827762557E-2
P5(1, 51) = 99921.7263263
P5(2, 51) = 99923.1929447
T5(1, 51) = 21.974
T5(2, 51) = 21.996
C= 2

L7= 18
M1= .021783484702
M2= 2.15417958661E-2
M3= 1.33977086358E-2
M4= 1.33978621668E-2
M5= 2.17837343299E-2
M6= 2.15415490107E-2
P5(1, 52) = 99901.3269974
P5(2, 52) = 99883.3275895
T5(1, 52) = 22.102
T5(2, 52) = 22.1285
C= 2

L7= 17
M1= 2.17249753269E-2
M2= 2.14187262742E-2
M3= 1.35737071595E-2
M4= 1.35587376206E-2
M5= 2.17010162964E-2
M6= 2.14423736422E-2
P5(1, 53) = 99856.4618065
P5(2, 53) = 99850.9953197
T5(1, 53) = 22.2145
T5(2, 53) = 22.2345
C= 2

L7= 16
M1= 2.17805312768E-2
M2= 2.13066562393E-2
M3= 1.34874336623E-2
M4= 1.34887377219E-2
M5= 2.17826371711E-2
M6= 2.13045963616E-2
P5(1, 54) = 99837.5290961
P5(2, 54) = 99824.3961947
T5(1, 54) = 22.319
T5(2, 54) = 22.3355
C= 2

A2= 1441.54984577
V1(1, 51) = 2.28237222222E-3
V1(2, 51) = 2.30902777778E-3
G9(1, 51) = 1.39996683598
G9(2, 51) = 1.39996589829
V(1, 51) = 3.85536640809E-3
V(2, 51) = 3.88744288593E-3
Q(1, 51) = 248.975122902
Q(2, 51) = 248.973889202
F2(1, 51) = 4667.04199083
F2(2, 51) = 4667.26791731
C1= 1

A2= 1465.41275233
V1(1, 52) = 2.37598611111E-3
V1(2, 52) = 2.37994722222E-3
G9(1, 52) = 1.39991408914
G9(2, 52) = 1.39991293862
V(1, 52) = 3.82023692653E-3
V(2, 52) = 3.86958287542E-3
Q(1, 52) = 242.536284956
Q(2, 52) = 242.584852661
F2(1, 52) = 4422.90669749
F2(2, 52) = 4423.09307435
C1= 1

A2= 1489.27242753
V1(1, 53) = .0024086
V1(2, 53) = 2.39915277778E-3
G9(1, 53) = 1.39985761951
G9(2, 53) = 1.39985675101
V(1, 53) = 3.80486336912E-3
V(2, 53) = 3.83968944878E-3
Q(1, 53) = 239.549873029
Q(2, 53) = 240.10112639
F2(1, 53) = 4177.27617474
F2(2, 53) = 4177.42786174
C1= 1

A2= 1537.0716074
V1(1, 54) = 2.40994166667E-3
V1(2, 54) = 2.38818055556E-3
G9(1, 54) = 1.39979695202
G9(2, 54) = 1.39979623743
V(1, 54) = 3.80671636643E-3
V(2, 54) = 3.85661517137E-3
Q(1, 54) = 233.173314243
Q(2, 54) = 233.167256147
F2(1, 54) = 3932.51063401
F2(2, 54) = 3932.64953807
C1= 1

L7= 23
M1= 2.06798723452E-2
M2= .02210452049
M3= 8.69593333767E-3
M4= 8.70728964056E-3
M5= 2.06568135681E-2
M6= 2.20756911252E-2
P5(1, 47) = 99923.0596158
P5(2, 47) = 99924.7928921
T5(1, 47) = 22.336
T5(2, 47) = 22.3335
C= 2

L7= 22
M1= .021005977938
M2= 2.19814794736E-2
M3= 9.89678567632E-3
M4= 9.89847522116E-3
M5= 2.10095640055E-2
M6= 2.19777275124E-2
P5(1, 48) = 99920.7263592
P5(2, 48) = 99918.5930961
T5(1, 48) = 22.1235
T5(2, 48) = 22.064
C= 2

L7= 21
M1= 2.11908814756E-2
M2= 2.19398126084E-2
M3= 1.10176263276E-2
M4= 1.10194203793E-2
M5= 2.11943320861E-2
M6= 2.19362406275E-2
P5(1, 49) = 99923.2596092
P5(2, 49) = 99916.193175
T5(1, 49) = 21.854
T5(2, 49) = 21.817
C= 2

L7= 20
M1= 2.16391899904E-2
M2= 2.17318475788E-2
M3= .012140842154
M4= 1.21267617972E-2
M5= 2.16140939129E-2
M6= 2.17570803798E-2
P5(1, 50) = 99909.9933789
P5(2, 50) = 99917.5264645
T5(1, 50) = 21.829
T5(2, 50) = 21.8555
C= 2

R2= 1417.92928402
V1(1, 47) = 1.51120555556E-3
V1(2, 47) = 1.63200555556E-3
G9(1, 47) = 1.40010888515
G9(2, 47) = 1.40010895631
V(1, 47) = 3.83638026831E-3
V(2, 47) = 3.87170243498E-3
Q(1, 47) = 259.269766168
Q(2, 47) = 258.575489973
F2(1, 47) = 5656.10449798
F2(2, 47) = 5655.79993809
C1= 1

R2= 1417.847366
V1(1, 48) = 1.73968888889E-3
V1(2, 48) = 1.84296944444E-3
G9(1, 48) = 1.40008279221
G9(2, 48) = 1.40008538494
V(1, 48) = 3.86331578826E-3
V(2, 48) = 3.91171202009E-3
Q(1, 48) = 257.584117458
Q(2, 48) = 257.477934435
F2(1, 48) = 5407.46763503
F2(2, 48) = 5406.97879158
C1= 1

R2= 1417.76554265
V1(1, 49) = 1.93764166667E-3
V1(2, 49) = 2.02299444444E-3
G9(1, 49) = 1.40005655568
G9(2, 49) = 1.40005814183
V(1, 49) = 3.85787034215E-3
V(2, 49) = 3.89095021227E-3
Q(1, 49) = 255.471955729
Q(2, 49) = 255.391129914
F2(1, 49) = 5158.75667345
F2(2, 49) = 5158.44522485
C1= 1

R2= 1417.68461448
V1(1, 50) = 2.13235277778E-3
V1(2, 50) = 2.17211666667E-3
G9(1, 50) = 1.40001695811
G9(2, 50) = 1.40001582735
V(1, 50) = 3.8212958348E-3
V(2, 50) = 3.87146498038E-3
Q(1, 50) = 249.90262013
Q(2, 50) = 250.476587827
F2(1, 50) = 4912.39551083
F2(2, 50) = 4912.63068043
C1= 1

2 MAY DATA TAPE, ARRAY STORAGE 70 to 92

LONG TUBE MODES 1 TO 23

A SIDE = 1082 w/ET, B SIDE = 815

A SIDE BIAS = 116.355 VOLTS, SIGMA = .004 VOLTS

B SIDE BIAS = 118.530 VOLTS, SIGMA = .002 VOLTS

L7= 3
M1= 1.93556544947E-2
M2= 2.97471600458E-2
M3= 7.96027427819E-3
M4= 7.95798672267E-3
M5= 1.93500922324E-2
M6= 2.97557109874E-2
P5(1, 90) = 100122.319728
P5(2, 90) = 100117.719879
T5(1, 90) = 22.924
T5(2, 90) = 22.946
C= 2

L7= 2
M1= 1.93428186644E-2
M2= 2.95718797566E-2
M3= 7.36683610694E-3
M4= 7.36027359172E-3
M5= 1.93255877202E-2
M6= 2.95982464275E-2
P5(1, 91) = 100113.986668
P5(2, 91) = 100108.586846
T5(1, 91) = 23.0475
T5(2, 91) = 23.065
C= 2

L7= 1
M1= 1.93485020825E-2
M2= 2.94815927542E-2
M3= 5.75217503748E-3
M4= 5.75164188301E-3
M5= 0.19346708719
M6= 2.94843255814E-2
P5(1, 92) = 100091.987392
P5(2, 92) = 100082.454372
T5(1, 92) = 23.1545
T5(2, 92) = 23.1665
C= 2

A2= 3083.55756811
V1(1, 90) = .0010720775
V1(2, 90) = 1.58916666667E-3
G9(1, 90) = 1.39723271782
G9(2, 90) = 1.39723154199
V(1, 90) = 4.00745340315E-3
V(2, 90) = 3.86410817764E-3
Q(1, 90) = 98.0261805388
Q(2, 90) = 98.0847719863
F2(1, 90) = 735.446701476
F2(2, 90) = 735.428994565
C1= 3

A2= 3289.9169161
V1(1, 91) = 3.50616388889E-4
V1(2, 91) = 1.25169722222E-3
G9(1, 91) = 1.39626185748
G9(2, 91) = 1.39626130193
V(1, 91) = 3.41758023771E-3
V(2, 91) = 3.28653332864E-3
Q(1, 91) = 78.8841818133
Q(2, 91) = 79.0394545003
F2(1, 91) = 491.323505933
F2(2, 91) = 491.387215374
C1= 3

A2= 3247.42718462
V1(1, 92) = 5.18435277778E-4
V1(2, 92) = 7.68546388889E-4
G9(1, 92) = 1.39405957027
G9(2, 92) = 1.39405835222
V(1, 92) = 2.65737993425E-3
V(2, 92) = 2.58514758487E-3
Q(1, 92) = 62.4738822122
Q(2, 92) = 62.481341567
F2(1, 92) = 244.457994698
F2(2, 92) = 244.41836835
C1= 3

L7= 7
M1= 1.96978973024E-2
M2= 3.02514702548E-2
M3= 9.21538579981E-3
M4= 9.21872129507E-3
M5= 1.97050269274E-2
M6= 3.02405247416E-2
P5(1, 86) = 100110.453451
P5(2, 86) = 100108.653511
T5(1, 86) = 22.946
T5(2, 86) = 22.957
C= 2

L7= 6
M1= 1.96552420912E-2
M2= 2.98502466619E-2
M3= 8.77073443167E-3
M4= 8.76899329938E-3
M5= 1.96513402086E-2
M6= .029856173594
P5(1, 87) = 100105.986932
P5(2, 87) = 100106.386918
T5(1, 87) = 23.009
T5(2, 87) = 22.997
C= 2

L7= 5
M1= .019421695586
M2= 3.00032158099E-2
M3= 8.58559374512E-3
M4= 8.60080628524E-3
M5= 1.94561082697E-2
M6= 2.99501480965E-2
P5(1, 88) = 100118.519853
P5(2, 88) = 100117.786543
T5(1, 88) = 22.942
T5(2, 88) = 22.9235
C= 2

L7= 4
M1= 1.94442159163E-2
M2= 2.96903060248E-2
M3= 8.21252180702E-3
M4= 8.20980148087E-3
M5= 1.94377751896E-2
M6= 2.97001439383E-2
P5(1, 89) = 100104.786971
P5(2, 89) = 100102.320386
T5(1, 89) = 22.871
T5(2, 89) = 22.8675
C= 2

A2= 2277.2397313
V1(1, 86) = 1.20260033333E-3
V1(2, 86) = .001772925
G9(1, 86) = 1.39873064618
G9(2, 86) = 1.39873006764
V(1, 86) = 3.94639007509E-3
V(2, 86) = 3.78962914126E-3
Q(1, 86) = 125.261842168
Q(2, 86) = 126.171562957
F2(1, 86) = 1720.59732656
F2(2, 86) = 1720.58029481
C1= 3

A2= 2444.23454976
V1(1, 87) = .00115996
V1(2, 87) = 1.69825555556E-3
G9(1, 87) = 1.39849976534
G9(2, 87) = 1.39850045383
V(1, 87) = 3.94858234415E-3
V(2, 87) = 3.80579577883E-3
Q(1, 87) = 119.499711957
Q(2, 87) = 119.552205302
F2(1, 87) = 1474.34880869
F2(2, 87) = 1474.41750862
C1= 3

A2= 2562.68177879
V1(1, 88) = 1.13337027778E-3
V1(2, 88) = .001679175
G9(1, 88) = 1.39820981482
G9(2, 88) = 1.39821066773
V(1, 88) = 3.95367037799E-3
V(2, 88) = 3.79850557268E-3
Q(1, 88) = 115.142705742
Q(2, 88) = 114.730068237
F2(1, 88) = 1227.71971513
F2(2, 88) = 1227.65065055
C1= 3

A2= 2800.16569539
V1(1, 89) = 1.10007472222E-3
V1(2, 89) = .0016188
G9(1, 89) = 1.39781728946
G9(2, 89) = 1.39781752694
V(1, 89) = 3.97836113687E-3
V(2, 89) = 3.83272001767E-3
Q(1, 89) = 106.848828971
Q(2, 89) = 106.925637415
F2(1, 89) = 981.878826346
F2(2, 89) = 981.909786003
C1= 3

L7= 11
M1= 2.01687600206E-2
M2= 3.10667020687E-2
M3= 1.09437869724E-2
M4= 1.09453907941E-2
M5= 2.01717157703E-2
M6= .031062149883
P5(1, 82)= 100155.451971
P5(2, 82)= 100152.052083
T5(1, 82)= 22.7365
T5(2, 82)= 22.741
C= 2

L7= 10
M1= 2.00759321761E-2
M2= .030679271764
M3= 1.02987880022E-2
M4= 1.02979722565E-2
M5= 2.00743420031E-2
M6= 3.06817019982E-2
P5(1, 83)= 100132.852714
P5(2, 83)= 100123.25303
T5(1, 83)= 22.748
T5(2, 83)= 22.732
C= 2

L7= 9
M1= 1.99335032367E-2
M2= 3.07978380696E-2
M3= 9.95826071926E-3
M4= 9.95918002327E-3
M5= 1.99353434123E-2
M6= 3.07949952073E-2
P5(1, 84)= 100129.986142
P5(2, 84)= 100126.252932
T5(1, 84)= 22.784
T5(2, 84)= 22.802
C= 2

L7= 8
M1= 1.99120659801E-2
M2= 3.03655674108E-2
M3= 9.44583570269E-3
M4= 9.45061696627E-3
M5= 1.99221449073E-2
M6= .030350204839
P5(1, 85)= 100120.986438
P5(2, 85)= 100117.719879
T5(1, 85)= 22.873
T5(2, 85)= 22.8805
C= 2

R2= 1464.8280754
V1(1, 82)= 1.39846944444E-3
V1(2, 82)= 2.06561666667E-3
G9(1, 82)= 1.39931603914
G9(2, 82)= 1.39931581967
V(1, 82)= 3.9693268518E-3
V(2, 82)= 3.80681083701E-3
Q(1, 82)= 187.556769771
Q(2, 82)= 187.509729907
F2(1, 82)= 2705.1861243
F2(2, 82)= 2705.20814995
C1= 3

R2= 1703.94953522
V1(1, 83)= 1.31928333333E-3
V1(2, 83)= 1.94187777778E-3
G9(1, 83)= 1.39920438482
G9(2, 83)= 1.39920520641
V(1, 83)= 3.93035161764E-3
V(2, 83)= 3.78539751984E-3
Q(1, 83)= 162.429681804
Q(2, 83)= 162.472079502
F2(1, 83)= 2458.18108388
F2(2, 83)= 2458.19897652
C1= 3

R2= 1799.3949478
V1(1, 84)= 1.28356388889E-3
V1(2, 84)= 1.90342222222E-3
G9(1, 84)= 1.39907448705
G9(2, 84)= 1.399073579
V(1, 84)= 3.96930196157E-3
V(2, 84)= 3.8100903458E-3
Q(1, 84)= 155.891537983
Q(2, 84)= 155.869763412
F2(1, 84)= 2213.10233765
F2(2, 84)= 2213.11783407
C1= 3

R2= 2062.27984196
V1(1, 85)= 1.22559722222E-3
V1(2, 85)= 1.79825833333E-3
G9(1, 85)= 1.39891808545
G9(2, 85)= 1.39891775901
V(1, 85)= 3.93793920573E-3
V(2, 85)= 3.79077506001E-3
Q(1, 85)= 137.097542682
Q(2, 85)= 136.969253484
F2(1, 85)= 1967.10953046
F2(2, 85)= 1967.19421295
C1= 3

L7= 15
M1= 2.06420535022E-2
M2= 3.13197261019E-2
M3= 1.31093950698E-2
M4= 1.31126939855E-2
M5= 2.06472479749E-2
M6= 3.13118466274E-2
P5(1, 78)= 100122.453057
P5(2, 78)= 100124.58632
T5(1, 78)= 22.817
T5(2, 78)= 22.824
C= 2

L7= 14
M1= 2.05748373205E-2
M2= 3.12362557395E-2
M3= 1.26046258608E-2
M4= 1.26067939628E-2
M5= 2.05783763662E-2
M6= .031230883764
P5(1, 79)= 100138.919182
P5(2, 79)= 100145.252307
T5(1, 79)= 22.844
T5(2, 79)= 22.8435
C= 2

L7= 13
M1= 2.04170092971E-2
M2= .03128980985
M3= 1.20384964394E-2
M4= 1.20362340659E-2
M5= 2.04131723645E-2
M6= 3.12956911941E-2
P5(1, 80)= 100142.119076
P5(2, 80)= 100145.385636
T5(1, 80)= 22.7885
T5(2, 80)= 22.7745
C= 2

L7= 12
M1= 2.03811194559E-2
M2= 3.10306964452E-2
M3= 1.13965909515E-2
M4= 1.13998398782E-2
M5= 2.0386296815E-2
M6= .031021852772
P5(1, 81)= 100162.318412
P5(2, 81)= 100162.985057
T5(1, 81)= 22.7155
T5(2, 81)= 22.7285
C= 2

A2= 1201.81707488
V1(1, 78)= 1.65664166667E-3
V1(2, 78)= 2.40793055556E-3
G9(1, 78)= 1.39963791204
G9(2, 78)= 1.39963756398
V(1, 78)= 3.9568957612E-3
V(2, 78)= 3.79152745744E-3
Q(1, 78)= 220.907885602
Q(2, 78)= 220.794256901
F2(1, 78)= 3690.55020761
F2(2, 78)= 3690.58630459
C1= 3

A2= 1273.56603318
V1(1, 79)= 1.59978888889E-3
V1(2, 79)= 2.33685833333E-3
G9(1, 79)= 1.39956842594
G9(2, 79)= 1.39956846152
V(1, 79)= 3.96384798627E-3
V(2, 79)= 3.81451068682E-3
Q(1, 79)= 210.030062814
Q(2, 79)= 209.94663801
F2(1, 79)= 3444.55745679
F2(2, 79)= 3444.59180294
C1= 3

A2= 1297.43085625
V1(1, 80)= 1.52758333333E-3
V1(2, 80)= 2.24641388889E-3
G9(1, 80)= 1.39949522876
G9(2, 80)= 1.39949591756
V(1, 80)= 3.97115840122E-3
V(2, 80)= 3.80986558293E-3
Q(1, 80)= 207.71685601
Q(2, 80)= 207.783165024
F2(1, 80)= 3197.87384292
F2(2, 80)= 3197.79836135
C1= 3

A2= 1369.16620388
V1(1, 81)= 1.44987222222E-3
V1(2, 81)= 2.12444722222E-3
G9(1, 81)= 1.39941391436
G9(2, 81)= 1.39941324551
V(1, 81)= 3.94659445156E-3
V(2, 81)= 3.79926004172E-3
Q(1, 81)= 197.662201775
Q(2, 81)= 197.546758048
F2(1, 81)= 2952.08816782
F2(2, 81)= 2952.06466314
C1= 3

L7= 19
M1= 2.11845011012E-2
M2= 3.06734514896E-2
M3= 1.27979055436E-2
M4= 1.27999662966E-2
M5= 2.11879122862E-2
M6= 3.06685131636E-2
P5(1, 74)= 100064.588293
P5(2, 74)= 100062.655024
T5(1, 74)= 22.6575
T5(2, 74)= 22.67
C= 2

L7= 18
M1= 2.10334323641E-2
M2= 3.11024618911E-2
M3= 1.34006577781E-2
M4= 1.34053818095E-2
M5= 2.10408471192E-2
M6= 3.10915014419E-2
P5(1, 75)= 100081.52107
P5(2, 75)= 100083.854326
T5(1, 75)= 22.7055
T5(2, 75)= 22.71
C= 2

L7= 17
M1= 2.09280506931E-2
M2= 3.11757582403E-2
M3= 1.35339078636E-2
M4= .013537772846
M5= 2.09340272779E-2
M6= 3.11668576805E-2
P5(1, 76)= 100093.320682
P5(2, 76)= 100093.254017
T5(1, 76)= 22.748
T5(2, 76)= 22.752
C= 2

L7= 16
M1= 2.08362835205E-2
M2= 3.13137152476E-2
M3= 1.35031398263E-2
M4= .013506032505
M5= 2.08419831239E-2
M6= 3.13051519663E-2
P5(1, 77)= 100098.187188
P5(2, 77)= 100096.787234
T5(1, 77)= 22.786
T5(2, 77)= 22.7875
C= 2

A2= 1130.2535181
V1(1, 74)= 1.67170555556E-3
V1(2, 74)= 2.31657777778E-3
G9(1, 74)= 1.39986234515
G9(2, 74)= 1.39986172985
V(1, 74)= 4.00602455314E-3
V(2, 74)= 3.83465437506E-3
Q(1, 74)= 236.681903767
Q(2, 74)= 236.615388286
F2(1, 74)= 4674.07117852
F2(2, 74)= 4674.17020793
C1= 3

A2= 1130.18912527
V1(1, 75)= 1.70146388889E-3
V1(2, 75)= 2.41638888889E-3
G9(1, 75)= 1.39981276825
G9(2, 75)= 1.39981255398
V(1, 75)= 3.94764703575E-3
V(2, 75)= 3.79272070831E-3
Q(1, 75)= 231.69435563
Q(2, 75)= 231.529467069
F2(1, 75)= 4428.78308986
F2(2, 75)= 4428.85467371
C1= 3

A2= 1154.06773998
V1(1, 76)= 1.73043333333E-3
V1(2, 76)= 2.46839444444E-3
G9(1, 76)= 1.39975912411
G9(2, 76)= 1.39975893597
V(1, 76)= 3.98496649815E-3
V(2, 76)= 3.8169821004E-3
Q(1, 76)= 229.623855866
Q(2, 76)= 229.496841829
F2(1, 76)= 4182.30022933
F2(2, 76)= 4182.37124893
C1= 3

A2= 1177.94386655
V1(1, 77)= 1.71229444444E-3
V1(2, 77)= 2.47325555556E-3
G9(1, 77)= 1.39970117327
G9(2, 77)= 1.39970111074
V(1, 77)= 3.96971685502E-3
V(2, 77)= 3.81640555113E-3
Q(1, 77)= 224.099601883
Q(2, 77)= 223.983523533
F2(1, 77)= 3936.75521671
F2(2, 77)= 3936.81374988
C1= 3

L7= 23
M1= 2.15013181279E-2
M2= 2.75934801927E-2
M3= 8.64186673148E-3
M4= 8.65948502126E-3
M5= 2.15451531539E-2
M6= .027537339449
P5(1, 70)= 99989.9240829
P5(2, 70)= 99994.5905961
T5(1, 70)= 22.507
T5(2, 70)= 22.4905
C= 2

L7= 22
M1= 2.13002637374E-2
M2= .02935519822
M3= 9.90701274673E-3
M4= 9.90067079672E-3
M5= 2.13038285761E-2
M6= 2.93502861194E-2
P5(1, 71)= 100023.8563
P5(2, 71)= 100027.056195
T5(1, 71)= 22.504
T5(2, 71)= 22.513
C= 2

L7= 21
M1= .02133360298
M2= 2.98074495818E-2
M3= 1.09294378389E-2
M4= 1.09320539565E-2
M5= 2.13387094837E-2
M6= .029800316449
P5(1, 72)= 100038.255826
P5(2, 72)= 100041.58905
T5(1, 72)= 22.559
T5(2, 72)= 22.569
C= 2

L7= 20
M1= 2.12031908882E-2
M2= 3.04251473911E-2
M3= 1.21363883533E-2
M4= 1.21363392073E-2
M5= 2.12031050263E-2
M6= 3.04252705974E-2
P5(1, 73)= 100058.855149
P5(2, 73)= 100065.521596
T5(1, 73)= 22.615
T5(2, 73)= 22.6225
C= 2

A2= 1178.41480438
V1(1, 70)= 1.23874166667E-3
V1(2, 70)= 1.56026944444E-3
G9(1, 70)= 1.40002718932
G9(2, 70)= 1.40002801448
V(1, 70)= 3.94725478007E-3
V(2, 70)= 3.88201423749E-3
Q(1, 70)= 245.596253114
Q(2, 70)= 244.585024644
F2(1, 70)= 5658.03117857
F2(2, 70)= 5658.00057826
C1= 3

A2= 1130.44721955
V1(1, 71)= 1.33547777778E-3
V1(2, 71)= 1.76586944444E-3
G9(1, 71)= 1.39999207575
G9(2, 71)= 1.39999163522
V(1, 71)= 3.9564554812E-3
V(2, 71)= 3.79665251817E-3
Q(1, 71)= 242.959542151
Q(2, 71)= 242.874196919
F2(1, 71)= 5412.02774954
F2(2, 71)= 5412.10912263
C1= 3

A2= 1130.38266996
V1(1, 72)= 1.46591666667E-3
V1(2, 72)= 1.95978333333E-3
G9(1, 72)= 1.39995156524
G9(2, 72)= 1.39995107904
V(1, 72)= 3.99698330312E-3
V(2, 72)= 3.82537877761E-3
Q(1, 72)= 241.349811853
Q(2, 72)= 241.231677264
F2(1, 72)= 5166.08247219
F2(2, 72)= 5166.19637857
C1= 3

A2= 1130.31824814
V1(1, 73)= 1.59436111111E-3
V1(2, 73)= 2.19714722222E-3
G9(1, 73)= 1.39990829951
G9(2, 73)= 1.39990793394
V(1, 73)= 3.99697725745E-3
V(2, 73)= 3.83858283091E-3
Q(1, 73)= 237.817756215
Q(2, 73)= 237.80778112
F2(1, 73)= 4920.6901336
F2(2, 73)= 4920.77042889
C1= 3

22 NOV DATA TAPE, ARRAY STORAGE 1 to 23
 LONG TUBE MODES 1 TO 23
 A SIDE = 1082, B SIDE = 815 w/ET
 A SIDE BIAS = 116.386 VOLTS, SIGMA = .001 VOLTS
 B SIDE BIAS = 118.565 VOLTS, SIGMA = .001 VOLTS

L7= 3
 M1= .018490192035
 M2= 2.87264513922E-2
 M3= 7.91407066141E-3
 M4= 7.91130949367E-3
 M5= 1.84837409273E-2
 M6= 2.87364773621E-2
 P5(1, 21) = 100131.519425
 P5(2, 21) = 100135.052642
 T5(1, 21) = 23.4955
 T5(2, 21) = 23.4765
 C= 2

A2= 3298.36366573
 V1(1, 21) = 1.07023444444E-3
 V1(2, 21) = 1.61364166667E-3
 G9(1, 21) = 1.39724027461
 G9(2, 21) = 1.39724101283
 U(1, 21) = 3.88608709735E-3
 U(2, 21) = 3.77006291312E-3
 Q(1, 21) = 96.3162854603
 Q(2, 21) = 96.3702494275
 F2(1, 21) = 736.004305686
 F2(2, 21) = 735.929256629
 C1= 3

L7= 2
 M1= .018344283291
 M2= 2.87352517611E-2
 M3= 7.3295620755E-3
 M4= 7.32851640203E-3
 M5= 1.83416652001E-2
 M6= 2.87393518666E-2
 P5(1, 22) = 100144.585662
 P5(2, 22) = 100152.252076
 T5(1, 22) = 23.401
 T5(2, 22) = 23.38
 C= 2

A2= 3289.94440357
 V1(1, 22) = 7.96608888889E-4
 V1(2, 22) = 1.20658611111E-3
 G9(1, 22) = 1.39627978494
 G9(2, 22) = 1.39628106952
 U(1, 22) = 3.12351855705E-3
 U(2, 22) = 3.01981990318E-3
 Q(1, 22) = 78.2673271481
 Q(2, 22) = 78.290518953
 F2(1, 22) = 491.503538049
 F2(2, 22) = 491.546984541
 C1= 3

L7= 1
 M1= 1.83776412599E-2
 M2= 2.85518091965E-2
 M3= 5.70875087783E-3
 M4= 5.70678761848E-3
 M5= 1.83713211248E-2
 M6= 2.85616316413E-2
 P5(1, 23) = 100150.785458
 P5(2, 23) = 100151.11878
 T5(1, 23) = 23.303
 T5(2, 23) = 23.288
 C= 2

A2= 3247.42476153
 V1(1, 23) = 4.85953055556E-4
 V1(2, 23) = 7.38970277778E-4
 G9(1, 23) = 1.39408685528
 G9(2, 23) = 1.39408670377
 U(1, 23) = 2.43128706521E-3
 U(2, 23) = 2.37889705775E-3
 Q(1, 23) = 62.9844457716
 Q(2, 23) = 62.1120211497
 F2(1, 23) = 244.463106058
 F2(2, 23) = 244.40428427
 C1= 3

L7= 7
M1= 1.87673471865E-2
M2= .029377286478
M3= 9.13488430655E-3
M4= 9.1370775279E-3
M5= 1.87718530944E-2
M6= 2.93702348915E-2
P5(1, 17) = 100150.718793
P5(2, 17) = 100143.452366
T5(1, 17) = 23.9415
T5(2, 17) = 23.951
C= 2

L7= 6
M1= 1.85977201535E-2
M2= 2.91093016012E-2
M3= 8.71759746794E-3
M4= 8.71765511724E-3
M5= 1.85978431399E-2
M6= 2.91091091033E-2
P5(1, 18) = 100131.386096
P5(2, 18) = 100125.386293
T5(1, 18) = 23.895
T5(2, 18) = 23.858
C= 2

L7= 5
M1= 1.85930321325E-2
M2= 2.89317597584E-2
M3= 8.52023908846E-3
M4= 8.51759531803E-3
M5= .018587262845
M6= 2.89407398668E-2
P5(1, 19) = 100126.986241
P5(2, 19) = 100122.919708
T5(1, 19) = 23.741
T5(2, 19) = 23.72
C= 2

L7= 4
M1= 1.84837252746E-2
M2= .028816574596
M3= 8.17185469296E-3
M4= 8.17185515219E-3
M5= 1.84837263133E-2
M6= 2.88165729766E-2
P5(1, 20) = 100132.052741
P5(2, 20) = 100125.319629
T5(1, 20) = 23.626
T5(2, 20) = 23.6085
C= 2

A2= 2492.52853095
V1(1, 17) = 1.22729166667E-3
V1(2, 17) = 1.85594166667E-3
G9(1, 17) = 1.39871668539
G9(2, 17) = 1.39871617043
Q(1, 17) = 3.94595523281E-3
Q(2, 17) = 3.81297676549E-3
R(1, 17) = 124.600721288
R(2, 17) = 124.548045966
F2(1, 17) = 1722.82113544
F2(2, 17) = 1722.79419113
C1= 3

A2= 2683.40517341
V1(1, 18) = 1.18424444444E-3
V1(2, 18) = 1.79613888889E-3
G9(1, 18) = 1.39849206743
G9(2, 18) = 1.3984934915
Q(1, 18) = 3.9543349948E-3
Q(2, 18) = 3.83179982045E-3
R(1, 18) = 118.132917229
R(2, 18) = 118.140610017
F2(1, 18) = 1476.20438489
F2(2, 18) = 1476.23308369
C1= 3

A2= 2873.46133034
V1(1, 19) = 1.17097083333E-3
V1(2, 19) = 1.76421944444E-3
G9(1, 19) = 1.39820594666
G9(2, 19) = 1.39820689182
Q(1, 19) = 3.97744264303E-3
Q(2, 19) = 3.8499141255E-3
R(1, 19) = 111.665500183
R(2, 19) = 111.73058865
F2(1, 19) = 1229.02266787
F2(2, 19) = 1228.92692728
C1= 3

A2= 3086.88480011
V1(1, 20) = .00112543
V1(2, 20) = 1.69856666667E-3
G9(1, 20) = 1.397815708
G9(2, 20) = 1.39781664483
Q(1, 20) = 3.9686260884E-3
Q(2, 20) = 3.84194785724E-3
R(1, 20) = 104.801488504
R(2, 20) = 104.811063544
F2(1, 20) = 982.83119229
F2(2, 20) = 982.655662565
C1= 3

L7= 11
M1= 1.93925675623E-2
M2= 3.01776574265E-2
M3= 1.08789809941E-2
M4= 1.08826478535E-2
M5= 1.93991040034E-2
M6= .0301674892
P5(1, 13)= 100087.987524
P5(2, 13)= 100088.187517
T5(1, 13)= 23.7405
T5(2, 13)= 23.7275
C= 2

L7= 10
M1= .019219898494
M2= 2.98805415976E-2
M3= 1.02430270622E-2
M4= 1.02472129508E-2
M5= 1.92277528474E-2
M6= 2.98623356818E-2
P5(1, 14)= 100111.120096
P5(2, 14)= 100109.720142
T5(1, 14)= 23.7375
T5(2, 14)= 23.756
C= 2

L7= 9
M1= 1.91598699701E-2
M2= 2.98007219558E-2
M3= 9.88535926594E-3
M4= 9.88913596791E-3
M5= 1.91671899993E-2
M6= 2.97893409367E-2
P5(1, 15)= 100132.719386
P5(2, 15)= 100137.052576
T5(1, 15)= 23.8065
T5(2, 15)= 23.817
C= 2

L7= 8
M1= 1.89680522037E-2
M2= 2.95836046428E-2
M3= 9.41446696699E-3
M4= 9.4140105231E-3
M5= .018967132571
M6= 2.95850390215E-2
P5(1, 16)= 100143.119043
P5(2, 16)= 100142.119076
T5(1, 16)= 23.887
T5(2, 16)= 23.8985
C= 2

A2= 1584.50487438
V1(1, 13)= 1.42666111111E-3
V1(2, 13)= 2.14245833333E-3
G9(1, 13)= 1.39930140678
G9(2, 13)= 1.39930206129
V(1, 13)= 3.95614108389E-3
V(2, 13)= 3.81908636491E-3
Q(1, 13)= 185.188165891
Q(2, 13)= 185.06075121
F2(1, 13)= 2708.77837607
F2(2, 13)= 2708.74642759
C1= 3

A2= 1871.47654231
V1(1, 14)= 1.35820833333E-3
V1(2, 14)= 2.04467222222E-3
G9(1, 14)= 1.39919053918
G9(2, 14)= 1.39918961505
V(1, 14)= 3.96049157924E-3
V(2, 14)= 3.8365995058E-3
Q(1, 14)= 159.935964903
Q(2, 14)= 159.811254993
F2(1, 14)= 2461.38417326
F2(2, 14)= 2461.43943212
C1= 3

A2= 1966.89550823
V1(1, 15)= .0013133
V1(2, 15)= 1.97173333333E-3
G9(1, 15)= 1.39905904645
G9(2, 15)= 1.39905850773
V(1, 15)= 3.95760441272E-3
V(2, 15)= 3.82162683884E-3
Q(1, 15)= 152.92845089
Q(2, 15)= 152.805427422
F2(1, 15)= 2216.04980227
F2(2, 15)= 2216.05438451
C1= 3

A2= 2253.67847492
V1(1, 16)= 1.25795833333E-3
V1(2, 16)= .0019013
G9(1, 16)= 1.39890312184
G9(2, 16)= 1.39890258568
V(1, 16)= 3.95314429478E-3
V(2, 16)= 3.83069564972E-3
Q(1, 16)= 135.596889132
Q(2, 16)= 135.617477173
F2(1, 16)= 1969.70885151
F2(2, 16)= 1969.79647325
C1= 3

L7= 15
M1= .019915933121
M2= 3.07320169458E-2
M3= 1.30745269158E-2
M4= 1.30758013726E-2
M5= .019917874453
M6= 3.07290215938E-2
P5(1, 9) = 100044.988938
P5(2, 9) = 100050.455425
T5(1, 9) = 23.6125
T5(2, 9) = 23.5915
C= 2

A2= 1297.58052161
V1(1, 9) = .001695675
V1(2, 9) = 2.52264166667E-3
G9(1, 9) = 1.39963344934
G9(2, 9) = 1.39963449481
Q(1, 9) = 3.98533989236E-3
Q(2, 9) = 3.84264478901E-3
O(1, 9) = 217.808486036
O(2, 9) = 217.747951908
F2(1, 9) = 3694.43735697
F2(2, 9) = 3694.33526858
C1= 3

L7= 14
M1= 1.98239683064E-2
M2= 3.06074728796E-2
M3= 1.25430576928E-2
M4= 1.25467922129E-2
M5= .019829870616
M6= 3.05983626448E-2
P5(1, 10) = 100063.78832
P5(2, 10) = 100063.654991
T5(1, 10) = 23.631
T5(2, 10) = 23.6455
C= 2

A2= 1345.38472406
V1(1, 10) = 1.62447777778E-3
V1(2, 10) = 2.42683888889E-3
G9(1, 10) = 1.39956435861
G9(2, 10) = 1.39956363114
Q(1, 10) = 3.96285828945E-3
Q(2, 10) = 3.83555416841E-3
O(1, 10) = 210.720236848
O(2, 10) = 210.598183638
F2(1, 10) = 3447.92636748
F2(2, 10) = 3447.97513589
C1= 3

L7= 13
M1= 1.97252013018E-2
M2= 3.04329322245E-2
M3= 1.19860542395E-2
M4= 1.19893336639E-2
M5= 1.97305981828E-2
M6= 3.04246079502E-2
P5(1, 11) = 100057.588524
P5(2, 11) = 100059.3218
T5(1, 11) = 23.6725
T5(2, 11) = 23.6805
C= 2

A2= 1393.18336868
V1(1, 11) = 1.55460833333E-3
V1(2, 11) = 2.31283888889E-3
G9(1, 11) = 1.39948635829
G9(2, 11) = 1.3994859539
Q(1, 11) = 3.94611505278E-3
Q(2, 11) = 3.80619107427E-3
O(1, 11) = 204.832612799
O(2, 11) = 204.718177213
F2(1, 11) = 3201.3582314
F2(2, 11) = 3201.37529737
C1= 3

L7= 12
M1= 1.95499350124E-2
M2= 3.03700796134E-2
M3= .011347551175
M4= 1.13521423314E-2
M5= .019557844808
M6= 3.03577970166E-2
P5(1, 12) = 100090.187451
P5(2, 12) = 100087.254214
T5(1, 12) = 23.7095
T5(2, 12) = 23.721
C= 2

A2= 1512.7863495
V1(1, 12) = 1.49073055556E-3
V1(2, 12) = 2.24140833333E-3
G9(1, 12) = 1.39939963865
G9(2, 12) = 1.39939907319
Q(1, 12) = 3.98811117168E-3
Q(2, 12) = 3.86157212046E-3
O(1, 12) = 192.727472404
O(2, 12) = 192.581760643
F2(1, 12) = 2955.7326086
F2(2, 12) = 2955.80052643
C1= 3

L7= 19
M1= 2.03692925447E-2
M2= 3.06510572031E-2
M3= .012786177898
M4= 1.27880941362E-2
M5= 2.03723452486E-2
M6= 3.06464642807E-2
P5(1, 5) = 99995.9238855
P5(2, 5) = 99996.6571947
T5(1, 5) = 23.7375
T5(2, 5) = 23.725
C= 2

L7= 18
M1= 2.03991088924E-2
M2= 3.07163806483E-2
M3= 1.33313056091E-2
M4= 1.33334838825E-2
M5= 2.04024420121E-2
M6= 3.07113625542E-2
P5(1, 6) = 100006.990188
P5(2, 6) = 100013.456642
T5(1, 6) = 23.694
T5(2, 6) = 23.687
C= 2

L7= 17
M1= .020205247953
M2= 3.08350100471E-2
M3= 1.35144623907E-2
M4= 1.35201326742E-2
M5= 2.02137254998E-2
M6= 3.08220779809E-2
P5(1, 7) = 100027.522846
P5(2, 7) = 100020.256418
T5(1, 7) = 23.6695
T5(2, 7) = 23.67
C= 2

L7= 16
M1= 2.01039792273E-2
M2= 3.08154463501E-2
M3= .013438386569
M4= 1.34405722555E-2
M5= 2.01072490394E-2
M6= 3.08104351864E-2
P5(1, 8) = 100026.322886
P5(2, 8) = 100030.122761
T5(1, 8) = 23.64
T5(2, 8) = 23.636
C= 2

A2= 1178.14760678
V1(1, 5) = 1.65431111111E-3
V1(2, 5) = 2.39676944444E-3
G9(1, 5) = 1.39984370349
G9(2, 5) = 1.39984433396
V(1, 5) = 3.96512443203E-3
V(2, 5) = 3.81822452069E-3
Q(1, 5) = 234.067884442
Q(2, 5) = 233.992532091
F2(1, 5) = 4681.51275575
F2(2, 5) = 4681.44496858
C1= 3

A2= 1202.02492049
V1(1, 6) = 1.72294166667E-3
V1(2, 6) = 2.50760555556E-3
G9(1, 6) = 1.39979870169
G9(2, 6) = 1.39979904723
V(1, 6) = 3.96914508876E-3
V(2, 6) = 3.83705244536E-3
Q(1, 6) = 228.812688555
Q(2, 6) = 228.719549566
F2(1, 6) = 4435.15829727
F2(2, 6) = 4435.08969699
C1= 3

A2= 1225.89920504
V1(1, 7) = 1.74390555556E-3
V1(2, 7) = 2.56265833333E-3
G9(1, 7) = 1.39974839328
G9(2, 7) = 1.39974835733
V(1, 7) = 3.97727941157E-3
V(2, 7) = 3.83138785303E-3
Q(1, 7) = 226.119777932
Q(2, 7) = 225.944009412
F2(1, 7) = 4187.76661976
F2(2, 7) = 4187.71916146
C1= 3

A2= 1249.77100725
V1(1, 8) = 1.71784722222E-3
V1(2, 8) = 2.54706666667E-3
G9(1, 8) = 1.39969378916
G9(2, 8) = 1.39969398279
V(1, 8) = 3.93853981122E-3
V(2, 8) = 3.81044071731E-3
Q(1, 8) = 220.841349846
Q(2, 8) = 220.758519258
F2(1, 8) = 3941.32166031
F2(2, 8) = 3941.27535516
C1= 3

L7= 23
M1= .020202452087
M2= 2.93121799076E-2
M3= 8.6689679161E-3
M4= 9.62290661663E-3
M5= 2.00951092978E-2
M6= 2.94687578641E-2
P5(1, 1) = 100003.5903
P5(2, 1) = 99997.5904974
T5(1, 1) = 24.206
T5(2, 1) = 24.2125
C= 2

L7= 22
M1= 2.03212315338E-2
M2= 2.96760657506E-2
M3= 9.82423789595E-3
M4= 9.82470330742E-3
M5= 2.03221942278E-2
M6= 2.96746609492E-2
P5(1, 2) = 99997.8571553
P5(2, 2) = 100001.990353
T5(1, 2) = 24.036
T5(2, 2) = 24.008
C= 2

L7= 21
M1= .020362310195
M2= .030117150659
M3= .010932702543
M4= 1.09336689502E-2
M5= 2.03641101418E-2
M6= 3.01144886588E-2
P5(1, 3) = 100009.523438
P5(2, 3) = 100006.590201
T5(1, 3) = 23.9
T5(2, 3) = 23.877
C= 2

L7= 20
M1= 3.04939684363E-2
M2= 3.03077982752E-2
M3= 1.20692009827E-2
M4= 1.20543089381E-2
M5= 2.04686811706E-2
M6= 3.03452409096E-2
P5(1, 4) = 99987.3908329
P5(2, 4) = 99984.1242737
T5(1, 4) = 23.7905
T5(2, 4) = 23.768
C= 2

A2= 1202.37070356
V1(1, 1) = 1.16174972222E-3
V1(2, 1) = 1.63291111111E-3
G9(1, 1) = 1.39997726256
G9(2, 1) = 1.39997697904
V(1, 1) = 3.94918075532E-3
V(2, 1) = 3.80539053827E-3
Q(1, 1) = 239.479942561
Q(2, 1) = 242.078186122
F2(1, 1) = 5673.25498425
F2(2, 1) = 5673.68531491
C1= 3

A2= 1178.35104516
V1(1, 2) = 1.30336111111E-3
V1(2, 2) = .001837125
G9(1, 2) = 1.39995078599
G9(2, 2) = 1.39995220091
V(1, 2) = 3.93687525446E-3
V(2, 2) = 3.80005481106E-3
Q(1, 2) = 240.514195995
Q(2, 2) = 240.466870892
F2(1, 2) = 5425.29679151
F2(2, 2) = 5424.97292363
C1= 3

A2= 1178.29309756
V1(1, 3) = 1.442238888889E-3
V1(2, 3) = 2.053188888889E-3
G9(1, 3) = 1.3999198731
G9(2, 3) = 1.39992103733
V(1, 3) = 3.97269444511E-3
V(2, 3) = 3.82409279681E-3
Q(1, 3) = 238.666453579
Q(2, 3) = 238.622672065
F2(1, 3) = 5176.81966623
F2(2, 3) = 5176.63758366
C1= 3

A2= 1178.21543243
V1(1, 4) = 1.57924166667E-3
V1(2, 4) = 2.26036944444E-3
G9(1, 4) = 1.39988490227
G9(2, 4) = 1.39988603706
V(1, 4) = 3.97064137869E-3
V(2, 4) = 3.83819443516E-3
Q(1, 4) = 235.279788721
Q(2, 4) = 235.861822836
F2(1, 4) = 4929.48453578
F2(2, 4) = 4929.3345886
C1= 3

22 NOV DATA TAPE, ARRAY STORAGE 24 to 33
SHORT TUBE MODES 1 TO 10
A SIDE = 1248, B SIDE = 815 (ET ALONGSIDE)

L7= 2
M1= 2.10981168293E-2
M2= 2.97542970407E-2
M3= 8.66987050134E-3
M4= 8.6746893448E-3
M5= 2.11098434778E-2
M6= 2.97377683449E-2
P5(1, 32) = 99837.7290895
P5(2, 32) = 99831.8626158
T5(1, 32) = 22.454
T5(2, 32) = 22.442
C = 116.4119

L7= 1
M1= 2.09685798082E-2
M2= 2.95141488499E-2
M3= 8.02169811907E-3
M4= 8.03841715247E-3
M5= 2.10122830717E-2
M6= 2.94527626303E-2
P5(1, 33) = 99842.9289184
P5(2, 33) = 99840.3956684
T5(1, 33) = 22.4235
T5(2, 33) = 22.368
C = 116.4093

A2= 650.525822711
V1(1, 32) = 1.07700027778E-3
V1(2, 32) = 1.47048611111E-3
G9(1, 32) = 1.39746594949
G9(2, 32) = 1.39746649615
V(1, 32) = 3.99821378266E-3
V(2, 32) = 3.87299059521E-3
Q(1, 32) = 75.9935012485
Q(2, 32) = 75.9129065127
F2(1, 32) = 1479.12444311
F2(2, 32) = 1479.11237336
C1 = 118.5701

A2= 1198.11604286
V1(1, 33) = 1.07977027778E-3
V1(2, 33) = .00146865
G9(1, 33) = 1.39574304228
G9(2, 33) = 1.3957454302
V(1, 33) = 4.04212645632E-3
V(2, 33) = 3.91417119562E-3
Q(1, 33) = 42.4283685067
Q(2, 33) = 42.2501706309
F2(1, 33) = 738.446363436
F2(2, 33) = 738.395883437
C1 = 118.5663

L7= 6
M1= 2.18818507746E-2
M2= 3.09835485827E-2
M3= 1.29018175474E-2
M4= 1.29074316502E-2
M5= 2.18913724531E-2
M6= 3.09700722513E-2
P5(1, 28) = 99897.7937803
P5(2, 28) = 99898.1937671
T5(1, 28) = 23.3805
T5(2, 28) = 23.3765
C= 116.4156

L7= 5
M1= 2.18828650073E-2
M2= 3.09512258393E-2
M3= 1.26879620871E-2
M4= 1.26937557462E-2
M5= 2.18923573024E-2
M6= 3.09370991414E-2
P5(1, 29) = 99886.8608066
P5(2, 29) = 99879.1943921
T5(1, 29) = 23.0705
T5(2, 29) = 23.0205
C= 116.4165

L7= 4
M1= 2.16050150645E-2
M2= .03060852328
M3= 1.10406172831E-2
M4= 1.10560594762E-2
M5= 2.16352333762E-2
M6= 3.05657718162E-2
P5(1, 30) = 99872.1946224
P5(2, 30) = 99867.7281026
T5(1, 30) = 22.873
T5(2, 30) = 22.837
C= 116.4152

L7= 3
M1= 2.13757525895E-2
M2= 3.01654696719E-2
M3= 9.66670738539E-3
M4= 9.67420175755E-3
M5= 2.13923247106E-2
M6= 3.01421012058E-2
P5(1, 31) = 99862.6616026
P5(2, 31) = 99864.3282145
T5(1, 31) = 22.6015
T5(2, 31) = 22.599
C= 116.4137

A2= 387.905559213
V1(1, 28) = 6.28991666667E-4
V1(2, 28) = 8.60593888889E-4
G9(1, 28) = 1.39918663613
G9(2, 28) = 1.39918676211
V(1, 28) = 3.94065472812E-3
V(2, 28) = 3.80946145986E-3
Q(1, 28) = 116.077297381
Q(2, 28) = 115.968916996
F2(1, 28) = 4447.59712346
F2(2, 28) = 4447.33053342
C1= 118.5793

A2= 387.838489862
V1(1, 29) = 9.04697222222E-4
V1(2, 29) = 1.23596111111E-3
G9(1, 29) = 1.39897078318
G9(2, 29) = 1.39897308592
V(1, 29) = 3.96806700887E-3
V(2, 29) = 3.83446895976E-3
Q(1, 29) = 117.055024283
Q(2, 29) = 116.945425871
F2(1, 29) = 3703.24109935
F2(2, 29) = 3702.87523621
C1= 118.5777

A2= 411.708158823
V1(1, 30) = 1.03213194444E-3
V1(2, 30) = 1.41388611111E-3
G9(1, 30) = 1.39866812869
G9(2, 30) = 1.39866972148
V(1, 30) = 4.03967404309E-3
V(2, 30) = 3.9115126516E-3
Q(1, 30) = 115.125197639
Q(2, 30) = 114.797918125
F2(1, 30) = 2961.11506582
F2(2, 30) = 2960.83359834
C1= 118.5759

A2= 483.349921531
V1(1, 31) = 1.10347138889E-3
V1(2, 31) = 1.50523055556E-3
G9(1, 31) = 1.39822366684
G9(2, 31) = 1.39822368234
V(1, 31) = 4.13748587483E-3
V(2, 31) = 4.00245412788E-3
Q(1, 31) = 102.982398438
Q(2, 31) = 102.814958167
F2(1, 31) = 2219.11165701
F2(2, 31) = 2218.97722217
C1= 118.573

L7= 10
M1= 1.94828237771E-2
M2= 2.35078384285E-2
M3= 4.12023509873E-3
M4= 4.11936070008E-3
M5= 1.94786891211E-2
M6= 2.35128283345E-2
P5(1, 24) = 99961.1250303
P5(2, 24) = 99951.8586684
T5(1, 24) = 23.9125
T5(2, 24) = 23.849
C = 116.4091

L7= 9
M1= 2.06663288792E-2
M2= 2.60707803001E-2
M3= 5.61943490022E-3
M4= 5.6171094395E-3
M5= 2.06577766427E-2
M6= 2.60815734983E-2
P5(1, 25) = 99929.6593987
P5(2, 25) = 99925.05955
T5(1, 25) = 23.709
T5(2, 25) = 23.68
C = 116.4103

L7= 9
M1= 1.66143042546E-2
M2= 3.65432356761E-2
M3= .592417329983
M4= .592055006661
M5= 1.66041429213E-2
M6= 3.65655992511E-2
P5(1, 26) = 99925.7928592
P5(2, 26) = 99926.2595105
T5(1, 26) = 23.6225
T5(2, 26) = 23.602
C = 116.4121

L7= 7
M1= 2.13769449594E-2
M2= 3.06977071842E-2
M3= .010932599242
M4= 1.09348213698E-2
M5= 2.13812899743E-2
M6= 3.06914689267E-2
P5(1, 27) = 99910.3933658
P5(2, 27) = 99917.4598
T5(1, 27) = 23.529
T5(2, 27) = 23.5065
C = 116.4143

A2= 579.865341231
V1(1, 24) = 2.72044166667E-4
V1(2, 24) = 3.1683388889E-4
G9(1, 24) = 1.39970586644
G9(2, 24) = 1.39970899995
Q(1, 24) = 4.06503781948E-3
Q(2, 24) = 3.92286921822E-3
R(1, 24) = 118.379340747
R(2, 24) = 118.427451996
F2(1, 24) = 7431.31692558
F2(2, 24) = 7430.50979396
C1 = 118.5833

A2= 507.893042353
V1(1, 25) = 1.69542222222E-4
V1(2, 25) = 2.06661111111E-4
G9(1, 25) = 1.39961444381
G9(2, 25) = 1.39961586542
Q(1, 25) = 4.04890436865E-3
Q(2, 25) = 3.91064105803E-3
R(1, 25) = 114.45331137
R(2, 25) = 114.548477594
F2(1, 25) = 6682.97516996
F2(2, 25) = 6682.69651431
C1 = 118.5821

A2= 459.898954401
V1(1, 26) = 4.43116666667E-5
V1(2, 26) = 9.42152777778E-5
G9(1, 26) = 1.39949880378
G9(2, 26) = 1.39949979557
Q(1, 26) = 4.06913306825E-3
Q(2, 26) = 3.93110463973E-3
R(1, 26) = 112.71908269
R(2, 26) = 112.852438793
F2(1, 26) = 5936.95169154
F2(2, 26) = 5936.7390681
C1 = 118.581

A2= 411.921535255
V1(1, 27) = 2.77407222222E-4
V1(2, 27) = 3.84483809889E-4
G9(1, 27) = 1.39935869064
G9(2, 27) = 1.39935978343
Q(1, 27) = 3.98010175096E-3
Q(2, 27) = 3.8422225963E-3
R(1, 27) = 114.009084511
R(2, 27) = 113.95145662
F2(1, 27) = 5191.70968126
F2(2, 27) = 5191.56630698
C1 = 118.5803

22 NOV DATA TAPE, ARRAY STORAGE 34 to 43
SHORT TUBE MODES 1 TO 10
A SIDE = 1248, B SIDE = 1082 (ET ALONGSIDE)

L7= 2
M1= 2.11068673513E-2
M2= 1.92383915261E-2
M3= 8.5414152305E-3
M4= 8.54152515999E-3
M5= 2.11071390003E-2
M6= 1.92391439279E-2
P5(1, 42)= 99716.1997539
P5(2, 42)= 99714.9997934
T5(1, 42)= 23.1375
T5(2, 42)= 23.155
C= 116.414

L7= 1
M1= 2.10180220532E-2
M2= 1.89718549347E-2
M3= 7.9608308125E-3
M4= 7.96091996144E-3
M5= 2.10182574224E-2
M6= 1.89716424818E-2
P5(1, 43)= 99689.1339776
P5(2, 43)= 99681.1342408
T5(1, 43)= 23.1935
T5(2, 43)= 23.196
C= 116.4154

R2= 961.442532391
V1(1, 42)= 1.59862777778E-3
V1(2, 42)= 1.46917777778E-3
G9(1, 42)= 1.39738043776
G9(2, 42)= 1.39737961015
W(1, 42)= 3.89704232584E-3
W(2, 42)= 3.9293682322E-3
Q(1, 42)= 77.5559475994
Q(2, 42)= 77.5580667521
F2(1, 42)= 1481.16097956
F2(2, 42)= 1481.2208758
C1= 118.5641

R2= 1866.40202641
V1(1, 43)= 1.59363611111E-3
V1(2, 43)= 1.45163055556E-3
G9(1, 43)= 1.39565757876
G9(2, 43)= 1.3956572478
W(1, 43)= 3.87217078566E-3
W(2, 43)= 3.90758428727E-3
Q(1, 43)= 40.4852083099
Q(2, 43)= 40.4847813162
F2(1, 43)= 740.17746519
F2(2, 43)= 740.126663099
C1= 118.5664

L7= 6
M1= 2.20919457451E-2
M2= 2.13136772985E-2
M3= 1.22642744075E-2
M4= .012264727611
M5= 2.20927621119E-2
M6= 2.13128897203E-2
P5(1, 38)= 99747.73205
P5(2, 38)= 99747.3987276
T5(1, 38)= 22.7055
T5(2, 38)= 22.7395
C= 116.4061

L7= 5
M1= 2.19476186489E-2
M2= 2.07267060278E-2
M3= 1.22862392545E-2
M4= 1.22849651904E-2
M5= 2.19453427147E-2
M6= 2.07288555782E-2
P5(1, 39)= 99760.7316224
P5(2, 39)= 99760.8649513
T5(1, 39)= 22.8725
T5(2, 39)= 22.9065
C= 116.4079

L7= 4
M1= 2.16804513138E-2
M2= 2.01330525786E-2
M3= .01078367659
M4= 1.07840726198E-2
M5= 2.16812475268E-2
M6= 2.01323132208E-2
P5(1, 40)= 99762.7982211
P5(2, 40)= 99762.0649118
T5(1, 40)= 22.9975
T5(2, 40)= 23.0185
C= 116.4099

L7= 3
M1= 2.14188330632E-2
M2= .019636250164
M3= 9.49164994974E-3
M4= 9.49128308276E-3
M5= .021418005992
M6= 1.96370091649E-2
P5(1, 41)= 99741.4655895
P5(2, 41)= 99733.8658395
T5(1, 41)= 23.0755
T5(2, 41)= 23.0945
C= 116.4124

A2= 483.683904774
V1(1, 38)= .000867785
V1(2, 38)= 6.44009444444E-4
G9(1, 38)= 1.39916292925
G9(2, 38)= 1.39916126622
V(1, 38)= 3.93590663602E-3
V(2, 38)= 3.96799928882E-3
Q(1, 38)= 134.062315597
Q(2, 38)= 134.061544924
F2(1, 38)= 4439.88330796
F2(2, 38)= 4440.16580913
C1= 118.5572

A2= 507.541445884
V1(1, 39)= 1.29884166667E-3
V1(2, 39)= 1.23526388889E-3
G9(1, 39)= 1.39892433635
G9(2, 39)= 1.39892264547
V(1, 39)= 3.94185532965E-3
V(2, 39)= 3.96932166216E-3
Q(1, 39)= 132.429168548
Q(2, 39)= 132.462968727
F2(1, 39)= 3700.30950116
F2(2, 39)= 3700.48682302
C1= 118.5571

A2= 555.327302625
V1(1, 40)= 1.50029888889E-3
V1(2, 40)= 1.40485277778E-3
G9(1, 40)= 1.39860660948
G9(2, 40)= 1.39860557941
V(1, 40)= 3.9597777402E-3
V(2, 40)= 3.99301895203E-3
Q(1, 40)= 126.755413494
Q(2, 40)= 126.752226131
F2(1, 40)= 2960.85892137
F2(2, 40)= 2960.9779958
C1= 118.5567

A2= 650.848095167
V1(1, 41)= 1.55101111111E-3
V1(2, 41)= .0014325
G9(1, 41)= 1.39814643243
G9(2, 41)= 1.39814547704
V(1, 41)= 3.85859355462E-3
V(2, 41)= 3.88713152386E-3
Q(1, 41)= 109.426014669
Q(2, 41)= 109.445018978
F2(1, 41)= 2220.55788819
F2(2, 41)= 2220.60112791
C1= 118.5615

L7= 10
M1= 1.92045975469E-2
M2= 1.99817050981E-2
M3= 4.31495883396E-3
M4= 4.31216735804E-3
M5= 1.91921735183E-2
M6= 1.99946402289E-2
P5(1, 34) = 99751.2652671
P5(2, 34) = 99751.6652539
T5(1, 34) = 22.4855
T5(2, 34) = 22.455
C= 116.4053

A2= 603.823379948
V1(1, 34) = 3.21725277778E-4
V1(2, 34) = 3.37506666667E-4
G9(1, 34) = 1.39971917232
G9(2, 34) = 1.39972063214
Q(1, 34) = 3.90359199425E-3
Q(2, 34) = 3.93326498791E-3
R(1, 34) = 130.541202897
R(2, 34) = 130.698108595
F2(1, 34) = 7407.33566674
F2(2, 34) = 7406.68396456
C1= 118.5636

L7= 9
M1= 2.05174603481E-2
M2= 2.11654991088E-2
M3= 6.08593848915E-3
M4= 6.08835932888E-3
M5= 2.05256216996E-2
M6= 2.11570833306E-2
P5(1, 35) = 99765.9981158
P5(2, 35) = 99768.9980171
T5(1, 35) = 22.346
T5(2, 35) = 22.339
C= 116.4042

A2= 531.847751579
V1(1, 35) = 2.13761666667E-4
V1(2, 35) = 2.22101944444E-4
G9(1, 35) = 1.3996244959
G9(2, 35) = 1.39962477969
Q(1, 35) = 3.82363623468E-3
Q(2, 35) = 3.85271521916E-3
R(1, 35) = 128.40652005
R(2, 35) = 128.291737492
F2(1, 35) = 6662.82519347
F2(2, 35) = 6662.36791147
C1= 118.5617

L7= 8
M1= 1.37892578789E-2
M2= 3.36707474954E-2
M3= .501423683043
M4= .501093939222
M5= 1.37801898536E-2
M6= 3.36929044608E-2
P5(1, 36) = 99759.2650039
P5(2, 36) = 99754.9984776
T5(1, 36) = 22.283
T5(2, 36) = 22.276
C= 116.4043

A2= 507.803073176
V1(1, 36) = 3.92394444444E-5
V1(2, 36) = 9.66566666667E-5
G9(1, 36) = 1.39950761204
G9(2, 36) = 1.39950791874
Q(1, 36) = 3.92279239176E-3
Q(2, 36) = 3.95463796482E-3
R(1, 36) = 128.932814812
R(2, 36) = 129.10268275
F2(1, 36) = 5919.83221932
F2(2, 36) = 5919.58602906
C1= 118.5608

L7= 7
M1= 2.14233756347E-2
M2= 2.22257704577E-2
M3= 9.89804820721E-3
M4= 9.89384627112E-3
M5= 2.14142809471E-2
M6= 2.22352097864E-2
P5(1, 37) = 99744.8654776
P5(2, 37) = 99746.6654184
T5(1, 37) = 22.5255
T5(2, 37) = 22.5725
C= 116.4043

A2= 483.766980051
V1(1, 37) = 3.41965555556E-4
V1(2, 37) = 3.57270833333E-4
G9(1, 37) = 1.399350942
G9(2, 37) = 1.39934864791
Q(1, 37) = 3.9260533392E-3
Q(2, 37) = 3.95201020353E-3
R(1, 37) = 132.143242952
R(2, 37) = 132.263992902
F2(1, 37) = 5179.20968816
F2(2, 37) = 5179.68587302
C1= 118.5585

LIST OF REFERENCES

1. Rudnick, I., "Unconventional Reciprocity Calibration of Transducers", Journal of the Acoustical Society of America, Vol. 63, 1978, p. 1923.
2. Swift, G.W., Migliori, A., and Garrett, S.L., "Two Methods For Absolute Calibration of Dynamic Pressure Transducers", Review of Scientific Instruments, Vol. 53, December 1982, pp. 1906-1910
3. American National Standards Institute, Inc., USA Standard Method for the Calibration of Microphones, ANSI S1.10-1966, Reaffirmed 1976.
4. MacLean, W.R., "Absolute Measurement of Sound Without A Primary Standard", Journal of the Acoustical Society of America, Vol. 11, July 1940, p. 140.
5. Cook, R.K., "Absolute Pressure Calibration of Microphones", National Bureau of Standards Journal of Research, Vol. 25, November 1940, pp. 489-505.
6. Sivian, L.J., "Absolute Calibration of Condenser Transmitters", Bell System Technical Journal, Vol. 10, 1932, pp. 96-115.
7. Rudnick, I. and Stein, M.N., "Reciprocity Free Field Calibration of Microphones to 100 Kc in Air", Journal of the Acoustical Society of America, Vol. 20, November 1948, pp. 818-825.
8. Simmons, B.D. and Biagi, F., "Pressure Calibration of Condenser Microphones above 10 000 cps", Journal of the Acoustical Society of America, Vol. 26, September 1954, pp. 693-695.
9. Beranek, L.L., Acoustic Measurements, Wiley, 1949
10. Bobber, R.J., Underwater Electroacoustic Measurements, U.S. Government Printing Office, 1969
11. Kinsler, Frey, Coppens, and Sanders, Fundamentals of Acoustics, Wiley, 3rd Edition, 1980

12. Wong, G.S.K., and Embleton, T.F.W., "Arrangement for Precision Reciprocity Calibration of Condenser Microphones", Journal of the Acoustical Society of America, Vol. 66, November, 1979, pp. 1275-1280.
13. Lord Rayleigh, "Some General Theorms Relating to Vibrations", Proceedings of the London Mathamatical Society, Vol. 4, pp. 357-368, 1873; Scientific Papers, Vol. I, Dover, New York, 1964
14. Lord Rayleigh, The Theory of Sound, Vol. I & Vol. II, Macmillan and Company, Ltd., 1877.
15. Lange, P.de, "On Thermophones", Proceedings of the Royal Society of London, Vol. A91, pp. 239-241, 1915.
16. Arnold, H.D. and Crandall, I.B., "The Thermophone as a Precision Soruce of Sound", Physical Review, Vol. 10, pp.22-38, 1917.
17. Ballantine, S., "Technique of Microphone Calibration", Journal of the Acoustical Society of America, Vol. 3, pp. 319-360, 1932.
18. Wente, E.C., "The thermophone", Physical Review, Vol. 19, pp. 333-345, 1922.
19. Wente, E.C., "A Condenser Transmitter as a Uniformly Sensitive Instrument For the Absolute Measurement of Sound Intensity", Physical Review, Vol. 10, pp. 39-63, 1917.
20. Foldy, L.L, and Primakoff, H., "A General Theory of Passive Linear Electroacoustic Transducers and The Electroacoustic Reciprocity Theorem, I", Journal of the Acoustical Society of America, Vol. 17, No.2, 1945, pp. 109-120.
21. Foldy, L.L. and Primakoff, H., "A General Theory of Passive Linear Electroacoustic Transducers and The Electroacoustic Reciprocity Theorem. II", Journal of the Acoustical Society of America, Vol. 19, No.1, 1947, pp. 50-58.
22. Morse, P.M., Vibration and Sound, The American Institute of Physics, 1976
23. Conte, D.V., Computerized Acquisition and Analysis of Acoustical Resonances, M.S. Thesis, Naval Postgraduate School, Monterey, California, 1983

24. Mehl, James B., "Analysis of Resonance Standing Wave Measurements", Journal of the Acoustical Society of America, Vol. 64, No. 5, 1978, pp. 1523-1525.
25. Wong, George S. and Embleton, Tony F.W., "Variation of Specific Heats and of Specific Heat Ratio in Air With Humidity", Journal of the Acoustical Society of America, Vol. 72, No. 2, 1984, pp. 555-559.
26. Bevington, Philip R., Data reduction and error analysis for the physical sciences, McGraw-Hill Book Company, 1969, Chapters 4, 5, and 11.
27. Churchill, Ruel V., Operational Mathematics, McGraw-Hill Book Company Inc., 1958, pp. 225-226
28. Holman, J. P., Experimental Methods for Engineers, McGraw-Hill Book Company, 1978, Chapter 3.
29. Private communication from Dr. V. Nedzelnitsky, U.S. Department of Commerce, National Bureau of Standards, Gaithersburg, MD., 20899
30. Burkhard, M.D., Corliss, E.L.R., Koidan, W., and Biagi, F., "Calibration for Carrier Operated Microphones and other Reversible Transducers", Journal of the Acoustical Society of America, Vol. 32, No. 4, April 1960, pp. 501-504.
31. Koidan, W., "Method for Measurement of E'/I' in the Reciprocity Calibration of Condenser Microphones", Journal of the Acoustical Society of America, Vol. 32, No. 5, May 1960, p. 661.
32. Bruel & Kjaer, Condenser Microphones and Microphone Preamplifiers for Acoustic Measurements, Data Handbook, revised September, 1982
33. Personal communication from Mr. James E. West, Acoustic Research Dept., AT&T Bell Laboratories, Murray Hill, N.J. 1983
34. Hunt, Frederick V., Electroacoustics, The Analysis of Transduction and Its Historical Background, American Institute of Physics, 1982

35. Personal communication from LT Michael B. Johnson, Physics Dept., Naval Postgraduate School, Monterey, Calif., 1984
36. Halliday, David, and Resnick, Robert, Fundamentals of Physics, Wiley, 2nd Edition, 1981, p. 501

INITIAL DISTRIBUTION LIST

	No. copies
1. Defense Technical Information Center Cameron Station Alexandria, Virginia 22304 - 6145	2
2. Superintendent Attn: Library, Code 0142 Naval Postgraduate School Monterey, California 93943	2
3. Prof. Isadore Rudnick UCLA Dept of Physics 405 Hilgard St. Los Angeles, CA., 90024	1
4. Prof. S. L. Garrett Physics Dept, Code 61gx Naval Postgraduate School Monterey, California 93943	6
5. Prof. O.B. Wilson Physics Dept, Code 61 Naval Postgraduate School Monterey, California 93943	1
6. LCDR C. L. Burmaster Physics Dept, Mail drop 9C USNA, Annapolis, Md., 21403	8
7. Dr. V. Nedzelnitsky U.S. Dept of Commerce, National Bureau of Standards, Gaithersburg, Md., 20899	1
8. LT. Michael B. Johnson c/o Physics Dept, Code 61 Naval Postgraduate School Monterey, Ca., 93943	1

- 9. George S. Wong 1
 Senior Research Officer
 National Research Council of Canada
 Physics Division
 Ottawa, Canada K1A0S1
- 10. John P. Keilman 1
 Knowles Electronics
 3100 N. Mannheim Rd.
 Franklin Park, Ill. 60131
- 11. Mr. Kerry Yarber 1
 c/o Physics Dept, Code 61
 Naval Postgraduate School
 Monterey, Ca., 93943
- 12. Daniel R. Flynn and M. R. Serbyn 1
 U.S. Dept. of Commerce
 National Bureau of Standards
 Washington, D.C.; 20234
- 13. Martin Greenspan 1
 12 Grandville Dr.
 Silver Springs, Md. 20901
- 14. James E. West 1
 Acoustic Research Dept.
 AT&T Bell Laboratories
 600 Mtn. Ave.
 Murray Hill, N.J. 07974
- 15. G. W. Swift 1
 P. O. Box 1663/MS764
 Los Alamos, N.M. 87545
- 16. Dr. Jorge C. Novarini 1
 Av. Cordoba 4190
 1188 Cap. Fed.
 Buenos Aires
 Argentina

END

FILMED

3-86

DTIC